Copigmentation and its Impact on the Stabilisation of Red Wine Pigments

Thesis submitted for the degree of Doctor of Philosophy

By

Stephanie Green Lambert
B.Sc. (Honours)

Department of Horticulture, Viticulture and Oenology

Faculty of Agricultural Science and Natural Resource Management

THE UNIVERSITY OF ADELAIDE
AUSTRALIA

October 2002

TABLE OF CONTENTS

Declaration

This work contains no material which has been accepted for the award of any other degree or diploma in any university or other tertiary institution and, to the best of my knowledge and belief, contains no material previously published or written by another person, except where due reference has been made in the text.

I give consent to this copy of my thesis, when deposited in the University of Adelaide Library, being available for loan and photocopying.

SIGNED : .. DATE : 15/10/02

Stephanie G Lambert

Acknowledgments

I would not have been able to complete my PhD programme without the support of many people. Thanks are due to :

- Assoc Prof Graham Jones and Dr Patrick Iland of Adelaide University who kept me enthused with their encouraging and enlightening supervision.
- All those involved with the Tannin Project from Adelaide University and the Australian Wine Research Institute.
- Dr Mark Buntine and Mr Phil Clements of the Chemistry Department of Adelaide University. From the former I received generous access to computational programs and advice in the molecular modelling component of the thesis, whist the latter performed the NMR analyses.
- Dr Kevin Wainwright of Flinders University for allowing me to use the potentiometric titration equipment.
- Mr Yogi Hayasaki of the Australian Wine Research Institute for performing the mass spectrometry.
- Southcorp Wines, Henschke Wines and Majella Wines for providing fruit for the winemaking experiments.
- Dr Robert Asenstorfer for inspiration which helped me to get started and continue on.
- Past and present members of the Oenology group, Ms Sally Elieff and Dr Jim Kennedy for their help and friendship.
- Ms Renata Ristic for help with the winemaking.
- Mr Mark Downey for all the technical advice and motivational prompts.
- Ms Jennie Gardner of Adelina Wines and Ms Julie Payne for keeping the wine passion well and truly alive.
- My mother in New Zealand who is still dreaming of verandahs overlooking vineyards…

This research was funded by the Australian Research Council and the Grape and Wine Research and Development Corporation.

Abstract

Copigmentation is the term used to describe the interaction between phenolic pigments and non-pigmented compounds which leads to increases in colour expression. It also produces shifts in the absorption maximum to longer wavelengths. In red wine this manifests itself as a shift from red to blue colour. In this study copigmentation interactions of two grape derived anthocyanins, malvidin-3-monoglucoside and malvidin-3-(p-coumaryl)glucoside, with various copigments were investigated. In particular, the mechanistic, equilibrium and thermodynamic aspects of copigmentation were studied. Various techniques were employed which included UV/visible spectroscopy, *semi empirical* molecular modelling calculations, ionisation constant determination by potentiometric titration and NMR structural studies of model solutions and applied spectral colour analysis of red wines.

The stability constants associated with intermolecular copigmentation were determined by monitoring the increase in colour expression with copigment addition. The strongest interaction of malvidin-3-monoglucoside occurred with the flavonol quercetin (K_a =2900 ±1300 $mol^{-1}L$). Other copigments had much lower stability constants. Monomeric and polymeric flavan-3-ols were relatively weak copigments; (-)-epicatechin, 260±40 $mol^{-1}L$; (+)-catechin,90±20 $mol^{-1}L$; procyanidin dimer B3, 330±33 $mol^{-1}L$ and seed tannin, 420±40 $mol^{-1}L$. The addition of potassium bitartrate, ethanol and sulphur dioxide resulted in a net decrease in copigmentation effects.

Self-association stability constants of malvidin-3-monoglucoside and malvidin-3-(p-coumaryl)glucoside were calculated using a model that predicted dimer concentration as a function of the observed and expected absorbance at pH 3.6. In the concentration range studied (5 $x10^{-5}$ to 3 $x10^{-3}$ $molL^{-1}$) malvidin-3-monoglucoside self associated (K_a = 4800±400 $mol^{-1}L$) whereas malvidin-3-(p-coumaryl)glucoside did not. At wine pH the absorbance of malvidin-3-(p-coumaryl)glucoside was approximately twice that of malvidin-3-monoglucoside. The greater colour expression of malvidin-3-(p-coumaryl)glucoside compared with that of malvidin-3-monoglcoside may be attributed to intramolecular stabilisation.

An examination of the notion that π-π stacking interactions between anthocyanins and copigments results in colour enhancement is presented. The lack of the characteristic spectral bands associated with charge transfer complexes between malvidin-3-monoglucoside and copigments suggests that there is no molecul; r orbital overlap between the π systems of the pigment and copigment. this was supported by copigmentation studies involving the aromatic

indicators, methyl red and methyl violet. It was concluded that the observed increase in absorbance of anthocyanins involved in self-association or intermolecular copigmentation is not a consequence of π-π interactions but a result of a shift in the anthocyanin equilibrium towards the formation of more coloured species.

Computational chemistry methods highlighted the structural and electronic properties of copigments which are relevant to their interaction with pigments The copigments which adopted coplanar conformations through their extended delocalised aromatic rings (eg quercetin) or that provided sufficient hydrogen bonding (eg seed tannin) were also the copigments that exhibited the higher stability constants with malvidin-3-monoglucoside.

Spectral methods were used to quantify the importance of copigmentation in retention and enhancement of colour expression in Shiraz and Pinot Noir wines. Copigmentation interactions accounted for up to 50% of the colour expression of a young Shiraz red wine but accounted for less than 14% in Pinot Noir wines. Copigmentation was correlated with increased red colour and a slight shift towards blue. Furthermore, the greater the degree of copigmentation at the completion of fermentation the more polymeric pigments present after 12 months ageing. This work demonstrates that the more anthocyanins present at completion of fermentation then the greater the future colour stability of the red wine.

Chapter 1

Introduction

1.1 Copigmentation

Phenolic compounds of grape berries and ultimately red wine, include anthocyanins, flavan-3-ols, procyanidins, flavonols, hydroxycinnamates and hydroxybenzoates (Singleton, 1988). Phenolic concentrations of red wines are dependent on that available in the grape berries at harvest and the method(s) by which the grapes are processed into wine. The colour of red wine reflects the concentration of the extracted phenolic compounds and on the reactions that they are involved in. Colour stability of red wines has been associated with polymeric pigment formation. One possible pathway in the formation of polymeric pigments may be via a phenomenon known as copigmentation.

Copigmentation is thought to involve interaction between phenolic constituents, which increases the colour expression and shifts the hue of the red wine towards blue. The interaction may involve solely the anthocyanins or it may involve interaction between an anthocyanin and another phenolic compound (termed copigment). Copigmentation can account for between 30 and 50% of the colour in a young red wine (Bolton, 2001).

1.2 The phenolic constituents of *Vitis vinifera* grapes and wines

1.2.1 Grape anthocyanins

Grape anthocyanins extracted from the skins of black grape berries during fermentation play an important role in the colour expression of a young red wine. The general structure of grape anthocyanins is a C15 skeletal structure as shown in Figure 1.1.

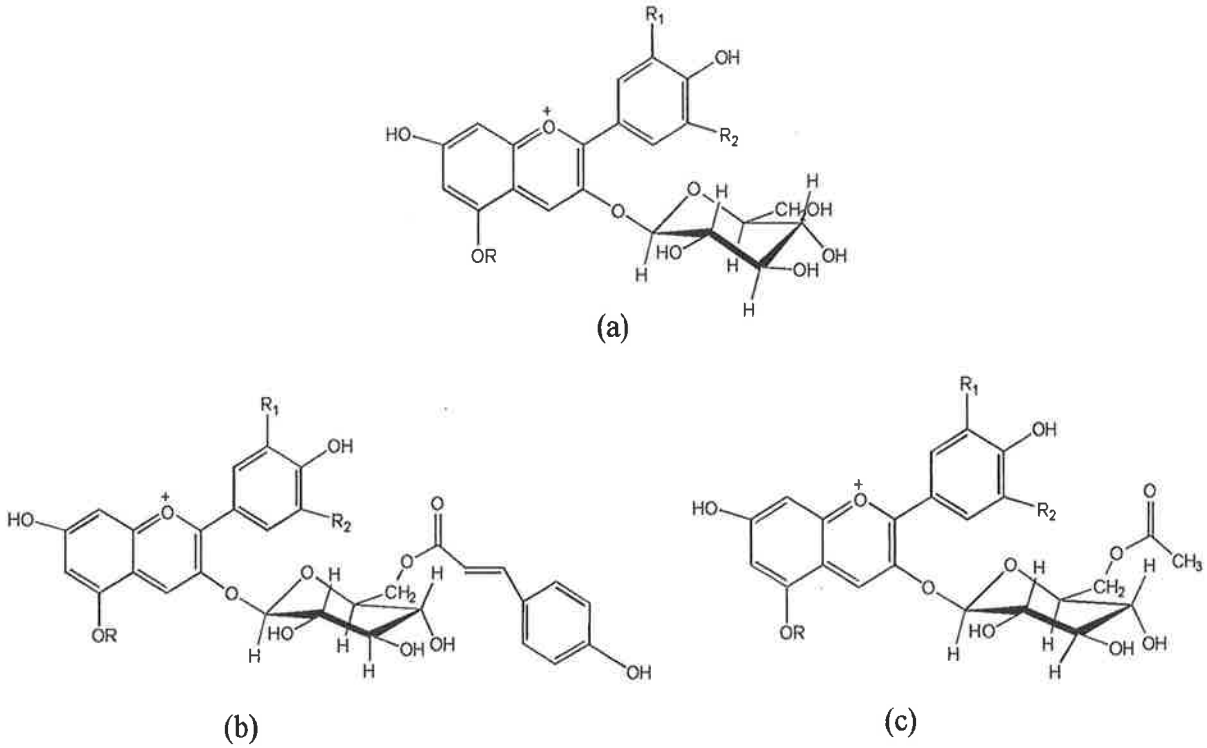

Figure 1.1 Grape anthocyanins, (a) representation of a grape anthocyanin glucoside (b) representation of a grape anthocyanin glucoside p-coumarate and (c) representation of a grape anthocyanin glucoside acetate. R = glucosyl for the diglucosides and R = H for the monoglucosides.

cyanidin :	R1 = OH	R2 = H
delphinidin :	R1 = OH	R2 = OH
malvidin :	R1 = OCH_3	R2 = OCH_3
peonidin :	R1 = OCH_3	R2 = H
petunidin :	R1 = OCH_3	R2 = OH

The glucose substituent may be acylated either by an acetate moiety or by hydroxycinnamic or benzoxybenzoic acids. Only the 3-monoglucosides and their related acylated derivatives are present in the skins of *V. vinifera* grape berries. Investigations involving the 3,5-diglucose substituted anthocyanins present in hybrid varieties have yielded great insight into general grape anthocyanin chemistry and it is likely that similar principles apply for the monoglucosides (Ribereau-Gayon, 1973).

The chemical behaviour or the reactivity of each derivative is dependent on the nature of the substitution pattern. There are however general structural characteristics and consequential

chemical reactivity characteristics for all the derivatives. These include presence of a hydroxyl group at C-7, the nucleophilic character of C-6 and C-8 and electrophilicity at C-4 and C-2. The glucose substituent influences the degree of these chemical reactivities by imparting changes in the electronic distribution (π, σ and n electrons) in the C ring through changes in configuration, polarity, degree of aromatic π electron interactions and steric constraints.

1.2.2 Non-pigmented phenolic constituents present in red wines

Phenolic compounds other than the anthocyanins present in *V. vinifera* grapes are outlined in Figure 1.2. Hydroxycinnamates are present principally as esters of tartaric acid, hydroxybenzoates as free acids or unidentified esters and flavonols as 3-glucosides and 3-glucuronides. The predominant phenolic constituent of red wines are monomeric and polymeric forms of flavan-3-ols (catechin and epicatechin, epigallocatechin and their 3-O-galloyl esters). The higher molecular weight polymers are referred to as proanthocyanidins or condensed tannins. The importance of these compounds to red wine colour stability and palate structure has been the focus of research for the past forty years but it is only in the last decade that chemical structural information has been obtained on some of the less complex members of this family of compounds.

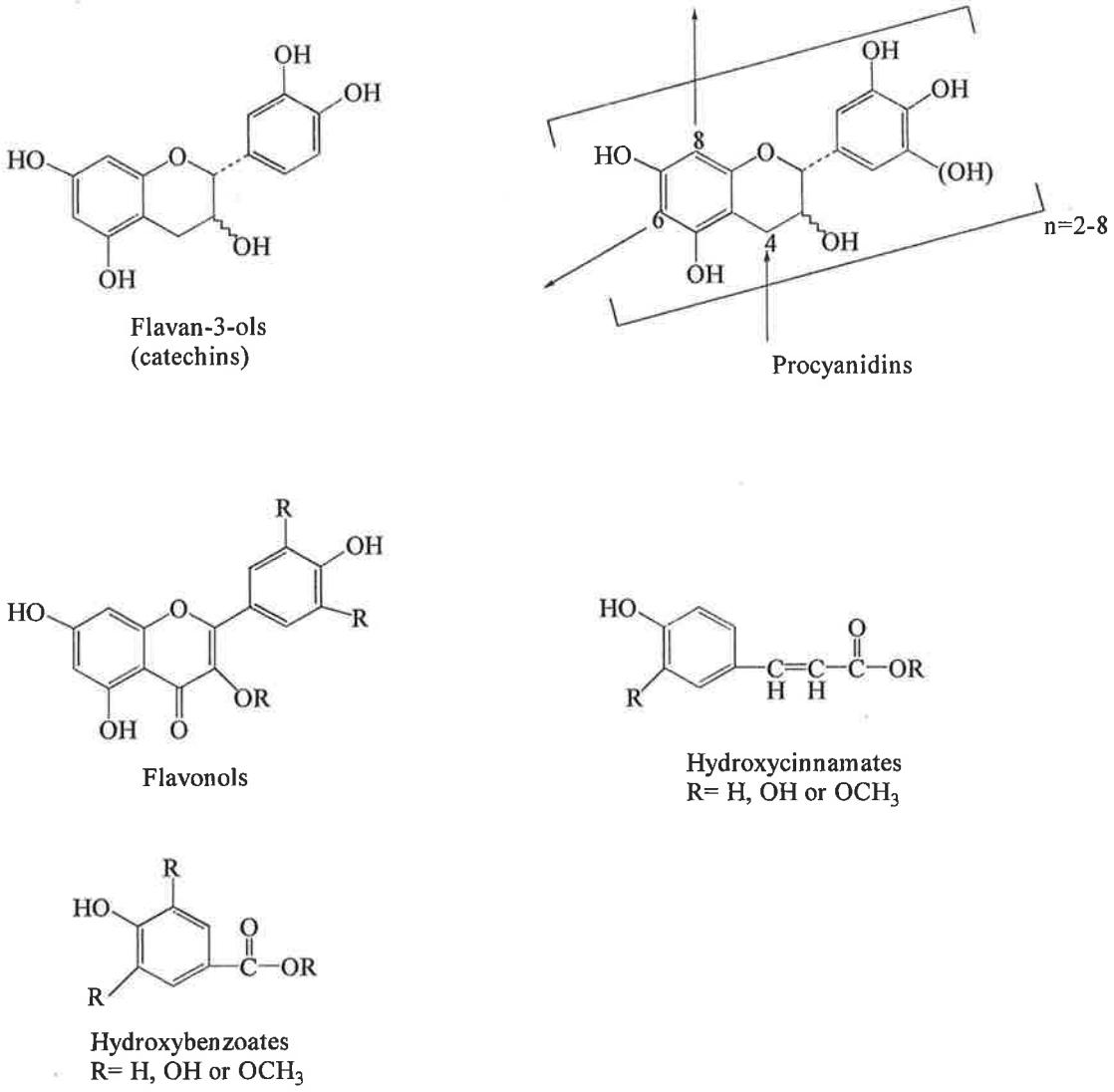

Figure 1.2 Non-pigmented phenolic compounds present in grape berries.

1.2.3 Concentration of phenolic compounds in red wine

Data presented by Singleton, (1988) showed a typical young red wine has a total phenolic concentration of approximately 1200 mgL^{-1} (Table 1.1 and Table 1.2) although wines may contain up to and in excess of 4 gL^{-1} phenolic compounds (Somers and Verette, 1988). The concentration of phenolic compounds of a red wine is dependent on the variety of grape berry, the viticultural practices and the techniques by which the grapes were processed to wine. During fermentation, the phenolics are extracted from the grape berry skins and seeds into the grape must, providing the pool of anthocyanins and other flavonoids available for further reaction during fermentation and maturation.

Table 1.1 Phenolic composition of young red wines (mgL^{-1})

	Young light red wine [a]	*Cabernet Sauvignon (after day 2 of fermentation)* [b]	*Cabernet Sauvignon (<1 month old)* [c]	*Cabernet Sauvignon (~3years old)* [d]
Non flavonoids: total	200			
Hydroxycinnamates	140		121	40-80
Hydroxybenzoates	40		49	20-40
Flavonoids: total	1000			
(+)-Catechin	100 (includes related species)	60	65	75-115
(-)-Epicatechin		34	34	
Flavonols			46	40-80
Polymeric flavan-3-ols	500		31 (B1 and B3)	
Malvidin-3-monoglucoside	400	148		60-110
Acylated derivatives		139		
Other anthocyanins		135		

(a) (Singleton, 1988)
(b) (Nagel and Wulf, 1979)
(c) (Archeir et al., 1992)
(d) (Ritchey and Waterhouse, 1999)

Table 1.2 Phenolic composition of commercial Australian red wines (mgL^{-1})

	Cabernet Sauvignon	*Shiraz*	*Pinot Noir*
(+)-Catechin[a]	32	22	75
(-)-Epicatechin[a]	20	21	35
Quercetin[b]	9.2	10.8	1.8
p-Coumaric acid[b]	4.7	6.1	1.8

(a) (Goldberg et al., 1998a)
(b) (Goldberg et al., 1998b)

Monomeric anthocyanin concentration declines during red wine aging while the concentration of polymeric pigments increases (Somers, 1971). The concentration of the monomeric anthocyanins declines due to either polymerisation or degradative processes. Degradation of anthocyanins may be enzymatic or non-enzymatic. The major enzymatic processes involve the enzymes released during crushing such as polyphenol oxidase, β-glucosidases and peroxidase (Calderon et al., 1992). Non-enzymatic degradation process involves oxidation reactions. Increased temperature and low sulphur dioxide concentration promotes the degradation of anthocyanins (Dallas and Laureano, 1994;Adams, 1973).

Another mode by which anthocyanin concentration declines is through complexation reactions. This includes copigmentation, which is the focus of this research.

1.3 Constituents involved in copigmentation and polymerisation

1.3.1 Introduction

The constituents involved in copigmentation are the grape anthocyanins and the flavan-3-ols, procyanidins, flavonols, hydroxycinnamates and hydroxybenzoates.

Previous studies of copigmentation generally have used the anthocyanin malvin-3,5-diglucoside. Copigments have included chlorogenic acid, rutin and quercetin as well as the major red wine occurring flavonoids (+)-catechin and (-)-epicatechin. The general chemistry of diglucoside anthocyanin copigmentation is assumed to be applicable to the monoglucoside anthocyanins found in red wines derived from *V. vinifera* grapes.

1.3.2 Anthocyanins

Anthocyanins exist within a delicately balanced equilibrium between many structural forms in solution. The colour of anthocyanins is variable, red in acidic solutions to reddish-violet and violet in weakly acidic or neutral solutions and finally blue in alkaline solutions (Markakis, 1982). The pH dependent structural transformations of the anthocyanins is outlined in Figure 1.3 (Brouillard and Lang, 1990). The equilibrium states presented in Figure 1.3 represent the thermodynamic equilibrium. The dynamic features of anthocyanin equilibrium are also important (Melo et al., 2000). The pH domain of the red colour may be shifted to higher pH values with the addition of a copigment. This is generally a strategy used by nature to obtain colour in plants. Addition of a copigment may impart similar changes in anthocyanin equilibrium reactions as that observed with pH jumps.

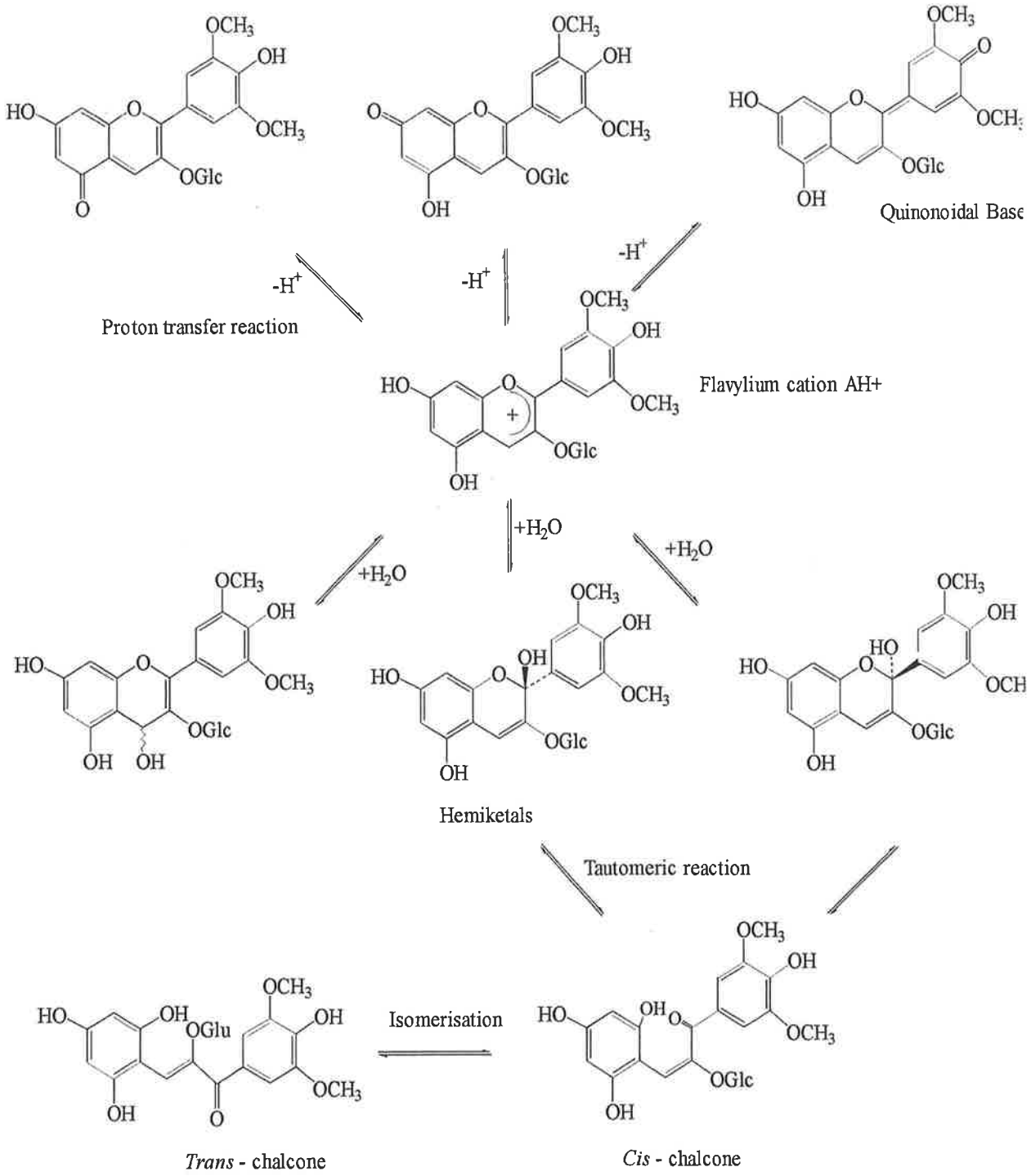

Figure 1.3 The reaction scheme of the anthocyanin equilibrium (Brouillard and Lang, 1990).

The flavylium ion, which appears red, is the centre link between all the structures. The quinonoidal base, hemiketal and the chalcone forms occur exclusively via the flavylium ion (Brouillard and Delaporte, 1977). The protonation-deprotonation reaction between the red flavylium cation and the quinonoidal base is fast with a pK_a of 4.25 (Brouillard and Delaporte, 1977). The hydration reaction is somewhat slower due to the endothermic nature of the reaction. The addition of water onto the flavylium ion is capable of forming four colourless

hemiketal diastereomers, pK_H of 2.6. A tautomeric reaction then occurs, pK 3, to form the yellow *cis* and *trans* chalcones.

At wine pH (3.5-3.6) the colour expression of monomeric anthocyanins is dependent on the pH and on the sulphur dioxide content of the wine. At wine pH, the colourless forms of the anthocyanin are dominant (Brouillard and Delaporte, 1977;Mazza and Brouillard, 1987). Sulphur dioxide is present in red wine as molecular SO_2 and as bisulphite ion, HSO_3^-. Molecular SO_2 and the bisulphite ion are required in wine to inhibit microbiological activity and act as an antioxidant. However the bisulphite ion also leads to unwanted reactions. Bisulphite reacts with the red flavylium ion form of an anthocyanin to form a colourless bisulphite addition product, essentially quenching the colour of the anthocyanin (Timberlake and Bridle, 1976).

1.3.3 Copigments

Studies of copigmentation has focussed on the involvment of flavonoid compounds (Brouillard et al., 1989;Baranac et al., 1996;Dangles and Brouillard, 1992;Baranac et al., 1997b;Baranac et al., 1997a;Baranac and Petranovic, 1997;Brouillard et al., 1991;Mazza and Brouillard, 1990). The common flavonoids present in red wines are the flavan-3-ols, (+)-catechin and its isomer (-)-epicatechin, and flavonols such as quercetin. Procyanidins, or dimers, trimers and higher oligomers of (+)-catechin and (-)-epicatechin, are also present. Characteristic of these flavan-3-ols is a C-15 skeletal structure and three hydroxyl groups at C-7, C-5 and C-4'. Procyanidins B1-B4 were first isolated from grapes by Weinges and Piretti, (1971). Further work has lead to the isolation and identification of the higher oligomers, dimers B5, B6, B8, 4 trimers ([epicatechin-(4β-6)-epicatechin-(4β-8)-epicatechin], [epicatechin-(4β-8)-epicatechin-(4β-6)-catechin], [epicatechin-(4β-8)-epicatechin-(4β-6)-epicatechin], [epicatechin-(4β-6)-epicatechin-(4β-8)-catechin]), and five galloyl esters (B2 3-*O*-gallate, B1 3-*O*-gallate, B4 3'-*O*-gallate, B2 3,3'-di-*O*-gallate, [epicayechin-(4β-8)-epicatechin 3-*O*-gallate-(4β-8)-catechin) in grape seeds (Ricardo da Silva et al., 1991) (Figure 1.4).

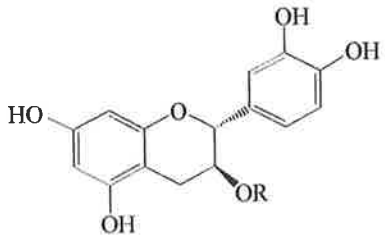

R= H (+)-catechin
R= 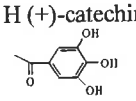

catechin-3-gallate

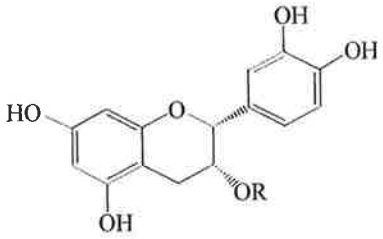

R= H (-)-epicatechin
R= 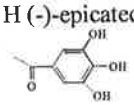

epicatechin-3-gallate

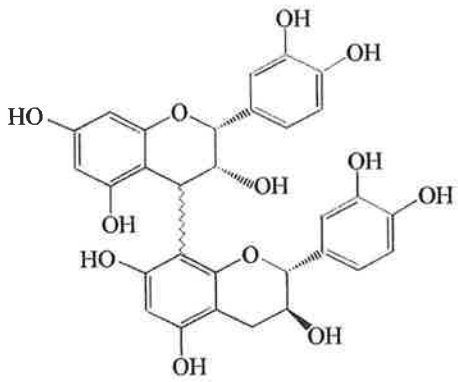

Procyanidin B-1
[epicatechin-(4β-8)-catechin]

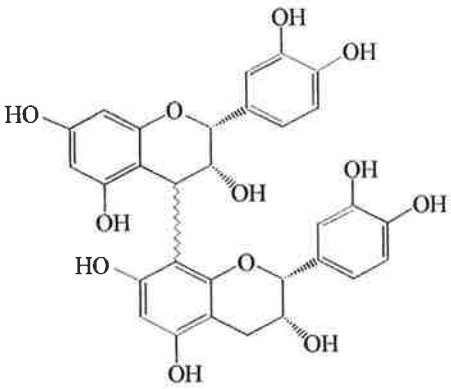

Procyanidin B2
[epicatechin-(4β-8)-epicatechin]

Figure 1.4 The flavan-3-ols, (+)-catechin, (-)-epicatechin and some higher oligomers.

All the flavan-3-ols monomers and higher oligomers may potentially act as copigments in red wine. Other possible copigments include flavonols such as quercetin and various phenolic acids (refer to Figure 1.2). The flavonols quercetin and rutin have been shown to exhibit strong copigmentation with anthocyanins (Liao et al., 1992;Baranac et al., 1997a;Gonnet, 1999;Baranac et al., 1996;Scheffeldt and Hrazdina, 1978). On the other hand, monomeric flavan-3-ols are rather poor copigments but (-)-epicatechin is a substantially better copigment than its stereoisomer, (+)-catechin (Brouillard et al., 1991;Mistry et al., 1991). Intermolecular copigmentation effects of procyanidins and higher oligomeric flavan-3-ols are still relatively unknown.

1.4 Copigmentation

1.4.1 Introduction

Research into the existence, effects and importance of copigmentation in red wine is a relatively new area even though the phenomena within biological systems containing

anthocyanins has been known for some time. The general effect of copigmentation is to cause an increase in colour expression. In spectroscopic terms this results in an increase in absorbance and a shift of absorbance maximum to longer wavelengths. Copigmentation of anthocyanins in red wine is expected to contribute to the overall colour expression of the wine.

Work performed in the early twentieth century by Willslatter and Zollinger, (1916) and Robinson and Robinson, (1931) on flower colour drew attention to the phenomena of copigmentation. They highlighted the ability of a copigment to enhance colour intensity and shift absorbance maximum to longer wavelengths causing a 'blueing' effect. More recent discoveries have included self-association and intramolecular copigmentation (Hoshino and Matsumoto, 1980;Dangles et al., 1993).

Copigmentation has been shown to occur with anthocyanins. Metal chelation, another mechanism that generally results in colour enhancement only occurs in *ortho*- dihydroxyl systems and therefore does not appear relevant to red wine systems where the principal anthocyanin is malvidin-3-monoglucoside (Bayer et al., 1966;Asen et al., 1972).

1.4.2 Intermolecular copigmentation

A mode of copigmentation is through the intermolecular association of an anthocyanin with a copigment. This mode of interaction has been of most interest to those investigating red wine colour characteristics as it is expected to have the greatest influence due to the large pool of possible copigments present in red wine.

Intermolecular copigmentation involving the diglucoside anthocyanins of the *Vitis* species have highlighted the general mechanisms involved with intermolecular copigmentation. Increase in absorbance and a shift of absorbance maximum to longer wavelengths upon copigment addition is commonly observed with all the anthocyanins. (Scheffeldt and Hrazdina, 1978;Brouillard et al., 1989). However it is the magnitude of this effect that varies between anthocyanins and different copigments.

Anthocyanins and copigments have varying affinities towards each other due to structural and electronic factors. Two mechanisms for complex interaction between anthocyanin and copigment have been postulated - (a) vertical stacking between the two constituents by aromatic π electron and/or hydrophobic interactions (Harborne, 1988;Brouillard et al., 1989;Goto et al., 1979) and (b) horizontal interactions via hydrogen bonding (Asen et al., 1972). In the literature vertical stacking of π aromatic systems has been commonly referred to

as π-π stacking however this terminology is misleading when used to describe copigmentation. Re-evaluation of the mode of interaction involved with copigmentation will be discussed in Chapter 2. Hydrogen bond formation is the less probable interaction since competition between hydrogen bond acceptors highly favours interaction with the solvent medium rather than with the other copigmentation partner. Both mechanisms of interaction have been observed with the copigment caffeine (Wigand et al., 1992).

1.4.3 Self-association

There is an observed increase in colour expression due to interactions between the anthocyanins themselves (Scheffeldt and Hrazdina, 1978). Hoshino and Matsumoto, (1980) observed the appearance of blue pigment floccules approximately 60 minutes after dissolving –3-5-cyanin diglucoside chloride in an aqueous solution. By following the conformational changes of the cyanin quinonoidal base by circular dichroism, Hoshino and Matsumoto, (1980) were able to conclude that the blue pigment precipitate was due to highly self-associated aggregates of the cyanin quinonoidal base. They postulated that the mechanism of self-association involved hydrophobic interactions between the aromatic nuclei of the anthocyanin, with the hydrophilic glucose substituent surrounding it in an appropriate spatial arrangement.

Results from visible absorption spectroscopy, circular dichroism and NMR studies of the diglucosides have suggested that the interactions involved overlap of aromatic π electrons and hydrophobic effects of the vertically stacked molecules. This has been suggested in preference to a hydrogen bonding mechanism as studies involving hirsutin (7-*O*-methylmalvin) quinonoidal base, which does not posses a phenolic hydroxy group necessary for H-bonding, still showed self-association (Hoshino et al., 1981). NMR studies have provided evidence of vertical stacking of the anthocyanins. It was shown that with increasing anthocyanin concentration the aromatic proton resonances all shifted to higher fields, a consequence of diamagnetic anisotropy caused by ring currents in neighbouring aromatic molecules (Hoshino, 1982). Nuclear Overhauser effect (NOE) NMR data has suggested that the anthocyanins do not have a superimposed stacking structure but instead exhibit a slight anticlockwise rotation (Figure 1.5) (Hoshino, 1991).

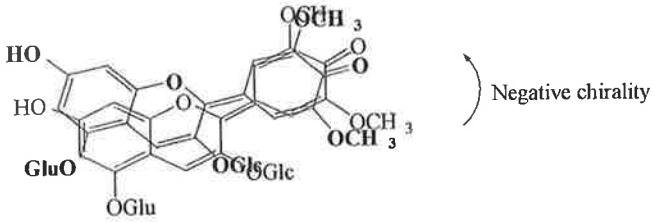

Figure 1.5 Self-association of the quinonoidal base of malvin-3,5-diglucoside (Hoshino, 1991).

Crystal structure analysis of malonylawobanin and flavocommelin, present in the flower petals of *Commelina communis*, have shown that they stack face to face in a cross-parallel arrangement (Kondo et al., 1992).

Hoshino et al., (1981) did not observe self association in the CD spectra of the monoglucoside anthocyanins and it was concluded that the monoglucosides are not significantly involved in self-association In contrast to the CD investigations the non-linear increase in the UV/visible spectral absorbance of malvidin-3-monoglucoside with increasing concentration indicated self aggregation (Asen et al., 1972;Timberlake, 1980). There have been no published studies investigating the self-association of the acylated anthocyanins.

1.4.4 Intramolecular copigmentation

Intramolecular copigmentation involves interaction between an aromatic pigment moiety and a copigment which are part of the same molecule. Acylation of the glucose substituent on the anthocyanin may impart colour stability through intramolecular copigmentation. This phenomena was initially observed in blue flowers which exhibited unusually stable colour, for example the Chinese bell flower, *Platycodon grandiflorum* (Saito et al., 1971) and the flowers of *Tradescantia reflexa* (Yoshitama, 1978). The anthocyanins present in these flowers were shown to be involved in stabilisation of the pigment as the removal of the acylating moiety on the glucose substituent on the anthocyanin resulted in anthocyanin decomposition.

This was further supported by the observation of the stability of the 'heavenly blue anthocyanin' from *Ipomoea purpurea* (Goto et al., 1986;Goto, 1987). The structure of the 'heavenly blue anthocyanin' (paeonidin-3-sophoroside-5-glucoside substituted with three caffeyl glucose residues) is shown in Figure 1.6.

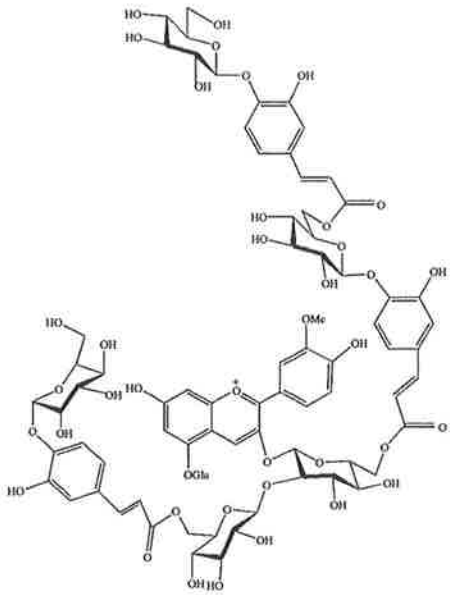

Figure 1.6 Structure of the 'Heavenly Blue Anthocyanin'.

Stability of the flavylium ion and quinonoidal base forms at plant pH was thought to be achieved through aromatic π electron interactions brought about via the intramolecular stacking of two of the caffeyl ester groups over the anthocyanin base structure (Figure 1.7). This arrangement is thought to prevent or inhibit the reaction of water with the carbons at C-2 and C-4, which would otherwise lead to the formation of the colourless hemiketal and chalcone forms.

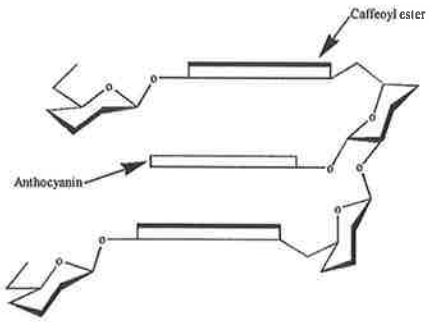

Figure 1.7 Intramolecular stacking through aromatic π electron interactions (Brouillard, 1981).

The exceptional colour stability of *Zebrina pendula* anthocyanin in the absence of copigments and metal ions also highlighted the phenomena of intramolecular copigmentation (Brouillard, 1981). A similar explanation has been suggested for the stability of delphinidin-3,3',5'-

triglucoside based blue ternatins present in the butterfly pea flower, *Clitoria ternatea* (Terahara et al., 1990).

1.5 **Factors influencing copigmentation**

1.5.1 Introduction

Copigmentation is dependent on many variables and each must be considered if an understanding of the mechanisms and importance of copigmentation is to be appreciated.

Research into flower colour has shown that the absorption spectra of most flowers can be mimicked in the laboratory by manipulation of pH, anthocyanin concentration and the molar ratio of anthocyanin to copigment (Asen et al., 1972). It should be noted however that in the case of flowers, chlorophyll or carotenoids, structural differences and interaction with other molecules present within the plant tissue may also influence colour expression. Investigations into the influence of factors influencing copigmentation have generally involved model aqueous systems. While this is not an ideal mimic of a red wine, it does provide an insight into the general chemical requirements needed for optimal copigmentation to occur.

Early studies into copigmentation between chlorogenic acid and malvin-3,5-diglucoside by Brouillard et al., (1989) gave the first theoretical and mechanistic insight as to the variables affecting copigmentation. Using UV/visible spectroscopy Brouillard et al., (1990) were able to extend the observations made by Timberlake and Bridle, (1976) to obtain stability and thermodynamic parameters associated with copigmentation.

The equilibrium reactions of intermolecular copigmentation involve the flavylium ion or neutral quinonoidal base of the anthocyanin (Equation 1.1).

1	$AH^+ \leftrightarrow (B + C_E) + H^+$	K_H
2	$AH^+ \leftrightarrow A + H^+$	K_a
3	$AH^+ + nCP \leftrightarrow AH(CP)^+_n$	K_1
4	$A + nCP \leftrightarrow A(CP)_n$	K_2

Equation 1.1 The copigment complex equilibrium profile (from Brouillard et al., 1989) where AH^+ is the flavylium ion, B is the hemiketal, C_E is the chalcone, A is the quinonoidal base and CP is the copigment.

A copigment may react directly with the flavylium ion form pushing the K_H equilibrium to the left-hand side (1, Equation 1.1). An increase in the flavylium ion concentration, in turn, leads to an increase in the quinonoidal base form (2, Equation 1.1) (Brouillard et al., 1991).

Values for K_1 and K_2 can be determined from the equilibrium concentrations of each species. These concentrations are derived from the absorbance values according to equations formulated from (a) the classical Benesi-Hildebrand equation (Equation 1.2) or (b) the mathematical model developed by Brouillard et al., (Equation 1.3) (Brouillard et al., 1989).

$$\text{(a)}\quad \frac{[CP]}{\varepsilon_{obs}-\varepsilon_O}=\frac{1}{\Delta\varepsilon K_1 K_2}-\frac{[CP]}{\Delta\varepsilon} \qquad \textbf{Equation 1.2}$$

where $\varepsilon_{obs} = A/C_o$ is the ratio of the measured absorbance divided by the concentration of the anthocyanin species(which is maintained constant), ε_o the molar absorption coefficient of the free anthocyanin, $\Delta\varepsilon$ the difference between the molar absorption coefficients of the free anthocyanin and its adduct, K_1 or K2 the association constant and [CP] the variable concentration of the copigment (in large excess).

or

$$\text{(b)}\quad \ln\left(\frac{A-A_O}{A_O}\right)=\ln\left(K_1\frac{\varepsilon_{AH(CP)_n+}}{\varepsilon_{AH+}}\right)+n\ln[CP] \qquad \textbf{Equation 1.3}$$

where A is the absorbance upon the addition of the copigment of concentration [CP], A_o the absorbance in the absence of copigment, $\varepsilon_{1,2}$ and ε_{AH+} the molar absorption coefficients for the adduct and the flavylium cation respectively.

Each equation has its specific limitations. The Benesi-Hildebrand equation must have constant ionic strength throughout. This is achieved by the addition of neutral anions. This limits its usefulness when investigating solvent and salt effects. On the other hand the equation used by Brouillard et al., (1989) implies some previous knowledge of the molar extinction coefficients of the individual species, which in some instances proves difficult.

1.5.2 Impact of anthocyanin structure

The ability of an anthocyanin to be involved in copigmentation is very much dependent on its chemical structure (Brouillard et al., 1989). Increased colour expression due to copigmentation increases with increasing methoxylation and glycosylation of the anthocyanin.

Analysis of the red-purple flowers of *Pharbitis nil* highlighted the effect of acylation of the glucose substituent on the anthocyanin on copigmentation (Dangles et al., 1993;Lu et al., 1992). It was observed that the most stable anthocyanins were those that had the larger number of caffeic acid residues on the pelargonidin glycoside. This stabilisation was attributed to increased intramolecular sandwich-like aromatic π electron stacking interactions.

The colour stability of the blue-purple flowers of *Eichhornia crassipes* may be attributed to substitution of the anthocyanin. The anthocyanins present in this flower are based on delphinidin but with different degrees of glycosylation and acylation. The investigation showed that as glycosylation increased so to did the molar extinction coefficient (ε) of the flavylium ion (Figueiredo et al., 1996).

When an anthocyanin has only a glucose substituent, dimers are formed between the anthocyanin and copigment. This may be attributed to steric hindrance preventing a second copigment molecule getting within an interaction distance of the anthocyanin chromophore.

1.5.3 Impact of copigment structure

As mentioned previously, intermolecular copigmentation occurs via the molecular stacking of anthocyanin and copigment. A copigment which exhibits planarity is expected to be an efficient copigment as hydrophobic effects are favourable. Also, due to the electron deficiency of the anthocyanin C ring (if flavylium ion stabilisation) it would be expected that a copigment which introduces electron density into the anthocyanin would form a stronger association with the anthocyanin (Mistry et al., 1991).

Monomeric flavan-3-ols such as (+)-catechin and (-)-epicatechin are rather poor copigments due to their reduced planarity (Brouillard et al., 1991;Mistry et al., 1991). However, (-)-epicatechin is a substantially better copigment than its stereoisomer, (+)-catechin as it can assume a near planer conformation. NMR studies have shown that the catechol sub group of flavan-3-ols can exist in either a quasi-equatorial or quasi-axial conformation (Porter et al., 1986). The dominant form in (+)-catechin is the quasi-axial conformation whereas in (-)-epicatechin it is the quasi-equatorial form. The quasi-axial form does not allow for the aromatic B ring to assume a near coplanar conformation with the C ring.

Malvin-3,5-diglucoside forms intermolecular copigment dimers with quercetin (Baranac et al., 1997a), morin (Baranac et al., 1997b) and apigenin (Baranac and Petranovic, 1997). However the equilibrium constants of the three systems are quite different with the malvin-3,5-

diglucoside and morin copigment complex having the greater stability relative to the quercetin and apigenin copigment complexes. The difference in stability between the three complexes may be attributed to the number of hydroxy groups present on the copigment B ring. Since apigenin possesses only one hydroxy group in its B ring it forms the weakest interaction. The *meta* position of the hydroxyl group of the morin in contrast to the *ortho* position of the hydroxy group of the quercetin allows for more efficient interaction with the anthocyanin.

1.5.4 Influence of concentration of anthocyanin in relation to copigment

Early studies of copigmentation by Asen et al., (1972) showed that copigmentation is dependent on the anthocyanin or copigment concentration and the molar ratio of the anthocyanin to copigment. For the phenomena of copigmentation to be observed by UV/visible spectroscopy the anthocyanin concentration must be greater than 10^{-5} $molL^{-1}$ and the anthocyanin to copigment molar ratio usually lies between 1:1 and 1:100 depending on whether the copigment is strong or weak (Asen et al., 1972).

Studies of malvidin-3,5-diglucoside with various copigments highlighted the influence of the anthocyanin to copigment molar ratio towards colour expression (Asen et al., 1972;Brouillard et al., 1989;Baranac et al., 1996). For example, rutin is a stronger copigment than chlorogenic acid since it gives a greater increase in colour expression with a molar ratio of malvin-3,5-diglucoside to rutin of 1:2 (Baranac et al., 1996) whereas the molar ratio of malvin-3,5-diglucoside to chlorogenic acid is at least 1:10 (Brouillard et al., 1989).

In red wines intermolecular copigmentation is limited by the concentration of the available copigments. For a typical young red wine the molar ratio of total anthocyanins to copigments ranges, for example, from 1:0.1 for (-)-epicatechin to 1:2. for the oligomeric flavan-3-ols (expressed as monomeric flavan-3-ol equivalents) (Nagal and Wolf, 1979;Singleton, 1988). Intermolecular copigmentation at similar anthocyanin to copigment molar ratios seen in red wines showed little colour enhancement (Asen et al., 1972;Brouillard et al., 1991). Intermolecular copigmentation generally required an excess of copigment to anthocyanin for colour enhancement to be observed (Mistry et al., 1991;Mazza and Brouillard, 1990;Miniati et al., 1992;Baranac et al., 1996;Baranac et al., 1997b;Baranac et al., 1997a;Baranac and Petranovic, 1997). In general, an increase in concentration of either constituent leads to an increase in copigment complex formation, which, in turn leads to enhanced absorbance and a shift to longer wavelength absorbance maximum. However, there is a critical concentration after which colour loss is observed (Dangles and Elhajji, 1994).

1.5.5 Influence of the solvent medium on copigmentation

The efficiency of copigmentation is very much dependent on the solvent medium. Variables such as pH, nature of the solvent and temperature must be considered. The complex nature of a red wine medium means that many factors are interacting to enhance or reduce copigmentation effects.

The effects of copigmentation have been observed over the pH range of 1.5-7.0 (at pH < 1.5 only an increase in absorbance is observed) with it being at its highest in the pH range 3 to 5 (Mistry et al., 1991;Brouillard and Dangles, 1994). Copigmentation is favourable in red wines as its pH (3.5-3.6) falls within the optimal copigmentation range. Because both the anthocyanin's and copigments chemical structure and electronic distribution are influenced greatly by pH, the effect of pH on copigmentation must be considered.

Copigmentation is greatly influenced by the nature of the solvent. Water has been shown to be the best solvent for copigment complex formation (Brouillard et al., 1989). Copigmentation, though less intense, may still occur in mixed solvents as long as water remains the dominant component. It is proposed that hydrophobic effects drives the close contact between anthocyanin and copigment and hence the unique quasi-tetrahedral structure of water is important (Brouillard et al., 1989). Polarity does not appear to be an important factor for the cosolvent. Whether the solvent is protic (acetic acid, dielectric constant 6.2) or weakly protic (N-methyl-formamide, dielectric constant 182) has little effect on copigmentation (Brouillard et al., 1991). The solvents which affect copigmentation the least are those that have one or more hydroxy substituents. This is a consequence of the hydroxyl group mimicking water molecules by hydrogen bonding to their neighbouring constituents, thus preventing the break up of water structure (Brouillard et al., 1991).

When considering copigmentation in red wine, other variables such as the ionic strength, glycerol, sulphur dioxide concentration and acetaldehyde content must be considered.

The ionic composition of the medium may influence copigmentation through ion pair stabilisation (Dangles and Brouillard, 1992). The flavylium ion has a positive charge, which would require balancing with a counter anion. The dissociated cation of the flavylium ion may be preferentially solvated by water or be counteracted by a solvent anion (Dangles and Brouillard, 1992;Bolton, 2001). The quinonoidal base on the other hand is a neutral species and copigmentation would not be expected to involve electron transfer interactions.

To date, no studies have been conducted to provide an insight into the influence of sulphur dioxide and acetaldehyde, which are two important constituents present in red wines, on copigmentation.

Increasing the temperature leads to a decrease in association between the anthocyanin and copigment and hence suggests that it is an exothermic process (Brouillard et al., 1989).

1.6 Role of copigmentation in polymeric pigment formation

1.6.1 Introduction

The formation of a chemical bond between two constituents is termed a polymerisation reaction. Polymerisation in wine involves random interaction and condensation between the phenolic constituents of wine.

Due to the great diversity of polyphenolic constituents in wine capable of acting as reagents, polymerisation has the potential to produce a wide variety of polymeric pigments. These may include small molecular weight dimers and trimers up to very complex oligomers. Isolation and structural elucidation of the higher molecular weight oligomers is difficult due to their large size and complexity.

Copigmentation does not involve chemical bond formation. However, copigmentation may be considered an intermediate interaction in the polymerisation between constituents as it essentially aligns the individual constituents, in an appropriate arrangement, which may ultimately lead to the formation of a chemical bond.

1.6.2 Intermediate interactions leading to polymerisation

Interactions involving aromatic π electrons similar to those hypothesised to occur in copigmentation is observed in many types of chemical systems. The π-π aromatic interaction is essentially a result of electron donor-acceptor or charge transfer mechanism and is important in host-guest complexation chemistry. Examples include DNA base pairing and DNA-drug chelation (Askew et al., 1989;Newcomb and Gellman, 1994); the weakly polar interactions present in proteins (Burley and Petsko, 1988;Burley and Petsko, 1986), the donor-acceptor chemistry of molecular tweezers (Zimmerman et al., 1989), the self assembling mechanisms of pseudorotaxanes (Anelli et al., 1991) and the aggregation in metalloporphyrins (Abraham et al., 1976;Hunter, 1989).

An example of an energetically favourable and structure stabilising interaction but where covalent bond formation does not occur is drug interchelation into the DNA double helix. This interaction has been shown to be a result of aromatic π electron interaction between two constituents arising from attractive interactions between partial positive and negative charges on atoms in the neighbouring aromatic groups (Newcomb and Gellman, 1994). This results in a parallel stacking arrangement. Aromatic-aromatic ring interaction in proteins is generally an edge to face interaction between the fractionally positive H atom on the edge of an aromatic side chains of the amino acids phenylalanine, tyrosine or tryptophan and the fractionally negative π electron cloud of an aromatic substituent of another protein amino acid side chain and/or ligand (Burley and Petsko, 1988). This is essentially a quadrupole-quadrupole interaction and leads to stabilisation of the protein tertiary structure or ligand incorporation.

An initial non-covalent interaction followed by covalent bond formation is seen within preorganised host chemistry. Preorganisation has been hypothesised to be the central determinant of complex stability. A preorganised host-guest interaction has been defined as those that are structurally arranged for binding and low solvation prior to complexation (Cram, 1986). Examples include the molecular tweezers, which are essentially rigid aromatic systems that act as preorganised hosts for electron donor-acceptor complexation, . and the metalloporphyrin host-guest complexes (Abraham et al., 1976;Hunter, 1989).

1.6.3 Mechanisms of polymer formation in red wine

1.6.3.1 Interflavan bond formation

The mechanism of polymerisation (covalent bond formation) involves an electrophilic - nucleophilic addition reaction between an anthocyanin and non-pigmented flavonoid. As long as the constituents possess an electrophilic and/or a nucleophilic centre they may be considered available for reaction and ultimately pigment polymer formation (Figure 1.8).

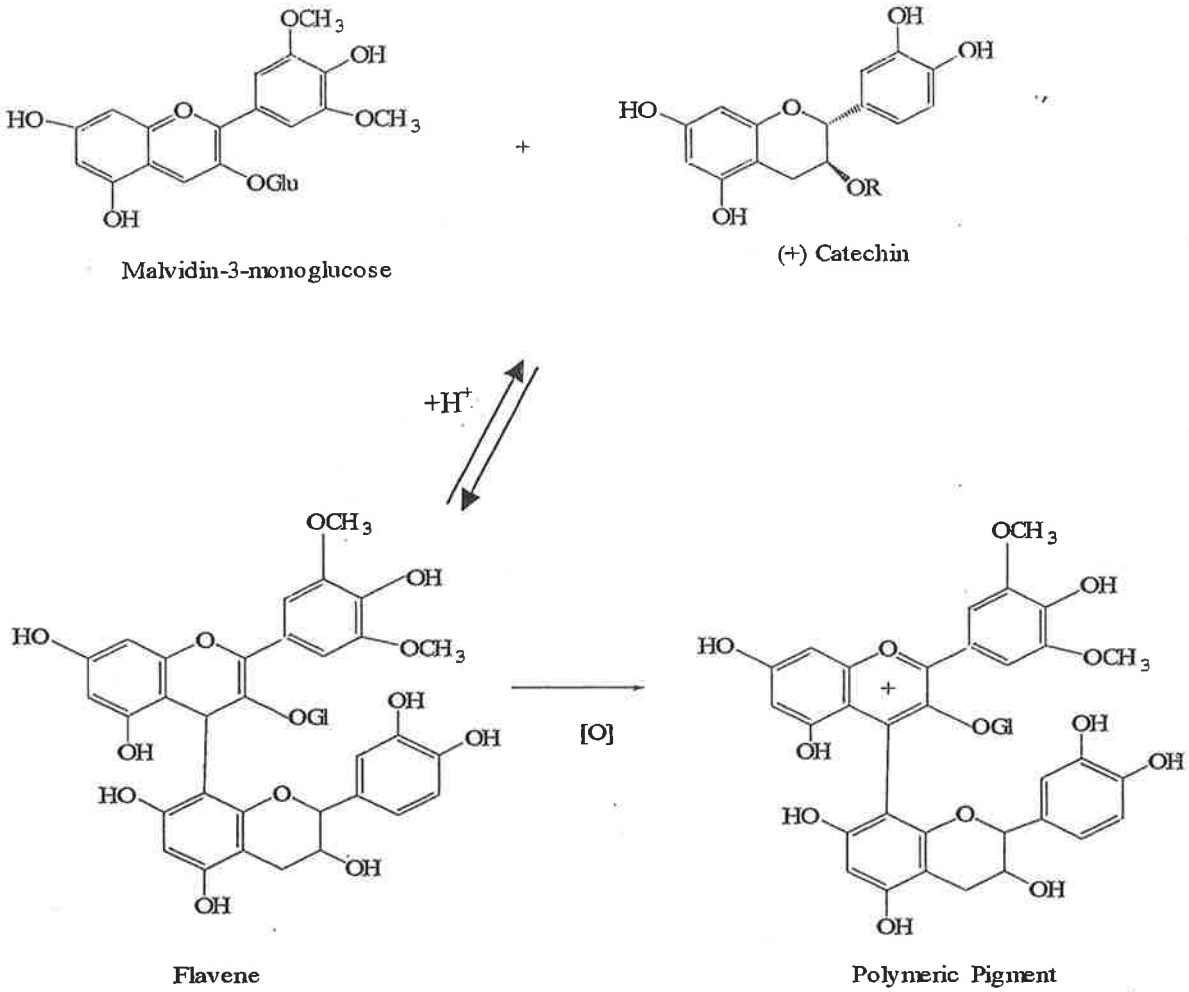

Figure 1.8 Polymeric pigment formation as proposed by Somers, (1971) with the interflavan bond formed between C4 of malvidin-3-monoglucoside and the C8 position of the flavan-3-ol.

Copigmentation may be important in the formation of interflavan covalent bonds as it electronically orientates and groups constituents together essentially preorganising the two constituents.

1.6.4 Polymeric pigments and red wine colour stability

It is thought anthocyanin incorporation into pigment polymers maintains polymer solubility by limiting the formation of the higher oligomers (Singleton and Trousdale, 1992). The formation of polymeric pigments is also considered to be beneficial to final red wine colour stability as they are resistant to the effects of changes in pH and bleaching by sulphur dioxide (Somers, 1971). Vitisins are wine pigments which evolve during wine ageing as a result of

interaction between wine anthocyanins and polyphenols. Vitisin derivatives have been successfully synthesized in the laboratory and have shown to feature more stable colours than the corresponding nonsubstituted flavylium analogs (Roehri-Stoeckel et al., 2001).

1.7 Work presented in this thesis

Previous research on copigmentation has concentrated on the chemistry of anthocyanin diglucosides and their acylated derivatives because they were more readily available. The work presented in this thesis examines the roles of malvidin-3-monoglucoside and its acylated derivative malvidin-3-(p-coumaryl)glucoside in copigmentation with various copigments found in grapes.. Flavonols and monomeric and polymeric flavan-3-ols were either obtained commercially, synthesised or extracted from grapes and used as copigments with the aforementioned anthocyanins. UV-vis spectroscopic studies of model aqueous solutions were investigated by varying temperature, pigment and copigment concentration and solvent composition. Potentiometric, NMR and coputational modelling studies were also carried out. A study investigating the copigmentation effects observed in a series of Shiraz and Pinot Noir wines is also presented.

Chapter 2

Copigmentation

2.1 Introduction

2.1.1 Intermolecular copigmentation

Phenolics extracted from red grapes during fermentation include anthocyanins, flavan-3-ols, procyanidins, as well as hydroxycinnamates and hydroxybenzoates. The anthocyanins extracted from the skin of red grapes of *V. vinifera* are all monoglucosides, of which malvidin-3-monoglucoside is the most dominant. In some cases the glucose moiety may be acylated to give malvidin-3-(*p*-coumaryl)glucoside or malvidin-3-(acetate)glucoside. At the completion of fermentation anthocyanin concentration decreases due to adsorption onto yeast, grape marc, enzymatic and non-enzymatic oxidation and as well polymeric pigment formation (Calderon et al., 1992;Dallas and Laureano, 1994;Adams, 1973). Reactions between anthocyanins and flavan-3-ols to form polymeric pigments have been verified (Liao et al., 1992;Somers and Wescombe, 1987;Timberlake and Bridles, 1979).

Copigmentation is thought to be an intermediate step in the formation of polymeric pigments through anthocyanin interaction with non-pigmented molecules (principally the flavan-3-ols). Essentially it allows for the two reactants to arrange themselves in a spatially favourable position so that a covalent bond may form between the two.

Anthocyanins and the copigments which have been studied in this investigation are shown in Figure 2.1. Monomeric flavan-3-ols (-)-epicatechin and (+)-catechin were chosen as they are principal components in red wine. Furthermore, the higher oligomeric proanthocyanidins are thought to be formed as a by product in the biosynthesis of the parent flavan-3-ols (Haslam, 1977)

The other red wine phenolic copigments included in this investigation are quercetin, quercetin-3-glucoside and caffeic acid. All are present in red wine (Singleton, 1988). By comparing data for quercetin, which has been shown to be a strong copigment (Baranac et al., 1996, 1997a), with that of quercetin-3-glucoside it was anticipated that information on the impact of the glucose group on intermolecular copigmentation would be gained.

Chlorogenic acid is a widespread, natural, colourless phenolic constituent whose intermolecular copigmentation effects have been extensively studied (Brouillard et al., 1989;Liao et al., 1992;Mazza and Brouillard, 1990;Wilska-Jezka and Korzuchowska, 1996) and was therefore included in this study to act as an internal standard.

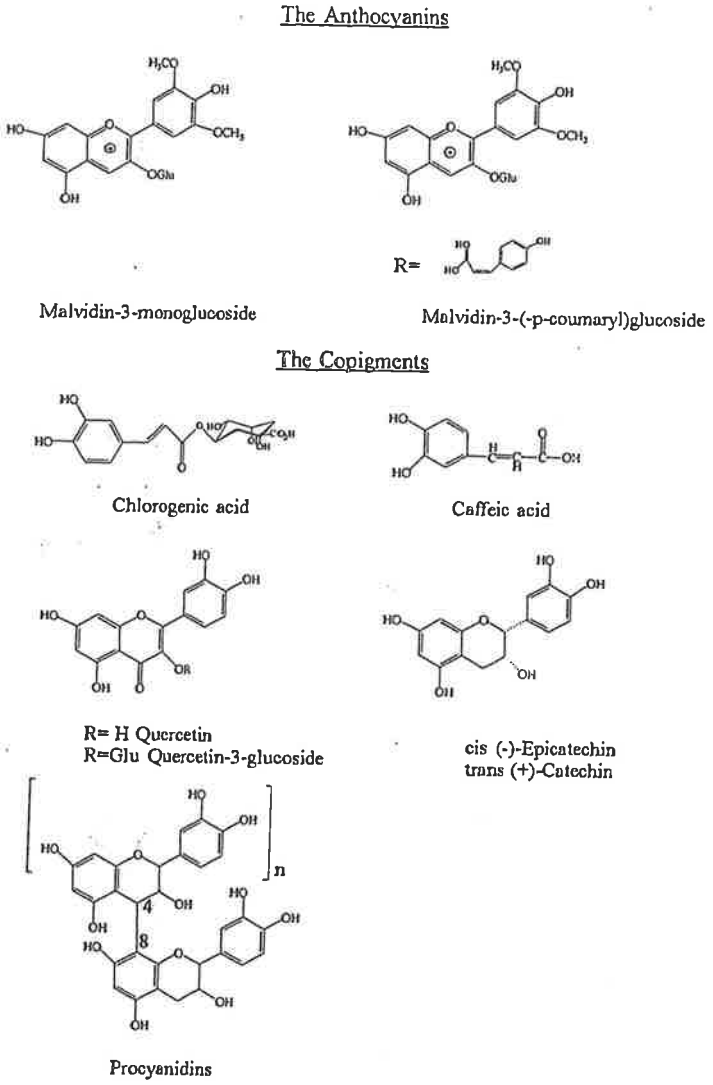

Figure 2.1 The phenolic constituents investigated in the copigmentation studies.

Model solutions were used in this study for simplicity as red wines contain a complex pool of copigments. Model solutions provide an insight into the more favourable and energetically stable chemical interactions that could be occurring between anthocyanins and copigments in

red wine. The constituents involved in intermolecular copigmentation in red wines differ as a result of regional and/or cultivar related variance. For example, in one study wines made from Pinot Noir grapes had a higher concentration of the monomeric flavan-3-ols (Goldberg et al., 1998a) compared to quercetin concentration whereas, in another study, wines made from Cabernet Sauvignon grapes contained a higher concentration of quercetin (Goldberg et al., 1998b).

2.1.2 Types of intermolecular interactions

Copigmentation was initially considered to originate from in plane hydrogen bonding between anthocyanin and copigment producing horizontal stacks (Asen et al., 1972;Chen and Hrazdina, 1981;Scheffeldt and Hrazdina, 1978). More recently vertical stacking has been proposed through π-π and/or hydrophobic interactions (Goto et al., 1979, Brouillard, 1988, Brouillard et al., 1989). Results from visible absorption spectroscopy, circular dichroism and NMR studies have suggested π-π vertical interactions (Chen and Hrazdina, 1981;Hoshino et al., 1982;Hoshino, 1991;Hoshino et al., 1981b) and subsequently adopted by other authors to explain copigmentation.

In essence π-π interaction has been used to describe the strong attractive interactions between π systems. π-π Interactions have been implicated as the driving force in governing the stabilisation and enhancement of colour observed with anthocyanin copigmentation. However it has been observed that π-π interactions rarely cause a distortion of the UV/visible spectra of two chromophores so the two interacting π systems do not distort each other molecular orbitals (Hunter and Sanders, 1990). It therefore seems a misrepresentation to justify copigmentation as a cause of simply π-π interactions without understanding the forces that drive such interactions.

The magnitude of the interaction may be driven by van der Waals forces and hydrophobic interactions , electrostatic forces and delocalisation of electrons in the molecular orbitals between the two aromatic systems (charge transfer) (Claessens and Stoddart, 1997;Dahl, 1994;Hunter and Sanders, 1990;Newcomb and Gellman, 1994;Price and Stone, 1987).

2.1.2.1 Van der Waals interactions

Van der Waals forces are the attractive interactions between closed shell molecules. They include the net attractive interactions between the partial charges of polar molecules.

Dipole-dipole interactions act between polar molecules that possess dipole moments. The interaction formed between two dipoles are maintained purely by electrostatic forces and can be explained in terms of Coulomb's law. The larger the dipole moment the greater the force. Ion-dipole interactions occur between either a cation or anion and a dipole. The strength of this interaction is directly proportional to the charge and size of the ion and the magnitude of the dipole.

A dipole moment may be induced in a nonpolar (or neutral) atom (or molecule) by the close proximity of an ion or a polar molecule. The force extorted by the ion or the polar molecule distorts the electron distribution of the neutral atom. The ease with which a dipole moment can be induced depends not only on the strength of the dipole but also on the polarizability of the neutral atom. In general, the larger the number of electrons and the more diffuse the electron cloud the greater the polarizability. The attractive forces that arise as a result of temporary induced dipoles may be quite weak

2.1.2.2 Hydrophobic interactions

Hydrophobic interactions are thought to result from positive attraction between two non polar molecules by van der Waals dispersion forces and the preference of water to interact with itself causing a net removal of water. Essentially it is a solvation effect that results in attraction between two molecules and there is increasing evidence that it is a initial principal driving force in intermolecular interaction (Haslam, 1998). Due to the dependency of the solvent composition on copigmentation it was hypothesised that hydrophobic effects direct π-π interaction (Brouillard et al., 1991b). However, Newcomb and Gellman, (1994) have suggested that π-π aromatic stacking interactions involve neither classical hydrophobic effect nor dispersion forces but simply involves attractive interactions between partial positive and negative charges on atoms in the two neighbouring aromatic rings.

2.1.2.3 Electrostatic interaction

Electrostatic interaction is the interaction between the undistorted electron clouds between two constituents. This contribution includes the interactions of all permanent charges and multipoles such as dipole-dipole and dipole-quadrupole. They have been implicated to be the major contributing factor in regard to geometrical orientation of the constituents (Williams, 1993;Pawliszyn et al., 1984;Hunter and Sanders, 1990).

2.1.2.4 Charge transfer complexes

The first type of interactions involving π orbitals of aromatic systems were observed with charge transfer complexes (Benesi and Hildebrand, 1949). Charge transfer involves molecular orbital overlap between the filled donor (π-rich) orbital (HOMO) of one molecule with the vacant acceptor (π deficient) orbital (LUMO) of the other molecule (Mulliken, 1952). In resonance terms, this type of interaction is a donor/acceptor model between the aromatic systems. Complexes may be stabilised by the cooperative forces of both n-π and π-π charge transfer (Slifkin, 1965;Okano et al., 1969).

Charge transfer complexes formed between good electron donors and good electron acceptors are characterised by either charge-transfer transitions in the UV/visible absorption spectrum or by a broadened UV/visible spectrum.

Mulliken's (1995) theory of electron delocalisation between orbitals explained many of the observed spectroscopic results involving aromatic systems (Szent-Gyorgyi, 1957). Consequently charge transfer was thought to constitute intermolecular π-π interactions and be the major driving force leading to interaction. The absence of charge transfer spectral bands in the absorbance spectra of stacked aromatic molecules contradicted this theory (Damiani et al., 1965;Damiani et al., 1967a;Damiani et al., 1967b). Subsequently the importance of charge transfer in dictating π-π interactions has been questioned (Hunter and Sanders, 1990;Dahl, 1994).

Hunter and Saunders, (1990) concluded that charge transfer transitions observed for such complexes are a consequence and not a cause of the π-π interaction and electron donor-electron acceptor complexes are simply a special case of π-π interaction. The donor-acceptor concept can be misleading when used to describe π-π interactions, as it is the properties of the atoms in the regions of intermolecular contact that control the strength and geometry of the interactions, rather than the overall molecular oxidation or reduction potential (Hunter and Sanders, 1990).

There has also been evidence that there is chiral distortion of the π electron cloud by a CH group in which an H atom is positioned above the π plane (Nishio et al., 1995). The π-CH interaction is a characteristic of delocalisation (electron transfer from π to σ*). In such an arrangement the δ^+ H is located above the δ^- π-orbital and is used to explain the edge to face

stacking of benzene dimers (Pawliszyn et al., 1984) and the aromatic side chains in proteins (Burley and Petsko, 1988).

2.1.2.5 Energetics associated with π-π interaction

The total attractive interaction is the sum of all the van der Waals contributions (only the dispersion interaction contributes if both molecules are non-polar). The strength of van der Waals interactions varies inversely with distance, so that they are significant only over a short range. In a more complete treatment the electrostatic contributions from quadrupole and higher-order multipole interactions should be considered, particularly if the molecules do not have dipole moments (Hunter and Sanders, 1990).

Van der Waals interactions are proportional to the area of the π orbital overlap. However this would lead to considerable π-π repulsion and therefore cannot be the dominating force controlling interaction. This is supported by the fact that many stacked π interacting molecules exhibit slightly offset π stacking rather than cofacial arrangement (Saenger, 1984;Hoshino, 1992;Hoshino et al., 1982;Hoshino et al., 1981a;Kondo et al., 1992). Hence there must be a large electrostatic barrier to π overlap which dominates the geometry of interaction (Hunter and Sanders, 1990).

The weakly bound dimers of benzene and s-tetrazine have provided insight into the dependence of intermolecular energies on conformational orientation (Pawliszyn et al., 1984). The attractive nature of the van der Waals interaction between two benzene rings would favour a face to face geometry. However this effect is small compared to the quadrupole-quadrupole repulsive electrostatic interaction. The electrostatic interaction of the homodimers in the stacked structure would be repulsive due to the approach of negative lobes in the case of benzene and positive lobes in the case of s-tetrazine. Face to face (parallel stacking) is one geometrical conformational on the multidimensional potential energy surface but does not generally represent local minima. In contrast, the opposite signs of the quadrupole moments of the two monomers leads to a stable face to face stacked structure of the benzene-s-tetrazine dimer.

Other researches have supported the view that aromatic-aromatic attraction arises from partial charges attributed to Coulombic interaction or multipole-multipole interactions (Hunter, 1993;Karlström et al., 1983;Hunter and Sanders, 1990).

Hunter and Saunders, (1990) recently presented a new model to describe intermolecular interactions associated with π electrons. A simple model of a π-system consists of a positively charged σ-framework sandwiched between two negatively charged π electron clouds. They go on further to conclude that π-π interactions are not due to an attractive electronic interaction between the two π systems but occur when the attractive interactions between π electrons and the σ framework outweigh unfavourable contributions such as π electron repulsion.

The attractive forces keeping two aromatic molecules together have strong geometrical requirements and appear to be driven principally by electrostatic forces between the two π conjugated systems. However, the energetics associated with the association comes from other factors and hence the electrostatic geometrical requirement may be outweighed by other energetic factors. For example, molecules that contain highly polarisable atoms or that have large steric constraints may be influenced more by van der Waals interactions.

In essence the geometries of π-π interactions are controlled by electrostatic interactions but the major energetic contribution comes from other factors and the total energy of interaction between two aromatic π-systems can be represented as:

$E_{Total} = E_{Electrostatic} + E_{Induction} + E_{Dispersion} + E_{Repulsion}$ (Buckingham, 1978;Hunter and Sanders, 1990).

2.1.2.6 Geometrical requirements of π-π interactions –a set of rules

Taking into account the energetics of π-π interactions Hunter and Sanders, (1990) have introduced some general rules for π-π interactions (Figure 2.2).

(i) π-π repulsion dominates in a face to face π stacked geometry. This type of stacking is unfavourable and not observed

(ii) π-σ attraction dominates in an edge or T-shaped geometry. This type of stacking is favourable and observed

(iii) π-σ attraction dominates in an offset π-stacked geometry. This type of stacking is favourable and observed

(iv) for interactions between highly charged atoms, charge-charge interactions dominate

(v) A favourable interaction with a neutral or weakly polarised site requires the following π polarisation (a) π deficient atom in a face to face geometry (b) π deficient atom in the vertical T group in the edge on geometry (c) π rich atom in the horizontal T group

(vi) Favourable interaction with a neutral or weakly polarised site requires the following σ polarisation (a) positively charged atom in the face to face geometry; (b) positively charged atom in the vertical T group; (c) negatively charged atom in the horizontal T group

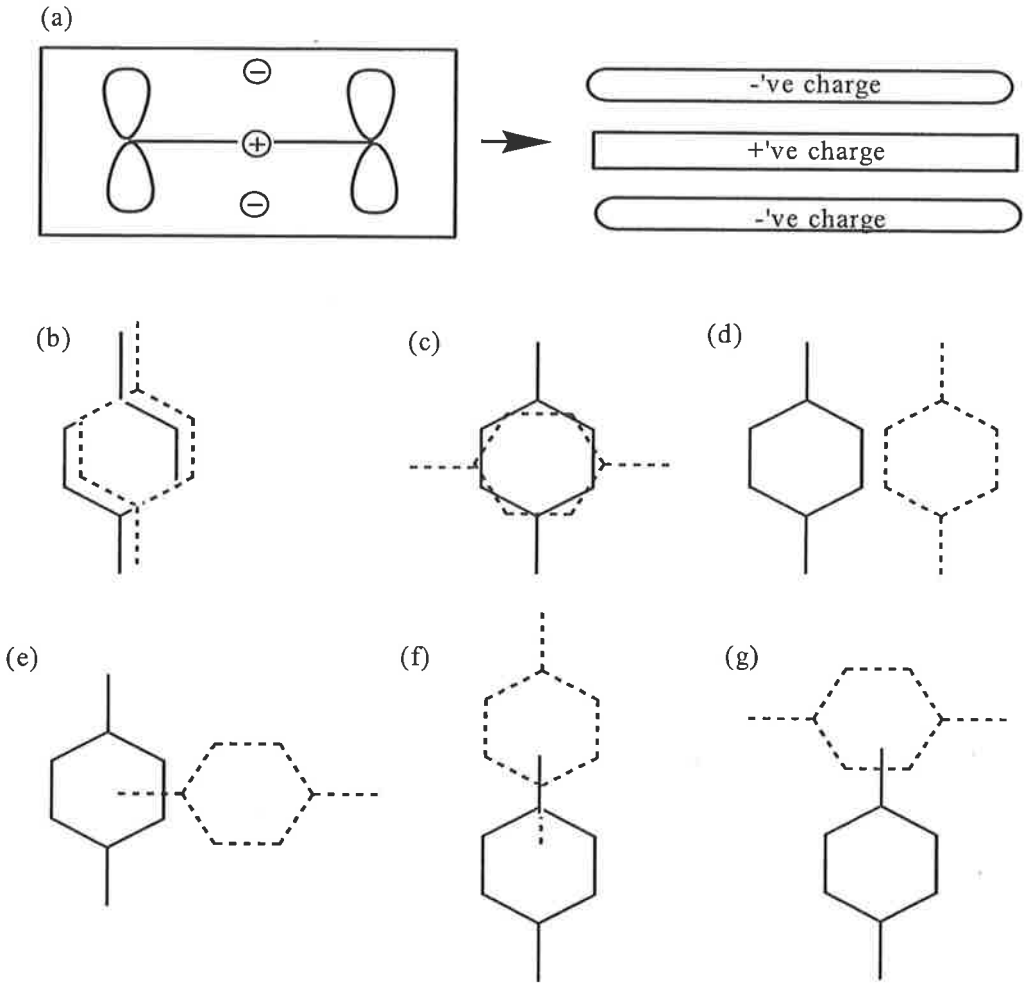

Figure 2.2 Possible interactions between π aromatic systems (Hunter and Sanders, 1990). (a) A simple model of a π-system consisting of a positively charged σ-framework sandwich between two negatively charged π electron clouds (b) face to face orientation (c) aoffset face to face orientation (d) edge to edge orientation and (e)-(g) T-shaped orientation.

The presence of strongly polarising atoms has a major influence on the electrostatic interactions and may in fact lead to face to face stacking (Price and Stone, 1987). In a face to face interaction an atom which is π deficient stabilises the interaction by decreasing the π repulsion, while a π rich atom destabilises the interaction further. Hence interaction between two π deficient (acceptor) atoms can be more favourable. If a face to face geometry is not significantly stabilised by the effects of polarisation then an offset π stacked geometry will be preferred as in the case of the double helical DNA (Saenger, 1984).

Investigations into π-π interactions between aromatic amino acids with riboflavin (Wright and McCormick, 1964) and more recently m^7GDP (Hsu et al., 2000) indicate that formation of a charge transfer complex coincides with tight face to face stacking. All crystals of 1:1 charge transfer complexes are formed from approximately plane to plane stacks of alternate donor-acceptor molecules so to maximise dispersion forces between planar molecules having delocalised π-electron systems (Haslam, 1998).

2.1.2.7 Anthocyanin copigmentation chemistry

Stacking of anthocyanins involved in self-association or intermolecular copigmentation is most likely due to a combination of hydrophobic, electrostatic and van der Waals forces between the aromatic rings present in anthocyanins and copigments. Factors that may influence the energetics of interaction may include the polarizability of the aromatic rings, steric constraints and substitution pattern of both anthocyanins and copigments.

Offset face to face stacking has been observed in anthocyanin 3,5 diglucosides aggregates (Hoshino et al., 1981a;Hoshino et al., 1982;Hoshino, 1992). This stacking arrangement is supported by the rules that govern the geometrical orientation as outlined by Hunter and Sanders, (1990).

It may be anticipated that a face to face geometry would be preferred between an electron deficient anthocyanin (flavylium ion) and a copigment. This type of interaction would lead to delocalisation of electrons between the π clouds of the molecules. However, it has been suggested that actual electron donation from the copigment may not occur. An electron rich copigment may specifically interact with the delocalised positive charge though simple Coulombic interactions (Hsu et al., 2000). In both cases, charge transfer complexes would be expected to form, which would be recognisable in the UV/visible spectrum.

If in fact it is the neutral quinonoidal base that is involved in copigmentation with copigments, the mode of π-π interaction may be quite different. When considering interactions between anthocyanins and copigments, the effects of steric constraints must also be taken into account.

While there is no doubt that intermolecular interaction occurs between anthocyanins and copigments it seems misleading to simply state them as due to π-π interactions. Interaction between π conjugated aromatic systems is in fact more complicated than first thought. It

seems nonsensical to explain copigmentation and the corresponding observed colour enhancement simply as a result of π-π interactions. In general, the formation of copigment complexes does not result in the presence of new significant spectral bands in the UV/visible spectrum. Anthocyanin copigmentation chemistry needs to be readdressed in light of the new physical models proposed for the nature of stacking interactions.

2.1.3 Use of ultraviolet/visible absorption to detect copigmentation

The absorption of ultraviolet radiation by a molecular species M involves a two step process. Upon radiation with a photon, M undergoes electronic excitation giving species M*. Relaxation processes cause the excited species M* to have a brief lifetime of about 10^{-8} to 10^{-9} s (Equation 2.1).

$$M + h\nu \rightarrow M^*$$

$$M^* \rightarrow M + \text{energy}$$

Equation 2.1 The absorption of ultraviolet radiation.

Wavelengths of absorption peaks can be related to the types of bonds that exist in the species under study as absorption of ultraviolet radiation generally results from excitation of bonding electrons (Skoog et al., 1998). Organic molecules such as anthocyanins may exhibit electronic transitions involving π, σ or non-bonding electrons (n). The spectral region (200-700nm) corresponds to transitions between n and π electrons and the π* excited state. Both transitions require the presence of π orbitals. In anthocyanins, these π orbitals are present in the form of benzene or dihydropyran rings. Generally, molar absorptivities for n to π* transitions are lower than the π to π* transitions.

Each functional group has a characteristic absorption maximum, λ_{max}(nm). Solvent effects and the degree of conjugation within the molecule may change λ_{max}. Delocalisation of the π-orbitals over four (or more) atomic centres causes a lowering of the energy levels of the π* orbitals, and absorption maxima are shifted to longer wavelengths. Hence, an increase in conjugation results in a shift to longer wavelengths.

Using UV/visible spectroscopy it was possible for Brouillard et al., (1990) to extend the observations made by Timberlake and Bridle, (1976) to obtain thermodynamic parameters associated with copigmentation. Measuring a sequence of absorption spectra with increasing copigment concentration and constant anthocyanin concentration gives a measure of the

ground state copigment-anthocyanin complex stability. As copigment concentration increases copigment-anthocyanin complex formation is also expected to increase with a corresponding increase in absorption.

To compare the effectiveness of various copigments accurate equilibrium stability constants (K) for copigment complex formation must be obtained. Anthocyanins are involved in complex equilibrium reactions (Equation 2.2, also presented in Chapter 1).

1	$AH^+ \leftrightarrow (B+C_E) + H^+$	K_h
2	$AH^+ \leftrightarrow A + H^+$	K_a
3	$AH^+ + nCP \leftrightarrow AH(CP)^+_n$	K_1
4	$A + nCP \leftrightarrow A(CP)_n$	K_2

Equation 2.2 Equilibria associated with the anthocyanins and formation of copigment complex where AH^+ is the flavylium ion, B is the hemiketal, C_E is the chalcone, A is the quinonoidal base of the anthocyanin and CP is the copigment.

It must be noted that an interaction that shifts equilibrium 3 towards product formation promotes further reactant (ie AH^+) formation via anthocyanin equilibria. The equation developed by Brouillard et al., (1989) calculates K_1, the stability constant, of the flavylium ion (the red form of the anthocyanin) and copigment complex (Equation 2.3).

$$\ln\left(\frac{A - A_O}{A_O}\right) = \ln\left(K_1 \frac{\varepsilon_{AH(CP)_n+}}{\varepsilon_{AH+}}\right) + n\ln[CP]$$

Equation 2.3 Formula relating copigment concentration and the change in absorbance of the anthocyanin to derive the stability constant of the copigment complex. Where A is the absorbance upon the addition of the copigment of concentration [CP], A_0 the absorbance in the absence of copigment, $\varepsilon_{AH(CP)}$ and ε_{AH+} the molar absorption coefficients for the complex and the flavylium ion respectively.

The temperature dependence of intermolecular copigmentation provides a means of calculating the enthalpy (ΔH) of the system via the van't Hoff equation : $d\ln K/dT = \Delta H/RT^2$.

Consequently, the Gibbs free energy (ΔG) and the entropy (ΔS) of the reaction may be derived so that a thermodynamic profile of individual intermolecular copigmentation may be obtained (Equation 2.4).

$$\Delta G = \Delta H - T\Delta S$$

$$\Delta G = -RT\ln K \text{ or } \ln K = -\Delta G/RT$$

Equation 2.4 The relation of Gibbs free energy with temperature, enthalpy, entropy and equilibrium constant. Where ΔG is the Gibbs free energy (kJ mol^{-1}), ΔH is the enthalpy(kJ mol^{-1}), T is the temperature in Kelvin, ΔS is the entropy(J K^{-1} mol^{-1}) and K is the equilibrium constant(mol^{-1} L).

The aim of this study is to use the methods developed by Brouillard et al., (1990) to determine the thermodynamic parameters of association between copigments and malvidin-3-monoglucoside and malvidin-3-(*p*-coumaryl)glucoside.

2.2 Materials and methods

2.2.1 Extraction, isolation and quantification of malvidin-3-monoglucoside and malvidin-3-(*p*-coumaryl)glucoside

Malvidin-3-monoglucoside and its *p*-coumarate ester were extracted and isolated from Shiraz grapes according to the methods of Willstätter and Zollinger, (1916) and Levy and Robinson, (1931). Differential partitioning of malvidin-3-monoglucoside against the other anthocyanins found in red grapes occurred upon washing grape skins with isoamyl alcohol at different pH. Preferential isolation of the malvidin-3-(*p*-coumaryl)glucoside was achieved through re-extraction of the isoamyl alcohol extract with a 1% sulphur dioxide solution. Precipitation and crystallisation was achieved with an ether/methanol solvent system (Asenstorfer, 2001). High Performance Liquid Chromatography was used to determine purity. The anthocyanins were stored as methanolic solutions in the freezer.

2.2.1.1 Determination of anthocyanin purity by HPLC

A Hewlett Packard series 1100 HPLC instrument fitted with a diode array detector was used with a reverse phase C-18 PLRP 5µm 100A° (Polymer laboratories) column equipped with a guard column of the same material. The solvent system was composed of water acidified with orthophosphoric acid (1.5% v/v) (buffer A) and 20% of buffer A in acetonitrile (buffer B).

The anthocyanins were eluted under the following conditions: 1mL/min flow rate (30°C), elution with linear gradients 8% to 27% B in 55 minutes, isocratic to 59 minutes then from 27% to 52% B to 64 minutes then isocratic at 52% B for 5 minutes followed by washing and reconditioning of the column. Detection was performed at 280nm and 520nm. An example of a chromatogram is shown in Figure 2.3.

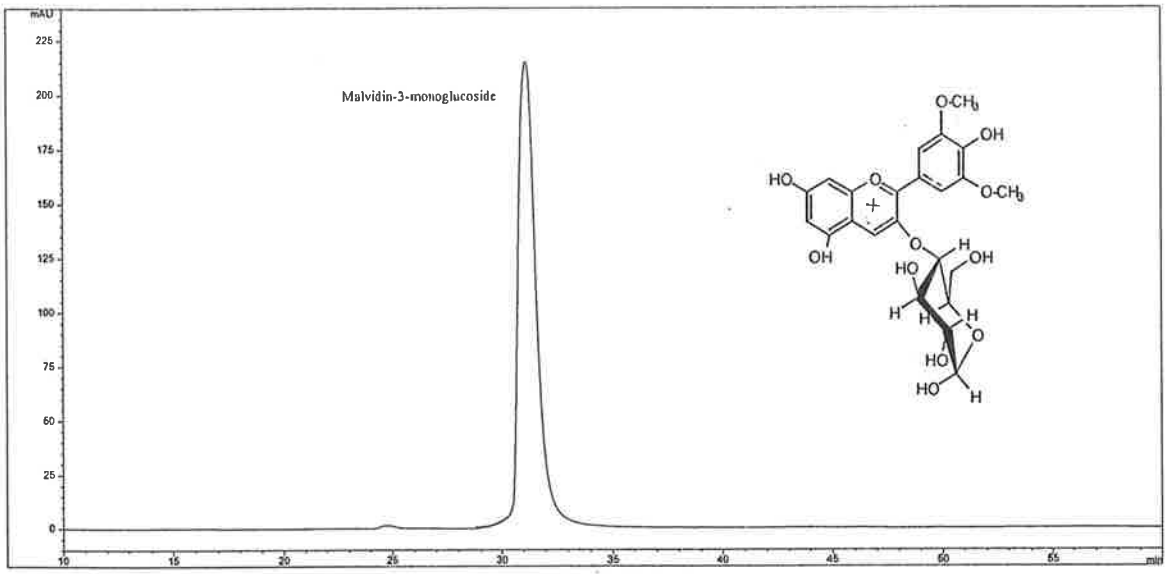

Figure 2.3 HPLC chromatogram of malvidin-3-monoglucoside isolated from Shiraz grape berries.

The peak with a retention time of 31.5 minutes was associated with malvidin-3-monoglucoside. The percentage purity of the anthocyanin was calculated by integration of the peak areas and only samples of greater than 95% purity were used.

2.2.2 Extraction, isolation and quantification of grape tannins

Two types of grape tannins were used:

(i) seed tannin extracted from seeds of Semillon grapes harvested at commercial ripeness (termed 'seed tannin (harvest)')

(ii) seed tannin extracted from seeds of Shiraz grapes at a vine development stage of 1 week after fruit set (termed 'post set seed tannin')

The method used for extraction, isolation and quantification of each seed tannin was similar except that ethanol was used as the extracting solution for seed tannin (harvest) whereas aqueous acetone was used for the post set seed tannin.

Seeds were manually separated from the skins and pulp of the grapes under a carbon dioxide atmosphere. A 50g sample of seeds was homogenised in a high-speed homogeniser (Ultra-turrax) with approximately 140mL of 70% (v/v) aqueous ethanol and extracted with shaking for one hour. The slurry was centrifuged (6,000 rpm, 30 min) and the supernatant and the precipitate separated. The precipitate was re-extracted with ethanol for thirty minutes and the supernatant's pooled. Solvent was removed under reduced pressure by rotary evaporation (35^{o}C) to give a concentrated solution of seed extract.

Condensed seed tannin was isolated according to a method developed by Kantz and Singleton, (1990). Sephadex LH-20 (Simga-Aldrich, preswollen in 50% methanol) was slurry packed into a glass column (3 x 22 cm) and equilibrated with milliQ water. All solvents contained 0.2% acetic acid. The ethanol extract was loaded on to the column with a flow rate of approximately 1.0 mL/min. Non-polymeric phenolics were removed by elution with 15 void volumes (approx. 1500mL) of 60% methanol. The polymeric fraction was then subsequently eluted with 10 void volumes of 50% acetone to give a red/orange solution. The solvent was removed under reduced pressure by rotary evaporation (35°C) to give a sticky residue. Purification of the residue was achieved by dissolving the isolate in a solution of ethyl acetate/ethanol with the addition of Na_2SO_4 to remove any residual water. After 24 hours the solvent was removed under reduced pressure to yield a buff coloured powder (0.36g). The powder was then freeze dried to remove any residual solvent and the purified product was then stored under P_2O_5 in the freezer.

2.2.2.1 Analysis of the seed tannin extract by Thin Layer Chromatography

The seed tannin extract was analysed using a method developed by Lea et al., (1979) with slight modifications. Spots were applied to silica gel 60 F_{254} plates (Merck and Co) containing a fluorescent indicator. The plates were developed with toluene:acetone:acetic acid (3:6:1). After drying the plates the compounds were observed under UV light which were revealed as dark spots on a green background. Exposure to daylight over several days resulted in the formation of dark brown spots on the plate. The Rf values for the compounds detected were (+)-catechin 0.71, (-)-epicatechin 0.67, (-)-epicatechin gallate 0.64 and seed tannin 0.21.

2.2.2.2 Purity of the seed tannin extract assessed by HPLC.

The column used in this analysis was a Merck LiChrospher reverse phase C-18 column (particle size 5µm, 250 x4 mm) protected by a guard column of the same material. The solvent system for the analysis of seed tannin was water acidified with orthophosphoric acid (0.2% v/v) (buffer A) and 20% buffer A in acetonitrile (buffer B).

The elution scheme for the seed tannin used a flow rate of 1mL/min (25°C) with a linear gradient of 0 to 15% B in 15 minutes, 15% to 16% B to 40 minutes, 16% to 25% B to 45 minutes, isocratic to 48 minutes then from 25% to 60% B to 50 minutes, 60% to 100% to 55

minutes, then isocratic for 5 minutes followed by washing and reconditioning of the column. Detection was made at 280nm. An example of a chromatogram is shown in Figure 2.4.

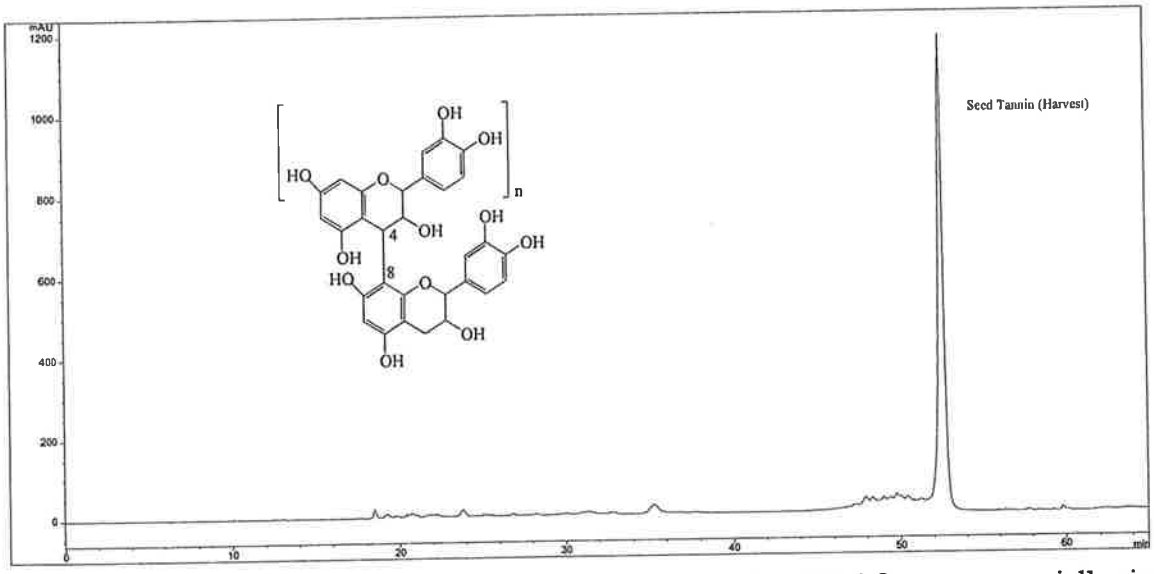

Figure 2.4 HPLC chromatogram of seed tannin extracted with ethanol from commercially ripe Semillon grapes.

Integration of the peak indicated that the extract contained greater than 95% tannin material.

2.2.2.3 Acid catalysis of the seed tannin in the presence of phloroglucinol

The subunit composition of the seed tannin extract was determined by the method developed by Kennedy and Jones, (2000). A solution was prepared in methanol that contained seed extract at a concentration of $5gL^{-1}$ with $50gL^{-1}$ phloroglucinol and $10gL^{-1}$ ascorbic acid and $0.1molL^{-1}$ HCl. This solution was placed in a water bath at 50°C and after 20 minutes the reaction was ceased by a five fold (v/v) addition of 4×10^{-3} $molL^{-1}$ aqueous sodium acetate.

2.2.2.3.1 Analysis of the reaction products produced from acid catalysis of the seed tannin by HPLC

A Merck LiChrospher reverse phase C-18 column (particle size 5µm, 250 x4 mm) with a guard column of the same material was used. The solvent system comprised 1% v/v aqueous acetic acid (buffer A) and methanol (buffer B). The elution scheme for the proanthocyanin products involved a flow rate of 1mL/min with a binary gradient of 5% B for 10 minutes, a linear gradient from 5 to 20% B in 20 minutes, a linear gradient from 20 to 40% B in 25 minutes. The column was then washed with 90% B for 10 minutes and then re-equilibrated with 5% B for 5 minutes (Kennedy and Jones, 2000).

Using the corrected relative mass response values calculated by Kennedy and Jones, (2000) the composition (in mgL^{-1}) of flavan-3-ol monomers and the phloroglucinol adducts in the seed tannin extract could be determined from which the proportional molar composition was obtained (Table 2.1).

Table 2.1 Summary of Semillon seed tannin (harvest) proanthocyanins following acid-catalysis in the presence of phloroglucinol with added ascorbic acid.

Compound	*Identification*	*Proportional composition (mole %)*
2	(-)-epicatechin-(4β→2)-phloroglucinol	29.2
3	(+)-catechin-(4β→2)-phloroglucinol	4.0
4	(-)-epicatechin-3-O-gallate-(4β→2)-phloroglucinol	39.9
5	(-)-epicatechin	2.4
6	(+)-catechin	9.2
7	(-)-epicatechin-3-O-gallate	15.2

The apparent mean degree of polymerisation (mDP) of 5.5 was calculated by dividing the molar sum of all subunits of the flavan-3-ol monomer and phloroglucinol adducts by the molar sum of all flavan-3-ol monomers. The sum of all the reaction products divided by the weight of the seed tannin gave a value of the conversion yield for the reaction; this was 73%. The 'post set seed' tannin sample gave a mDP of 4.8 and a conversion yield of 87%. The proportional composition of the proanthocyanins were similar to the seed tannin (harvest) except that there was more (-)-epicatechin-(4β→2)-phloroglucinol relative to (-)-epicatechin-3-O-gallate-(4β→2)-phloroglucinol.

2.2.3 Synthesis of procyanidin dimer B3

The procyanidin B3 dimer was synthesised according to a modified method of Eastmond (1974). The synthesis involved the formation of the flavan-3,4-diol from (±)-taxifolin (purchased from ICN) with $NaBH_4$. The flavan-3,4-diol was then reacted with (+)-catechin to give a mixture of procyanidins (Figure 2.5).

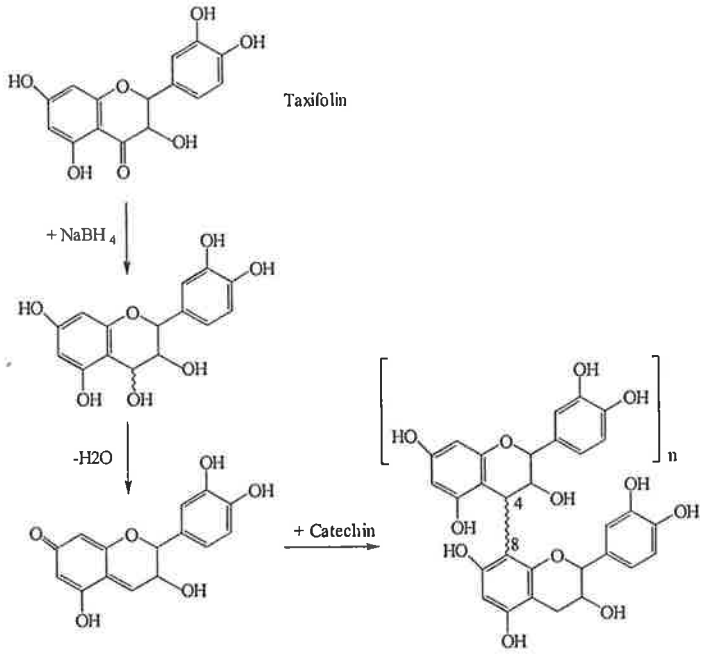

Figure 2.5 Reaction scheme for procyanidin dimer synthesis

Taxifolin (0.25g) and (+) catechin (0.25g) were dissolved in ethanol (10mL) with stirring (40°C) under an atmosphere of N_2. Sodium borohydride (0.2g) in ethanol (10mL) was added over 30 minutes. When evolution of H_2 had almost ceased (~2 hours) water (50mL) was added and the solution adjusted to pH 5.0 with 10% acetic acid. The mixture was allowed to stand for 1 hour and then extracted with ethyl acetate (4 x 40mL). The combined extracts were dried with Na_2SO_4 and filtered. The solvent was evaporated under reduced pressure to give a yellow solid.

This solid was then chromatographed on a Sephadex LH 20 column using methanol as the elutant. 15mL fractions were collected and monitored by ultraviolet absorption at 280nm and by thin layer chromatography. Examination of the UV data and TLC plates showed that the reaction product was composed of five components. The fractions containing each component were bulked together and the solvent evaporated under reduced pressure leaving solid residues. The first fraction (present in tubes 16-23) consisted of degradative products of the reaction starting material. The second fraction (present in tubes 24-29) was a dull yellow powder (0.076g). The third fraction (present in tubes 30-36) was a golden yellow powder (0.055g). The fourth fraction (present in tubes 38-49) was a cream brown powder (0.043g). The final fraction (present in tubes 50+) was a dark brown powder (0.009g).

Preliminary structural analysis indicated that fractions 2 and 3 and fraction 4 were similar with the only defining factor being that of purity. TLC Rf values for each powder product in relation to that of (+)-catechin indicated procyanidin product formation. Hydrolysis of the powder products in *n*-butanol-HCl (95:5) confirmed that each product was a procyanidin (Swain and Hillis, 1959, Porter et al., 1986). The reaction involved the autoxidation of the procyanidin to the cyanidin anthocyanidin as shown in Figure 2.6. The formation of cyanidin was followed during the course of the reaction by monitoring the increase in absorbance maxima to a maximum of 550nm.

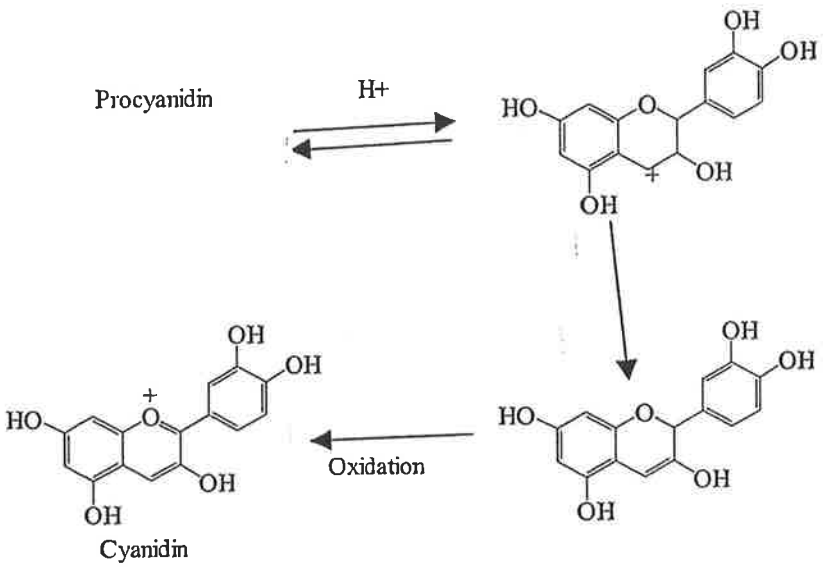

Figure 2.6 Mechanism for the conversion of procyanidin to cyanidin (Porter et al., 1986).

2.2.3.1 Mass spectrometric analysis of the procyanidin material

Analysis of the procyanidin products was performed by electrospray mass spectrometry in the positive and negative mode using an API-300 mass spectrometer with an ionspray interface (PE Sciex, Thornhill, Ontario, Canada) connected to a HPLC (LC-MS) system. The ion spray and orifice potentials were 5.5 kV and 30 V for the positive ion mode and –4.5 kV and –30 V for the negative ion mode respectively. Scans were recorded within 100 and 2500m/z. Electrospray is a gentle ionisation technique and fragmentation of the molecular entity present in the sample was not expected to occur. Examination of the peaks corresponding to a dimer 577m/z (negative mode) or 579m/z (positive mode) indicated whether it was a fragmentation product or a whole entity. The absence of a M-1 peak indicated a molecular ion. The synthesised yellow product was subsequently identified as the procyanidin dimer, B3, while the other products were mixtures of dimers and trimers.

2.2.3.2 HPLC of procyanidin products

HPLC was used in conjunction with mass spectrometry to identify the degree of polymerisation of the products. The presence of a single peak indicated purity. The retention times of the procyanidins determined in this study were similar to the retention times for procyanins observed by other researchers (Escribano-Bailon et al., 1992;Ricardo da Silva et al., 1991a;Pekic et al., 1998;Rigaud, 1993;Ricardo da Silva et al., 1991b;Lazarus et al., 1999).

A Merck LiChrospher reverse phase C-18 column (particle size 5µm, 250 x4mm) (temperature of 30°C) protected with a guard column made from the same material was used to test the purity of the synthesised product. The solvent system was the same as that used to analyse anthocyanins. For the procyanidin dimers the elution scheme was a flow rate of 1mL/min, with a linear gradient of 0 to 5% B in 5 minutes, 5% to 20% B to 15 minutes, linear for 10 minutes then from 20% to 100% to 30 minutes followed by washing and reconditioning of the column. Detection was made at 280nm. A representative chromatogram is shown in Figure 2.7. Integration of the peaks indicated greater than 90% purity.

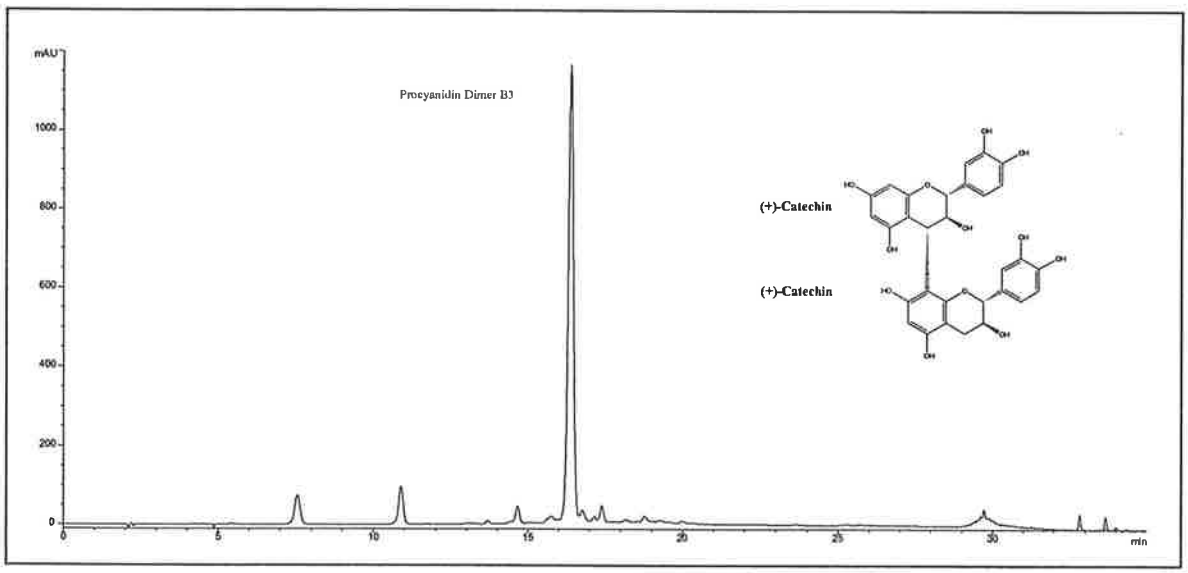

Figure 2.7 HPLC chromatogram of the synthesised procyanidin product that was identified as the procyanidin dimer B3.

A summary of the chemical analyses performed on the synthesised procyanidin products is presented in Table 2.2. Results identified the dull yellow powder (fraction 2) as procyanidin dimer B3.

Table 2.2 Quantification of the synthesised procyanidin products formed from the reaction of (+)-catechin with (±)taxifolin.

Product	*Fraction*	*Sephadex LH-20* [a]	*TLC Rf* [b]	*Positive procyanidin test*	*m/z* [c] *positive mode*	*HPLC peaks (RT mins)*
(+)-catechin		1:1.00	0.79	x	-	17.1 (16.4)
Dull-yellow	1	1:1.52	0.71	√	579	16.4
Golden-yellow	2	1:1.95	0.69	√	579,867,1155	16.4,16.8,(18.2, 19.3)
Cream-brown	3	1:2.51	0.67	√	579,867,1155	16.8,(16.4,18.2, 19.3)
Brown	4	1:3.38	n.d	√	n.d	n.d

[a] Ratio of elution volume to that of (+)-catechin. [b] TLC plate: Merck 1.05735. Solvent: the TLC solvent system employed was ethyl acetate/methyl ethyl ketone/formic acid/water (5:3:1:1 v/v/v/v). The HPLC retention times of 17.1, 16.4,16.8 and 18.2/19.3 minutes correspond to the catechin, dimer, and either procyanidin dimers or trimers respectively.Fraction 4 was not fully analysed as it contained a complex mixture of procyanidins.

2.2.4 Other compounds used to investigate intermolecular copigmentation

Caffeic acid (trans-3-(3,4-dihydroxy-phenyl)-propenoic acid), chlorogenic acid (5-*O*-caffeoylquinic acid), quercetin (3,5,7,3',4'-pentrahydroxyflavone), quercetin-3-glucoside,

(-)-epicatechin, (+)-catechin, mannose and proline were purchased from Sigma Aldrich.

2.2.5 Physical methods

2.2.5.1 General

Analytical grade chemicals and solvents were used in all preparations. Distilled, 0.45μm filtered water was used to make up all solutions.

2.2.5.2 Solutions used for the spectroscopic analysis

The stock solution used for visible spectroscopy experiments was a universal buffer solution developed by Davies, (1959). The buffer solution was prepared from citric acid (0.1 molL^{-1}), potassium dihydrogen orthophosphate (0.1 molL^{-1}), sodium tetraborate (0.05 molL^{-1}), trishydroxymethylaminomethane (0.1 molL^{-1}) and potassium chloride (0.1 molL^{-1}) in distilled water. This gave a buffer mixture for use over the pH range 2 to 12 by addition of either 0.4 molL^{-1} HCl or NaOH. Ionic strength was constant at 0.09 molL^{-1}. A PHM85 precision pH meter (Radiometer) with glass electrode was used to measure the pH of the solution. Buffer solutions of pH 4.00 and 7.00 were used for the pH meter calibration (NBS standards, Merck).

The stock solution of malvidin-3-monoglucoside (50μL) was dissolved in 1M HCl (4.95mL) and the absorbance at 520nm recorded so that the solution concentration of malvidin-3-monoglucoside could be determined using an extinction coefficient of 27,900 (Asenstorfer, 2001). Similarly, the solution concentration of malvidin-3-(*p*-coumaryl)glucoside in acidified ethanol (99.5%) was determined using an extinction coefficient of 30,800 (Asenstorfer, 2001).

Concentrated solutions of the anthocyanin or copigment were prepared in the universal buffer solution at a pH of 3.6. A concentrated quercetin or quercetin-3-glucoside solution was prepared in methanol due to their lower solubilities in the buffer solvent. A certain volume of the concentrated solutions were then mixed together and made up to 1mL with the buffer solution to give the appropriate anthocyanin and copigment concentration. Solutions used in the UV/visible spectroscopy analysis contained anthocyanin at a concentration of either 5 x 10^{-5} molL^{-1} (25 mgL^{-1}) for malvidin-3-monoglucoside or 6 x 10^{-6} molL^{-1} (4 mgL^{-1}) for malvidin-3-(*p*-coumaryl)glucoside with anthocyanin to copigment molar ratios ranging from 1:1 to 1:100 for all copigments except for quercetin (1:1 to 1:2) and quercetin-3-glucoside (1:1 to 1:20). A total of sixteen anthocyanin and copigment solutions were prepared. Solutions were analysed by UV/visible spectroscopy immediately after preparation.

The ratio of the extinction coefficient of the flavylium ion and the copigment complex ($\varepsilon AH(CP)_n^+ / \varepsilon AH^+$) was determined as a function of the absorbance difference between a solution containing malvidin-3-monoglucoside (concentration 5 x10^{-5} molL^{-1}) in the absence and in the presence of high levels of added copigment (anthocyanin to copigment molar ratio was 1:500). Solutions were prepared in 1 molL^{-1} HCl.

To determine the influence of temperature on intermolecular copigmentation, two solutions were prepared for each temperature. One solution contained malvidin-3-monoglucoside (concentration 5 x10^{-5} molL^{-1}) in the buffer solution and the other contained the same concentration of malvidin-3-monoglucoside with copigment added at a molar ratio of 1:90 (1:2 and 1:20 for quercetin and quercetin-3-glucoside respectively).

Investigations involving the indicator dyes methyl red or methyl violet at a concentration of 5 x10^5 molL^{-1} with (-)-epicatechin involved preparation of a stock solution of indicator dye and (-)-epicatechin in the universal UV/visible buffer solution at pH 3.6. Eleven solutions were prepared in total with a indicator dye to (-)-epicatechin molar ratio ranging from 1:1 to 1:250. At an indicator dye concentration of 1 x10^{-4} molL^{-1} eight solutions were prepared with a

methyl red to (-)-epicatechin molar ratio ranging from 20 to 200. To determine the increase in absorbance with increasing methyl red concentration, thirteen solutions were prepared ranging in concentration from 1 $x10^{-5}$ to 2 $x10^{-4}$ $molL^{-1}$.

2.2.5.3 Measure of copigmentation

UV/visible absorption spectra of the anthocyanin solutions with and without copigment were recorded on a GBC Cintra 40 spectrometer fitted with a thermostated cell holder. A personal computer was used to record all the spectra. Temperature was varied by a circulating water bath.

All spectra were recorded using quartz 10mm cells (1mm cells were used when anthocyanin concentration was 5 $x10^{-4}$ $molL^{-1}$) over the range 250-750nm. Unless otherwise stated, temperature was 298K. The spectral bandwidth of the spectrometer was set to 2nm with a scan rate of 1000nm per minute.

2.3 Results and discussion

2.3.1 Intermolecular copigmentation between malvidin-3-monoglucoside and various copigments

Thermodynamic parameters associated with intermolecular copigmentation between malvidin-3-monoglucoside and various copigments were determined at a representative average pH of red wine of 3.6. A malvidin-3-monoglucoside concentration of 5 x 10^{-5} $molL^{-1}$ ($25mgL^{-1}$) was chosen to minimise the effect of possible self-association of the anthocyanin. This concentration also fell in the range of values determined for one year old red wines in the studies described in Chapter 6.

A preliminary study of the effect of pH on colour expression of malvidin-3-monoglucoside was carried out. At pH <2 the flavylium ion was the dominant species present with a wavelength absorption maximum (λ_{max}) at 520nm (Figure 2.8). When increasing the pH value up to pH 4 the absorbance maximum (λ_{max}) was still at 520nm but the absorbance was reduced in intensity. In acidic to moderately acidic solutions the flavylium ion form of malvidin-3-monoglucoside existed. However its concentration relative to the other forms decreased proportionally with the increasing pH of the solvent system hence absorbance at 520nm decreased. At higher pH's (>4) there was a shift to longer wavelengths (pH 7.8 λ_{max} = 588nm) and an increase in absorbance at this wavelength.

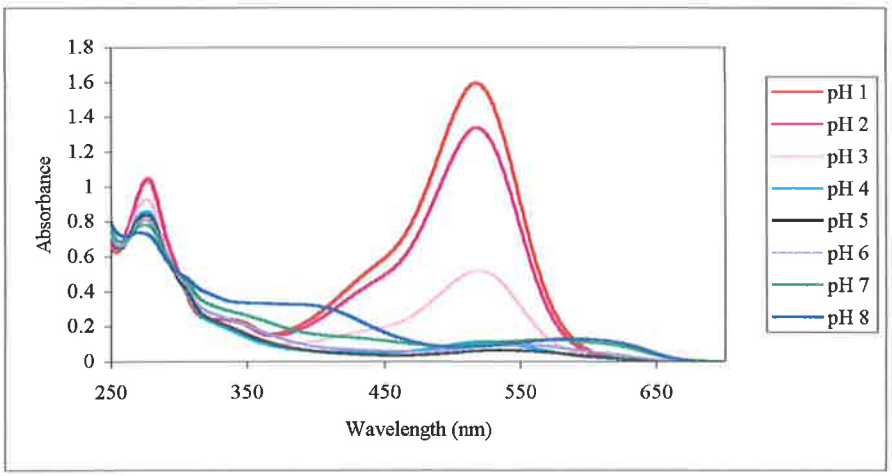

Figure 2.8 The change in the absorption profile of malvidin-3-monoglucoside's (5 x10^{-5} mol L^{-1}) over the wavelength range (250-700nm) at different pH values.

Brouillard et al., (1989) has shown that optimal intermolecular copigmentation occurs in the pH range 3.0 to 5.0. Since red wine pH falls in this range, intermolecular copigmentation may

significantly counteract the reduction in colour expression due to the hydration reactions of anthocyanins.

The free copigments lack absorbance in the visible range (400 –750nm). Hence the observed shift of absorbance maximum to longer wavelengths (λ_{max}) and an increase in absorbance was a characteristic of intermolecular copigmentation as shown in Figure 2.9, Figure 2.10 and Figure 2.11. At high concentrations of procyanidin dimer and seed tannin light scattering occurred indicating either aggregation or, particularly in the case of seed tannin, poor solubility.

Chlorogenic acid has a pK_a of 3.45 and therefore at pH 3.6 a significant contribution of the chlorogenate anion would have been present (Brouillard et al., 1989). It has previously been shown that the carboxylic group does not contribute to the copigment effect (Brouillard et al., 1991). The procyanidin dimer is a neutral species at pH 3.6. Caffeic acid was fully protonated as the stepwise protonation of the singly protonated dianion of caffeate ($caffeate^{2-}$) are 8.72 and 4.41 (Linder and Voye, 1987). No pK_a values have been reported for quercetin however it was expected to be fully protonated at pH 3.6.

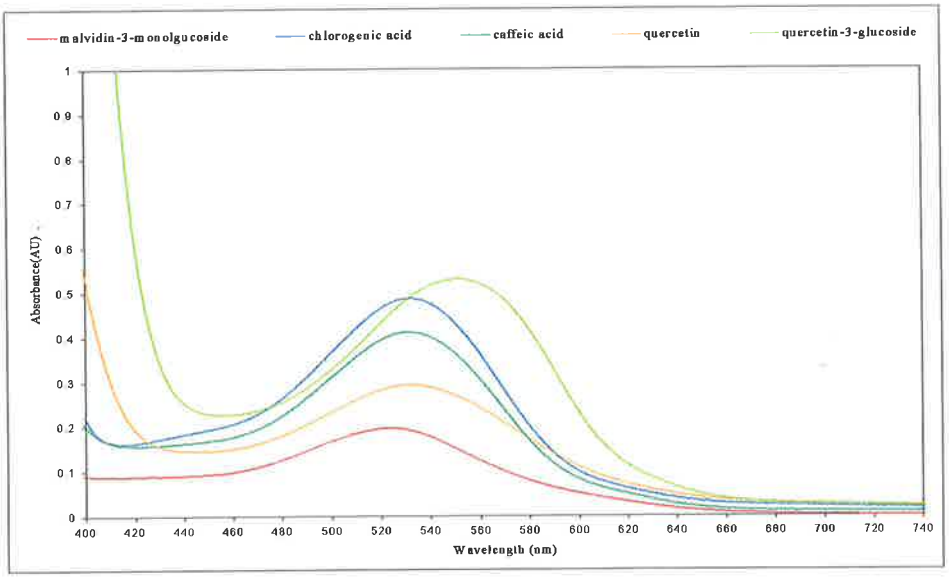

Figure 2.9 Absorption spectra of malvidin-3-monoglucoside in the absence and presence of chlorogenic acid, caffeic acid, quercetin and quercetin-3-glucoside. All spectra have been standardised to a malvidin-3-monoglucoside concentration of 5 x10^{-5}molL^{-1} with an anthocyanin to copigment molar ratio of 1:100 for chlorogenic acid and caffeic acid, 1:2 for quercetin and 1:20 for quercetin-3-glucoside (Temperature 298K, pH 3.6 and ionic strength 0.09 molL^{-1}).

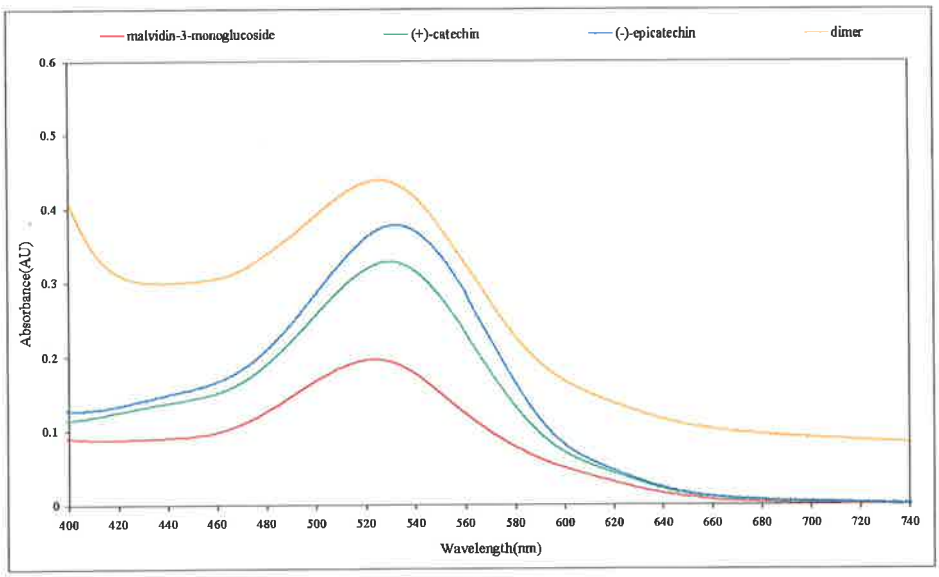

Figure 2.10 Absorption spectra of malvidin-3-monoglucoside in the absence and presence of (+)-catechin, (-)-epicatechin and procyanidin dimer. All spectra have been standardised to a malvidin-3-monoglucoside concentration of 5 x10^{-5}molL^{-1} with an anthocyanin to copigment molar ratio of 1:100 for all copigments (Temperature 298K, pH 3.6 and ionic strength 0.09 molL^{-1}).

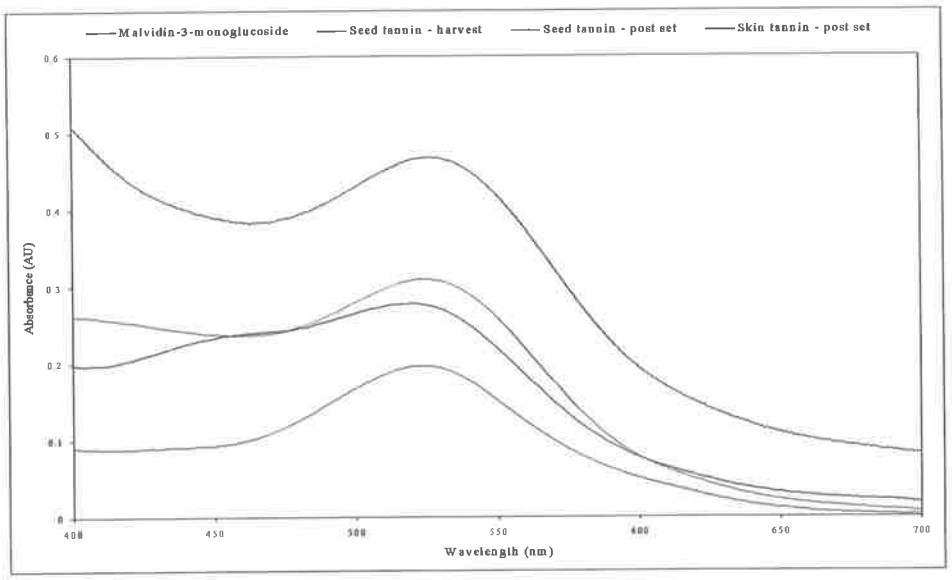

Figure 2.11 Absorption spectra of malvidin-3-monoglucoside in the absence and presence of seed tannin (harvest) and post set seed tannin. All spectra have been standardised to a malvidin-3-monoglucoside concentration of 5 $x10^{-5}molL^{-1}$ with an anthocyanin to copigment molar ratio of 1:100 for all copigments (Temperature 298K, pH 3.6 and ionic strength $0.09molL^{-1}$).

Intermolecular copigmentation between malvidin-3-monoglucoside and the copigments chlorogenic acid, caffeic acid, quercetin, quercetin-3-glucoside, (+)-catechin, (-)-epicatechin, procyanidin dimer, seed tannin (harvest) and post set seed tannin was quantitative as shown in Figure 2.12, Figure 2.13, and Figure 2.14.

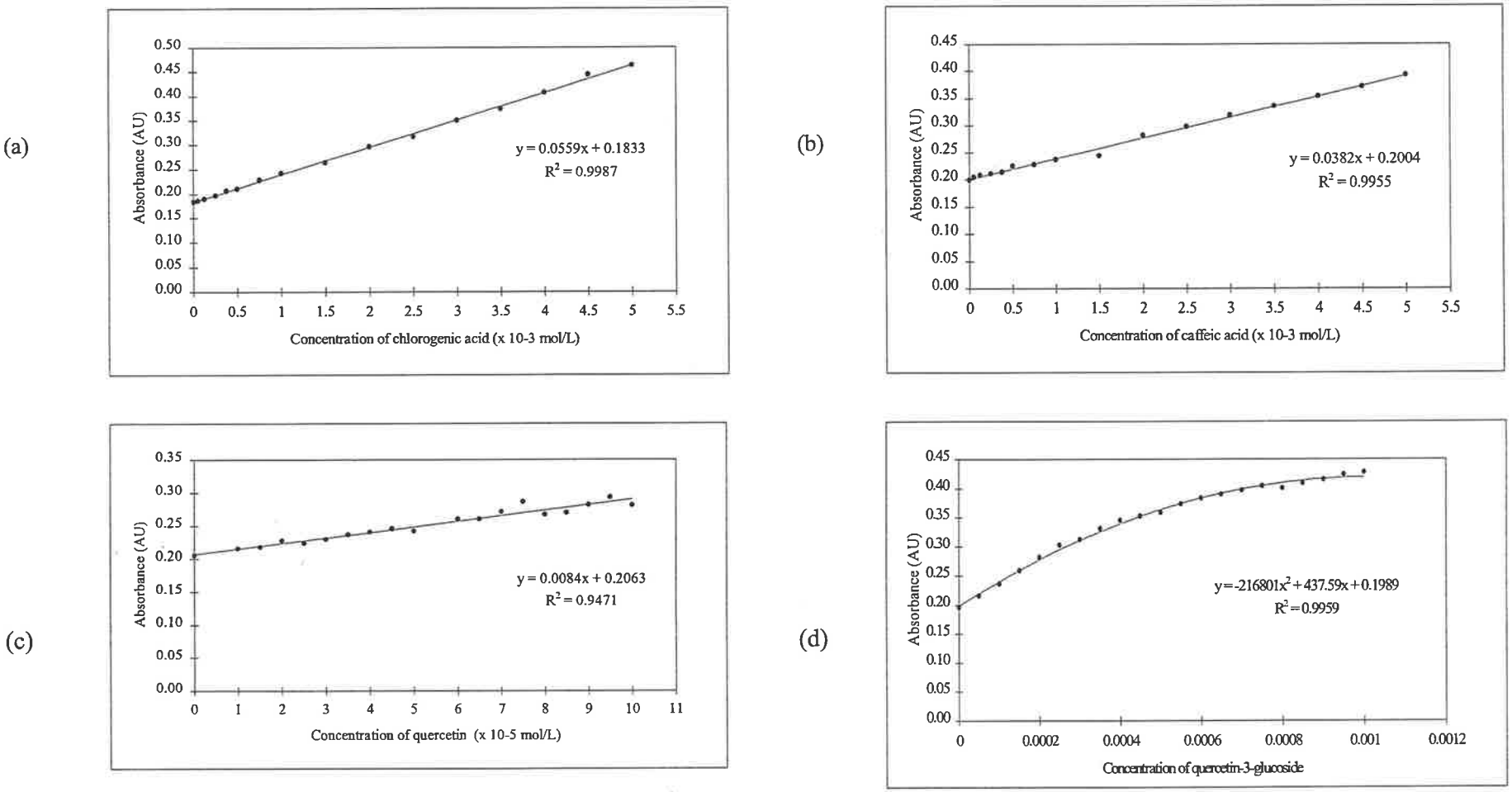

Figure 2.12 The change in absorbance maxima with constant malvidin-3-monoglucoside concentration (5 x10^{-5} molL^{-1}) with increasing (a) chlorogenic acid (b) caffeic acid (c) quercetin (d) quercetin-3-glucoside (Temperature 298K, pH 3.6 and ionic strength 0.09 molL^{-1}).

(a)

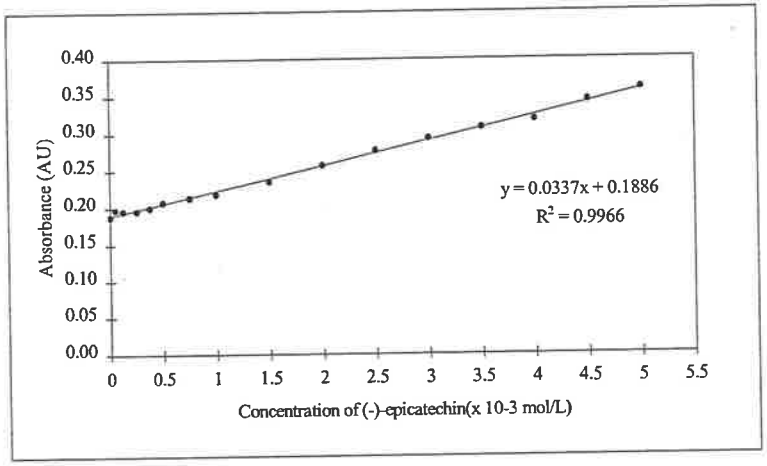

(b)

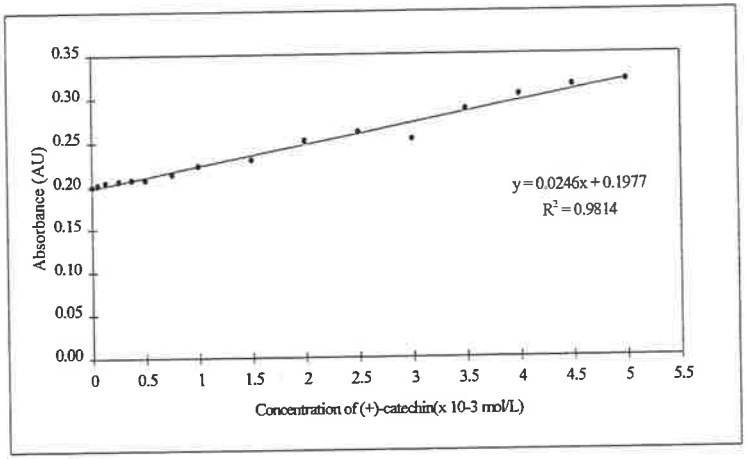

(c)

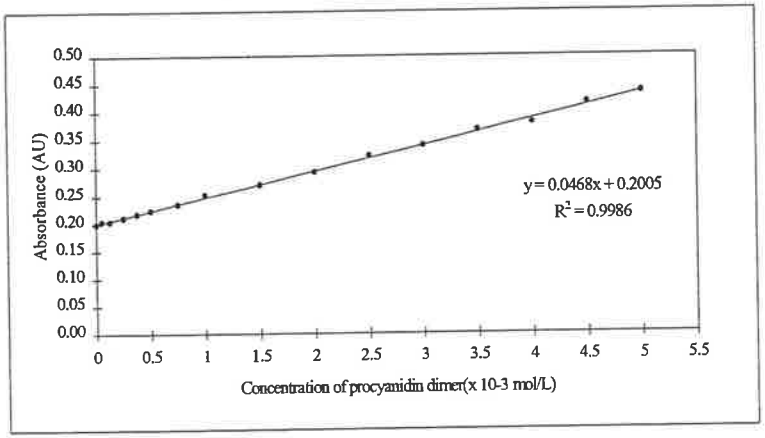

(d)

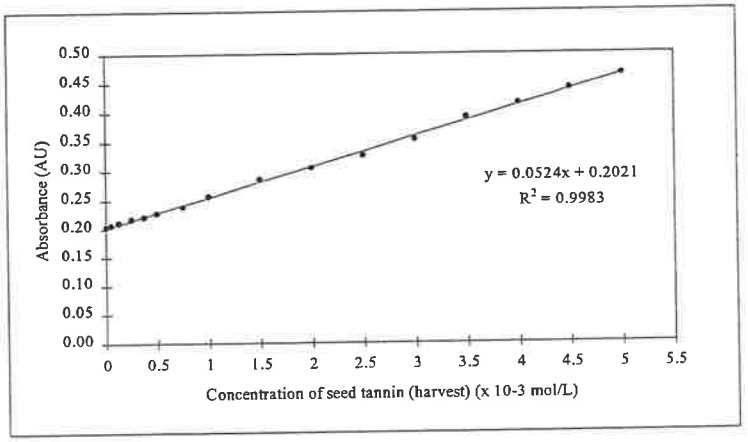

Figure 2.13 The change in absorbance maxima with constant malvidin-3-monoglucoside concentration (5 x10^{-5} molL^{-1}) with increasing (a) (-)-epicatechin (b) (+)-catechin (c) procyanidin dimer (d) seed tannin (harvest) (Temperature 298K, pH 3.6 and ionic strength 0.09 molL^{-1}).

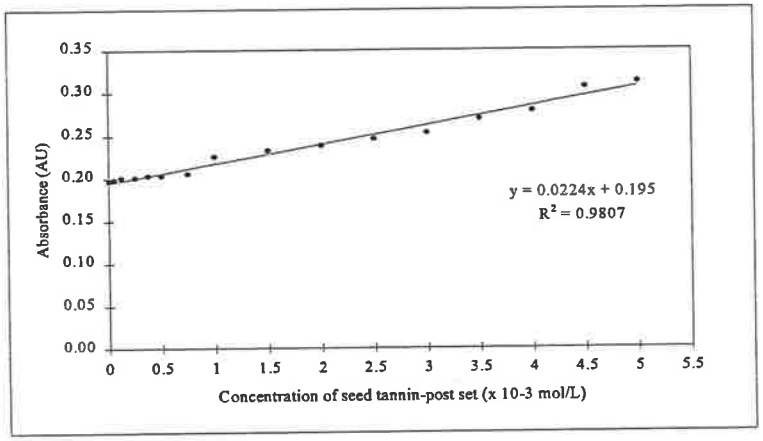

Figure 2.14 The change in absorbance maxima with constant malvidin-3-monoglucoside concentration (5 x10^{-5} molL^{-1}) with increasing post set seed tannin (Temperature 298K, pH 3.6 and ionic strength 0.09 molL^{-1}).

The individual copigments caused unique changes in the spectral profile of malvidin-3-monoglucoside as shown in Table 2.3. In general, as the degree of polymerisation increased for the flavan-3-ols polymers, so too did the increase in absorbance the post set seed tannin being an exception). However, this effect was not mirrored in the shift of absorbance maximum to longer wavelengths (λ_{max}) indicating that very different electronic transitions in the visible range were occurring. The post set seed tannin sample caused the least change in the spectral profile of malvidin-3-monoglucoside. A possible explanation for the reduction in copigmentation of the tannin extracts at post set may be due to the composition of their extension and terminal units. This may be a consequence of not only the degree of maturity of the grape seeds but also due to varietal differences as the seed tannin (harvest) was extracted from Semillon grape berries while the post set sample was sourced from Shiraz grape berries (Kennedy and Jones, 2000).

Table 2.3 The change in wavelength of the absorbance maximum (λ_{max}) and absorbance ($A-A_0/A_0$) of malvidin-3-monoglucoside (5×10^{-5} molL^{-1}) with the addition of various copigments.

Copigments	*Maximum anthocyanin to copigment molar ratio studied*	$\lambda-\lambda_0$	$A-A_0/A_0$
Chlorogenic acid	1:100	10.66	1.53
Caffeic acid	1:100	8.10	0.96
Quercetin	1:2	8.53	0.37
Quercetin-3-glucoside	1:20	27.31	1.18
(-)-Epicatechin	1:100	9.39	0.92
(+)-Catechin	1:100	5.12	0.64
Procyanidin dimer	1:100	5.97	1.18
Seed Tannin - harvest	1:100	1.71	1.28
Seed Tannin- post set	1:100	2.10	0.59

(A, λ and A_0, λ_0 are absorbance and absorbance maxima in the presence and absence of copigment. UV buffer solution, l = 10mm, ionic strength = 0.09 molL^{-1}.)

A lower concentration of quercetin was required to cause an equivalent shift in absorbance maximum (λ_{max}) and maximum absorbance of malvidin-3-monoglucoside to that expressed by the other copigments. Hence of all the copigments investigated quercetin had the highest affinity towards malvidin-3-monoglucoside. The flavonols quercetin and quercetin-3-

glucoside caused the greatest change in the absorbance maximum (λ_{max}) of malvidin-3-monoglucoside.

Proline and mannose, which are both present in red wine, exhibited no copigmentation with malvidin-3-monoglucoside, in fact a slight decrease in absorbance was observed (data not shown). Other researchers have also found that sugars do not seem to influence the colour stability of anthocyanins (Malien-Aubert et al., 2001;Scheffeldt and Hrazdina, 1978).

2.3.1.1 Determination of the thermodynamic parameters for intermolecular copigmentation

Values for the ratio of extinction coefficients r_1 ($\varepsilon AHCP^+/\varepsilon AH^+$) were determined by measuring the ratio of absorbance at 520nm of malvidin-3-glucoside in the presence of excess copigment and malvidin-3-monoglucoside at pH <1. Values of 0.76 were determined for chlorogenic acid, 0.81 for procyanidin dimer, 0.89 for caffeic acid, 0.84 for (-)-epicatechin, 0.81 for (+)-catechin, 0.67 for seed tannin, 0.78 for quercetin and 0.71 for quercetin-3-glucoside (Chapter 3). These values correlated well with previously reported values (Brouillard et al., 1991).

A plot of $\ln((A-A_0)/A_0)$ vs ln[CP] gave a slope equal to the stoichiometric constant (n) and the stability constant (K_1) was derived from the vertical intercept of the line of best fit. Plots of this type were produced for the anthocyanin-copigment systems and are represented in Figure 2.15, Figure 2.16 and Figure 2.17. As the concentration of chlorogenic acid, procyanidin dimer or seed tannin (harvest) increased there was a linear increase in the colour expression. While addition of caffeic acid or (+)-catechin to malvidin-3-monoglucoside did give a linear increase in the absorbance (Figure 2.12(b) and Figure 2.13(b)) they did not fit the quantitative natural log plots as exemplified by deviation from linearity. At (-)-epicatechin concentrations of less than 7.5×10^{-4} $molL^{-1}$ there was also deviation from linearity. The stoichiometry of the interactions fitted a 1:1 model for chlorogenic acid, quercetin, (-)-epicatechin, procyanidin dimer, seed tannin (harvest) and post set seed tannin indicating that one moiety of malvidin-3-monoglucoside interacts with one moiety of copigment. Caffeic acid, quercetin-3-glucoside and (+)-catechin did not fit this first order relationship. This would indicate that more complex interactions were occurring in these systems. However, their calculated thermodynamic parameters are included for completeness.

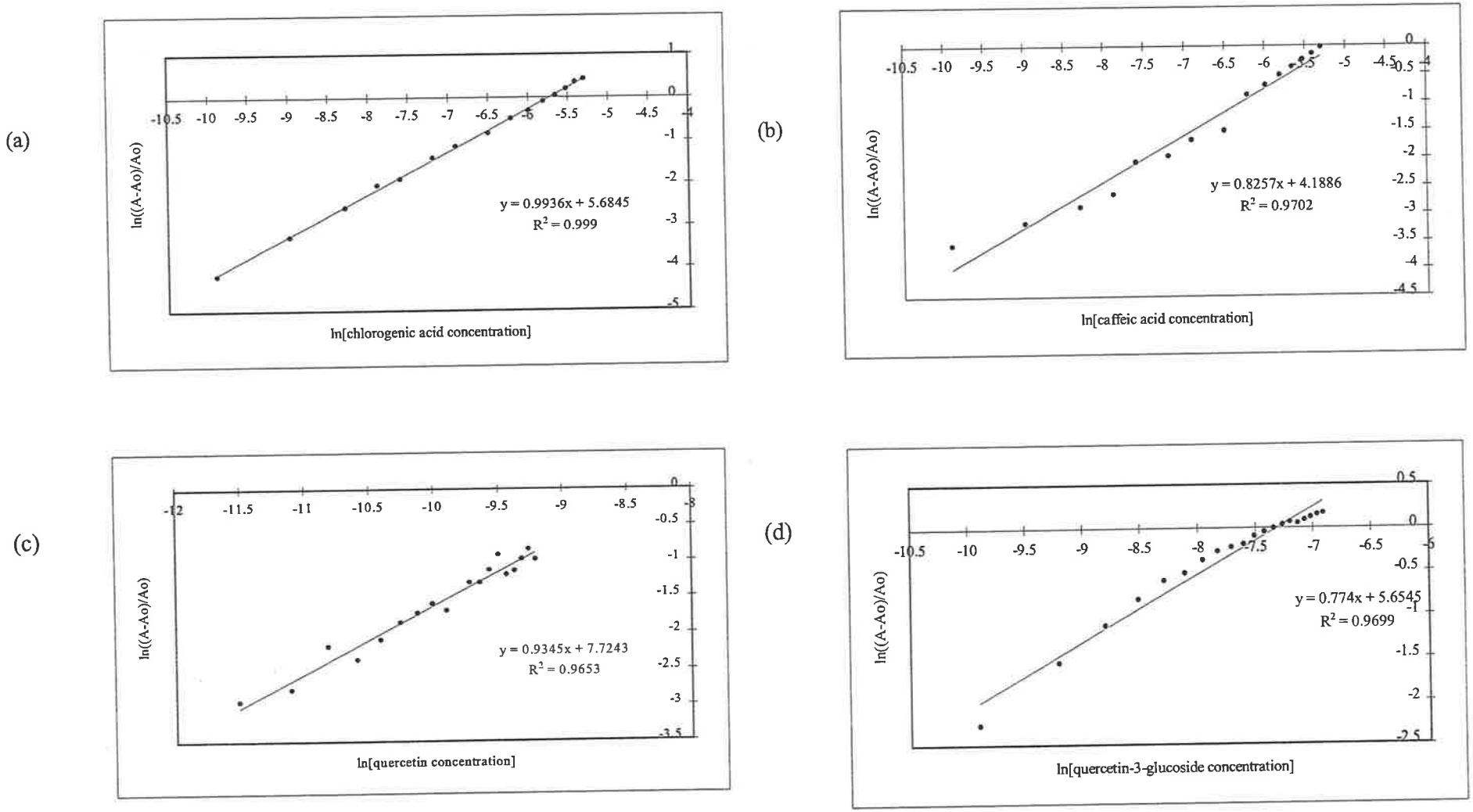

Figure 2.15 A plot of $\ln[((A-A_o)/A_o)]$ vs ln[copigment] (a) chlorogenic acid (b) caffeic acid (c) quercetin (d) quercetin-3-glucoside. Experimental conditions the same as Figure 2.12.

(a)

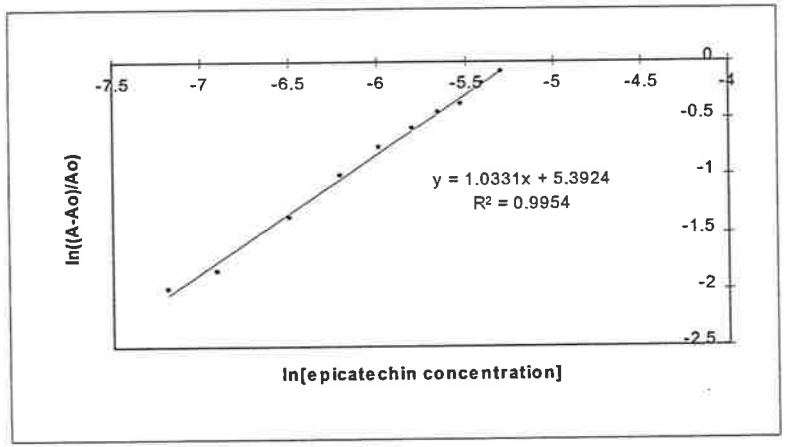

(b)

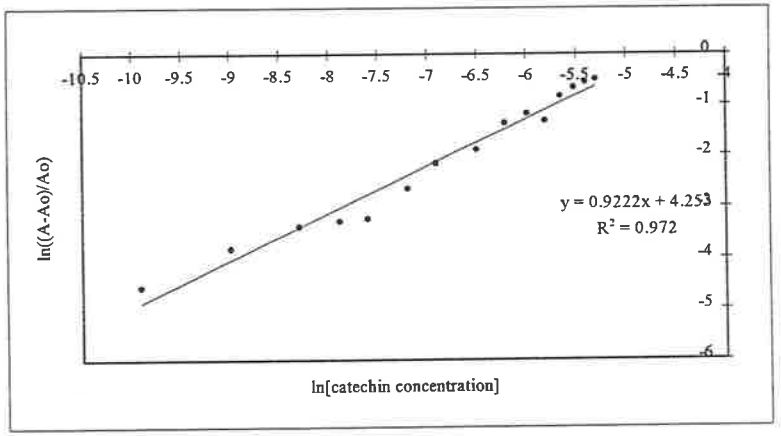

(c)

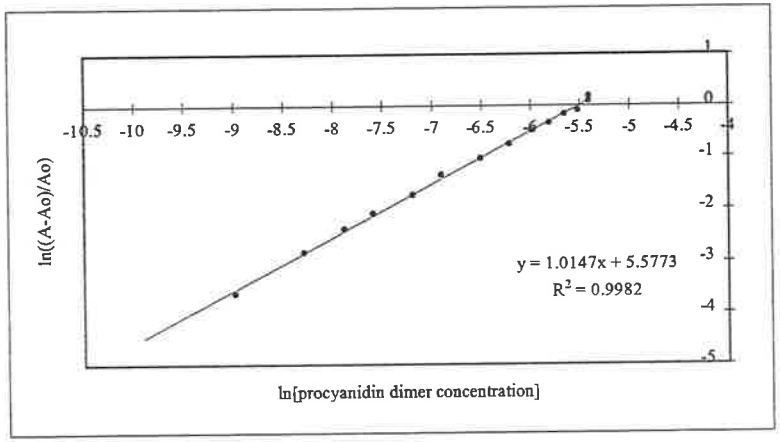

(d)

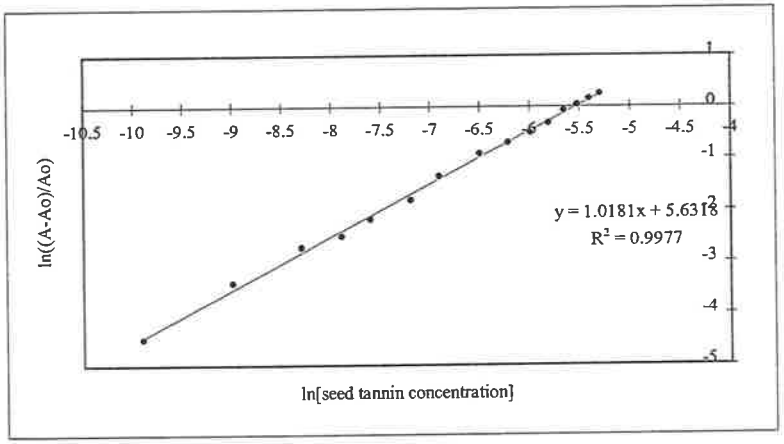

Figure 2.16 A plot of $\ln[((A-A_o)/A_o)]$ vs ln[copigment] (a) (-)-epicatechin (b) (+)-catechin (c) procyanidin dimer (d) seed tannin-harvest. Experimental conditions the same as Figure 2.13.

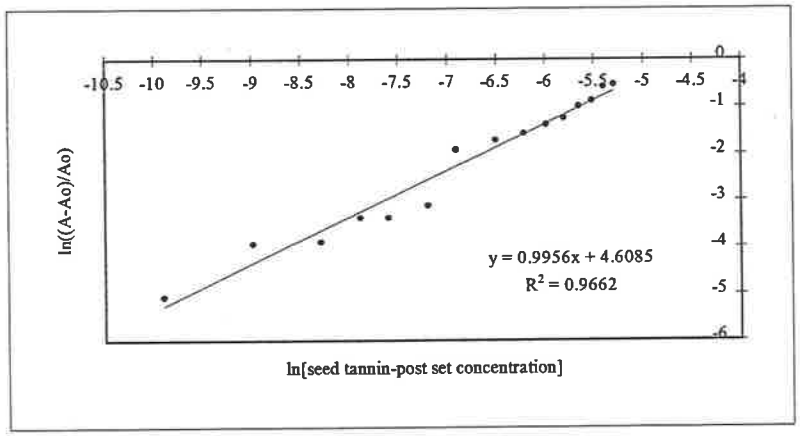

Figure 2.17 A plot of $\ln[((A-A_0)/A_0)]$ vs ln[copigment] post set seed tannin. Experimental conditions the same as Figure 2.14.

Temperature had a significant effect on intermolecular copigmentation. In the experiment the molar ratio of anthocyanin to copigment was sufficient for significant copigmentation to occur. The impact of temperature was expected to be the same at other molar ratios (Baranac et al., 1997a). A plot of $\ln((A-A_0)/A_0)$ vs the reciprocal of temperature gave a slope of $-\Delta H/R$ from which the enthalpy (H) and subsequently the entropy (S) could be determined (Figure 2.18 and Figure 2.19)

The values for n, stability constant (K_1), Gibbs free energy (ΔG), enthalpy (ΔH) and entropy (ΔS) for malvidin-3-monoglucoside with various copigments are reported in Table 2.4. The negative value for the Gibbs free energy in all the systems indicated that interaction between anthocyanin and copigment was spontaneous.

Table 2.4 The stability and thermodynamic parameters calculated for malvidin-3-monoglucoside (5×10^{-5} mol L^{-1}) with various copigments. Measurements were made in a universal aqueous buffer solution at 298K, ionic strength 0.09 mol L^{-1} and pH 3.6.

Copigments	*Range of anthocyanin to copigment molar ratio*	*Stoichiometry*	K_1 $mol^{-1}L$	ΔG $kJmol^{-1}$	ΔH $kJmol^{-1}$	ΔS $JK^{-1}mol^{-1}$
Chlorogenic acid	1:1 to 1:100	0.99	390.2±29	-14.77	-14.16	2.04
Caffeic acid	1:1 to 1:100	0.83	70±20	-10.67	-12.75	-6.96
Quercetin	1:1 to 1:2	0.93	2900±1300	-19.76	-31.76	-5.42
Quercetin-3-glucoside	1:1 to 1:20	0.77	400±100	-14.87	-13.59	4.29
(-)-Epicatechin	1:1 to 15:100*	1.03	260.5±40	-13.80	-18.04	-14.23
(+)-Catechin	1:1 to 1:100	0.92	90±20	-11.07	-17.29	-20.88
Procyanidin dimer	1:1 to 1:100	1.01	330±33	-14.35	-9.23	17.16
Seed tannin-harvest	1:1 to 1:100	1.02	420±40	-14.95	-33.30	-61.53
Seed tannin-post set	1:1 to1:100	1.00	150±55	-12.42	n.d	n.d

* ratios less than 1:15 were not used in this calculation
n.d = not determined

(a)

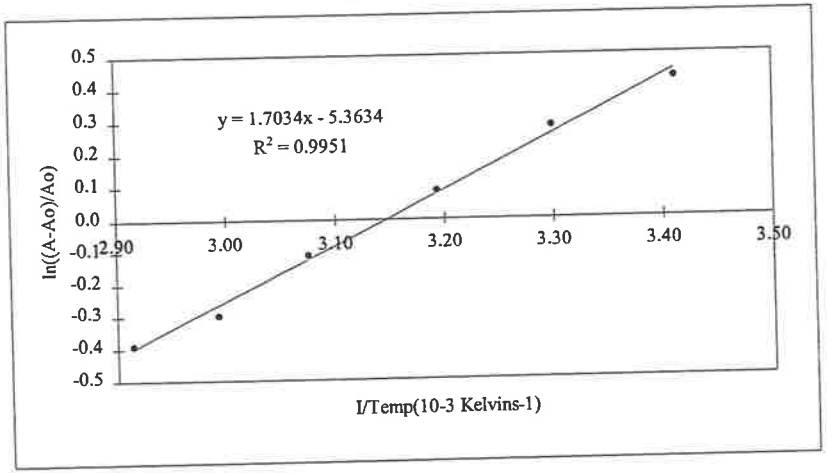

(b)

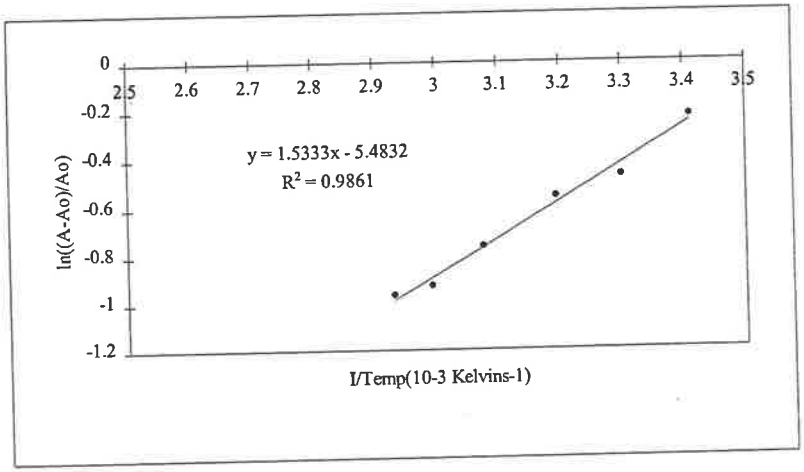

(c)

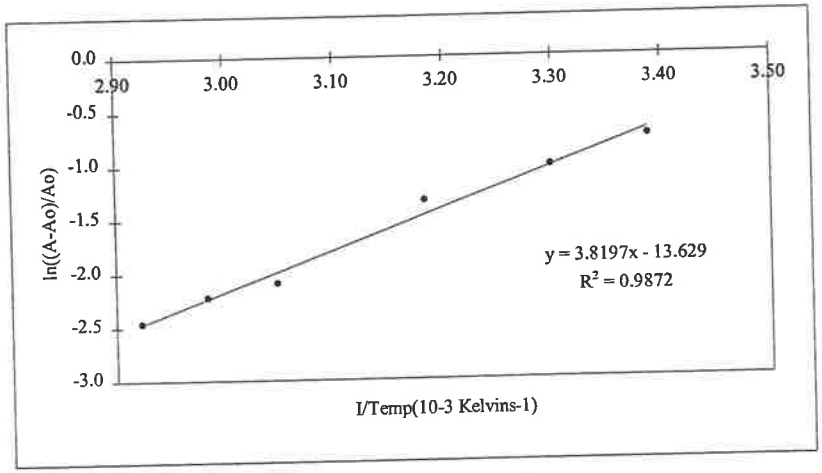

(d)

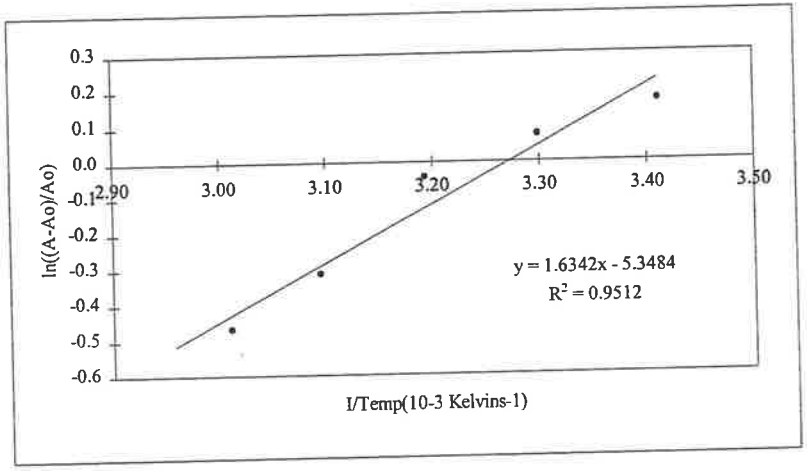

Figure 2.18 A plot of $\ln[((A-A_o)/A_o)]$ vs the reciprocal temperature. Malvidin-3-monoglucoside concentration 5 $x10^{-5}$ $molL^{-1}$ (a) chlorogenic acid (b) caffeic acid (c) quercetin (d) quercetin-3-glucoside.

(a)

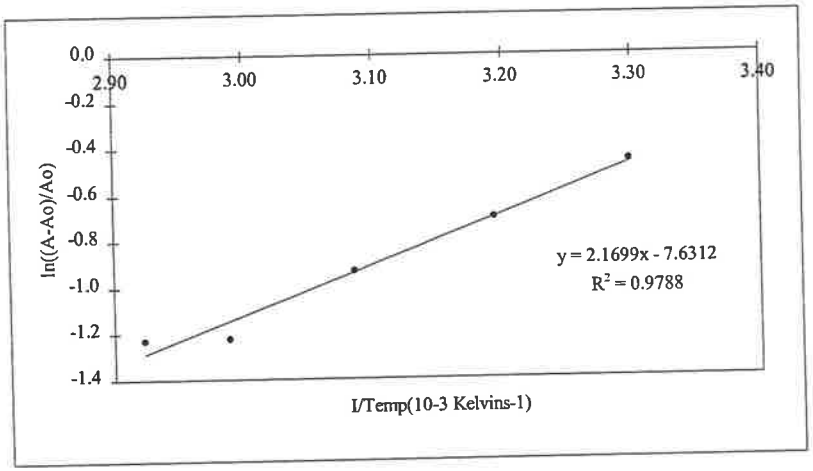

(b)

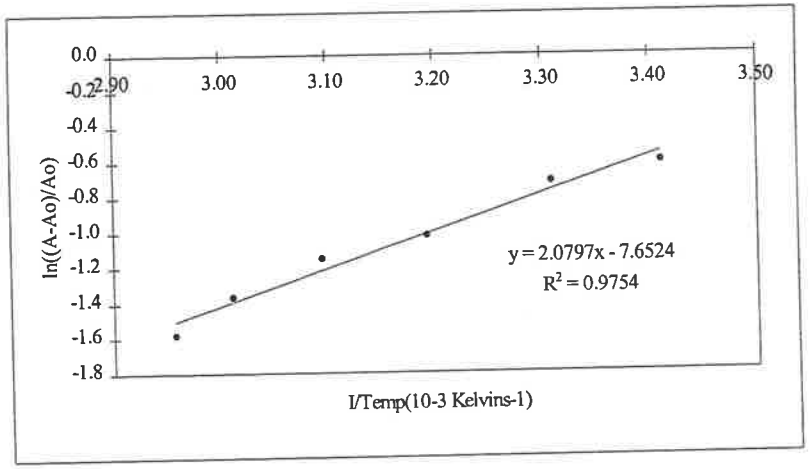

(c)

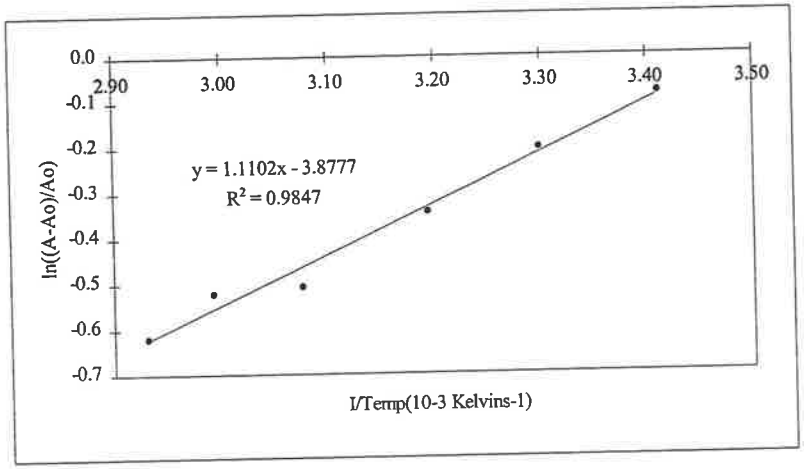

(d)

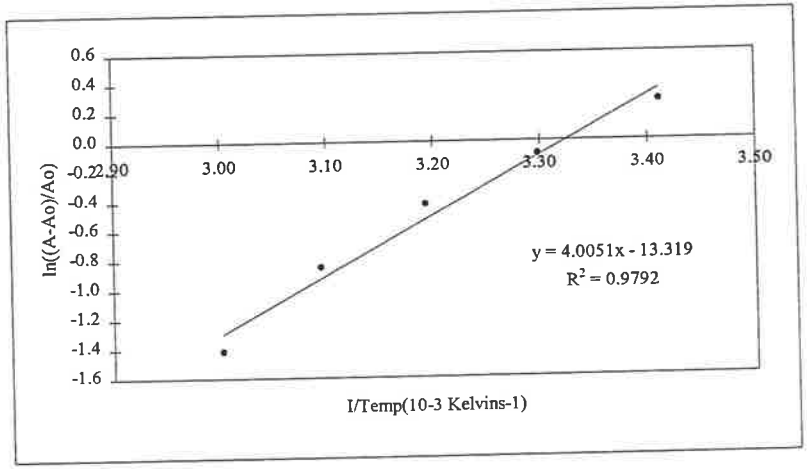

Figure 2.19 A plot of $\ln[((A-A_o)/A_o)]$ vs the reciprocal temperature. Malvidin-3-monoglucoside concentration 5 $x10^{-5}$ $molL^{-1}$ (a) (-)-epicatechin (b) (+)-catechin (c) procyanidin dimer (d) seed tannin-harvest.

Quercetin formed the most stable complex as exemplified by its high stability constant (2900 $mol^{-1}L$) and large negative Gibbs free energy (-19.76 $kJmol^{-1}$). The K_1 obtained in this study was higher than that obtained for the malvin-3,5-diglucoside - quercetin interaction (650 $mol^{-1}L$) as reported by Baranac et el., (1997a) whereas the stability constant for the malvidin-3-monoglucoside - chlorogenic acid interaction was similar to that determined for malvin-3,5-diglucoside (390 $mol^{-1}L$) as reported by Brouillard et al., (1989).

The values for the enthalpies indicate, as expected, that the intermolecular copigmentation was exothermic (Brouillard et al., 1989). The entropies of intermolecular copigmentation were negative or only slightly positive. A negative entropy indicated more order in the system, as would be expected when two individual constituents come together to form one entity. Each copigment has a unique relationship with malvidin-3-monoglucoside so that the Gibbs free energy and hence the stability constants are very much dependent on the combination of the individual thermodynamic parameters. For example, procyanidin dimer has a relatively low enthalpy, which was counteracted by its large positive entropy (this will be discussed further in the following section).

2.3.1.2 Comparison of abilities of copigments to form complexes with malvidin-3-monoglucoside

The most effective copigments were the flavonols quercetin and quercetin-3-glucoside. Both required much lower relative concentrations than other copigments to significantly change the absorption profile of malvidin-3-monoglucoside. Quercetin was more likely to form an intermolecular copigment complex with malvidin-3-monoglucoside than all the other copigments. The flavonols also caused the greatest change in the absorbance maximum (λ_{max}) of malvidin-3-monoglucoside.

Caffeic acid was a poor copigment, which may be due to the absence of an extensive aromatic π network. The derived stability constants presented here indicate the stability of the copigment complex of malvidin-3-monoglucoside with (+)-catechin should be quite similar to that with caffeic acid. However, in one study pre-fermentation addition of caffeic acid or (+)-catechin to a red wine resulted in a 60% and 10% colour increase respectively (Darias-Martin et al., 2001). This difference may be a result of further side reactions due to the complex phenolic composition of the wines and not simply to intermolecular copigmentation. It is possible that the caffeic acid is decarboxylated by yeast to form vinyl phenol, which then

reacts with malvidin-3-monoglucoside to form a Pigment A – like compound (Fulcrand et al., 1996).

Comparison of the entropies of association between malvidin-3-monoglucoside and the flavan-3-ol monomers (-)-epicatechin and (+)-catechin highlighted the importance the structure of the copigment on intermolecular copigmentation. Firstly, comparison of the two monomers showed, as expected, the greater stability of (-)-epicatechin with malvidin-3-monoglucoside relative to (+)-catechin. The *cis* configuration of (-)-epicatechin imparts a quasi planar arrangement through the delocalised π aromatic rings (Porter et al., 1986;Fronczek et al., 1984;Spek et al., 1984). This planar arrangement resulted in lower steric hindrance with malvidin-3-monoglucoside. This was in contrast to malvidin-3-monoglucoside interacting with (+)-catechin where steric constraints made the interaction less favourable. (+)-Catechin has a *trans* substituent configuration at position C2 and C4 in its C ring making it non-planer.

Both (-)-epicatechin and (+)-catechin had relatively large negative entropies whereas the procyanidin dimer had an equally large positive entropy. This suggests that the interaction of (-)-epicatechin or (+)-catechin with malvidin-3-monoglucoside resulted in a copigment complex that was more solvated than the corresponding individual constituents. The malvidin-3-monoglucoside/procyanidin dimer copigment complex gave a system that was more disordered than the individual constituents. The inability of the procyanidin dimer to form a compact complex with malvidin-3-monoglucoside may be due to formation of a copigment complex that was less solvated than its individual constituents. While the entropy was more favourable for the procyanidin dimer relative to monomeric (-)-epicatechin, the enthalpy was not. Entropy therefore appears to be the driving force in this reaction as the procyanidin dimer has a greater overall stability constant.

The abilities of the seed tannin extracts to act as copigments was dependent on their structural composition which was a function of time of harvest, variety of the grapes and perhaps the extraction technique. The mean degree of polymerisation was 5 for the post set seed tannin and seed tannin (harvest). Hence the difference in the stability constants must be due to the nature of the constituents making up the tannin chains. The extension unit for the tannin extracted from the Shiraz berries at post set was predominantly (-)-epicatechin in nature, whereas in the Semillon harvest berries the extension units were mainly (-)-epicatechin-3-O-gallate.

2.3.1.3 Influence of anthocyanin concentration on intermolecular copigmentation

To better represent the concentration of anthocyanins at the completion of fermentation, an experiment was undertaken where the malvidin-3-monoglucoside concentration was held constant at 5 x10^{-4} molL^{-1} (250 mgL^{-1}) whilst (-)-epicatechin or seed tannin (harvest) concentration was increased. The flavan-3-ols were chosen as the copigments as they represent the majority of the compounds extracted from grape seeds. With these systems there was increased colour expression although the cause of the increase in colour intensity did not appear to be straightforward as stability constants for these systems were reduced relative to those determined at the lower anthocyanin concentration (Table 2.5).

Table 2.5 The thermodynamic parameters calculated for malvidin-3-monoglucoside (5 x10^{-4} mol L^{-1}) and (-)-epicatechin or seed tannin (harvest). A universal aqueous buffer solution at 298K, ionic strength 0.09 molL^{-1} at pH 3.6 was used. The values in the parentheses are the stability constants as presented in section 2.3.1.1.

Copigments	*Ratio*	*Stoichiometry*	*K_1 mol^{-1}L*	*ΔG kJ mol^{-1}*
(-)-Epicatechin	1:1 to 1:15	0.73	39 (260)	-9.12
Seed Tannin (harvest)	1:1 to 1:15	0.91	48 (420)	-9.59

However the change in absorbance was much higher for the higher malvidin-3-monoglucoside concentration compared to that of the lower concentration as exemplified by the $((A-A_0)/A_0)$ (Table 2.6).

Table 2.6 The difference in absorbance of malvidin-3-monoglucoside in the absence and presence of copigments for a 1:15 molar ratio of anthocyanin to copigment.

	$((A-A_0)/A_0)$ at malvidin-3-monoglucoside conc. of 5 x10^{-5} molL^{-1} (25mgL^{-1})	*$((A-A_0)/A_0)$ at malvidin-3-monoglucoside conc. of 5 x10^{-4} molL^{-1} (250mgL^{-1})*
(-)-Epicatechin	0.14	0.90
Seed Tannin	0.16	0.39

The stoichiometric ratios of 0.73 and 0.91 for (-)-epicatechin and seed tannin (harvest) respectively indicated that the interactions contributing to colour enhancement did not involve simple dimeric interactions, as observed at the lower malvidin-3-monoglucoside

concentration. The reduction in the stability constants associated with intermolecular copigmentation at the higher anthocyanin concentration was thought to be due to strong self-association between malvidin-3-monoglucoside constituents.

2.3.2 Self-association of malvidin-3-monoglucoside

Self-association of malvidin-3-monoglucoside was investigated in the same manner as intermolecular copigmentation. Absorbance data was collected for 20 different concentrations ranging from 5 $x10^{-5}$ $molL^{-1}$ to 3 $x10^{-3}$ $molL^{-1}$. The maximum concentration of malvidin-3-monoglucoside used represents the maximum absorbance capability of the spectrometer. A non-linear increase in absorbance at 520nm with increasing concentration was observed which was believed to be due to aggregate formation. At concentrations above 2.5 $x10^{-4}$ $molL^{-1}$ the resulting absorbance does not fit a linear relationship and cannot be predicted. This was similar to results observed by Asen et al., (1972) and Timberlake, (1980). To determine the thermodynamic parameters associated with self-association of malvidin-3-monoglucoside the formula of Brouillard et al., (1989) had to be modified to account for the incremental increase in colour and the associated increase in malvidin-3-monoglucoside concentration. Estimation of the stability constant of self-association of anthocyanins was difficult due to the presence of several unknown variables these being the concentration of the malvidin-3-monoglucoside dimer and the molar absorptivity of the species.

The expected absorbance of malvidin-3-monoglucoside at a particular concentration may be calculated as a function of the estimated molar absorptivity (27,900) and concentration of the coloured forms of malvidin-3-monoglucoside at pH 3.6. The concentration of the coloured species of malvidin-3-monoglucoside may be calculated using the Henderson-Hasselbach equation and the pK_H (2.66) of malvidin-3-monoglucoside (refer to equation 2.6, section 2.3.5).

To estimate the increase in absorbance due to malvidin-3-monoglucoside dimerisation (AHD) a plot of the expected absorbance vs the difference between the observed absorbance and the expected absorbance was produced (Figure 2.20).

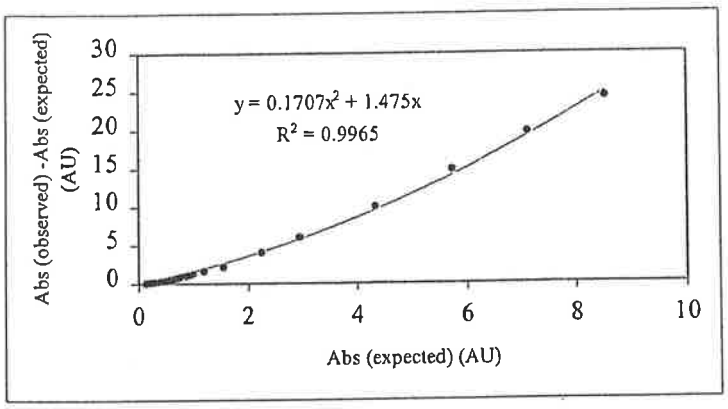

Figure 2.20 A plot of A_{obs}-A_{exp} vs A_{exp} at 520nm. Malvidin-3-monoglucoside concentration $5x10^{-5}$ molL^{-1} to $3x10^{-3}$ molL^{-1} at 298K, pH 3.6, ionic strength 0.09molL^{-1}.

Absorbance due to the dimer (AHD) was therefore equal to AHD =$1.707\ x10^{-1}x^2 + 1.475x$. This predicts that 1.475 was added over and above the colour expected at a particular malvidin-3-monoglucoside concentration.

The stability constant may then be estimated as a function of the absorbance associated with the malvidin-3-monoglucoside dimer (AHD) (Figure 2.21).

$$K\frac{[AHD]}{[AH^+]^2} = \frac{(AHD)/\varepsilon_{AHD}}{(A_{exp})^2/(\varepsilon_{AH^+})^2}$$

$$K = \frac{(AHD).(\varepsilon_{AH^+})^2}{(A_{exp})^2.\varepsilon_{AHD}}$$

$$(AHD) = \frac{(A_{exp})^2.\varepsilon_{AHD}.K}{(\varepsilon_{AH^+})^2}$$

$$(AHD) = (A_{exp})^2.c$$

where : $c = \frac{\varepsilon_{AHD}.K}{(\varepsilon_{AH^+})^2}$

Figure 2.21 The relationship between the stability constant (K) and the absorbance due to malvidin-3-monoglucoside self-association.

Then from above, absorbance of the malvidin-3-monoglucoside dimer (AHD) = $0.1707(A_{exp})^2$ and therefore $c = \frac{\varepsilon_{AHD}.K}{(\varepsilon_{AH^+})^2} = 0.1707$. An estimate of the molar absorptivity is required to determine the stability constant of malvidin-3-monoglucoside dimer formation. It is assumed that copigmentation involves minimal interaction between the two individual species that is there is no orbital overlap between the aromatic π networks (Hunter and Sanders, 1990). Thus it may be assumed that $\varepsilon_{AHD} \approx \varepsilon_{AH+}$ is equivalent to that of the

individual species that is monomeric malvidin-3-monoglucoside (27,900) (Hunter et al., 1989 and Scott, 1964). The stability constant (K) is related to the value of ε_{AHD} and the greater the value of ε_{AHD} the smaller the stability constant.

The enthalpy (ΔH) and entropy (ΔS) of self-association was determined in a similar manner as to that for intermolecular copigmentation. The values for A and A_0 were adjusted to account for the colour increase associated with dimer formation in a similar manner to that used for the calculation of the stability constant (Figure 2.22).

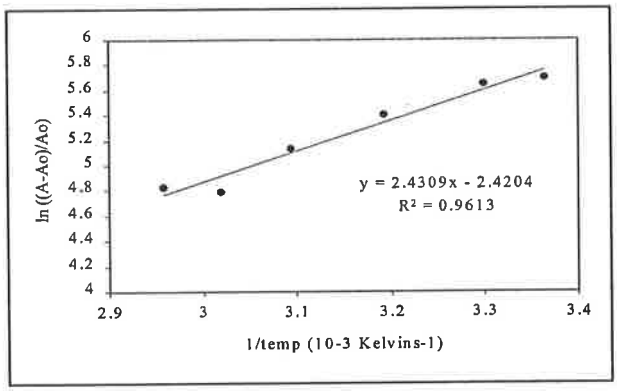

Figure 2.22 A plot of $\ln[((A-A_0)/A_0)]$ vs the reciprocal of temperature for malvidin-3-monoglucoside.
Malvidin-3-monoglucoside concentration 5 x10^{-5} molL^{-1} to 3 x10^{-3} molL^{-1} at pH 3.6, ionic strength 0.09 molL^{-1}

The stability constant for malvidin-3-monoglucoside self-association was larger than that calculated for intermolecular copigmentation (Table 2.7). Self-association of malvidin-3-monoglucoside was favourable as indicated by the negative value of the Gibbs free energy.

Table 2.7 Stability and thermodynamic parameters calculated for malvidin-3-monoglucoside (5 x 10^{-5} mol L^{-1}to 3 x 10^{-3} molL^{1}). A universal aqueous buffer solution at 298K, ionic strength 0.09 molL^{-1} at pH 3.6 was used.

Copigments	*Ratio*	*Assumed stoichiometry*	K_1 *mol^{-1}L*	ΔG *kJmol^{-1}*	ΔH *kJmol^{-1}*	ΔS *J K^{-1}mol^{-1}*
Malvidin-3-monoglucoside	1:1 to 1:59	1:1	4800±400	-21.00	-20.21	2.64

The mode of self-association is still not entirely understood. It has recently been proposed that colour stabilisation may be achieved via interaction between the various forms of the anthocyanin (Houbiers et al., 1998). Using NMR, equilibrium constants were determined for flavylium ion self-association and for the flavylium ion/Z-chalcone copigmentation of 3700

and 3080 $mol^{-1}L$ respectively (Houbiers et al., 1998). The values correlate well with the stability constant presented in this study.

2.3.3 Comparision between self-association and intermolecular copigmentation of malvidin-3-monoglucoside

In red wines, anthocyanins would not be exclusively involved in one form of interaction as malvidin-3-monoglucoside may be a substrate in both self-association and intermolecular copigmentation simultaneously. The impact of these competitive interactions on the resulting colour expression was investigated. An experiment was conducted in which malvidin-3-monoglucoside and (-)-epicatechin were considered copigments. The change in absorbance at 520nm with increasing malvidin-3-monoglucoside (5 x 10^{-5} to 3 x10^{-3} $molL^{-1}$) and (-)-epicatechin concentration (5 x 10^{-5} to 3 x10^{-3} $molL^{-1}$) was compared with the results observed for the self-association of malvidin-3-monoglucoside.

The increase in absorbance with addition of malvidin-3-monoglucoside and (-)-epicatechin was the same as that observed with addition of solely malvidin-3-monoglucoside (Figure 2.23). The addition of (-)-epicatechin did not contribute to a further increase in colour expression. A plot of $A_{obs} - A_{exp}$ vs A_{exp} was similar to that of malvidin-3-monoglucoside in the absence of (-)-epicatechin and hence the stability constant was not significantly different than that calculated for the self-association of malvidin-3-monoglucoside. It may be concluded that there was a preference for the self-association of malvidin-3-monoglucoside over intermolecular copigmentation with (-)-epicatechin. Scheffeldt and Hrazdina, (1978) observed that at higher concentrations of malvin-3,5-diglucoside at pH 3.2 the intermolecular copigmentation effect became insignificant in relation to self-association.

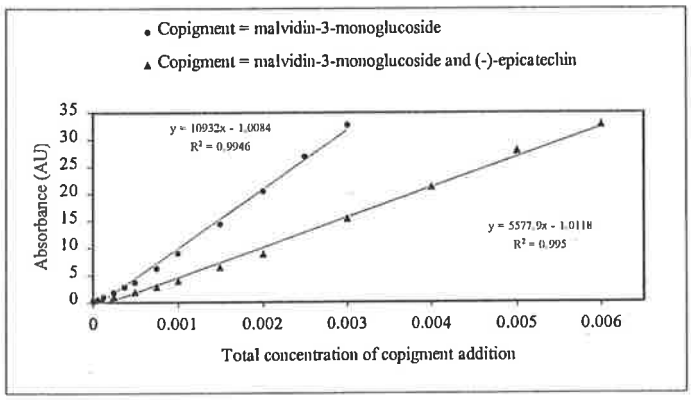

Figure 2.23 A plot of absorbance vs the total concentration of copigment added. Copigment either malvidin-3-monoglucoside or malvidin-3-monoglucoside plus (-)-epicatechin. Malvidin-3-monoglucoside concentration 5x10^{-5} $molL^{-1}$ at 298K, pH 3.6, ionic strength 0.09$molL^{-1}$.

2.3.4 Intermolecular copigmentation of malvidin-3-(*p*-coumaryl)glucoside

Intermolecular copigmentation between malvidin-3-(*p*-coumaryl)glucoside and chlorogenic acid and procyanidin dimer was studied. The change in absorbance with copigment addition was minimal ($(A-A_0)/A_0$) (530nm) was equal to 0.48 for chlorogenic acid and 0.26 for procyanidin dimer. The lack of significant intermolecular copigmentation may be attributed to the *p*-coumaryl which was attached to the glucose substituent as it is thought that the major colour stabilising mechanism of acylated anthocyanins is through intramolecular copigmentation (Goto et al., 1986;Goto, 1987;Brouillard, 1981).

2.3.5 Self-association of malvidin-3-(*p*-coumaryl)glucoside

Absorbance of malvidin-3-(*p*-coumaryl)glucoside at varying concentrations showed a linear increase as shown in Figure 2.24. The absorbance maximum was 530nm.

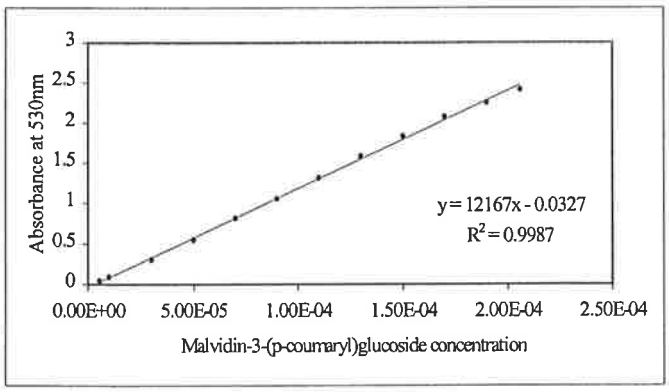

Figure 2.24 Increase in absorbance with increasing malvidin-3-(*p*-coumaryl)glucoside concentration. at 298K, pH 3.6, ionic strength 0.09 $molL^{-1}$ and 10%(v/v) alcohol.

The absorbance of malvidin-3-(*p*-coumaryl)glucoside was approximately twice that of malvidin-3-monoglucoside at the same concentration. In dilute aqueous solutions it was possible to estimate the percent contribution of the coloured forms of malvidin-3-O-(6-p-coumaryl) to the overall colour at pH 3.6 using equation 2.6.

$$pH = pK_a + \log\frac{\alpha}{1-\alpha}$$

Equation 2.6 The Henderson-Hasselbalch equation where α is the degree of dissociation (Clark, 1928).

The pK_{H1} of malvidin-3-O-(6-p-coumaryl) is 3.01 and greater than that of malvidin-3-monoglucoside (pK_{H1} = 2.66) (Asenstorfer, 2001). Hence at wine pH of 3.6, there was approximately 20% of malvidin-3-(*p*-coumaryl)glucoside in the coloured forms, while for malvidin-3-monolgucoside this was reduced to 10%. Consequently the absorbance of

malvidin-3-(*p*-coumaryl)glucoside due to the coloured forms in a dilute solution was approximately twice that of malvidin-3-monoglucoside. This was consistent with the knowledge that the *p*-coumaric acid substituent stabilises the anthocyanin from hydration at the C2 position through intramolecular copigmentation.

Self-association of malvidin-3-(*p*-coumaryl)glucoside was investigated using the same model as outlined for malvidin-3-monoglucoside. The concentration of malvidin-3-(*p*-coumaryl)glucoside ranged from 5.5 x10^{-6} molL^{-1} to 2.06 x10^{-4} molL^{-1} (Figure 2.25).

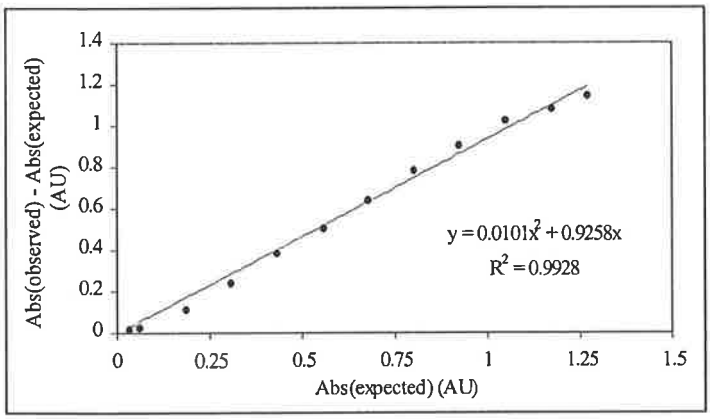

Figure 2.25 A plot of A_{obs}-A_{exp} vs A_{exp}. Malvidin-3-(*p*-coumaryl)-glucoside concentration of 5.5 x10^{-6} molL^{-1} to 2.06 x10^{-4} molL^{-1} at 298K, pH 3.6, ionic strength 0.09 molL^{-1} and 10% (v/v) alcohol.

In contrast to malvidin-3-monoglucoside the absorbance of malvidin-3-(*p*-coumaryl)glucoside was linear in nature. This suggests that in the concentration range measured malvidin-3-(*p*-coumaryl)glucoside did not form self-association dimers. Intramolecular copigmentation is therefore the major colour stabilising mechanism in malvidin-3-(*p*-coumaryl)glucoside (Figure 2.26) (Goto and Kondo, 1991).

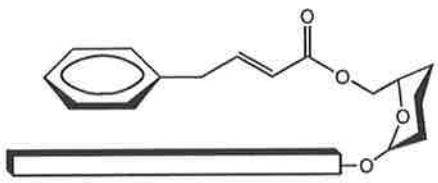

Figure 2.26 A diagrammatic representation of malvidin-3-(*p*-coumaryl)glucoside showing intramolecular copigmentation of the *p*-coumaric acid with the aromatic ring of the anthocyanin. The flavonoid portion of the anthocyanin is represented by the large rectangle.

2.3.6 The use of anthocyanin analogues to investigate the phenomenon of copigmentation

To provide insight into the mechanism of copigmentation, that results in observed colour enhancement, analogues representing anthocyanin aromatic π-conjugated systems were

investigated. Indicator dyes were used as they are highly conjugated, coloured and do not involve any complex equilibrium reactions (Figure 2.27).

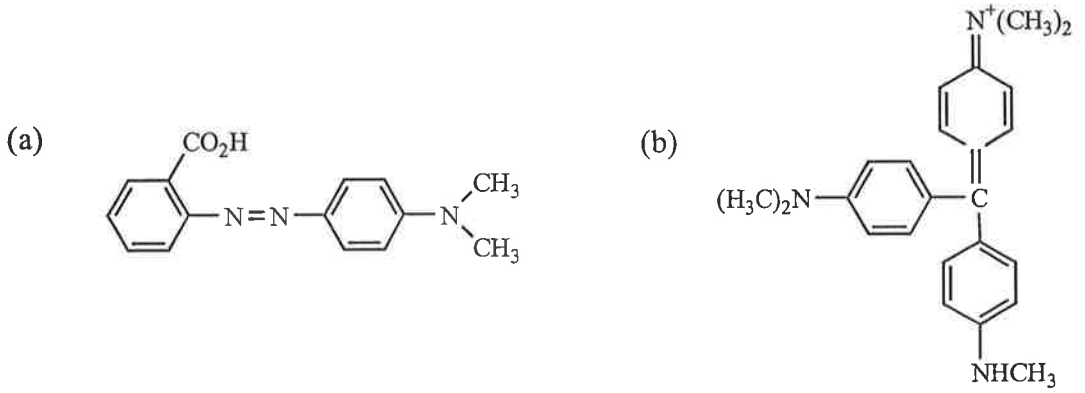

Figure 2.27 Chemical structures of (a) methyl red and (b) methyl violet.

Methyl red (pK_a 4.8) and methyl violet (pK_a estimated as 4.03) both have distinctly different colours in their nonionized and ionized forms. At pH 3.6 methyl red is red in colour and has an overall balanced neutral charge. Methyl violet is blue in colour and has a net positive charge. (-)-Epicatechin was used as the copigment in this investigation as it is a neutral species at pH 3.6.

At a methyl red and methyl violet concentration equal to that used in the copigmentation studies involving malvidin-3-monoglucoside (5×10^{-5} molL^{-1}) there was no significant change in the absorbance spectrum with the addition of (-)-epicatechin. Increasing the concentration of methyl red to 1×10^{-4} molL^{-1} only caused a slight increase in the absorbance when (-)-epicatechin was added. The absorbance increase of methyl red with addition of (-)-epicatechin was considered negligible in comparison to that observed with malvidin-3-monoglucoside (Table 2.8).

Table 2.8 Change in absorbance of malvidin-3-monoglucoside and methyl red with the addition of (-)-epicatechin at pH 3.6.

	Maximum anthocyanin to copigment molar ratio	$(A-A_0)/A_0$
Malvidin-3-monoglucoside (5×10^{-5} molL^{-1})	1:100	0.92
Methyl red (5×10^{-5} molL^{-1})	1:250	0.02
Methyl red (1×10^{-4} molL^{-1})	1:200	0.24

In the case of methyl violet, as (-)-epicatechin concentration was increased there was a slight decrease in absorbance of the peak at 585nm and a slight wavelength shift of the peak at 663nm to 680nm (molar ratio of methyl violet to copigment 1:200). There was no observed increase in absorbance with increasing (-)-epicatechin concentration.

The results indicated that (-)-epicatechin did not engage in π-π interactions that resulted in increased absorbance with either the neutral methyl red or positively charged methyl violet. The increased absorbance observed in the self-association or intermolecular copigmentation studies of malvidin-3-monoglucoside could not be emulated using the indicator dyes as analogues.

The absorbance spectra of malvidin-3-monoglucoside in the absence and presence of copigment at pH <1, where the flavylium ion is dominant showed no characteristic charge transfer bands. Similarly, no such electronic interaction was observed at pH 3.6 where both flavylium ion and quinonoidal base forms of the anthocyanin are present. Furthermore, the values calculated (at pH <1) to estimate $\varepsilon_{AHCP}/\varepsilon_{AH+}$ indicate that the molar absorptivities of the copigment complexes are less than that of malvidin-3-monoglucoside. Thus it would be unexpected to see an increase in absorbance with copigment complex formation.

The absence of the formation of charge transfer complexes, together with the absence of enhancement of colour expression of the indicator dyes with (-)-epicatechin, suggests that it was not π-π interaction which caused increased absorbance of malvidin-3-monoglucoside when involved in copigmentation. The major discriminating factor between the indicator dyes and the anthocyanins is that anthocyanins are involved in complex equilibrium reactions between coloured and colourless species at pH 3.6. Hence, it was thought that the observed increase in absorbance of anthocyanins when involved in copigmentation, was not due to aromatic π electron interactions, but a result of a shift in the anthocyanins equilibrium to the formation of more coloured species.

This was further supported by the adherence to Beer's law of methyl red as its concentration was increased. As methyl red concentration was increased from 1 $x10^{-5}$ to 2 $x10^{-4}$ $molL^{-1}$ there was a linear increase in absorbance ($R^2 = 0.9979$). This indicates that the equilibrium between the red form of methyl red and its non coloured (or other coloured forms) is not altered by increasing methyl red concentration. Furthermore, if self-association of methyl red is taking place then it is not affecting the molar absorptivity of methyl red. This data supports

the idea that anthocyanins do self-associate and that this self-association causes a shift in the equilibria to give more of the red coloured species.

Observed shifts of malvidin-3-monoglicosides absorbance maximum to longer wavelengths with the addition of copigments (in particular the flavonols) may indicate that there is slight delocalisation of electrons between molecular orbitals (Table 2.3). However, the major contributing factor to the colour enhancement would be due to the increase in the concentration of the coloured anthocyanin forms.

Intermolecular interaction of anthocyanins involved in self-association and intermolecular copigmentation promote the equilibrium reactions of the anthocyanins to shift towards the coloured species. This in turn increases their concentration and accounts for the increase in absorbance observed in the copigmentation studies presented in this chapter. Attractive interaction between π electrons (anthocyanin or copigment) and the σ framework (anthocyanin or copigment) which outweigh unfavourable π electron repulsion result in copigment complex formation (Hunter and Sanders, 1990). This subsequently promotes a shift in anthocyanin equilibrium towards the formation of the coloured species. The driving forces contributing to the magnitude of the interaction are van der Waals (Hunter and Sanders, 1990), dipole-dipole (Cozzi and Siegel, 1995) and non classical hydrophobic interactions (Newcomb and Gellman, 1994). Therefore it may be concluded that the phenomenon of copigmentation is not due to π-π interaction as such but an indirect consequence of π-σ interaction between anthocyanins and copigments.

2.3.7 Relevance of copigmentation on red wine colour

The model solution studies, as presented in this study, gave a quantitative basis for assessing the influence of not only self-association relative to intermolecular copigmentation but also the ability of the individual copigments to enhance the colour expression of anthocyanins.

In the intermolecular copigmentation studies, the molar ratio of anthocyanin to copigment was such that significant intermolecular copigmentation could be observed and the corresponding thermodynamic parameters of the copigment complex determined. The relative stability constants of intermolecular copigmentation between anthocyanin and copigment gave an indication of the ability of a particular copigment to stabilise the coloured forms of the anthocyanin. This calculated stability constant is a property of the association and therefore would be the same at any concentration.

In a young red wine, the anthocyanin to copigment ratio differs significantly to that used in this investigation (Iland, 1997;Singleton, 1988;Goldberg et al., 1998b;Goldberg et al., 1998a). For example, the total anthocyanin to monomeric flavan-3-ols concentration in a young red wine is approximately 8.1 $x10^{-4}$ to 3.5 x 10^{-4} $molL^{-1}$ or a molar ratio of 1 to 0.42 (Table 1.1, Chapter 1). To observe an increase in absorbance due to copigmentation the concentration of the copigment (in mgL^{-1}) used in this investigation was greater than that present in red wines. Hence, the contribution of intermolecular copigmentation to the observed colour expression may be insignificant.

Self-association of the anthocyanins and in particular the acylated anthocyanins gave the highest relative stability constants. Hence, the main mechanism stabilising colour in a young red wine may be via self-association. Intermolecular copigmentation may play a more significant role in the colour expression of an aged red wine or wines with low anthocyanin concentration due to the greater concentration of anthocyanins relative to copigments. For example, the total anthocyanin to monomeric flavan-3-ol concentration for a Cabernet Sauvignon red wine after 3 years ageing is 1.2 $x10^{-4}$ to 2.6 $x10^{-4}$ $molL^{-1}$ or a molar ratio of 1:2.2 (Table 1.1, Chapter 1).

It should be noted that in the complex medium of a red wine both self-association and intermolecular copigmentation would be occurring and that the stability constants determined in this investigation indicate the more favourable interactions. For example, red wines which have higher concentrations of acylated anthocyanins and flavonols would be expected to exhibit greater colour expression.

2.4 Conclusion

Intermolecular copigmentation between the anthocyanin malvidin-3-monoglucoside and various non-coloured organic copigments resulted in increased absorbance and a shift in the absorbance maximum of the anthocyanins to longer wavelengths. The maximum molar ratio of anthocyanin to copigment was 1 to 100 with the exception of quercetin and quercetin-3-glucoside where it was 1 to 2 and 1 to 20 respectively. The extent of these spectral changes differed between the copigments. The flavonols were the best copigments. This was attributed to their extensive π aromatic conjugation, their many potential H-bonding sites and particularly in the case of quercetin to its planar conformation.

The monomeric flavan-3-ols (+)-catechin and (-)-epicatechin were relatively weak copigments compared with their higher oligomers, procyanidin dimer B3 and seed tannin (harvest). The effectiveness of the seed tannin in increasing colour intensity through intermolecular copigmentation with malvidin-3-monoglucoside appears to be dependent on the proportional composition of the components making up the tannin.

The greater colour enhancement as the total concentration of malvidin-3-monoglucoside was increased, indicated that self-association was more favourable than intermolecular copigmentation. The two-fold increase in the observed colour enhancement of malvidin-3-(*p*-coumaryl)glucoside relative to malvidin-3-monoglucoside is attributed to stabilisation by intramolecular copigmentation. Intramolecular copigmentation stabilisation may also explain the lack of self-association and intermolecular copigmentation of malvidin-3-(*p*-coumaryl)glucoside.

It is misleading to state the observed colour enhancement associated with copigmentation is due to π-π interaction between the aromatic rings of the constituents. The absence of characteristic spectral changes associated with charge transfer complexes and the lack of copigmentation of anthocyanin analogues indicated that there was no delocalisation of electrons between the π aromatic clouds. The observed increase in absorbance of malvidin-3-monoglucoside when involved in self-association or intermolecular copigmentation results from a shift in the anthocyanin equilibrium reactions towards the formation of more coloured species. It was concluded that the phenomenon of copigmentation is not due to π-π interaction

as such but an indirect consequence of π-σ interaction between anthocyanins and themselves or copigments.

Chapter 3

Factors influencing copigmentation

3.1 Introduction

The enhancement in colour expression due to copigmentation between an anthocyanin and a copigment is dependent on the solvent. Variables such as pH, sulphur dioxide, ethanol and acetaldehyde have all shown to affect copigmentation. To understand the importance of copigmentation on red wine colour stability, these variables were investigated.

3.1.1 Influence of pH on intermolecular copigmentation

Chemical structure and electronic distribution of malvidin-3-monoglucoside is influenced by pH (Figure 3.1). At wine pH (3.5-3.6), the colourless chalcone and hemiketal forms are dominant (Brouillard and Delaporte, 1977;Mazza and Brouillard, 1987). In very acidic solvent the red flavylium ion is the dominant form. The proportion of each form depends on the pH of the solvent medium and therefore the effect of pH on intermolecular copigmentation must be considered.

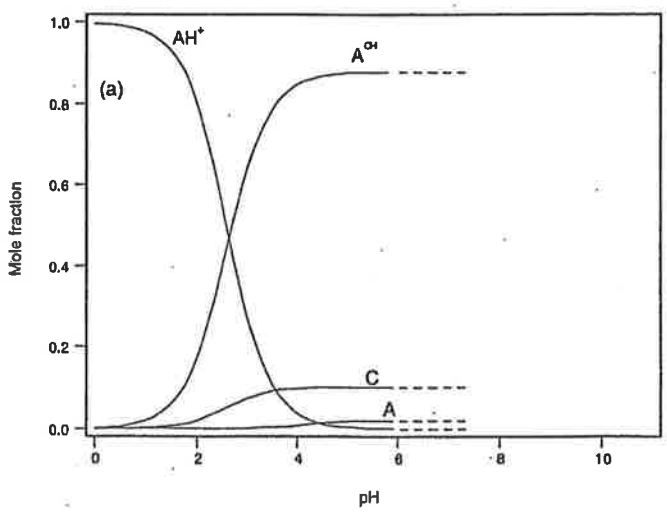

Figure 3.1 The speciation diagram of malvidin-3-monoglucoside utilising pK values of pK_a = 4.25, pK_H = 2.60 (Brouillard and Delaporte, 1977).

Intermolecular copigmentation occurs in the pH range 1.5-7.0 with it being at its highest between pH 3.0 to 5.0 (Mistry et al., 1991, Brouillard and Dangles, 1994). Williams and Hrazdina, (1979) observed intermolecular copigmentation at pH <2.0 but only a shift in absorbance maximum occurred without a simultaneous increase in absorbance.

Colour enhancement through intermolecular copigmentation is due to stabilisation of the coloured forms of malvidin-3-monoglucoside, the flavylium ion (AH^+) and quinonoidal neutral base (A). The flavylium ion form is in rapid equilibrium with the hemiketal, chalcone and quinonoidal base forms (refer to Equation 2.2, Chapter 2, equilibriums 1 and 2). The presence of a copigment pushes the equilibrium towards copigment complex formation (Equation 2.2, equilibriums 3 and 4). This in turn reduces the overall concentration of flavylium ion and quinonoidal base. To counteract this reduction the equilibrium readjusts at the expense of the hemiketal and chalcone and it is therefore thought that copigmentation reduces the hydration reaction (Dangles et al., 1993b).

3.1.2 Influence of sulphur dioxide on intermolecular copigmentation

Sulphur dioxide is present in red wine as molecular SO_2 and as bisulphite ion (HSO_3^-). Molecular SO_2 is the active form and is required in wine to inhibit microbiological activity. The bisulphite ion acts as an antioxidant but leads to unwanted reactions by reacting with the red flavylium ion form of an anthocyanin to form a colourless bisulphite addition product, essentially quenching the colour of the anthocyanin (Figure 3.2) (Berke et al., 1998;Brouillard and El Hage Chahine, J, 1980).

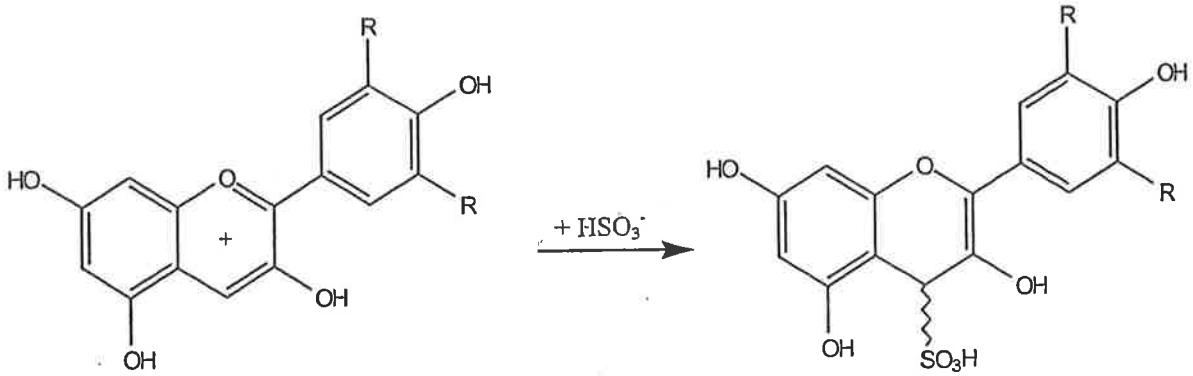

Anthocyanin

Figure 3.2 Formation of the bisulphite addition product anthocyanin–4-sulphonic acid.

The influence of sulphur dioxide on the copigment complex was first investigated by Somers and Pocock, (1990). Significant colour loss is observed after dilution of a red wine due to the constituents in the copigment complex reverting back to their free forms whereupon the anthocyanin is quickly bleached by sulphur dioxide. The influence of sulphur dioxide at concentrations seen in red wines (approximately 15 mgL^{-1} free SO_2 and 60 mgL^{-1} total SO_2) has not been investigated.

3.1.3 Influence of ethanol on intermolecular copigmentation

Copigmentation is at its most energetically favourable in pure water. Introduction of a cosolvent such as ethanol changes the thermodynamics parameters of interaction and ultimately reduces copigmentation (Brouillard et al., 1989). Attractive hydrophobic forces acting between the aromatic rings of the anthocyanin and copigment are reduced due to the disruption of the tight tetrahedral network of water molecules by cosolvent molecules. Consequently reducing the driving force for complexation (Dangles and Broulliard, 1992).

3.1.4 Influence of acetaldehyde on intermolecular copigmentation

The formation of adducts between anthocyanins and copigments in the presence of acetaldehyde is well known (Somers and Wescombe, 1987;Saucier et al., 1997;Timberlake and Bridle, 1976;Timberlake and Bridle, 1977;Fulcrand et al., 1996;Rivas-Gonzalo et al., 1995;Romero and Bakker, 1999). The formation of anthocyanin/flavan-3-ol adducts occurs via $CH_3CH<$ bridging between the C8 or C6 positions of the individual flavonoids. The mechanism of condensation by acetaldehyde has been shown to be a Baeyer-type condensation where the acetaldehyde reacts as its carbonium ion at position 8(6) of a flavan-3-ol, which then in turn reacts with the anthocyanin (Timberlake and Bridle, 1977). This condensation of flavanols involving acetaldehyde occurs in the early stage of red winemaking (Saucier et al., 1997). The influence of acetaldehyde on intermolecular copigmentation is unknown.

3.1.5 Influence of potassium bitartrate on intermolecular copigmentation

Both potassium and tartaric acid are naturally found in grape berries. Tartaric acid is a weak organic diprotic acid and exists in three forms with their relative proportions a function of pH (Figure 3.3).

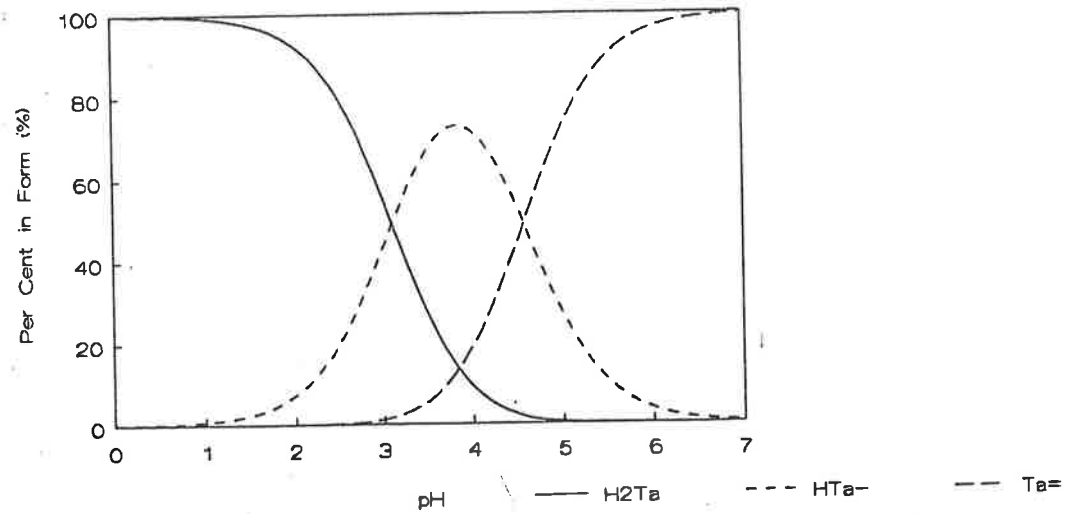

Figure 3.3 The relative proportion of the three forms of tartaric acid over a pH range. Using the pKa_1 of tartaric acid, 2.98 and pK_2 of 4.34.

At red wine pH (3.6) the dominant species is the bitartrate anion. This species readily associates with free potassium cations to form potassium bitartrate. As a consequence wine is a supersaturated solution of potassium bitartrate. The precipitation of potassium bitartrate can cause major stability problems in wines. A wine is considered stable when it contains no potassium bitartrate in excess of its solubility (2.77g/L at 12% alcohol, 20°C) (Berg and Keefer, 1958). Potassium bitartrate has greater solubility in red wines due to the presence of polyphenolics such as tannins.

Bitartrate anions are thought to be involved in an ion-pairing effect with the flavylium ion copigment complexes (Bolton, 2001). The negative charge of the anion acts as a counter charge to the positive flavylium ion. The influence of potassium bitartrate on intermolecular copigmentation must therefore be considered as a factor in the copigmentation of anthocyanins in red wines.

3.2 Materials and methods

3.2.1 Preparation of solutions

The stock solution to make up all the solutions used in the UV/visible spectroscopy analysis was the same as outlined in section 2.2.5.2.

3.2.1.1 Influence of pH on intermolecular copigmentation

The intermolecular copigmentation between chlorogenic acid and malvidin-3-monoglucoside was measured over a pH range from 1 to 8 by addition of either 1 $molL^{-1}$ HCl or 1 $molL^{-1}$ NaOH to a universal buffer solution containing $5x10^{-5}$ $molL^{-1}$ malvidin-3-monoglucoside and chlorogenic acid $5x10^{-3}$ $molL^{-1}$.

Solutions of malvidin-3-monoglucoside in the absence and presence of copigments at pH 1 and 7.8 were prepared and the absorbance measured. Solutions at pH 1 were prepared in 1.0 $molL^{-1}$ HCl while those at pH 7.80 were prepared using the universal buffer solution with pH adjusted to pH 7.8.

To determine the stability constant of malvidin-3-monoglucoside with (-)-epicatechin at pH 3.0 and 4.0, solutions were prepared as previously described in section 2.2.5. Addition of either 0.4 $molL^{-1}$ HCl or 0.4 $molL^{-1}$ NaOH gave solutions of pH 3.0 and 4.0 respectively. Ionic strength was 0.09 $molL^{-1}$. Sixteen sample solutions were made up in total with a constant malvidin-3-monoglucoside concentration of 5 $x10^{-5}$ $molL^{-1}$ and an anthocyanin to copigment ratio from 1:1 to 1:100.

3.2.1.2 Influence of sulphur dioxide on intermolecular copigmentation

The influence of sulphur dioxide on intermolecular copigmentation between malvidin-3-monoglucoside and (-)-epicatechin was determined in solutions of sulphur dioxide with concentrations between 0 and 150 mgL^{-1}. The effect of sulphur dioxide was tested at two distinct malvidin-3-monoglucoside concentrations, 5 $x10^{-5}$ $molL^{-1}$ and 5 $x10^{-4}$ $molL^{-1}$. The molar ratio of malvidin-3-monoglucoside to (-)-epicatechin was 1:100 in both cases. All solutions were prepared in the universal buffer solution at pH 3.6.

3.2.1.3 Influence of ethanol on intermolecular copigmentation

Solutions of malvidin-3-monoglucoside (5 x10^{-5} molL^{-1}) with either chlorogenic acid or (-)-epicatechin at an anthocyanin to copigment molar ratio 1:1 to 1:100 were prepared. All solutions were made up in universal buffer solution at pH 3.6 with varying ethanol concentrations. For chlorogenic acid, ethanol concentrations of 2, 4, 6 and 8% were used. Solutions at ethanol concentrations of 2, 6, 10 and 12% were used for (-)-epicatechin. Enthalpy and entropy was determined for each ethanol concentration as a function of temperature in the same manner as outlined in section 2.2.5.

3.2.1.4 Influence of acetaldehyde on intermolecular copigmentation

Mixed solutions of malvidin-3-monoglucoside (5 x 10^{-5} molL^{-1}) and (-)-epicatechin (5 x 10^{-3} molL^{-1}) were prepared in universal buffer solution at pH 3.6. Concentrations of added acetaldehyde ranged from 0 to 150 mgL^{-1}. The effect of acetaldehyde in the absence and presence of copigment was determined.

For HPLC analysis, solutions containing 5 x10^{-5} molL^{-1} malvidin-3-monoglucoside, 5 x10^{-3} molL^{-1} copigment and 250ppm (mgL^{-1}) acetaldehyde were prepared in universal buffer solution at pH 3.6. The copigments under investigation were (-)-epicatechin, procyanidin dimer and seed tannin (harvest). The solutions were prepared in quadruplicate. One sample was measured directly by HPLC while the other three were placed in airtight containers and stored in the dark until required. Standard solutions of malvidin-3-monoglucoside in the absence of copigment and malvidin-3-monolgucoside plus copigment in the absence of acetaldehyde were also prepared.

3.2.1.5 Influence of potassium bitartrate on intermolecular copigmentation

The influence of potassium bitartrate on intermolecular copigmentation between malvidin-3-monoglucoside and seed tannin (harvest) was determined in the absence and presence of ethanol. The universal buffer solution was prepared with potassium bitartrate concentration of 2.5 gL^{-1} with either 0% ethanol or 12% ethanol. The pH was adjusted to 3.6 with the addition of 0.4M HCl. Solutions were then prepared with a malvidin-3-monoglucoside concentration of 5 x10^{-5} molL^{-1} and seed tannin (harvest) concentration ranging from 0 to 5 x10^{-3} molL^{-1}. Sixteen sample solutions were made up in total. A similar experiment was conducted with a malvidin-3-monoglucoside concentration of 5 x10^{-4} molL^{-1} and seed tannin (harvest) concentration range from 0 to 7.50 x 10^{-3} molL^{-1}.

3.2.2 Physical methods

3.2.2.1 Investigating copigmentation with Ultraviolet/visible spectroscopy

A GBC Cintra 40 spectrometer fitted with a thermostated cell holder was used in all experiments as described in section 2.2.5.3. Absorption spectra of the sample solutions were recorded using quartz cells (10mm) over the range 250-750nm. For malvidin-3-monoglucoside concentration of greater than 5 $x10^{-4}$ $molL^{-1}$ or when pH<1, 1mm quartz cells were used. Unless otherwise stated, the temperature was 298K.

3.2.2.2 Measurement of condensation products by HPLC

HPLC analysis was performed as described for the anthocyanins presented in section 2.2.1.1.

3.3 Results and discussion

3.3.1 Influence of pH on intermolecular copigmentation

3.3.1.1 General trends

The change in absorbance of malvidin-3-monoglucoside in the presence of chlorogenic acid was pH dependent (Figure 3.4). The values for maximum absorbance were used to compare the individual samples since absorbance maximum (λ_{max}) changed with increasing pH.

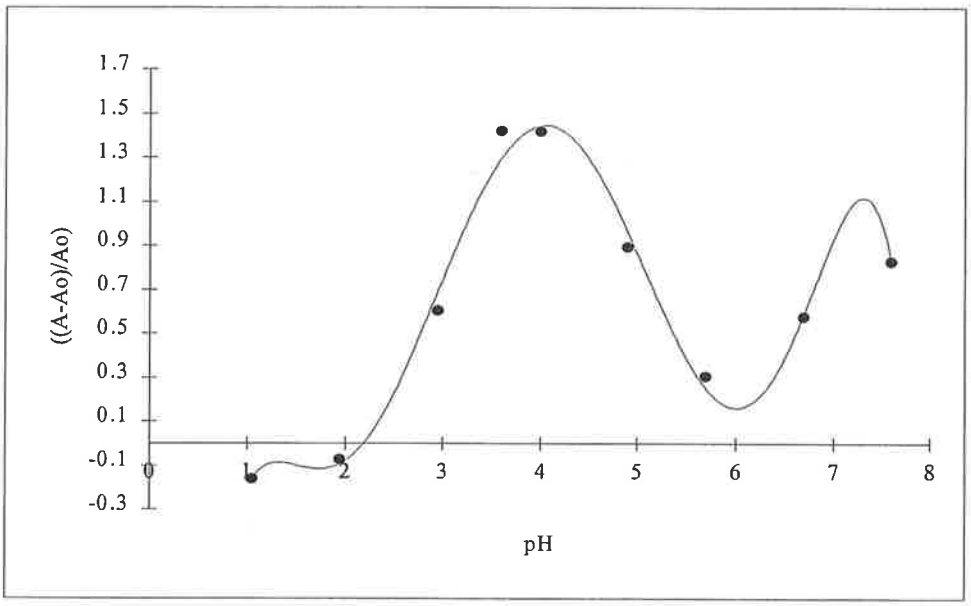

Figure 3.4 Change in absorbance of a solution of mavlvidin-3-monoglucoside (5 x10^{-5} mol L^{-1}) and chlorogenic acid with an anthocyanin to copigment molar ratio of 1:100 (Temperature 298K, *l* = 10mm). The solid line represents the line of best fit for a 6^{th} order polynomial.

The negative result for $((A-A_0)/A_0)$ at pH<2 indicated the decreased colour expression of the copigment complex relative to that of the red flavylium ion. However, copigmentation did occur as is evident by a shift of the absorbance to longer wavelengths (Table 3.1).

Table 3.1 The percentage increase in colour expression and change in absorbance maximum ($\Delta\lambda_{max}$) with the addition of chlorogenic acid (3×10^{-3} molL^{-1}) to a solution containing malvidin-3-monoglucoside (5×10^{-5} molL^{-1}) relative to a solution of malvidin-3-monoglucoside (5×10^{-5} molL^{-1}) only.

pH	$\Delta\lambda_{max}$	*% increase in colour relative to malvidin-3-monoglucoside*
1.05	9.39	-16
1.95	13.23	-7
2.95	11.52	60
3.60	10.66	153
4.00	10.77	141
4.90	6.40	89
5.70	-5.54	30
6.70	-9.39	57
7.60	-2.56	83

Between pH 2.0 and 4.0, malvidin-3-monoglucoside had low absorbance in the visible region due to the dominance of the colourless hemiketal forms. There was a significant increase in colour expression with the addition of chlorogenic acid. Intermolecular copigmentation was less pronounced between pH 4.0 and 6.0 due to the increased presence of the quinonoidal forms (A, A^-, A^{2-}) of malvidin-3-monoglucoside. At pHs greater than 6.0 there was a slight increase again, this was in contrast to the results of chlorogenic acid with malvin where a steady decrease was observed (Brouillard et al., 1991).

Intermolecular copigmentation between malvidin-3-monoglucoside and chlorogenic acid was at its greatest at pH 3.6. Chlorogenic acid has a pK_a of 3.45 so at pH 3.6 a significant amount of the chlorogenate anion would have been present (Brouillard et al., 1989). Brouillard et al., (1991) however concluded that the conjugated π system of chlorogenic acid is the major pre-determining factor in imparting intermolecular copigmentation effects and the negative charge on the carboxylic group of the chlorogenate anion does not affect copigmentation. Copigments with higher pK_as may however exhibit maximum intermolecular copigmentation at slightly higher pHs.

The results confirm that intermolecular copigmentation causes the greatest increase in colour expression at pH 3.6 which corresponds with typical red wine pH.

3.3.1.2 Malvidin-3-monoglucoside and copigments at pH<1

Direct interaction between copigment and the flavylium ion form of malvidin-3-monoglucoside was investigated by measuring the change in UV/visible absorption at pH <1. Malvidin-3-monoglucosides visible absorbance at 520nm was at its maximum under these conditions. To ensure copigmentation, excess copigment was added so that the anthocyanin to copigment molar ratio was 1:500 (Figure 3.5 and Figure 3.6).

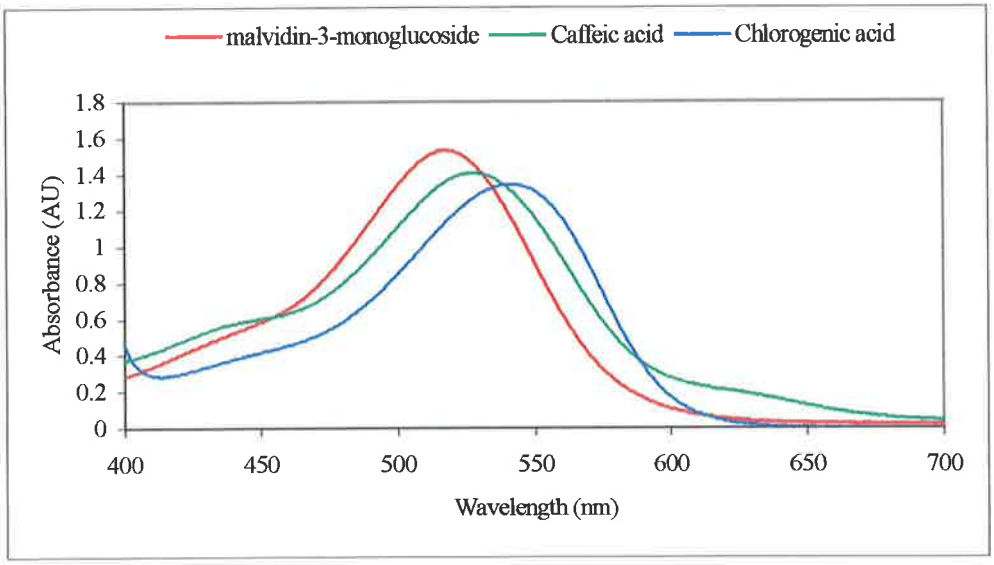

Figure 3.5 The absorption spectra of malvidin-3-monoglucoside (5 x10^{-5} molL^{-1}) and caffeic acid or chlorogenic acid (x500) at pH <1 (Temperature was 298K, l = 10mm).

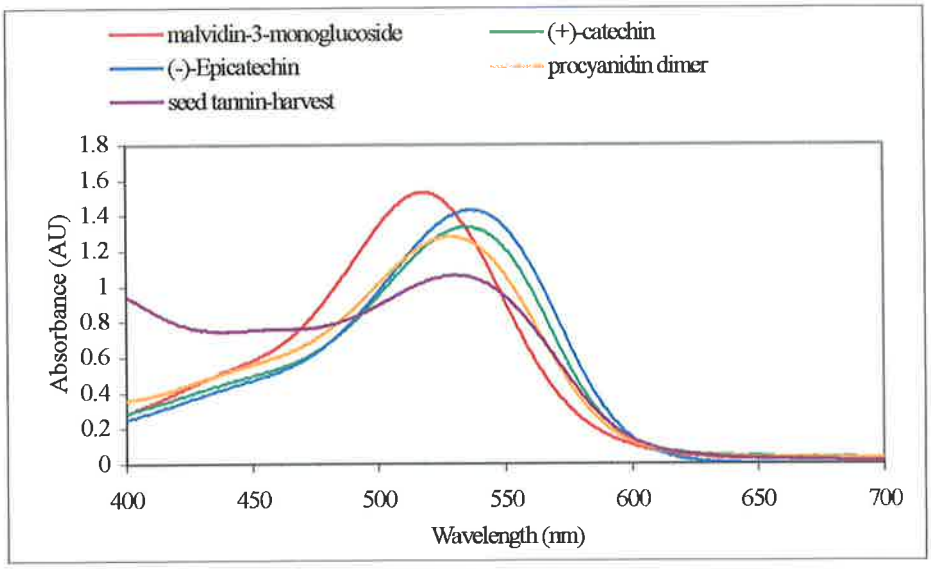

Figure 3.6 The absorption spectra of malvidin-3-monoglucoside (5 x10^{-5} molL^{-1}) and the flavan-3-ol derived copigments (x500) at pH < 1.0 (Temperature 298K, l = 10mm).

In all cases there was a shift of the absorbance maximum (λ-λ_o) to longer wavelengths and a decrease in absorbance when a copigment was added to a solution containing malvidin-3-monoglucoside (Table 3.2).

Table 3.2 Intermolecular copigmentation at pH < 1.

	λ-λ_0	A/A_o *at 520nm*
Malvidin-3-monoglucoside	-	-
Caffeic acid	8.53	0.89
Chlorogenic acid	23.89	0.76
(+)-Catechin	16.21	0.81
(-)-Epicatechin	18.77	0.84
Procyanidin dimer	11.10	0.81
Seed tannin-harvest	12.80	0.67

Where A/λ and A_o/λ_0 correspond to absorbance/absorbance wavelength maximum in the presence and absence of copigment

The results of A/A_o were used to estimate the extinction coefficients (ε) for the malvidin-3-monoglucoside and copigment complexes which were required in the calculations performed in section 2.3.1.1. (Equation 3.2).

$$A = \varepsilon lc \qquad \text{Beers Law}$$

$$A_0 = \varepsilon_{AH+}[AH^+]_0 l$$

$$A = \varepsilon_{AH+}[AH^+]l \; + \; \varepsilon_{AH(CP)+n}[AH(CP)_n{}^+]l$$

$$\text{Therefore } A/A_0 \propto \varepsilon_{AH(CP)n}/\varepsilon_{AH+}$$

Equation 3.2 The relationship of Beer's Law to the extinction coefficient of the copigment complex.

The absorbance profiles of malvidin-3-monoglucoside with quercetin and quercetin-3-monoglucoside were more difficult to determine due to their low solubility in the universal buffer solution. The copigments were prepared as saturated solutions in methanol and introduced into a solution of malvidin-3-monoglucoside at pH 1.0. The values for A/A_0 were calculated for quercetin and quercetin-3-glucoside as 0.78 and 0.71 respectively.

In all cases the calculated estimate values of $\varepsilon_{AH(CP)n}/\varepsilon_{AH+}$ were less than 1. This would indicate that the molar absorptivity of the copigment complex is less than the flavylium ion. An outcome which supports the hypothesis that enhancement in colour due to copigmentation is a consequence of a shift in the anthocyanin equilibrium towards the formation of the coloured species.

3.3.1.3 Malvidin-3-monoglucoside and copigments at pH 7.80

Intermolecular copigmentation of malvidin-3-monoglucoside and various copigments was determined at pH 7.8. Brouillard et al., (1989) suggest that the dominant anthocyanin form at this pH would be the neutral quinonoidal base (A) while others suggest it would be the mono-anion (A^-) or di-anion (A^{2-}) of the quinonoidal form (Asenstorfer, 2001). Addition of copigment resulted in colour enhancement. An example is shown in Figure 3.7.

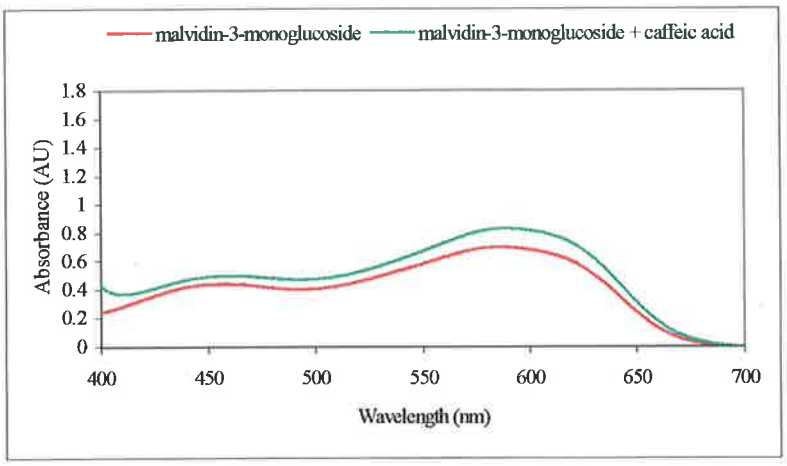

Figure 3.7 The absorption spectra of malvidin-3monoglucoside (5 x10^{-5} molL^{-1}) with caffeic acid (8 x10^{-3} molL^{-1}) at pH 7.8 (Temperature was 298K, l =10mm).

The quantitative addition of copigment to a solution of malvidin-3-monoglucoside (5 x10^{-5} molL^{-1}) resulted in very little shift of absorbance maximum to longer wavelengths. However absorbance did increase, denoting intermolecular copigmentation (Table 3.3). Very little colour enhancement was observed when quercetin was added to a solution containing malvidin-3-monoglucoside at pH 7.8. Intermolecular copigmentation at pH 7.8 was far less pronounced than that observed at pH 3.6 (Chapter 2).

Table 3.3 The effect of intermolecular copigmentation on the absorbance maximum (λ_{max}) and absorbance for malvidin-3-monoglucoside (5 x10^{-5}mol L^{-1}) with various copigments at pH 7.8.

Copigments	*Ratio anthocyanin to copigment*	λ-λ_0	A-A_0/A_0
Chlorogenic acid	1 to 160	1.15	0.138
Caffeic acid	1 to 160	1.57	0.198
Quercetin	1 to 1.8	0.29	0.049
Procyanidin dimer	1 to 160	0.72	0.397

where A/λ and A_0/λ_0 correspond to absorbance/absorbance wavelength maximum in the presence and absence of copigment

Intermolecular copigmentation of the quinonoidal base forms of malvidin-3-monolgucoside and the copigments was not a simple 1:1 relationship. The increase in absorbance as the concentration of chlorogenate anion increased (ln((A-A_o)/A_o) vs ln[copigment]) fitted a quadratic relationship (R^2 = 0.9903). Similarly, the interaction of malvidin-3-monoglucoside with the

doubly protonated caffeate anion (L^-) and neutral procyanidin dimer fitted quadratic relationships, $R^2 = 0.9960$ and 0.9604 respectively.

3.3.1.4 Influence of pH on the stability of malvidin-3-monoglucoside and (-)-epicatechin

The stability constants of malvidin-3-monoglucoside (5×10^{-5} molL^{-1}) and (-)-epicatechin at pH 3.0 and 4.0 were compared to that determined at pH 3.6 (K = 261.5 mol^{-1}L). Experimental conditions, except for the pH of the solutions, were identical to those used in the initial studies (section 2.3.1.1). (-)-Epicatechin was chosen as the copigment in this investigation due to its neutral charge at all pHs.

Intermolecular copigmentation, as typified by a shift of absorbance maximum to longer wavelengths and an increase in absorbance, was at its greatest at pH 3.6 (Figure 3.8). This result was in agreement to that observed of malvidin-3-monoglucoside with chlorogenic acid (section 3.3.1.1). Using the mathematical method developed by Brouillard et al., (1989), the stability constants for malvidin-3-monoglucoside and (-)-epicatechin at pH 3.0 and 4.0 were calculated as 223.2 and 74.03 mol^{-1}L respectively. These results were in agreement with previous findings involving copigmentation of malvin-3,5-diglucoside with either caffeic or ferulic acid where the stability constant at pH 3.65 was greater than that at pH 2.5 (Markovic et al., 2000).

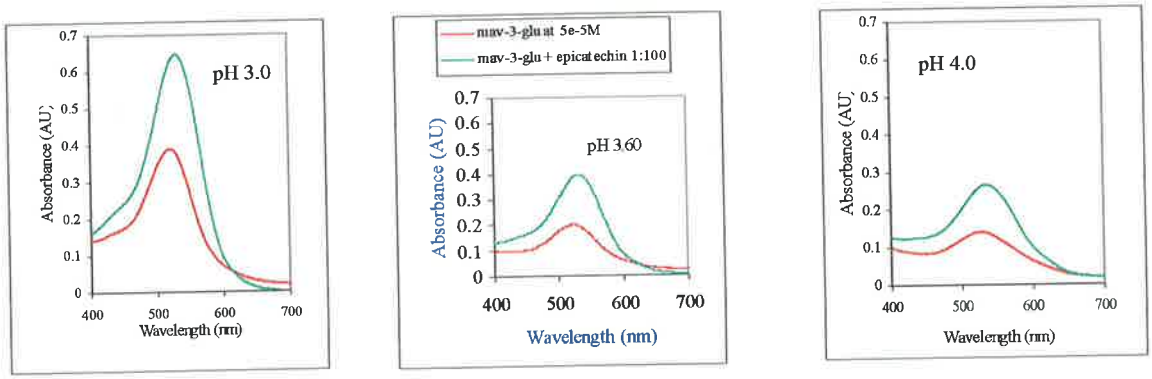

(a)

λ-λ_o = 9.38

((A-A$_o$)/A$_o$) at 520nm = 0.58

(b)

λ-λ_o = 9.39

((A-A$_o$)/A$_o$) at 520nm = 0.92

(c)

λ-λ_o = 6.83

((A-A$_o$)/A$_o$) at 520nm = 0.79

Figure 3.8 The absorption spectral profiles of malvidin-3-monoglucoside and (-)-epicatechin at various pHs at an anthocyanin to copigment molar ratio of 1:100. Malvidin-3-monoglucoside concentration is 5×10^{-5} molL^{-1} (a) pH 3.0 (b) pH 3.6 and (c) pH 4.0. All solutions were made up in universal buffer solution, at 298K and l = 10mm.

In conclusion, pH influenced intermolecular copigmentation between malvidin-3-monoglucoside and (-)-epicatechin. The colour enhancement observed with the addition of a copigment was a consequence of the stabilisation of the coloured forms (flavylium ion and/or quinonoidal neutral base) of malvidin-3-monoglucoside. The initial greater concentration of coloured species of the anthocyanins at pH 3.0 compared to 3.6 resulted in a less significant shift in the equilibrium associated with anthocyanins (Figure 3.1). Hence the copigmentation effect was less pronounced. At pH 4.0 anthocyanins exist predominantly as the colourless hemiketal. The reduction in the copigmentation effect at this pH suggests that the hemiketal did not form a copigment complex with the copigment. Hence the observed copigmentation was reduced. This supports the view that enhancement in colour due to copigmentation is a consequence of a shift in the anthocyanin equilibrium towards formation of the coloured species.

3.3.2 Influence of sulphur dioxide on intermolecular copigmentation

Experiments were undertaken to determine the affect of sulphur dioxide bleaching on the copigment complex. Two distinct malvidin-3-monoglucoside concentrations were used, either 5×10^{-5} molL^{-1} (25 mgL^{-1}) or 5×10^{-4} molL^{-1} (250 mgL^{-1}). Model solutions of malvidin-3-monoglucoside and (-)-epicatechin at an anthocyanin to copigment molar ratio of 1:100 with increasing concentration of sulphur dioxide were prepared and absorbance monitored at 520nm.

As sulphur dioxide concentration was increased in solutions containing malvidin-3-monoglucoside in the absence and presence of (-)-epicatechin there was a reduction in absorbance at 520nm (Figure 3.9 and Figure 3.10). At a malvidin-3-monoglucoside concentration of 5×10^{-5}molL^{-1} (25mgL^{-1}) the copigment complex was bleached with increasing concentration of sulphur dioxide (Figure 3.9). At a malvidin-3-monoglucoside concentration of 5×10^{-4} molL^{-1} (250 mgL^{-1}) there was a consistent 50% difference in colour expression between the anthocyanin and copigment complex solutions at all sulphur dioxide concentrations (Figure 3.10). The greater buffering capability of malvidin-3-monoglucoside at this concentration may be due to self-association of the anthocyanin (section 2.3.2). Thus anthocyanin self-association aggregates are more resistant to sulphur dioxide bleaching.

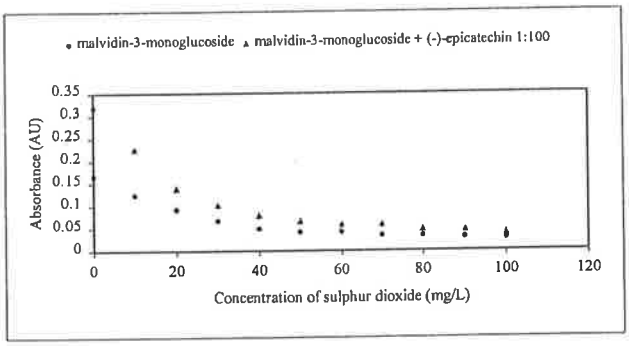

Figure 3.9 The change in absorbance with increasing sulphur dioxide concentration for malvidin-3-monoglucoside (5 x10^{-5} molL^{-1}) in the absence and presence of (-)-epicatechin (5 x10^{-3} molL^{-1}) at 298K pH 3.60 and l = 10mm.

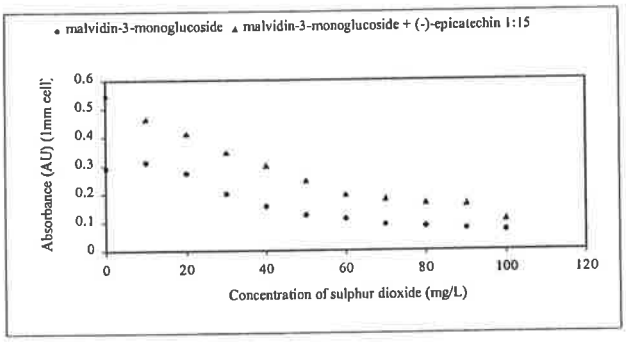

Figure 3.10 The change in absorbance with increasing sulphur dioxide concentration for malvidin-3-monoglucoside (5 x10^{-4} molL^{-1}) in the absence and presence of (-)-epicatechin (7.5 x 10^{-3} molL^{-1}) at 298K, pH 3.60 and l = 1mm.

As the concentration of sulphur dioxide concentration increased, the percentage of total colour loss also increased (Figure 3.11).

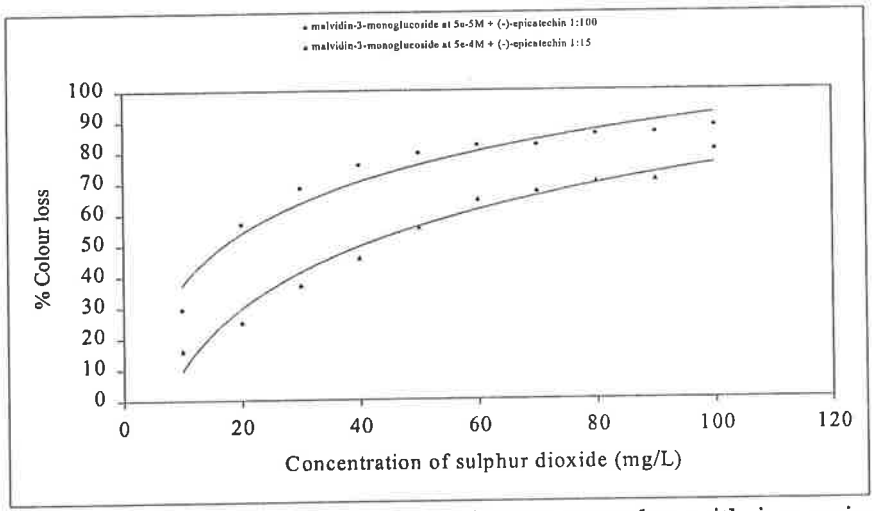

Figure 3.11 The percentage colour loss of the copigment complex with increasing sulphur dioxide concentrations. The concentration of malvidin-3-monoglucoside was either 5 x10^{-5} molL^{-1} or 5 x10^{-4} molL^{-1} with an anthocyanin to copigment molar ratio of 1:100 and 1:15 respectively.

In conclusion, the results highlighted the significant affect sulphur dioxide had on the copigment complexes. Sulphur dioxide reduced the overall colour enhancement observed when malvidin-3-monoglucoside was involved in copigmentation. This may have important consequences when related to a red wine. At a representative free sulphur dioxide level found in red wines (20mg/L) there was significant overall colour loss observed for low and medium/high concentrations of malvidin-3-monoglucoside (57% and 25% respectively). However the presence of acetaldehyde must be considered as it will reduce the concentration of free sulphur dioxide and hence the overall colour loss may be less than that calculated here.

3.3.3 Influence of ethanol on intermolecular copigmentation

As ethanol concentration increased the observed enhancement in colour expression due to intermolecular copigmentation was reduced ($(A-A_0)/A_0$) (Table 3.4).

Table 3.4 The affect of ethanol concentration on absorbance maximum ($\lambda-\lambda_o$) and absorbance on solutions of malvidin-3-monoglucoside (5 $x10^{-5}$ $molL^{-1}$) and copigment (5 $x10^{-3}$ $molL^{-1}$).

(a) chlorogenic acid molar ratio of 1:100 (anthocyanin to copigment).

% Ethanol	$\lambda-\lambda_o$	$A-A_o/A_o$
0	10.66	1.53
2	11.09	1.31
4	10.66	1.23
6	11.52	1.08
8	10.24	1.05

(b) (-)-epicatechin molar ratio of 1:100 (anthocyanin to copigment)

% Ethanol	$\lambda-\lambda_o$	$A-A_o/A_o$
0	9.39	0.92
2	9.81	0.89
6	5.12	0.50
10	5.97	0.55
12	4.70	0.54

(A/λ and A_0/λ_0 are absorbance/absorbance wavelength maximum in the presence and absence of copigment. UV buffer solution, l = 10mm, ionic strength = 0.09 $molL^{-1}$)

Intermolecular copigmentation colour enhancement was reduced by approximately 40% when ethanol concentration was similar to that observed in red wine (12%). Dufour and Sauvaitre, (2000) observed a 50% reduction in colour expression between anthocyanins and various unsaturated cyclic aroma substances such as acetosyringone and syringaldehyde in the presence of 10% ethanol.

Intermolecular copigmentation between malvidin-3-monoglucoside and chlorogenic acid or (-)-epicatechin is more exothermic (-ΔH favourable) in water/ethanol mixtures than in water (Table 3.5). This would have indicated a more favourable interaction. However, this was not the case, as emphasised by a decrease in stability constants and an increase in Gibbs Free Energy values as ethanol concentration increased.

Table 3.5 The thermodynamic parameters calculated for malvidin-3-monoglucoside (5 $x10^{-5}$ mol L^{-1}) and either chlorogenic acid or (-)-epicatechin at different ethanol concentrations. In a universal aqueous buffer solution at 298K, ionic strength 0.09 $molL^{-1}$ and pH 3.60.

(a) chlorogenic acid molar ratio of 1:1 to 1:100 (anthocyanin to copigment).

% Ethanol	R^2	*Stoichiometry*	K_1 $Mol^{-1}L$	ΔG $kJ\ mol^{-1}$	ΔH $kJ\ mol^{-1}$	ΔS $JK^{-1}\ mol^{-1}$
0	0.999	0.99	390	-14.77	-14.16	2.04
2	0.981	0.82	120	-11.91	-19.50	-25.47
4	0.991	0.99	300	-14.17	-17.71	-11.89
6	0.997	1.02	320	-14.32	-33.59	-64.63
8	0.997	1.00	280	-13.93	-30.26	-54.78

(b) (-)-epicatechin molar ratio of 1:15 to 1:100 (anthocyanin to copigment)

% Ethanol	R^2	*Stoichiometry*	K_1 $Mol^{-1}L$	ΔG $kJ\ mol^{-1}$	ΔH $kJ\ mol^{-1}$	ΔS $JK^{-1}\ mol^{-1}$
0	0.995	1.03	260	-13.80	-18.04	-14.23
2	0.984	1.03	260	-13.77	-20.76	-23.44
6	0.985	1.05	160	-12.61	-23.43	-36.31
10	0.949	1.09	240	-13.60	-21.24	-25.60
12	0.936	0.76	38	-9.01	-31.00	-73.75

A similar study involving malvidin-3-monoglucoside in the presence of (-)-epicatechin however found a greater stability constant in the presence of 12% ethanol than without (Mirabel et al., 1999). The discrepancy in the results may be a consequence of two factors.

Firstly, Mirabel et al., (1999) used a malvidin-3-monoglucoside concentration of 1.01 x 10^{-3} $molL^{-1}$ and hence would have included a significant proportion of self-association interactions. However self-association of anthocyanins is also inhibited by the presence of ethanol (Miniati et al., 1992). Secondly, the use of only 5 data points in the analysis may have also introduced errors into the calculations as the intercept (used to calculate stability constant) is determined by extrapolation and a larger number (than 5) data points is preferred.

However other researchers in agreement to the results presented here have observed a decrease in stability constants with increasing ethanol concentrations. Stability constants of malvidin-3-monoglucoside and acetosyringone or syringaldehyde were reduced by 1/3 with the addition of 10% ethanol (Dufour and Sauvaitre, 2000).

There was no clear trend between the calculated stability constants and the percentage ethanol present. In general the stoichiometry of the interactions was 1:1 indicating that one malvidin-3-monoglucoside constituent interacted with one copigment constituent.

As previously mentioned the Gibbs Free Energy, and hence the probability that the equilibrium lies towards product formation, depends on two important factors, the enthalpy and entropy. Addition of ethanol had a much larger effect on the entropy of the interaction than on the enthalpy.

The more favourable enthalpy with the addition of ethanol may be explained due to two factors. Firstly, ethanol weakens the cohesive forces holding the water molecules together causing a distortion of the tight tetrahedral network so that the net desolvation is less enthalpatically costly than in pure water. Consequently hydrophobic forces, which are a major driving force in copigment complex formation, are less energetically costly. Secondly, water has a very low polarizability (α = 1.47 $Å^3$) so the dispersion forces between pure water and the solute molecules would be weak and hence the addition of ethanol increases the solubility of the constituents (Dangles and Brouillard, 1992). This in turn reduces the energy required for interaction.

The greatest change in the thermodynamic parameters upon ethanol addition was the large decrease in entropy (ie system became more ordered). This indicated that the copigment complex was much more solvated in this solvent system compared to that in pure water. As

ethanol concentration increased the bulk solvent became more disordered with corresponding enhanced solvation of the copigment complex.

The driving force of complex formation is due to the preference of water to interact with itself in the bulk solution rather than with apolar molecules (Dangles and Broulliard, 1992). Introduction of a cosolvent is expected to reduce the hydrophobic forces leading to complexation and hence make complexation less exothermic. However with the addition of ethanol the interaction becomes more exothermic. Perhaps more importantly is the large decrease in entropy of interaction (Figure 3.12). It has been suggested that the copigment complex is preferentially solvated by the cosolvent to form a micelle like hydrophobic environment. This in turn is less enthalpically costly (Sigel et al., 1985).

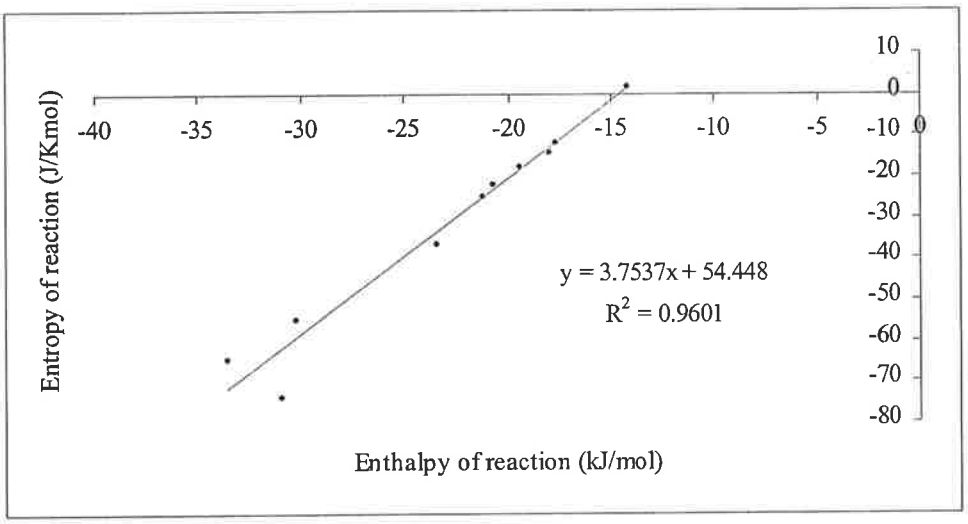

Figure 3.12 The relationship between enthalpy and entropy associated with intermolecular copigmentation as a function of ethanol concentration.

3.3.4 Influence of acetaldehyde on intermolecular copigmentation

HPLC analysis of a young red wine has shown that acetaldehyde reacts with flavonoids in the early stages of red winemaking (Saucier et al., 1997). Since intermolecular copigmentation was expected to be significant at this stage in a wines development, an experiment was carried out to determine the influence of acetaldehyde on copigmentation. A preliminary study of the direct affect of acetaldehyde on intermolecular copigmentation was investigated by measuring the change in absorbance of malvidin-3-monoglucoside (5×10^{-5} molL^{-1}) and (-)-epicatechin (5×10^{-3} molL^{-1}) with increasing concentration of acetaldehyde. It was found that acetaldehyde did not influence the colour expression of the copigment complex to any significant extent.

Model solutions of malvidin-3-monoglucoside in the presence of either (-)-epicatechin, procyanidin dimer or seed tannin (harvest) with and without acetaldehyde were analysed by HPLC over 25 days. Only the solutions that contained seed tannin (harvest) showed a significant increase in red polymer pigment concentration. This occurred both in the presence and absence of acetaldehyde. However, it was by far more pronounced in the presence of acetaldehyde which exhibited 80% greater red polymer formation than in the absence of acetaldehyde. This effect was at its maximum at 12 days and there was a slight decrease in red polymer pigment concentration at 25 days suggesting that some precipitation of a polymeric type acetaldehyde condensation product had occurred. No new pigments were detected. However this was probably a consequence of the low concentration of malvidin-3-monoglucoside (5×10^{-5} molL^{-1}) used in this investigation. Higher initial concentrations of malvidin-3-monoglucoside are required to observe new pigment formation (Fulcrand et al., 1996;Rivas-Gonzalo et al., 1995;Es-Safi et al., 1999;Saucier et al., 1997).

It may be concluded that acetaldehyde does not influence copigmentation in regards to colour expression. The copigment complex may in fact have been beneficial to the formation of acetaldehyde condensation products by aligning the two constituents in an appropriate arrangement.

3.3.5 Influence of potassium bitartrate on intermolecular copigmentation

To approximate red wine conditions an experiment was undertaken that included the addition of potassium bitartrate with and without ethanol. Potassium bitartrate has a solubility of 2.8 gL^{-1} at 20°C and an ethanol concentration of 12%. At concentrations exceeding 2.8gL^{-1} the wine is considered tartrate unstable. Potassium bitartrate in red wine is more soluble. However an addition of 2.5 gL^{-1} (0.0133 molL^{-1}) was chosen as a representative concentration. This addition of potassium bitartrate added 0.0133 molL^{-1} ionic strength to the solutions at 0.09 molL^{-1}. Consequently, ionic strength was only slightly higher than the estimate for wines ($75\text{-}85 \times 10^{-3}$ molL^{-1}) (Abgueguen and Bolton, 1993). The concentration of the salt was also insignificant in contributing to copigmentation through ion pair formation as concentrations exceeding 1 molL^{-1} are required to observe an effect (Figueiredo and Pina, 1994).

The addition of potassium bitartrate caused a significant reduction in the observed colour enhancement of malvidin-3-monoglucoside (25 mgL^{-1}) in the presence of a copigment. This reduction was best represented by plotting the relative enhancement of the individual intermolecular copigmentation solution in relation to absolute absorbance increase with the

absorbance of malvidin-3-monoglucoside in the absence of potassium bitartrate as the baseline (Figure 3.13).

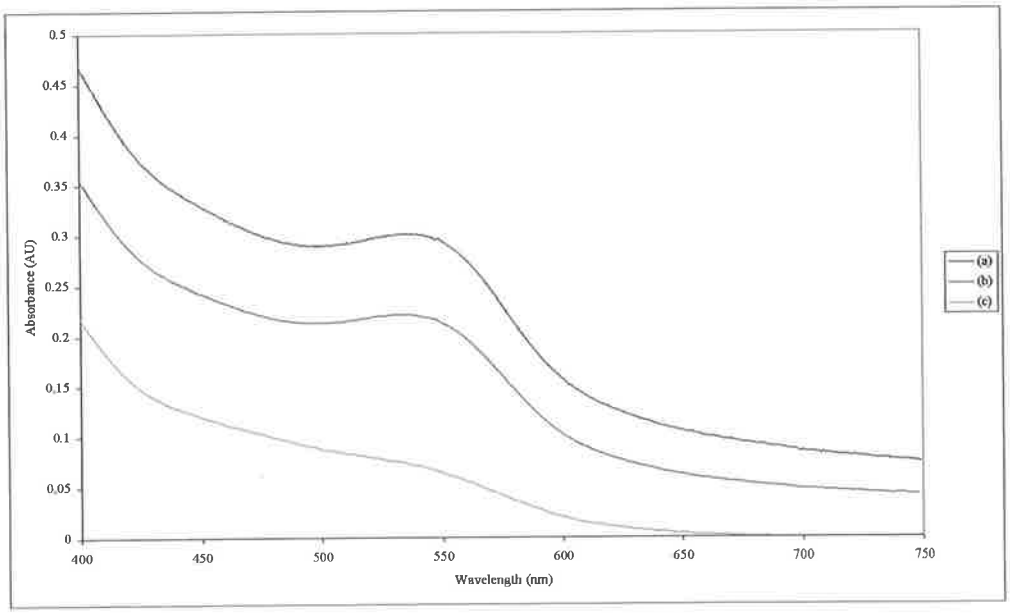

Figure 3.13 A graph of A-A_0 with malvidin-3-monoglucoside concentration 5 x10^{-5} mol L^{-1} and seed tannin molar ratio of 1:100 (a) seed tannin (b) seed tannin plus 2.5 gL^{-1} KHT (c) seed tannin plus 2.5 gL^{1} KHT plus 12% ethanol (Temperature 298K, pH 3.6, *l*= 10mm).

The addition of potassium bitartrate influenced intermolecular copigmentation between malvidin-3-monoglucoside and seed tannin (harvest) as was evident by the reduction in the stoichiometry (1.02 to 0.72) and reduction in the stability constant (417 to 56 mol^{-1} L) (Figure 3.14 (a)). Addition of 12% ethanol caused even more disruption, evident by the stoichiometry (0.49), which indicated that there was different types of interactions occurring simultaneously. The interactions could not be fitted to first order analysis (Figure 3.14 (b)).

(a) (b)

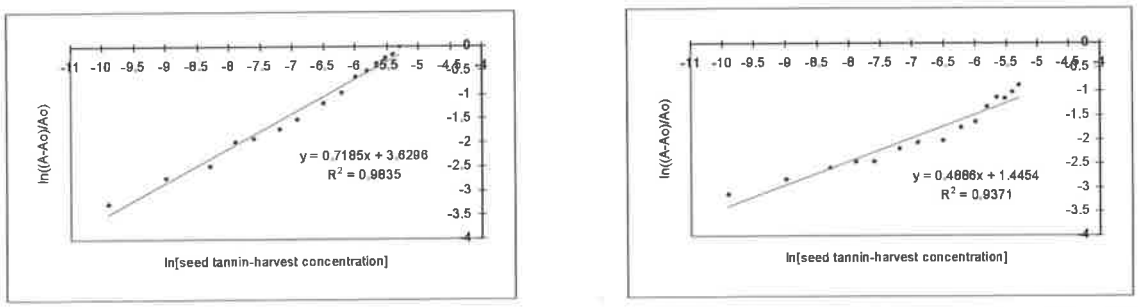

Figure 3.14 A plot of ln[((A-A_o)/A_o)] vs ln[seed tannin (harvest)]. Malvidin-3-monoglucoside concentration of 5 x10^{-5} $molL^{-1}$ with increasing seed tannin (harvest) concentration. With a potassium bitartrate concentration of (a) 2.5gL^{-1} (b) 2.5gL^{-1} and ethanol concentration of 12 % (Temperature 298K, pH 3.6 and ionic strength 0.1 $molL^{-1}$).

Increasing the concentration of malvidin-3-monoglucoside to 250 mgL^{-1} caused a slight increase in colour expression with the addition of potassium bitartrate however addition of 12% ethanol again caused a significant reduction (Figure 3.15).

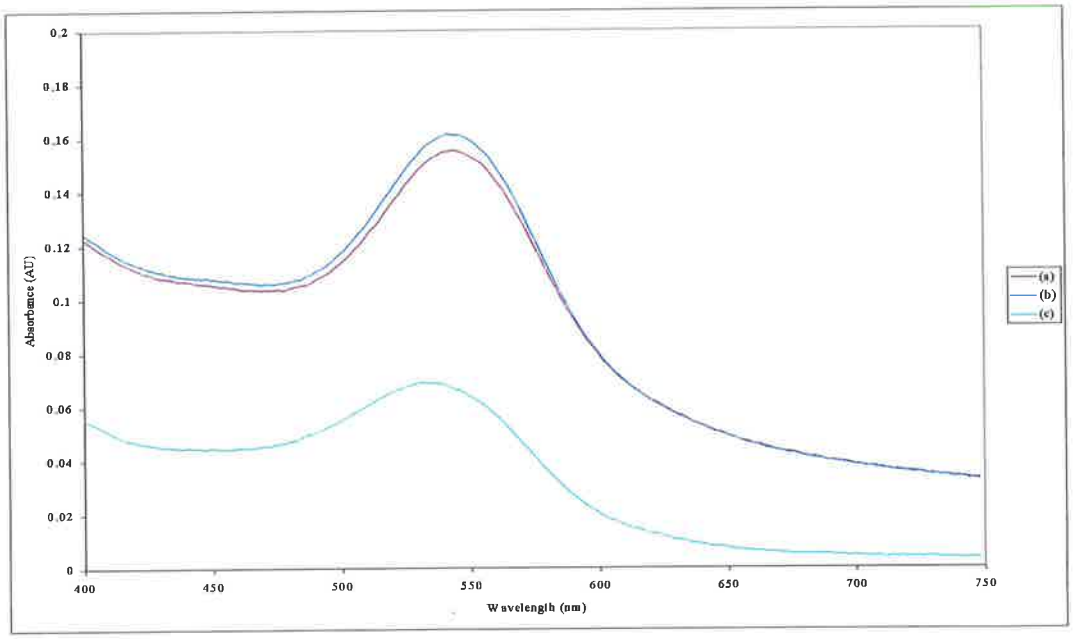

Figure 3.15 A graph of $A-A_0$ with malvidin-3-monoglucoside concentration 5 $x10^{-4}$ mol L^{-1} and seed tannin (harvest) molar ratio of 1:15 (a) seed tannin (b) seed tannin plus 2.5 gL^{-1} KHT (c) seed tannin plus 2.5 gL^{1} KHT plus 12% ethanol (Temperature 298K, pH 3.6, l= 1mm).

The stability constant of intermolecular copigmentation at this malvidin-3-monoglucoside concentration was slightly reduced in the presence of potassium bitartrate (20.39 $mol^{-1}L$) compared to in the absence of potassium bitartrate (47.79 $mol^{-1}L$). With the addition of 12% ethanol the data could not be fitted to first order functions suggesting a more complex interaction (Figure 3.16). Addition of ethanol resulted in disassociation of the malvidin-3-monoglucoside aggregates and hence the colour absorbance decreased.

(a) (b)

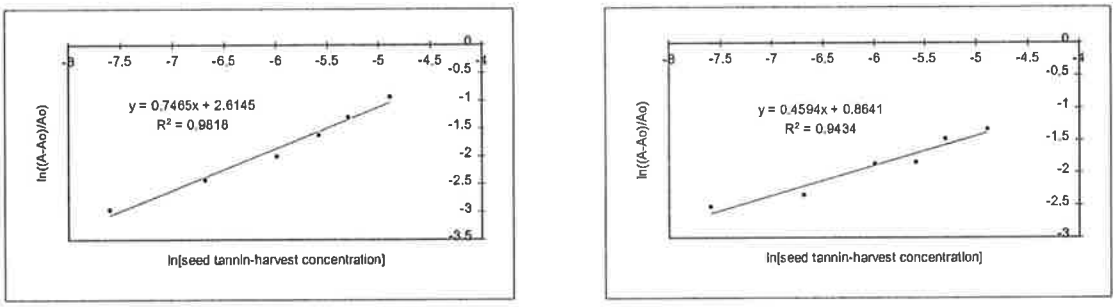

Figure 3.16 A plot of $\ln[((A-A_o)/A_o)]$ vs ln[seed tannin (harvest)]. Malvidin-3-monoglucoside concentration of 5 $x10^{-4}$ $molL^{-1}$with increasing seed tannin (harvest) concentration. With a potassium bitartrate concentration of (a) $2.5gL^{-1}$ (b) $2.5gL^{-1}$ and ethanol concentration of 12 % (Temperature 298K, pH 3.6 and ionic strength 0.1 $molL^{-1}$).

3.4 Conclusion

To obtain a full appreciation of the process of copigmentation in red wine the role of the solvent variables such as pH, sulphur dioxide, ethanol and salt concentration must be understood.

The maximum copigmentation result occurred at pH 3.6 for chlorogenic acid. However copigments with higher pK_as may exhibit maximum intermolecular copigmentation at slightly higher pHs. When variables such as sulphur dioxide, ethanol and potassium bitartrate were introduced into a model system intermolecular copigmentation was reduced. In all cases the maximum absorbance decreased with increasing concentration of sulphur dioxide, ethanol or potassium bitartrate. The effect was less pronounced at higher anthocyanin concentrations. Acetaldehyde did not affect intermolecular copigmentation between malvidin-3-monoglucoside and the copigments.

Intermolecular copigmentation increases colour expression at red wine pH 3.5-3.6. However the observed colour enhancement is not only dependent on anthocyanin concentration but also on the solvent system.

Chapter 4

Studies of copigmentation by potentiometric titration and nuclear magnetic resonance

4.1 Introduction

4.1.1 The use of potentiometric titrations to determine the ionisation constants and the copigmentation of malvidin-3-monoglucoside

Malvidin-3-monoglucoside undergoes structural transformations at various pHs (Brouillard et al., 1978;Timberlake and Bridle, 1967;Brouillard and Dubois, 1977;Brouillard and Delaporte, 1977). Ionisation constants are associated with the proton transfer reactions of the flavylium ion and quinonoidal base forms of malvidin-3-monoglucoside. The hydration reaction of the flavylium ion to form the hemiketal may be considered as a pK_H as the reaction is pH dependent.

The use of UV/visible spectroscopy to determine ionisation constants, depends upon the direct determination of the ratio of unionised molecular species to ionised species in a series of non-absorbing buffer solutions (Albert and Serjeant, 1971). UV/visible spectroscopy is applicable to systems that have pK values spanning the very acidic (<2) to the alkaline (>11) pH range. The limitation of the spectroscopic method is that knowledge of spectroscopic parameters such as absorption maxima and molar extinction coefficients is required. The ionisation constants of malvidin-3-monoglucoside were first investigated using UV/visible spectroscopy by Brouillard and Delaporte, (1977). The ionisation constant (pK_a) of the transformation of the flavylium ion form of the anthocyanin to the quinonoidal base was 4.25. The hydration constant (pK_H) of the flavylium ion to the colourless hemiketal was 2.50.

Using NMR a pK_a for the protonation of the flavylium ion to form the quinonoidal base may be calculated as 3.20 (Houbiers et al., 1998).

Another method that may give insight into the structural transformations of malvidin-3-monoglucoside is potentiometric titration. Potentiometric titration is commonly used for the determination of ionisation constants of organic compounds and also for the determination of stability constants for ligand host complexes. The ionic strength must be held constant so that the activity coefficients of the species are also held constant. When the ionic strength of the

supporting electrolyte is much greater than that of the species studied, changes in the concentration of the titrated species parallel those of their activities and stability constants are quoted as those of concentration alone (Equation 4.1).

$$[M_3v.H_n] \leftrightarrow M_3v.H_{n-1} + H^+$$

$$K_a = \frac{[M_3v.H_{n-1}][H^+]}{[M_3v.H_n]}$$

Equation 4.1 The acid dissociation of malvidin-3-monoglucoside.

An advantage of potentiometric titration is that a concentration of malvidin-3-monoglucoside, similar to that observed in red wine may be used. Potentiometric titration is not suitable for investigating species which have pK_as outside the pH range 2-11. Potentiometric titration is an alternative method to determine the ionisation constants of malvidin-3-monoglucoside and the influence of the presence of a copigment on the ionisation constants.

4.1.2 Investigation of copigmentation by nuclear magnetic resonance (NMR)

NMR spectroscopy has been extensively used in anthocyanin chemistry investigations. In addition to structure elucidation, NMR has been useful in understanding the complex equilibrium reactions involved in anthocyanin chemistry (Santos et al., 1993;Mistry et al., 1991;Cheminat and Brouillard, 1986). NMR spectroscopy has been useful in determining intermolecular interactions observed with copigmentation, such as that seen in self-association (Houbiers et al., 1998;Hoshino, 1992;Hoshino et al., 1981;Hoshino, 1982) and in intramolecular copigmentation (Gläbgen et al., 1992). Copigment complexes involving anthocyanin diglucosides have been analysed by NMR spectroscopy (Mistry et al., 1991;Wigand et al., 1992).

4.2 Materials and methods

4.2.1 Ionisation constants of malvidin-3-monoglucoside by potentiometric titration

The potentiometric titrations were performed using a Metrohm E665 Dosimat equipped with an autoburette and a Ross 8103 combination pH electrode. The titration data was controlled and collected in constant millivolt units using an IBM compatible program, AUTOTIT7. The potential readings during the titration were monitored by an Orion Research 720 Digital voltmeter. All titrations were carried out in a 10mL titration vessel, which was thermostated to 298K, by circulation of water through an outer jacket of the vessel.

A fine stream of welding grade argon, which had been humidified with 0.100 $molL^{-1}$ sodium chloride solution, was bubbled through the titration solution. The titration solution was stirred magnetically to aid mixing.

The titrant used for all the titrations was 0.094 $molL^{-1}$ sodium hydroxide that was protected from carbon dioxide by a drying tube containing silica gel. The titrant was standardised by titration of a 5 $x10^{-3}$ $molL^{-1}$ potassium hydrogen phthalate. Three replicates of these titrations were performed and the concentration of sodium hydroxide was taken as an average of the three measures.

The reference electrode was filled with 0.100 $molL^{-1}$ sodium chloride. Prior to analysis the electrode was allowed to stand for at least 12 hours to equilibrate before use. Calibration was carried out by titrating a solution of 0.01 $molL^{-1}$hydrochloric acid. The calibration was performed with constant volume increments. From the data the standard potential of the electrode (E_0) and pK_W values were determined.

The dissociation constant for the acidic protons on malvidin-3-monoglucoside were determined by titration of an acidic solution of the anthocyanin with standardised 0.094 $molL^{-1}$ sodium hydroxide. Malvidin-3-monoglucoside was weighed out to give as close as possible a 1.00 x 10^{-3} $molL^{-1}$ solution in 0.01 $molL^{-1}$ hydrochloric acid and 0.10 $molL^{-1}$ sodium chloride. A sample of this solution was taken and its absorbance measured in 1 $molL^{-1}$ hydrochloric acid. Using the extinction coefficient for malvidin-3-monoglucoside (27,900) and the dilution factors, the actual concentration of the mavlidin-3-monoglucoside solution was determined to be 5.4 $x10^{-4}$ $molL^{-1}$. Three replicate runs were performed.

Chlorogenic acid solution of 1 $x10^{-3}$ $molL^{-1}$ was made up in 0.010 $molL^{-1}$ hydrochloric acid and 0.10 $molL^{-1}$ sodium chloride were prepared. To the 10mL titration vessel 5mL of the chlorogenic acid solution and $5cm^3$ of the malvidin-3-monoglucoside were added. Three titration runs were collected for each of the chlorogenic acid concentrations.

The data, which had been collected in millivolts, were converted into pH units using a modified form of the Nernst equation,

$$pH = \frac{E_0 - E}{59.15}$$

Plots of the volume of sodium hydroxide added vs pH were then produced using Igor® wavematrics package. Acid dissociation constants were derived from the experimental data using a PC, using the Superquad program (Gans et al., 1985). The Superquad program determines the acid dissociation constants by minimisation of an error-square sum based on the measured electrode potentials. The program also allows for the refinement of the reactant concentrations and/or the standard electrode potential. The calculated fit of a single run was deemed to be statistically acceptable if it had a chi squared value less than 12.60 so to fit the 95 percent confidence level.

4.2.2 Investigation of copigmentation by ^{1}HNMR

All spectra were recorded on a Varian Inova 600 MHz Spectrometer. A buffer solution was prepared using deuterated formic acid and deuterated sodium formate in D_2O to give a pH of 3.6. A stock solution of malvidin-3-monoglucoside was prepared from a freeze dried sample of the isolated product (Chapter 2). The actual concentration of malvidin-3-monoglucoside in the stock solution was determined by UV/visible spectroscopy (Chapter 2, section 2.2.5.2). Similarly a stock solution of seed tannin in the buffer solution was prepared. Four solutions were prepared in the buffer solution comprising malvidin-3-monoglucoside at a concentration of 2.2 $x10^{-4}$ $molL^{-1}$ and seed tannin concentrations of 0, 2.5, 5 and 7.5 $x10^{-3}$ $molL^{-1}$. An internal standard of tertiary butanol (2 $x10^{-4}$ $molL^{-1}$) was used to quantify the results. The solutions were stored in the fridge for no longer than 24hrs before the analysis was carried out.

One dimensional NMR analysis was performed on the four solutions. A 2D ROESY NMR spectra was performed on the solution containing malvidin-3-monoglucoside (2.2 $x10^{-4}$ $molL^{-1}$) and seed tannin (harvest) (7.5 $x10^{-3}$ $molL^{-1}$). A ROESY experiment was conducted to determine possible through space interactions (cross peaks) between the anthocyanin and copigment. Due to operational restraints, the solutions were stored in the fridge overnight and scanned approximately 24hrs after being prepared.

4.3 Results and Discussion

4.3.1 Ionisation constants of malvidin-3-monoglucoside

Two types of titrations were carried out in the investigation of the ionisation constants of malvidin-3-monoglucoside. Firstly, pKs for the malvidin-3-monoglucoside were characterised, then secondly the change in the pKs with the addition of chlorogenic acid was investigated.

Titration of malvidin-3-monoglucoside in the presence and absence of chlorogenic acid against sodium hydroxide gave characteristic similar curves (Figure 4.1). The only difference observed between the two titrations was the volume of sodium hydroxide, which may be accounted for by the increase in hydrogen ion concentration from the chlorogenic acid addition.

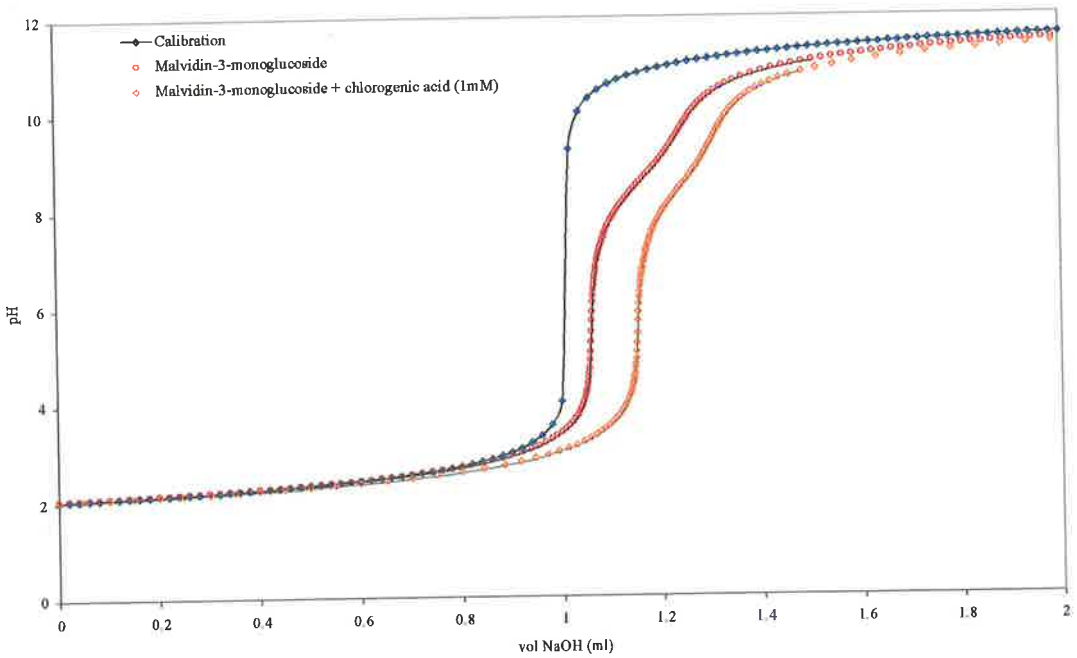

Figure 4.1 The experimental titration profiles of (a) Calibration: 0.01 $molL^{-1}$ HCl (b) Malvidin-3-monoglucoside: 5.4 $x10^{-4}$ $molL^{-1}$ and 0.01 mol L^{-1} HCl (c) Malvidin-3-monoglucoside (5.4 $x10^{-4}$ $molL^{-1}$) plus chlorogenic acid (1 $x10^{-3}$ $molL^{-1}$) and 0.01 $molL^{-1}$ HCl. All solutions were made up in milli Q water and 0.10 $molL^{-1}$ NaCl.

The solid lines through the experimental points are the curves of best fit, over the pH range investigated, extracted from the Superquad computational program. Calibration of the electrode was achieved by titrating 0.01 $molL^{-1}$ hydrochloric acid against 0.1 $molL^{-1}$ sodium hydroxide. This titration gave an electrode potential value of 379.4 and a pK_w of –13.72.

In the absence of chlorogenic acid, the calculated best fit gave ionisation constants of 2.36, 7.59, 8.59 and 9.17 for a malvidin-3-monoglucoside concentration of 5.4 $x10^{-4}$ $molL^{-1}$. In the presence of chlorogenic acid, the calculated best fit gave the same pK values as in the absence of copigment. The only added pK value was for the chlorogenic acid dissociation (pK_a 3.45). The addition of a copigment had no effect on the pKs of malvidin-3-monoglucoside.

The complex nature of the pH dependent transformations involving malvidin-3-monoglucoside made it difficult to assign the derived pKs to any particular transformation. The pK value of 2.36 determined by potentiometric titration does not coincide with any published pK values for malvidin-3-monoglucoside. It could, however, support the proposal by Asenstorfer, (2001) that the pK_{a1} and pK_{H1} of malvidin-3-monoglucoside are 1.76 and 2.66 respectively in representing a half way point between these two pKs.

Potentiometric titration indicated that the ionisation constants of malvidin-3-monoglucoside (5.4 $x10^{-4}$ $molL^{-1}$) were not affected by the presence of chlorogenic acid. Self-association and intermolecular copigmentation is thought to stabilise the red flavylium and/or the quinonoidal base form of malvidin-3-monoglucoside from hydration which forms the colourless hemiketal (Dangles et al., 1993). Results presented in Chapter 2 indicate that copigmentation is a result of a shift in anthocyanin equilibria towards formation of the coloured species. Thus, the pK_H is affected by copigment addition but the equilibrium between the flavylium ion and quinonoidal base (pK_a) is unaffected by the presence of a copigment (Brouillard et al., 1991). The formation of the coloured species is expected to be the dominant step. Thus, as expected, no change in the ionisation constants of malvidin-3-monoglucoside occurred with copigment addition.

The green colour of the final solution (pH 11) indicated that there was some blue quinonoidal di-anion (λ_{max} 596) occurring simultaneously with the yellow chalcone (Asenstorfer, 2001). As no spectroscopic data were collected during potentiometric titration, relative amounts of each form could not be determined.

The potentiometric titration method was unable to provide insight into the pK_a of the flavylium ion deprotonation to the quinonoidal base. No pK_a was detected at 4.25 as reported by Brouillard and Delaporte, (1977) but this was probably a consequence of the experimental conditions which favoured hemiketal and chalcone formation. For preference to be given to the equilibrium reaction of malvidin-3-monoglucoside to go from flavylium ion to quinonoidal base rather than hemiketal and chalcone formation, the reaction must be fast. Potentiometric

titration of malvidin-3-monglucoside took up to 4 hours to complete and therefore hydration occurred.

A typical young red wine contains a total anthocyanin concentration of approximately 400 mgL^{-1} (8.1 $x10^{-4}$ $molL^{-1}$) (Chapter 1). This is greater than the concentration of malvidin-3-monoglucoside which was used to determine the pK_a of 4.25 (4.4 mgL^{-1} or 0.9 $x10^{-5}$ $molL^{-1}$). Self-association of malvidin-3-monoglucoside has been accounted for in this investigation and hence better represents the pK_a's of malvidin-3-monoglucoside in red wine. Malvidin-3-monoglucoside is involved in complex proton transfer reactions involving both monomeric and dimerisation macro and micro ionisation constants.

4.3.2 Investigation of intermolecular copigmentation by ^{1}H nuclear magnetic resonance

To ensure consistency between NMR and UV/visible spectroscopy analyses, in regards to copigmentation, all solutions were prepared at a pH of 3.6 and a constant ionic strength of 0.1 $molL^{-1}$. Constant ionic strength assured that there was no interference from ionic activity on copigmentation of malvidin-3-monoglucoside.

The ^{1}HNMR spectra of malvidin-3-monoglucoside gave the characteristic shifts for the various structural conformations of the anthocyanin (Bakker and Timberlake, 1985;Cheminat and Brouillard, 1986;Santos et al., 1993;Fulcrand et al., 1996;Harborne, 1989). The protonation/deprotonation equilibrium is in fast exchange (Brouillard and Delaporte, 1977). Hence, the flavylium ion and quinonoidal base form appeared as a single set of signals. The precise chemical shift values were dependent on the anthocyanin concentration and the position of the equilibrium (pH dependent) (Mistry et al., 1991). The upfield shift of the proton at position 4 at pH 3.6 relative to that observed in acidic conditions (Santos et al., 1993) indicated that the equilibrium lay towards the neutral quinonoidal base (A). At pH 3.6 the chemical shifts of the nuclei indicated the presence of the quinonoidal base, hemiketals and the *cis* and *trans* chalcones (Figure 4.2).

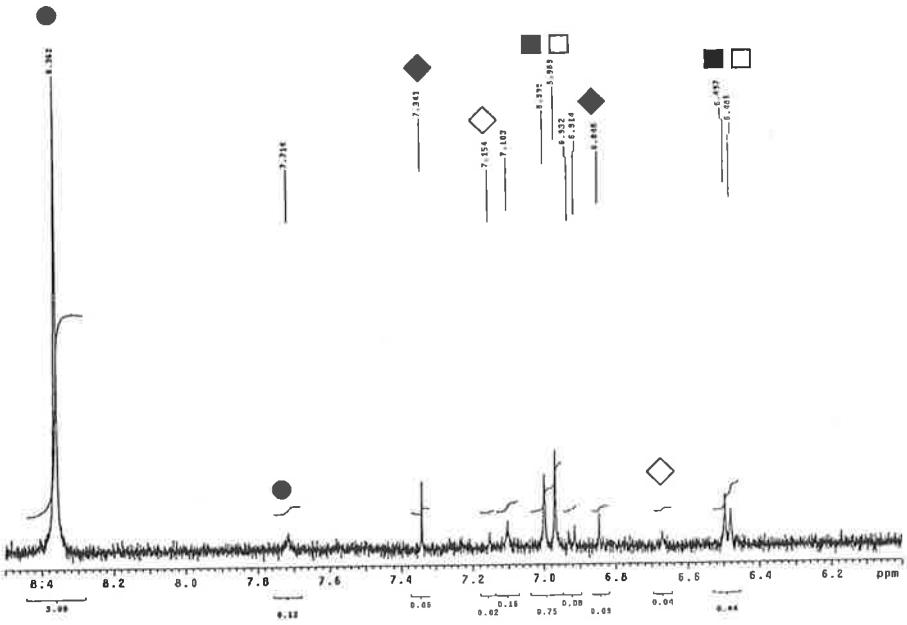

Figure 4.2 ^{1}HNMR spectra for the aromatic portion of malvidin-3-monoglucoside (2.2 x10^{-4} molL^{-1}) where ● is proton shifts associated with the quinonoidal base, ■/ R and S hemiketal and ◆/ *trans* and *cis* chalcone, pH 3.6 and ionic strength 0.1 molL^{-1}.

In agreement with other researchers, peaks associated with the quinonoidal base were detected at 8.36ppm (H4) and at δ7.71ppm (H2' and H6') (Cheminat and Brouillard, 1986;Mistry et al., 1991). The H4 proton associated with the hemiketals and chalcones occurs further upfield (between δ6.60ppm and δ6.80ppm) (Santos et al., 1993). The 2' and 6' protons of the R/S hemiketal resonated at δ7.00ppm and δ6.97ppm. Protons 6 and 8 of the hemiketal (δ6.50ppm and δ6.48ppm) were assigned from the literature (Cheminat and Brouillard, 1986;Santos et al., 1993). The peaks at δ7.34ppm and δ7.15ppm were for the 2' and 6' protons of the *trans* and *cis* chalcones respectively. The protons associated with the glucoside moiety resonated between δ3.20 and δ4.00ppm.

With the addition of seed tannin (harvest), there was a noticeable difference between the colour of the samples (Figure 4.3 and Figure 4.4). The more intense colour and slight change in hue of the sample containing the seed tannin (harvest) indicated that intermolecular copigmentation was occurring.

Figure 4.3 A comparison of the colour of the samples submitted for NMR analysis (a) malvidin-3-monoglucoside (2.2 x10^{-4} molL^{-1}) (b) malvidin-3-monoglucoside (2.2 x10^{-4} molL^{-1}) plus seed tannin (harvest) (7.5 x10^{-3} molL^{-1}).

(a) (b)

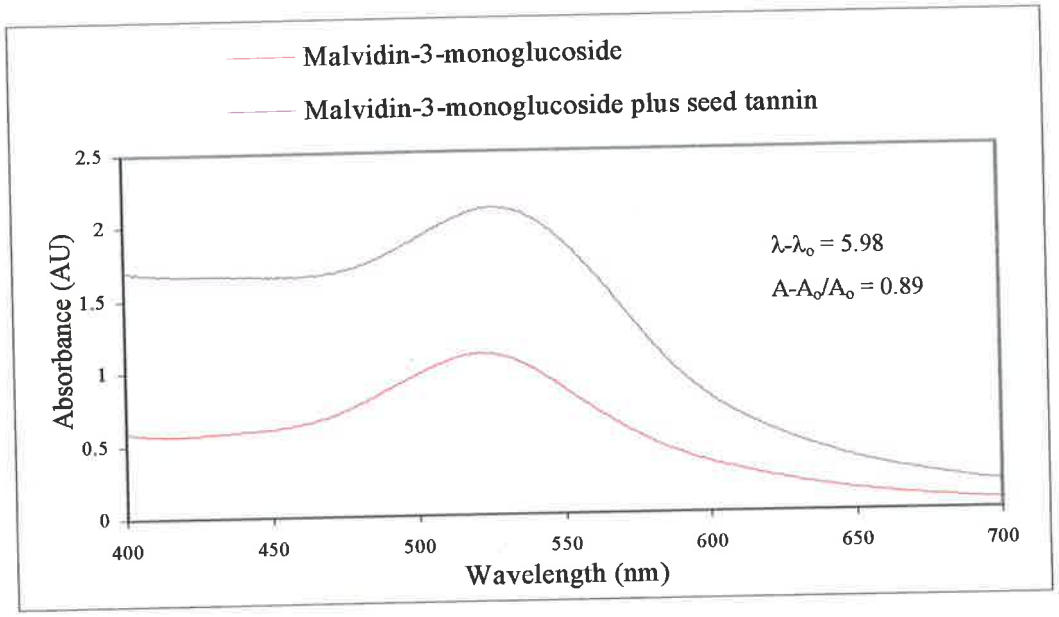

Figure 4.4 The change in the absorbance spectra of malvidin-3-monoglucoside (2.2 x10^{-4} molL^{-1}) with the addition of seed tannin (7.5 x10^{-3} molL^{-1}).

In contrast to the visible differences, the ^{1}HNMR spectra exhibited no observable change in shifts of the peaks associated with malvidin-3-monoglucoside (Figure 4.5). No changes in the chemical shifts associated with the protons of the R/S hemiketals and the *cis* and *trans* chalcones are observed.

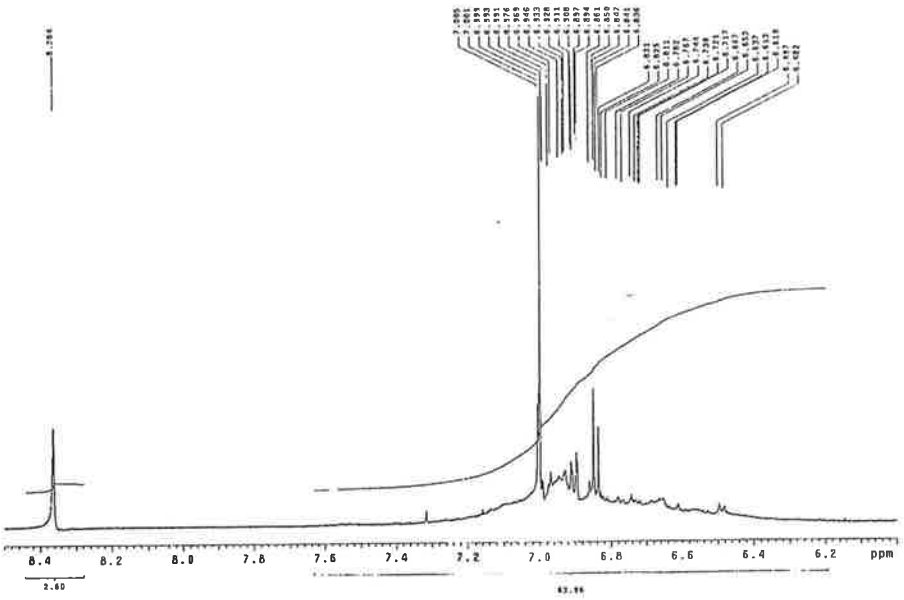

Figure 4.5 The ^{1}HNMR spectra of malvidin-3-monoglucoside (2.2 x10^{-4} molL^{-1}) with seed tannin (7.5 x10^{-3} molL^{-1}), pH 3.6 and ionic strength 0.1 molL^{-1}.

Furthermore quantification of the intensity of the peaks by using an internal standard (t-butanol) indicated that the proton at position 4 (δ8.36ppm) associated with the quinonoidal base did not increase in intensity. Enhancement in the intensity of the proton signals associated with the coloured species relative to the proton signals of R or S hemiketal has been observed in NMR experiments conducted with malvin chloride and chlorogenic acid or caffeine (Mistry et al., 1991).

The two dimensional ROESY spectra did not show any cross peaks between the anthocyanin and seed tannin (harvest) (Figure 4.6). The cross peaks that are present are associated with the protons on the seed tannin (harvest). It was difficult to ascertain the involvement of the peaks at a chemical shift of approximately 7.0ppm as many nuclei resonated in this region. There was no cross peak observed with the H4 proton of the quinonoidal base or for the protons of the hemiketal and chalcone forms.

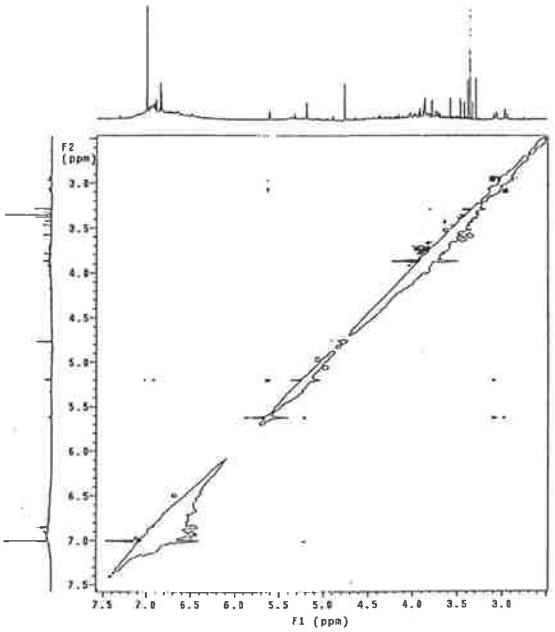

Figure 4.6 ROESY of malvidin-3-monoglucoside (2.2 x10^{-4} molL^{-1}) and seed tannin (7.5 x10^{-3} molL^{-1}), pH 3.6 and ionic strength 0.1 molL^{-1}.

The ^{1}HNMR data suggests that the anthocyanin equilibrium lay towards the quinonoidal base form rather than the flavylium ion at wine pH of 3.6. This would infer that the quinonoidal base is the primary form involved in copigmentation. The stability constants calculated (Chapter 2) for intermolecular copigmentation are still valid. The difference in absorbance between the flavylium ion and the copigment complex at acidic pH was used to estimate the extinction coefficients and hence the concentration of the copigment complex at pH 3.6.

4.4 Conclusion

The ionisation constants determined by potentiometric titration are thought to represent combined ionisation and hydration constants associated with malvidin-3-monoglucoside. The ionisation constants of malvidin-3-monoglucoside were not altered with the addition of a copigment due to the overall balancing of the equilibrium reactions.

The ^{1}HNMR data showed no change in the shifts of the proton signals associated with malvidin-3-monoglucoside upon addition of a copigment. It may be expected that an enhancement in the intensity of the proton signals associated with the coloured species relative to the proton signals of the hemiketals and chalcones would occur with copigmentation. Under the experimental conditions used in this study no significant change was observed. This may however be due to concentration factors which made such changes undetectable. The ^{1}HNMR data suggested a significant proportion of the quinonoidal base is present at red wine pH 3.6.

Chapter 5
Molecular modelling studies

5.1 Introduction

The relatively new chemical tool of molecular modelling or computational chemistry has been used to complement laboratory experimental methods. Computational chemistry provides a means by which the geometry, energies and other properties of a known or unknown molecule maybe determined. Until recently the calculations were very time consuming. However, with the rapid developments in computer technology, modern computers are powerful enough to handle large molecules with ease. Hence, computational chemistry may provide vital insight into a chemical system in addition to laboratory experimental studies.

5.2 Theoretical background to geometry optimisation calculations

The potential energy surface (PES) describes the energy associated with a particular conformation of a molecule (Figure 5.1). It is necessary to find the lowest energy conformation (global minimum) of a molecule. There is only one global minimum for a molecule, however there are additional regions of low energy termed local minima. Therefore, the global minimum represents the most stable conformation, the local minima, less stable conformations and the saddle point represents transition conformations between minima.

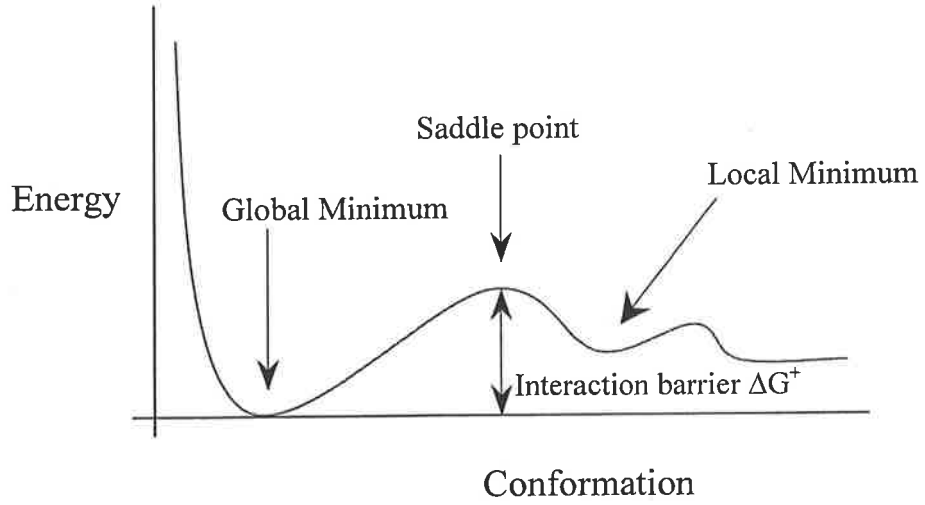

Figure 5.1 A representation of a two-dimensional potential energy profile showing the energy barriers associated with a conformation.

The ability of a geometrical optimisation to converge to a minimum will depend on the starting geometry, the potential energy function used and the settings for the convergence criteria.

5.2.1 Electronic structure models

In general, there are two types of quantum mechanical methods, *semi empirical* and *ab initio.* Both use approximations to solve the Schrödinger equation (Equation 5.1).

$$H\Psi = E\Psi$$

Equation 5.1 Schrödinger equation

Where H is the Hamiltonian operator, Ψ is the wavefunction of the positions and momenta of particles and E is the energy of the system. For the hydrogen atom, this equation may be solved exactly. However as the number of electrons increases the equation becomes more difficult to solve. Wavefunctions (Ψ) may also be used to represent the molecular wave function. Each electron is treated separately, each with its own one-electron wave function or orbital, leading to orbital approximation (Equation 5.2).

$$\Psi = \phi_1\phi_2\phi_3\phi_4.....\phi_n$$

Equation 5.2 The molecular wavefunction

The goal of quantum molecular calculations is the production of a molecular wavefunction Ψ. This may be achieved if all the constituent molecular orbitals ϕ_n are solved. A basis set is used to assign a group of atomic functions to each atom within a molecule to approximate its orbitals so that a theoretical calculation may be performed (Foresman and Frish, 1996). The choice of an appropriate basis set for a specific molecule to solve its geometric minimisation calculation is essential.

Some mathematical approximations are necessary as a concession between computational speed and accuracy of results. Electronic structure methods are characterised by their mathematical approximations to their solution (Grant and Richards, 1996). Both *semi empirical* and *ab initio* methods are based on the Hartree Fock approach where a Fock-matrix is constructed and the Hartree-Fock equations are iteratively solved. The *semi empirical* methods use simplified Fock operators making them more computationally practical compared to *ab initio* methods that use the complete Fock operator to construct the wave equation (Hehre and Huang, 1995). Whilst *ab initio* methods offer a higher quality of quantitative predictions

for more complex molecules, they are limited in their practical application because of its heavy demands on computer time.

5.3 Application of computational chemistry to copigmentation studies

Semi empirical methods are efficient and can be applied (with care) to very large molecules for which they are the only, computationally practical, quantum-mechanical method. MNDO (Modified Neglect of Differential Overlap) basis set is one of the older *semi empirical* methods and is an appropriate basis set for systems containing extensive π aromatic conjugation (Dewer and Thiel, 1977). Katritzky et al., (1990) concluded that the MNDO basis set can be used to obtain geometries for aromatic compounds which are in reasonable agreement with experimental values, except for those molecules where the number of heteroatoms in the ring exceeds the number of carbon atoms. As this was not the case in the systems investigated in this research, MNDO was chosen as the basis set. One limitation of the MNDO method is that hydrogen bonds are virtually non-existent. It also tends to over estimate the repulsion between non-bonded atoms (Foresman and Frish, 1996).

Early *semi empirical* (HMO, ω-SCF and PPSCF ASMO CI) computational studies of the structures of the anthocyanins has provided insight into their conformation (Kurtin and Song, 1968). These basis sets showed consistency with respect to predicting the electronic properties of the ground state anthocyanin molecules. Molecular orbital computations of anthocyanin excited states have also been studied using PPP SCF MO CI (Song et al., 1972). It has been suggested that in conformational studies MNDO is more efficient than the more recently developed AM1 and PM3 programs (Berski and Latajka, 1997).

Only some of the copigments being investigated in this study have already been analysed by crystal structure analysis (Einstein et al., 1985;Fronczek et al., 1993;Rossi et al., 1986;Spek et al., 1984). In some instances, such as in the case of catechin, only derivatives have been characterised. Comparing the computationally calculated bond distances and angles against those defined by crystal structure determination is a way of testing the suitability of the computational method for predicting geometric energy minimised structures for all copigments.

Geometry optimisation in the gas phase using the MNDO basis set in Gaussian 94 (Frisch et al., 1995) was used to calculate energies. The calculated bond lengths, interatomic distances and dihedral angles of the copigments may help explain the reasons for the more favourable copigmentation of some copigments relative to others, as presented in Chapter 2. Correlation

between the computer generated minimised structures and the experimental stability constants may therefore provide information in predicting suitable copigments into the investigation of pigment-copigment interactions.

5.4 Results and discussion

5.4.1 Justification of Modified Neglect of Differential Overlap (MNDO) analysis

The crystal structures of the flavonoid monomers and their derivatives provide an important data base for testing the accuracy of the algorithms used for the theoretical study of the conformations of the polymeric procyanidins. The nomenclature used in assigning bond angles and distances is presented in Figure 5.2.

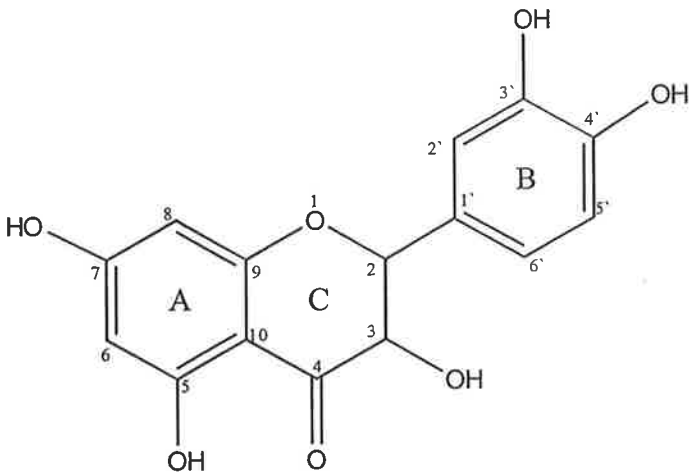

Figure 5.2 Quercetin structure illustrating the nomenclature used for structure analysis.

The bond angles and distances calculated by MNDO for quercetin, matched well with those determined by crystal structure analysis (Rossi et al., 1986). The dihedral angle between the B and C planes indicated a planer molecule as exemplified by an angle of 7° and 0° for the crystal structure (Rossi et al., 1986) and the MNDO geometry minimised structure respectively (Table 5.1).

Table 5.1 The bond distances and angles of quercetin as determined by crystal structure analysis (Rossi et al., 1986) and MNDO calculations.

	Crystal Structure	*MNDO*
O1-C2	1.37	1.37
C2-C1`	1.48	1.49
C2-C3	1.36	1.39
C3-C4	1.45	1.51
C4-C10	1.42	1.48
O1-C2-C3	121.26°	117.56°
C2-C3-C4	120.33°	122.11°
O1-C2-C1`-C2`	7°	0°

The MNDO method estimated the bond distances in the heterocyclic ring. There was a slight discrepancy between crystal structure analysis and MNDO in determining the bond distance of the carbons connected to the C4. The C4 short bond distance as determined by crystal structure analysis is a consequence of hydrogen bonding between the hydroxyl group on C5 with the oxygen on C4. C-C bond lengths calculated by MNDO methods are nearly all longer than experimental values (Katritzky et al., 1990).

The intramolecular bond between C5 and the oxygen at C4 has been reported to be equal to 2.59Å (Rossi et al., 1986). MNDO predicted an intramolecular distance of only 2.26Å. Similarly the hydroxyl group on C3 had the same H bonding distance whereas the crystal structure indicated a distance of 2.71Å. Hence MNDO tends to ignore the stronger electrostatic properties of some H-bond interactions over others. The shortest reported O-H ··· O bonds have oxygen-oxygen distance of 2.40Å (Pauling, 1960). Therefore, while MNDO appeared to have predicted hydrogen bonding (even if rather excessively) it also seemed to be adding a degree of symmetry to the molecule which does not necessarily exist according to the crystal structure determination.

With five hydroxyl groups, quercetin is involved in hydrogen bonding interactions. Two of these hydroxyl groups, C5-OH and C3-OH, are involved in intramolecular hydrogen bonding with the only hydrogen bond acceptor on the molecule itself, the exocyclic oxygen. The other three participate in intermolecular hydrogen bonding interactions with the two solvent waters of crystallisation (Rossi et al., 1986). The exocyclic oxygen is electron withdrawing, hence there are several resonance forms of the skeleton flavone structure. Ideally, the phenyl ring

would exist at a conformation perpendicular to the pyrone ring to minimise the steric hindrance between atoms. However, in order to maximise the positive contribution from a conjugated electron system, the two rings should be planer. Planer conformations of flavonoid structures exist when stabilisation of the negative charge on the exocyclic oxygen is possible. Stabilisation occurs in known crystal structures through hydrogen bonding. These interactions are strong enough to overcome the small potential energy barrier and permit the molecule to achieve planarity.

The crystal structures of (+)-catechin derivatives and (-)-epicatechin were compared with the geometrically minimised structures as determined by MNDO (Table 5.2). The crystal structure of (-)-epicatechin has been fully characterised (Fronczek et al., 1984;Spek et al., 1984). (+)-Catechin on the other hand has not been crystallised in a form suitable for structure determination. Hence (+)-catechin derivatives have been used as models and several have been analysed (Baudry et al., 1978;Einstein et al., 1985;Fronczek et al., 1993).

A comparison between the bond distances and bond angles of (+)-catechin as determined by computational analysis with the crystal structure of 6-bromo-3,3`,4`,5,7-penta-*O*-methyl catechin (Einstein et al; 1985) showed reasonable correlation. The crystal structure presented here was for a (+)-catechin derivative and therefore the heterocyclic ring system in (+)-catechin might have a somewhat different structure.

The crystal structure of (-)-epicatechin has been fully elucidated so its comparison with the MNDO results perhaps provided a more reliable result (Fronczek et al., 1984;Spek et al., 1984). As mentioned previously (-)-epicatechin differs from (+)-catechin only in that it has *cis* conformation about the C2-C3 position. Intramolecular hydrogen bonding was absent in the crystalline (-)-epicatechin and also in the MNDO calculated structure (-)-epicatechin. It should be noted that intermolecular H-bonding is possible from the hydroxyl groups.

Table 5.2 The bond distances and angles of (+)-catechin (Einstein et al., 1985) and (-)-epicatechin (Spek et al., 1984) as determined by crystal structure analysis and MNDO.

	(+)-Catechin		*(-)-Epicatechin*	
	Crystal Structure	*MNDO*	*Crystal Structure*	*MNDO*
O1-C2	1.44	1.41	1.46	1.41
C2-C1`	1.52	1.53	1.53	1.53
C2-C3	1.50	1.58	1.44	1.40
C3-C4	1.47	1.56	1.51	1.56
O1-C2-C3	111.10°	111.25°	110.50°	112.32°
C2-C3-C4	112.50°	111.07°	109.50°	109.72°
O1-C2-C3-C4	-60.0°	-51.3°	-64.0°	-52.0°
C2-C3-C4-C10	46.0°	36.6°	47.0°	39.2°
C3-C4-C10-C9	-17.0°	-15.0°	-18.0°	-14.7°
C4-C10-C9-O1	1.0°	1.6°	1°	-0.79°
C10-C9-O1-C2	-14.0°	-16.0°	-	-13.2°
C9-O1-C2-C3	42.0°	41.0°	-	40.3°
O1-C2-C1`-C2'	-	126.5°	152.2°	141.4°

Einstein et al., (1985) observed that C2 was above the plane of ring A while C3 was below the plane and that the two atoms attached to these positions (C1`(ring B) at C2 and O at C3) were located either below (half chair) or above (sofa) this plane. The B ring may also be equatorial (E conformer) or axial (A conformer). Hence, the flavan-3-ols possess a high degree of conformational flexibility. The C ring conformation may be described in the terms of the equilibrium as shown in Figure 5.3.

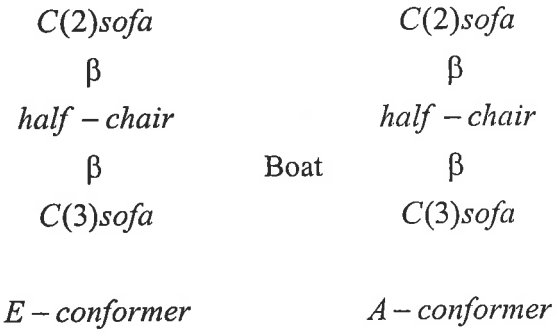

Figure 5.3 The conformations that exist for the C ring of the flavan-3-ols (Porter et al., 1986).

In the ideal C2 sofa the C3-C4-C10-C9 dihedral angle would be zero, and in the C2-C3 half chair, it would be equal to the C2-O1-C9-C10 value (Baudry et al., 1978). The boat conformation represents the high-energy transition state for the conversion of E to A conformers, or vice versa. Substitution at the C4 position by a hydroxy aryl substituent strongly favours the E-conformation.

Both the (+)-catechin and (-)-epicatechin geometry optimised structures assumed half chair conformers (C3-C4-C10-C9 = C10-C9-O1-C2) (Table 5.2). The O1-C2-C3-C4 dihedral angle, of –51° and –52° for (+)-catechin and (-)-epicatechin, respectively verifies the quasi-equatorial position of ring B (Baudry et al., 1978;Einstein et al., 1985;Spek et al., 1984). The angle was slightly underestimated by MNDO analysis (60° for crystal structures).

In conclusion, good agreement was observed between the known crystal structures of the flavan-3-ols and quercetin and those calculated using molecular modelling. There were slight discrepancies in the dihedral angles but the overall geometries were very similar. Hence MNDO can be used with confidence when analysing the anthocyanins and the other copigments.

5.4.2 Molecular modelling of anthocyanins and copigments

Malvidin-3-monoglucoside and malvidin-3-(*p*-coumaryl)glucoside were optimised as the flavylium ion form giving the molecule a net charge of +1 (Figure 5.4, Figure 5.5). Double bonds were delocalised throughout the aromatic π network. Both structures had a B ring that was out of plane with the A and C rings. The addition of an acylating group, in this case *p*-coumaric acid, resulted in a net decrease in the energy of the system (Table 5.3). The B ring and the glucose substituent were non-planar with respect to the heterocyclic ring by an angle of 55° or more. MNDO analysis of the neutral quinonoidal base also put the B ring out of plane with the A and C rings. PPP *semi empirical* SCF ASMO CI computational analysis of anthocyanidin quinonoidal bases has shown that the twist of the B ring is 45° or more (Kurtin and Song, 1968). It has been suggested that the neutral quinonoidal base is planar which would be favourable for self-association. Intramolecular copigmentation of malvidin-3-(p-coumaryl)glucoside, of *p*-coumaric acid interaction with the aromatic π rings, was not observed in the geometrically optimised structure of the flavylium ion form calculated by MNDO.

Table 5.3 The energy associated with formation of malvidin-3-monoglucoside and malvidin-3-(*p*-coumaryl)glucoside as calculated by MNDO.

	Malvidin-3-monoglucoside	*Malvidin-3-(p-coumaryl)glucoside*
Energy kJ mol^{-1}	-1215.24	-1366.35

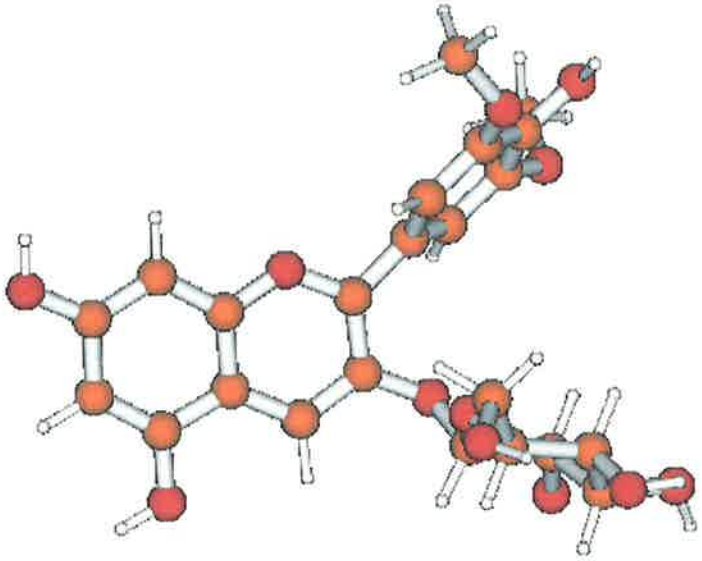

Figure 5.4 MNDO geometry optimised structure of malvidin-3-monoglucoside

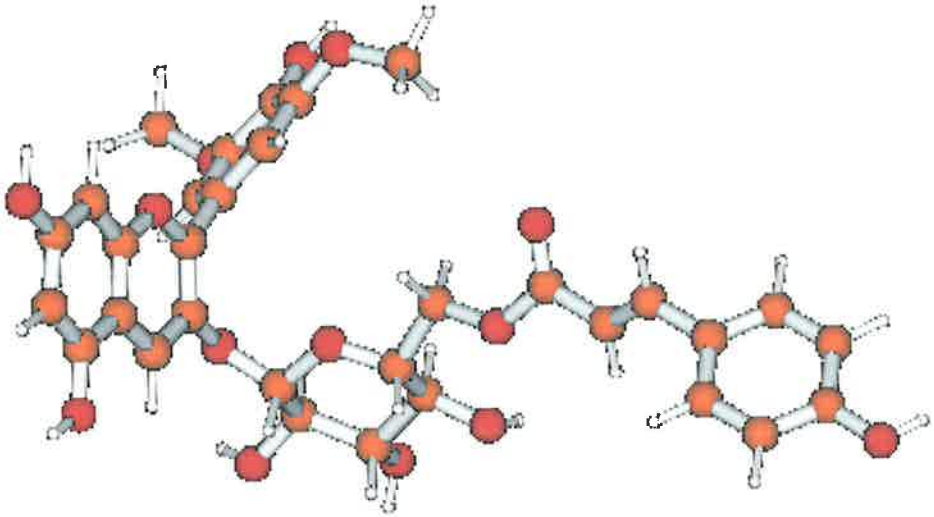

Figure 5.5 MNDO geometry optimised structure of malvidin-3-(p-coumaryl)glucoside

The geometry optimised structures of quercetin and quercetin-3-glucoside are shown in Figure 5.7, Figure 5.8, Figure 5.9 and Figure 5.10. The glucose substituent must impart a significant affect on the conformation and energetics of the copigments, as the stability constant with malvidin-3-monoglucoside varied between the systems (Chapter 2).

Due to stabilisation of its exocyclic oxygen through intramolecular H-bonding quercetin is a planar molecule (Section 5.4.1). The fractional atomic charge on the quercetin exocyclic oxygen calculated by MNDO was –0.403555 whereas in quercetin-3-glucoside it was –0.309212 indicating the much greater electron withdrawing capability of quercetin over its glucosylated derivative. The glucose substituent not only reduced the electron donating capability of the exocyclic oxygen but also imparted greater steric constraints about the aromatic rings. These combined effects leads to a non-planar B-ring (Table 5.4).

Table 5.4 The calculated dihedral angles of the flavonol copigments through the O-C2-C1`-C6` (illustrated in Figure 5.6) as determined by *semi empirical* calculations using Gaussian 94.

	Quercetin	*Quercetin-3-glucoside*
Dihedral Angle	0°	78°

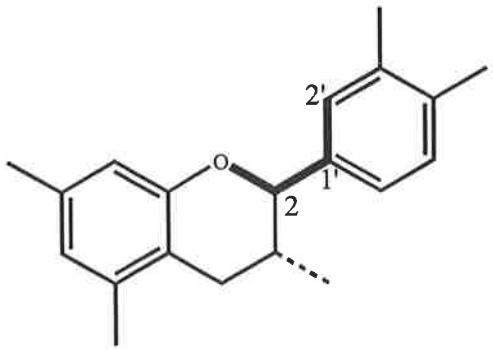

Figure 5.6 An illustration of the bonds (in bold) through which the dihedral angles were calculated for Table 5.4 and Table 5.6.

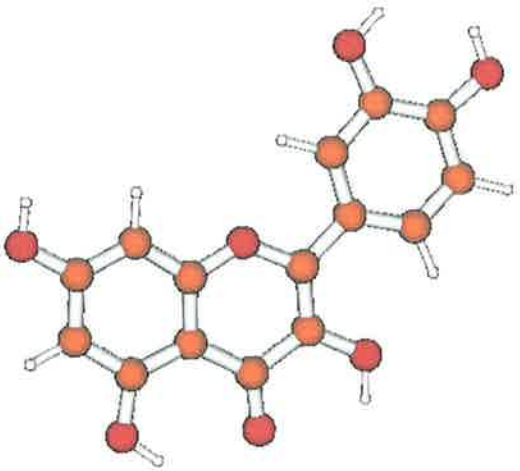

Figure 5.7 MNDO geometry optimised structure of quercetin.

Figure 5.8 View perpendicular to the AC ring for quercetin.

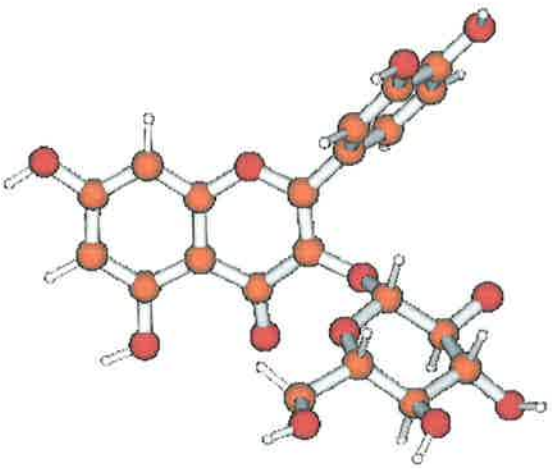

Figure 5.9 MNDO geometry optimised structure of quercetin-3-glucoside.

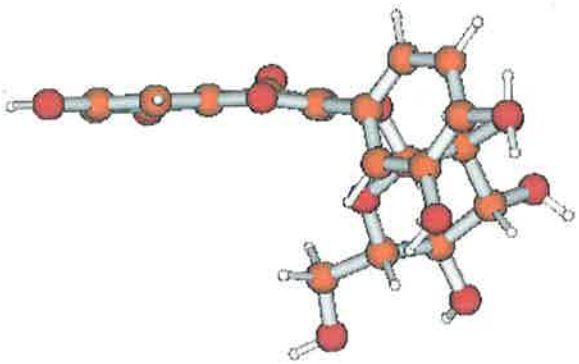

Figure 5.10 View perpendicular to the AC ring for quercetin-3-glucoside.

(+)-Catechin differs from (-)-epicatechin only in its stereochemistry of the hydroxy group at the C3 position. This had a slight influence on the energy associated with the conformer as demonstrated by the calculated energies where (+)-catechin was 3.44 kJ mol^{-1} lower in energy than (-)-epicatechin. Furthermore, as the degree of polymerisation increased, the corresponding energy of formation also decreased (Table 5.5).

Table 5.5 The energy associated with formation of the flavan-3-ols as calculated by MNDO.

	(+)-Catechin	*(-)-Epicatechin*	*Procyanidin dimer B3*	*Seed tannin pentamer*
Energy kJ mol^{-1}	-949.50	-946.06	-1796.94	-4264.74

The geometry optimised structures of (+)-catechin and (-)-epicatechin are shown in Figure 5.11, Figure 5.12, Figure 5.13 and Figure 5.14.

The conformation of the B3 (+)-catechin-(+)-catechin procyanidin as determined by geometry optimisation using MNDO showed a puckered C ring between a C2 sofa and a C2-C3 half chair (Figure 5.15). The first crystal structure of a B type procyanidin derivative to be obtained was that of (2R, 3S, 4R)-3`,4`,5,7-tetramethoxy-4-(2,4,6-trimethoxyphenyl)flavan-3-ol (Porter et al., 1986). MM2 computational calculations concluded that procyanidins containing (-)-epicatechin units had C-rings adopting a half chair E-conformation whereas those containing (+)-catechin units favoured a sofa E conformation (Porter et al., 1986).

The seed tannin pentamer strongly favoured the E-conformer as the substituents at the C4 position caused strain and repulsion effects between the aromatic rings so that the B ring assumed quasi-equatorial arrangement (Figure 5.16). It has been generally assumed that both (+)-catechin and by analogy (-)-epicatechin and their various derivatives including flavan-3,4 diols and procyanidins all adopt preferred C ring conformations with the C2 aryl group (B ring) equatorial (Table 5.6). However, if the substituent at C3 is bulky then the C ring may adopt an axial conformation with the B ring (Porter et al., 1986).

Table 5.6 The calculated dihedral angles of the flavan-3-ol copigments through the O-C2-C1`-C6` (illustrated in Figure 5.6) as determined by gas phase *semi empirical* calculations using Gaussian 94.

	(+)-Catechin	*(-)-Epicatechin*	*Procyanidin*	*Seed tannin pentamer*
Dihedral Angle	*126°*	*141°*	*122°, 128°*	*49°, 49°, 133°, 51°, 1438°* -

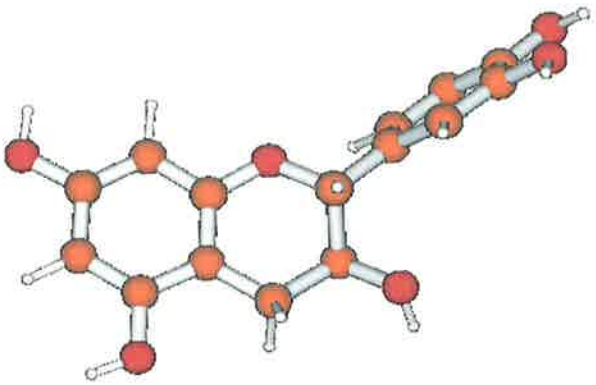

Figure 5.11 MNDO geometry optimised structure of (+)-catechin.

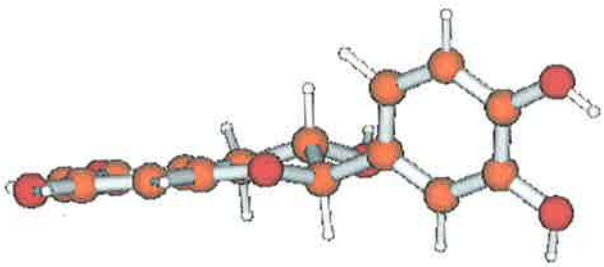

Figure 5.12 View perpendicular to the AC ring for (+)-catechin.

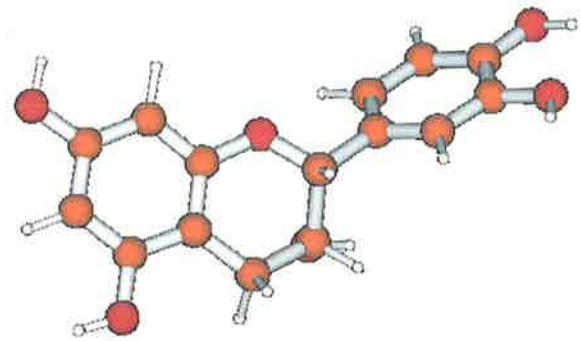

Figure 5.13 MNDO geometry optimised structure of (-)-epicatechin.

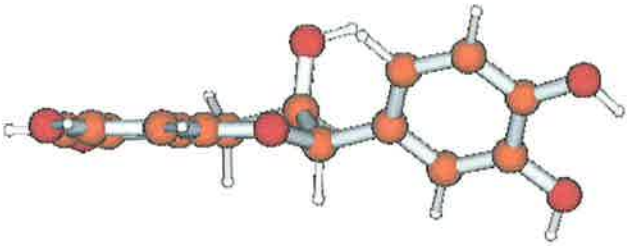

Figure 5.14 View perpendicular to the AC ring for (-)-epicatechin.

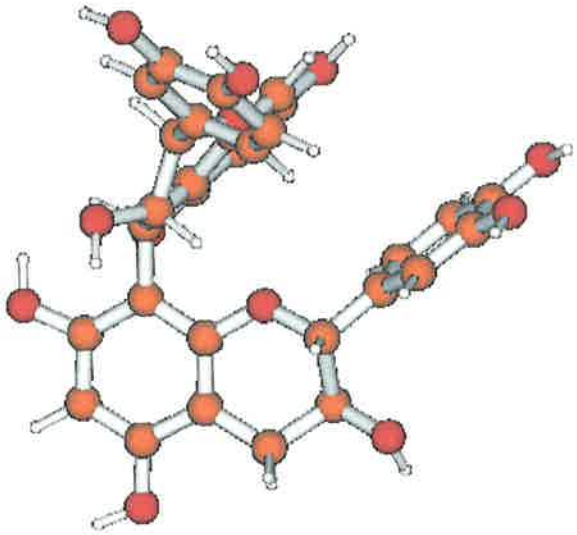

Figure 5.15 MNDO geometry optimised structure of procyanidin B3.

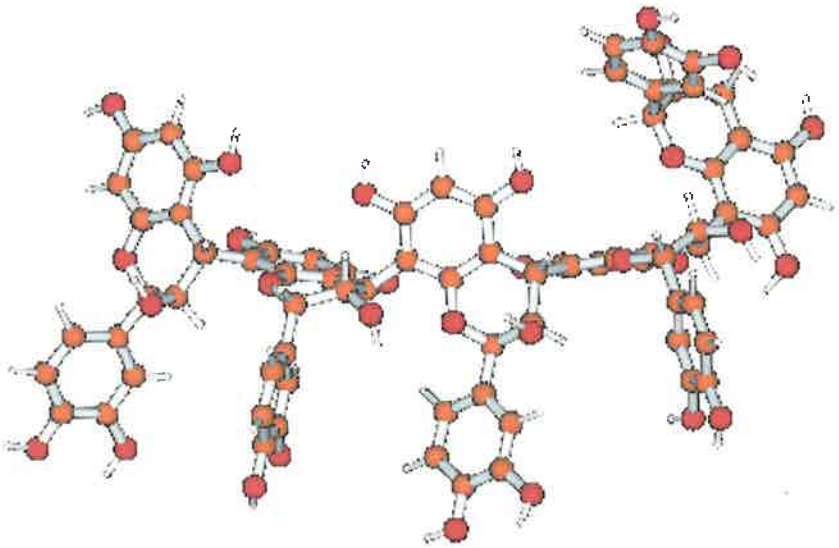

Figure 5.16 MNDO geometry optimised structure of the seed tannin pentamer with *trans* 3-4 linkages and *cis* 2-3 linkages.

5.4.3 Relationships between the calculated geometry optimised structures of copigments and their abilities to form copigment complexes with anthocyanins

Two general conclusions may be drawn from the computational geometry optimisation studies on the copigments and their stability constants with malvidin-3-monoglucoside calculated in Chapter 2. Firstly, the copigments which adopted coplanar conformations through their extended delocalised aromatic rings (eg, quercetin) or secondly that provided sufficient cavity space (eg, seed tannin) were also the copigments that exhibited the higher stability constants with malvidin-3-monoglucoside.

Of all the copigments investigated, quercetin exhibited the greatest stability with malvidin-3-monoglucoside (Chapter 2). The polarization effects of the carbonyl oxygen present in the C ring of quercetin and its planar conformation suggest that it would form an offset face to face stacking arrangement with malvidin-3-monoglucoside (Hunter and Saunders, 1990). The π deficient quercetin reduces the effect of π electron repulsion between the two aromatic systems allowing for interaction. van der Waals and solvophobic effects are optimised in face to face stacking and therefore the magnitude of the interaction is greater than in systems where π-π repulsion dominates. By analogy quercetin-3-glucoside would interact with malvidin-3-monoglucoside in a similar manner however the stability of interaction is reduced due to increased steric factors associated with the glucoside substituent. Furthermore the reduction in the electron withdrawing capacity of the exocyclic oxygen in quercetin-3-glucoside resulted in a less π deficient cloud relative to that of quercetin.

While the procyanidin B3 adopted a conformer similar to that of (+)-catechin (ring puckered half chair/sofa) rather than the more favourable (-)-epicatecin (half chair) it more readily formed an intermolecular complex with malvidin-3-monoglucoside than (-)-epicatechin (Chapter 2). Perhaps one explanation may be due to the increased electron donating/accepting capabilities of the higher oligomeric copigment. Intermolecular hydrogen bonding between the procyanidin and malvidin-3-monoglucoside may be the dominant interaction mechanism. This may also be the case with the seed tannin. The large cavity and the many potential H-bonding sites provided stabilisation for the intermolecular complex with malvidin-3-monoglucoside.

5.4.4 Intermolecular copigmentation complexes

To mimic intermolecular copigmentation an anthocyanin and copigment were orientated so that the aromatic rings were in alignment and the bulky substituents pointed away from each other. The anthocyanin was a positively charged flavylium ion while the copigment was

neutral. This was then submitted for geometry optimisation using MNDO. Two systems were investigated, one with just the anthocyanin and copigment and the other with a water molecule between the two species.

Simple donor acceptor models have been examined by *semi empirical* MNDO methods using benzene as a model for the aromatic ring and small molecules such as methanol and ammonia as the donor species (Malone et al., 1997). In all systems studied the results of the MNDO calculations gave minima beyond the 3.05A limit of interaction, as was the case in this investigation. Manually following the iterations of the geometry optimisation indicated that hydrogen bonding was occurring between the two species but this collapsed and the species moved away from each other. Hence the MNDO software does not work for multiple molecules.

The inability of MNDO to model interacting aromatic systems suggests that it does not allow for spatial charge distribution of the π electron systems. Coupled with this MNDO did not adequately predict hydrogen bonding interaction between the aromatic rings. Researchers using CHARMM (Chemistry at Harvard Macromolecular Mechanics; Brooks et al., 1983) have shown some intermolecular associations (Rathore et al., 1997).

5.5 Conclusion

The *semi empirical* MNDO geometry optimisation calculations provided information on the conformation of the anthocyanins and copigments investigated in this research. The geometry optimised structures of the monomeric compounds calculated by MNDO correlated with reported crystal structures.

The effective copigmentation of the flavonol quercetin, relative to the other copigments, with malvidin-3-monoglucoside was attributed to its deficient π system and its planer conformation. The higher oligomeric flavan-3-ols were more effective copigments than their monomeric forms due to their large cavity size and many potential hydrogen bonding sites. Both the flavylium ion and the neutral quinonoidal base forms of the anthocyanins exhibited non-planarity.

MNDO was a suitable basis set to use for determining the copigments optimised geometry. Hence MNDO may potentially be used to predict the suitability of copigments towards intermolecular copigmentation with anthocyanins.

MNDO did not adequately predict attractive π-σ interactions, polarization effects or hydrogen bonding interactions between compounds and therefore is not a suitable basis set for geometry optimisation of copigment complexes.

Chapter 6

Use of copigmentation measures in a set of red wines

6.1 Introduction

6.1.1 UV/visible spectroscopic determination of copigmentation in red wines

UV/visible spectroscopy can be used to evaluate the colour characteristics of red wines. An example is the methodology developed by Somers and Evans, (1977) for the determination of the components which contribute to the colour expression of a red wine. In the approach of Somers and Evans, (1977) several important chemical assumptions are made. The first assumption is that monomeric anthocyanins are instantly bleached by sulphur dioxide. Non sulphur dioxide bleachable components indicate protection of the C4 and C2 positions of the anthocyanin through molecular associations between species - these species are generally referred to as polymeric pigments. According to this definition the sulphur dioxide resistant pigments such as the vitisins and pigments A and B would also be classed as polymeric pigments. The second assumption is that acetaldehyde preferentially binds sulphur dioxide, so it is assumed that colour expression after this addition includes the red colour contribution from monomeric anthocyanins that were previously bleached. Essentially it measures the total colour of the wine. The third assumption is that anthocyanins are entirely in the red coloured flavylium ion form at pH < 1.

Copigmentation is also a factor that must be considered when assessing red wine colour as it involves interaction between the phenolic compounds (Brouillard et al., 1989;Levengood, 1996;Wilson and Allen, 1994).

In 1990 Somers and Pocock proposed a method to estimate the influence of copigmentation in the expression of red wine colour. They hypothesised that as a red wine is diluted and the concentration of copigment and anthocyanin declines the amount of copigment complex that can form also declines and hence colour expression is reduced. Hence the difference between the total colour measure and the colour measure of the diluted sample is a means of determining copigment complex concentration. Subsequent to the dilution approach, formulas

have been derived to determine quantitatively the copigmentation effect present in a red wine (Levengood, 1996).

The total colour expression of a red wine is a function of the concentration of monomeric anthocyanin [A], anthocyanins in the copigment complex [C] and polymeric pigments Ep[P]. These individual components which contribute to the total colour of a red wine are calculated using a series of formulas which take into account the extinction coefficients and fractions of each component present at pH 3.6 (Equation 6.1). Total colour of a red wine at pH 3.6 may be calculated as a function of all the component concentrations. It would be expected that this result would correlate well with the result obtained from the measurement of total red colour (A^{acet}_{520nm}) with the addition of acetaldehyde as proposed by Somers and Evans, (1977).

Concentration of monomeric anthocyanin (mgL^{-1})	$[A] = [(A^{100}-A^{SO2})/E^{A}] - [C]$
Concentration of anthocyanins in the copigment complex (mgL^{-1})	$[C] = (A^{acet}-A^{20})/(E^{C}-E^{A}frac)$
Polymeric pigments (AU)	$Ep[P] = A^{SO2}$
Total Colour (TC) (AU)	$TC = (E^{a}frac[A]) \times (E^{c}[C]) \times Ep[P]$
% Colour due to anthocyanins	$E^{A}[A]frac/TC \times 100$
% Colour due to copigment complex	$E^{C}[C]/TC \times 100$
% Colour due to polymeric pigments	$Ep[P]/TC] \times 100$

Equation 6.1 The copigmentation formulas developed by Levengood, (1996).
where:
E^{A} = 0.066 $AUmg^{-1}$ (based on the molar absorptivity (Linskens and Jackson, 1998) and molecular weight of malvidin-3-glucoside)
E^{C} = 3 x 0.066 = 0.198 $AUmg^{-1}$ (based on the enhancement of pelargonidin-3-glucoside in an aqueous solution (Davies and Mazza, 1993))
frac at pH 3.6 = 0.086 (estimate from the dissociation curve for malvidin using the pKa values of Brouillard and Delaporte, (1977))

It is assumed that anthocyanins in the copigment complex form are also fully bleached upon the addition of sulphur dioxide.

To date the application of the copigmentation formulas to red wines has not been extensively studied. The initial investigation conducted by Levengood, (1996) gave some insight into copigmentation measures for a set of Cabernet Sauvignon wines. In this chapter the occurrence of copigmentation in a set of experimental Shiraz and Pinot Noir wines are explored.

6.2 Materials and methods

6.2.1 General

In 1998, commercially ripe Shiraz grapes (22-25°Brix) were sourced from 14 vineyards representing different climatic and viticultural conditions. In some locations, samples were taken from vines where different irrigation regimes or trellising systems had been applied. The vineyards included two from the Riverland (a hot climate), five from the Barossa Valley (warm climate), two from Eden Valley (a cool climate), four from the Coonawarra (a cool climate) and one from Adelaide University's Waite vineyards (a warm climate). The aim was to obtain a range of grape samples that would provide a set of wines varying in colour values.

Similarly, commercially ripe Pinot Noir grapes were sourced from 5 vineyards in 1998. Four samples were from the Eden Valley region and were taken from vines where different irrigation regimes or trellising had been applied and one sample was taken from Adelaide University's Waite vineyard.

All wine samples were adjusted to pH 3.6 using 0.10 $molL^{-1}$ NaOH and centrifuged (3000rpm) twice prior to analysis. A 500mL solution of acidic buffer was prepared in distilled water by adding (i) 47.14mL of 32% HCl to give a final concentration of 0.960 $molL^{-1}$ and (ii) 60mL of absolute ethanol to give a final concentration of 12%. A 500mL solution of wine medium buffer was prepared in distilled water by adding (i) 1.25g KHT to give a final concentration of 0.01329 $molL^{-1}$and (ii) 60mL of absolute ethanol to give a final concentration of 12%. The measurements using the varying conditions were carried out as outlined below. Maturation of the red wines was carried out in a cool room adjusted to 14^0C.

In the case of the Shiraz wines, a heating trial was carried out for one month in sealed containers by placing the pH adjusted (3.6) wine samples in an incubator adjusted to 45^oC. After one month the wine samples were removed and analysed directly.

The anthocyanin concentration of berries used to make the wines, was determined by ethanol extraction of skin homogenates and visible spectroscopy as determined by Iland et al., (2000).

6.2.2 Ultraviolet/visible spectroscopy evaluation of a set of red wines

The spectrometer used was a GBC Cintra 40 spectrometer fitted with a thermostated cell holder. A Microbits personal computer was used to record all the UV/visible absorption

spectra. Absorption spectra of the sample solutions were recorded using quartz 10, 2 or 1mm cells. Temperature was controlled at 298K. The spectral bandwidth of the spectrometer was set to 2nm with a scan rate of 1000nm per minute.

The colourimetric coordinates were computerised in the CIELAB scale for the CIE D65/10° standard observer using the GBC Cintra 40 spectrometer. In this scale, each colour was numerically specified by a unique set of three cylindrical coordinates: L for lightness, a* and b* indicate change in hue from red to green and from yellow to blue respectively.

6.2.2.1 Somers and Evans spectral measures to determine red wine colour indices

A^{520} and A^{420} : Absorbance was recorded at 520nm and 420nm in a 1mm-quartz cell. The reading was corrected for cuvette pathlength by multiplying by 10.

A^{acet} : 20µl of a 10% acetaldehyde solution was added to 2mL of wine and after 45 minutes the wine sample was placed into a 1mm quartz cuvette and the absorbance measured at 520nm and 420nm. The reading was corrected for cuvette pathlength by multiplying by 10.

A^{SO2} : 30µl of a 20% $Na_2S_2O_5$ was added to 2mL of wine and mixed. The wine sample was placed in a 2mm quartz cuvette and absorbance measured at 520nm. The reading was corrected for cuvette pathlength by multiplying by 5.

A^{HCl} : 100µl of wine sample was added to 10mL of 1.0 $molL^{-1}$ HCl. After 3 hours the wine sample was placed in a 10mm quartz cuvette and absorbance measured at 520nm and 280nm. The reading was corrected for dilution by multiplying by 101.

All calculations were performed as outlined in the reference of Somers and Evans, (1977)

6.2.2.2 The copigmentation formulas of Levengood

A^{100} : 100µl of wine sample was added to 10mL of acidic buffer. After 3 hours the wine sample was placed in a 10mm quartz cuvette and absorbance measured at 520nm. The reading was corrected for dilution by multiplying by 101.

A^{20} : 100µl of wine sample was added to 1.9mL of wine condition buffer. The wine sample was placed in a 10mm quartz cuvette and absorbance measured at 520nm. The reading was corrected for dilution by multiplying by 20.

$A^{20/Acet}$: 100µl of wine sample was added to 1.9mL of wine condition buffer. In addition 20µl of a 10% acetaldehyde solution was added and left to equilibrate for 45 minutes The wine sample was placed in a 10mm quartz cuvette and absorbance measured at 520nm. The reading was corrected for dilution by multiplying by 20.

A^{SO2} : 30µl of a 20% $Na_2S_2O_5$ was added to 2mL of wine and mixed. The wine sample was placed in a 2mm quartz cuvette and absorbance measured at 520nm. The reading was corrected for cuvette pathlength by multiplying by 5.

The calculations were performed as outlined in section 6.1.1.

6.2.3 Quantitative analysis of the red wines by HPLC

The instrument used was a Hewlett Packard series 1100 HPLC machine fitted with a diode array detector. A reverse phase C-18 PLRP 5µm 100A° (Polymer laboratories) column equipped with a guard column of the same material was used. The solvent system comprised of water acidified with orthophosphoric acid (1.5% v/v) (buffer A) and 20% of buffer A in acetonitrile (buffer B). The wines were eluted under the following conditions: 1mL/min flow rate, elution with linear gradients 8% to 27% B in 55 minutes then from 27% to 52% B to 64 minutes then isocratic at 52% B for 5 minutes followed by washing and reconditioning of the column. Detection was performed at 280nm and 520nm.

6.2.4 Statistical Methods

Single factor ANOVA (with replication) analysis was utilised to test whether there was significant difference between the colour measures of the wines at the different stages of maturation (Appendix 1 and 2). Using Tukey's test for pairwise comparison, it was possible to separate the red wines into groups according to their total colour expression (TC) or copigment complex concentration as shown in Table 6.1 and Table 6.2, in section 6.3.1.

Two way ANOVA (with replication) was used to test the significance of adding sulphur dioxide to the 1 in 20 diluted samples used to calculate the copigment complex. (Appendix 3).

6.3 Results and discussion

6.3.1 Grouping of the wines into different colour characteristic categories

Based on total colour expression (TC) and concentration of the anthocyanins in the copigment complex [C] (simply referred to as copigment complex) the Shiraz wines could be grouped into four distinct groups (Table 6.1). The Pinot Noir wines formed two distinct groups in regard to total colour expression but there was no significant difference in the copigment complex concentration between the wines (Table 6.2).

Table 6.1 Total colour expression (TC) (AU) and concentration of copigment complex [C] (mgL^{-1}) for red wines (measured at completion of fermentation) made from Shiraz grapes sourced from various vineyards. Each value represents the mean of three replicates (two replicates in the case of Coonawarra 1). Values followed by different letters are significantly different at the 5% level.

	Wine	*Avg. TC*	*Avg. [C]*
1	*Waikerie Red*	4.85^{a}	9.83^{a}
2	*Waite*	5.75^{ab}	12.48^{a}
3	*Waikerie Yellow*	6.11^{ab}	14.05^{a}
4	*Eden Valley 1*	6.84^{ab}	17.16^{a}
5	*Nurioopta Irrigated*	7.96^{b}	19.54^{ab}
6	*Nurioopta Non Irrigated*	11.23^{c}	30.41^{bc}
7	*Barossa 1*	11.87^{c}	29.33^{bc}
8	*Barossa 2*	11.89^{c}	31.42^{cd}
9	*Coonawarra 1*	12.08^{c}	32.76^{cd}
10	*Coonawarra 3*	12.17^{c}	33.42^{cd}
11	*Coonawarra 2*	13.19^{cd}	32.99^{cd}
12	*Eden Valley 2*	13.20^{cd}	34.16^{cd}
13	*Coonawarra 4*	13.53^{cd}	36.73^{cd}
14	*Barossa 3*	15.25^{d}	42.34^{d}

Table 6.2 Total colour (TC) (AU) and concentration of the copigment complex [C] (mgL^{-1}) for red wines made from Pinot Noir grapes sourced from various vineyards. Each value represents the mean of three replicates. Values followed by different letters are significantly different at the 5% level.

	Wine	*Avg. TC*	*Avg. [C]*
1	*Eden Valley 2*	2.55^{a}	2.11^{a}
2	*Eden Valley 1*	2.77^{ab}	2.05^{a}
3	*Waite*	2.87^{ab}	2.37^{a}
4	*Eden Valley 4*	3.14^{b}	1.81^{a}
5	*Eden Valley 3*	3.17^{b}	1.50^{a}

6.3.2 Relationship between the components contributing to total colour and the measure of total colour expression of red wine

The focus of this research was to determine the influence of copigmentation on total red wine colour. Relationships between the components contributing to total colour and the measure of total colour expression (TC) of a red wine were investigated.

6.3.2.1 The Shiraz wines

The lower the concentration of anthocyanins in the wine, the lower the copigment complex concentration (Table 6.3). It may have been expected that these wines would have expressed the same percentage contribution of copigmentation to their total colour expression as the wines with the higher phenolic concentrations. However, this was not the case as highlighted by the positive correlation between the percentage contribution of copigmentation to total colour expression and the concentration of copigment complex (Shiraz r = 0.877***, data not shown). In general, the lower the concentration of the copigment complex, the less the contribution of copigmentation towards total colour expression. The effective formation of copigment complex in a red wine is dependent upon sufficiently high concentrations of anthocyanins.

Table 6.3 Mean values of the concentration of the copigment complex (C), monomeric anthocyanin (A), polymeric pigment (Ep[P]), percentage contribution of copigment complex, monomeric anthocyanin and polymeric pigment to total colour expression and the total colour expression (TC) for the Shiraz wines at the completion of fermentation.

Wine	*[C]* (mgL^{-1})	*[A]* (mgL^{-1})	*Ep[P]* *AU*	*%[C]*	*%[A]*	*%[P]*	*TC* *AU*
Waikerie Red	9.8	311	1.1	40.2	36.4	23.4	4.9
Waite	12.5	336	1.4	43.0	33.2	23.9	5.6
Waikerie Yellow	14.0	333	1.4	45.1	31.2	23.7	6.1
Eden Valley 1	17.1	411	1.1	49.6	34.3	16.2	6.8
Nurioopta Irrigated	19.5	480	1.4	48.5	34.4	17.1	8.0
Nurioopta Non Irrigated	30.4	593	1.8	52.7	30.6	16.6	11.2
Barossa 1	29.3	664	2.3	48.6	31.9	19.5	11.9
Barossa 2	31.5	606	2.2	52.4	28.9	18.7	11.9
Coonawarra 1	32.8	603	2.2	53.6	28.5	17.9	12.1
Coonawarra 3	33.4	602	2.1	54.4	28.1	17.6	12.2
Coonawarra 2	33.0	689	2.8	49.5	29.7	20.9	13.2
Eden Valley 2	34.2	709	2.4	51.0	30.7	18.3	13.2
Coonawarra 4	36.4	681	2.5	53.2	28.5	18.2	13.5
Barossa 3	42.3	747	2.6	55.0	27.8	17.2	15.3

The concentration of total monomeric anthocyanin concentration was 747 mgL^{-1} for the highly coloured Barossa 3 wine. However the concentration of anthocyanins in the copigment complex was only 42.3 mgL^{-1}. As previously mentioned, anthocyanins exist predominantly in the colourless hemiketal and yellow chalcone forms at pH 3.6. To put the value obtained for the concentration of copigment complex into context with total anthocyanin concentration a comparison between the Barossa 3 wine and a model solution with a similar total anthocyanin concentration ([A] + [C]) was made (Table 6.4).

Table 6.4 The calculation of the concentration of anthocyanin in copigment complex for the highly coloured Barossa 3 Shiraz wine and a model malvidin-3-monoglucoside solution at pH 3.6.

	Aacet (AU)	*A20 (AU)*	*Difference in AU*	*[C]*
Barossa 3	15.89	7.75	8.14	42 mgL^{-1}
[A] +[C]	789 mgL^{-1}			
Malvidin-3-monoglucoside absorbance	14.39 [a]	6.84 (0.342 [b] x 20)	7.55	39 mgL^{-1} [d]
Concentration associated with the absorbance value	1.55 $x10^{-3}$ $molL^{-1}$ 764.8 mgL^{-1} [c]	7.75 $x10^{-5}$ $molL^{-1}$ 38.2 mgL^{-1}		

(a) Using the absorbance values of malvidin-3-monoglucoside as its concentration increased as presented in Chapter 2 section 2.3.2.
(b) Calculated using calibration y=5349.7x-0.0725 where x is the concentration of malvidin-3-monoglucoside and y is the absorbance (max = 1). Determined at pH 3.6 in a universal buffer solution.
(c) Calculated using the extinction coefficient of 27,900 for malvidin-3-monoglucoside (493.43 $gmol^{-1}$).
(d) Calculated as per the copigmentation formulas

A model solution at pH 3.6, containing a malvidin-3-monoglucoside concentration of 764.8 mgL^{-1} gave an absorbance value of 14.39AU. The observed absorbance value for a 20 fold dilution of the model solution was calculated using the calibration formula determined for dilute solutions of malvidin-3-monoglucoside (refer to Table 6.4). The discrepancy between the overall colour expression (7.55AU) between the concentrated solution and the 20 fold diluted sample was similar to that observed in the Barossa 3 wine and may be attributed to the phenomenon of copigmentation. An analogous calculation with Waikerie red and an anthocyanin model solution exhibited a similar correlation between calculated copigment complex concentration and anthocyanin concentration. The value of the concentration of anthocyanins in the copigment complex gives no indication of what mode of copigmentation the anthocyanins are involved in i.e. self-association, intermolecular or intramolecular. The agreement between the wine and the model solutions in regards to the concentration of anthocyanins in the copigment complex would however support the notion that the principal mode of copigmentation at high total anthocyanin concentrations would be self-association.

At all stages in the production and maturation of the wines, total colour was significantly positively correlated at the 0.1% level with the concentration of monomeric anthocyanin, anthocyanins in the copigment complex and polymeric pigment (Figure 6.1).

After fermentation:

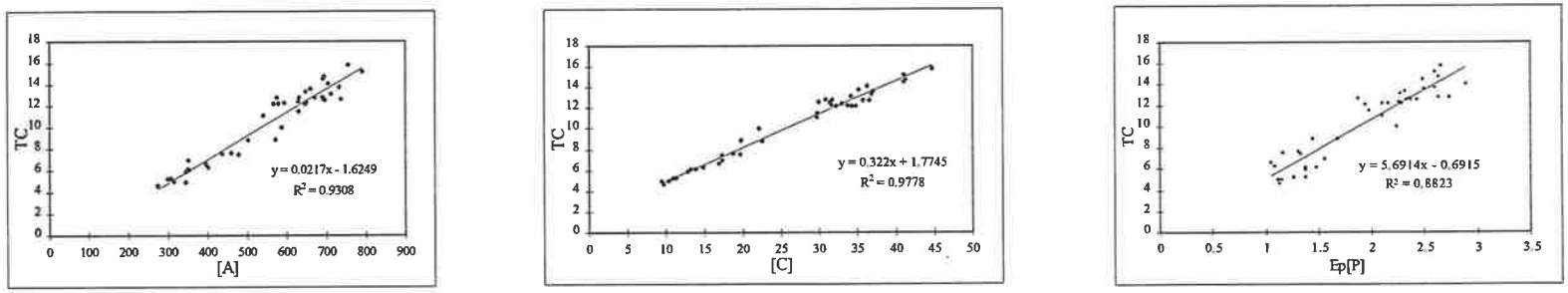

After 6 months ageing:

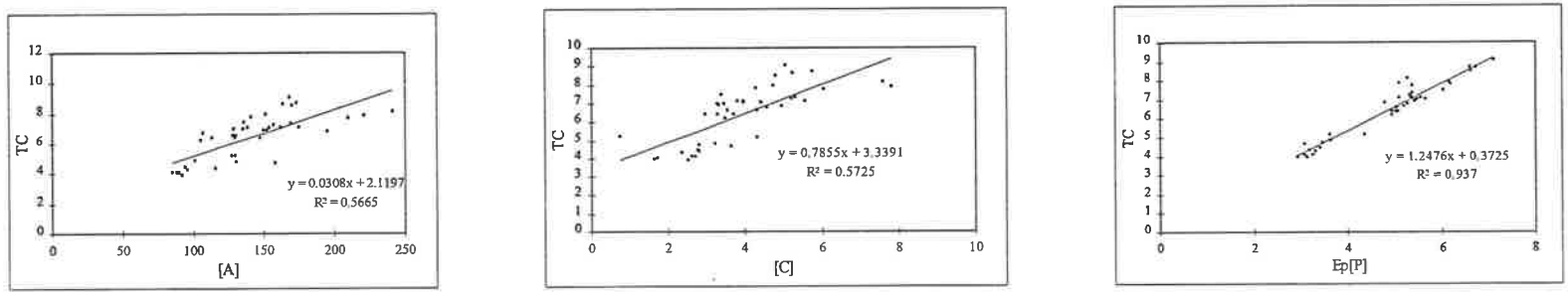

After 12 months ageing:

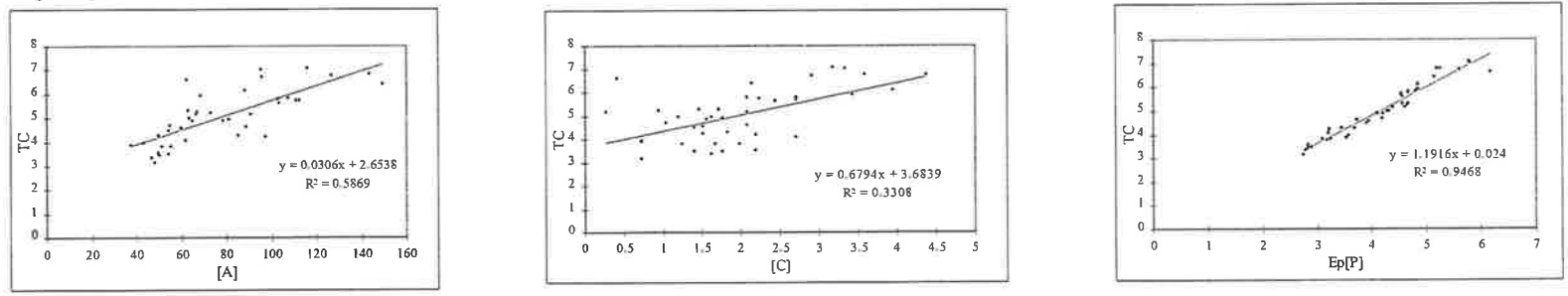

Figure 6.1 Relationship between the anthocyanin [A] (mgL^{-1}), copigment complex [C] (mgL^{-1}) and polymeric pigment Ep[P] (AU) concentration and the total colour (TC) (AU) expression of the set of Shiraz wines. All relationships were statistically significant at the 0.1% level.

At the completion of fermentation, there was a positive correlation for all three parameters however it was highest for the copigment complex concentration (Table 6.5). Even though the relationship between copigment complex concentration and total colour gave the highest correlation (r = 0.9888***) at the completion of fermentation the component that maintained a high degree of correlation throughout maturation was Ep[P] (r = 0.9393, 0.9660, 0.9730***).

Table 6.5 Correlation coefficients (r) for the relationship between (i) monomeric anthocyanin (A)(mgL^{-1}) (ii) copigment complex (C) (mgL^{-1}) (iii) polymeric pigment concentration (Ep[P]) (AU) and (iv) percentage copigment complex %[C] with total colour expression for a set of Shiraz wines

	After fermentation	*After 6 months ageing*	*After 12 months ageing*
[A]	0.9648***	0.7509***	0.7661***
[C]	0.9888***	0.7399***	0.5752***
Ep[P]	0.9393***	0.9660***	0.9730***
%[C]	0.8078***	not.signf.	not.signf.

At the completion of fermentation, the greater the concentration of copigment complex, the higher the total colour (TC) expression. To determine the relationship between anthocyanins in the copigment complex relative to monomeric anthocyanin concentration, a graph of [C]/[A] versus total colour (TC) expression was produced (Figure 6.2). The ratio of [C]/[A] increased when the anthocyanin was involved in copigmentation as opposed to being in its monomeric form. The positive correlation indicates that the more anthocyanins engaged in copigmentation at the completion of fermentation, the greater the total colour.

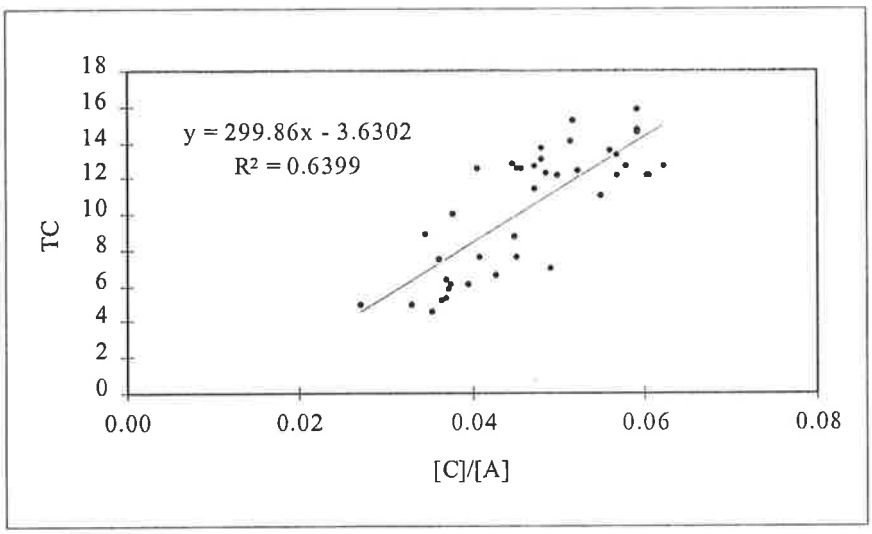

Figure 6.2 The relationship between [C]/[A] and the total colour (TC) expressed by a Shiraz wine at completion of fermentation. Statistically significant at the 0.1% level.

There was no relationship after 6 and 12 months ageing which may be attributed to the increasing importance of the polymeric pigment component to total colour (TC) expression. The relationship between polymeric pigment concentration and total colour expression was the most dominant at 6 and 12 months ageing.

The composition of the Shiraz wines changed during the course of maturation (Table 6.6). The trend of decreasing anthocyanin and copigment complex concentration with corresponding increasing polymeric pigment concentration supports the thought that copigmentation is a intermediate step in the formation of the colour stable red wine polymeric pigments.

Table 6.6 Mean values of the concentration of monomeric anthocyanins (A), copigment complex (C), polymeric pigment (Ep[P]), total colour expression (TC) and the percentage composition of the constituents for a set of Shiraz wines.

	After fermentation	*After 6 months ageing*	*After 12 months*
[A] (mgL^{-1})	553.73 ±152	140.19 ±36.99	77.27 ±27.98
[C] (mgL^{-1})	26.73 ±10.53	3.90 ±1.55	1.96 ±0.95
Ep[P](AU)	1.95 ±0.57	4.86 ±1.17	4.19 ±0.91
TC (AU)	10.38 ±3.43	6.42 ±1.52	5.02 ±1.12
%[C]	49.66 ±5.08	11.85 ±3.46	7.68 ±2.92
%[A]	31.07 ±3.30	12.51 ±2.16	8.64 ±1.941
%Ep[P]	19.27 ±2.84	75.64 ±4.58	83.68 ±4.02

The percentage contribution of the copigment complex contributing to total colour reduced to 11.85% after 6 months ageing. The percentage contribution of copigment complex in this set of Shiraz wines was considerably less than that observed in a set of 6 month old Cabernet Sauvignon wines which had on average 40% copigment complex (Levengood, 1996).

6.3.2.2 The Pinot Noir wines

Colour analysis of the Pinot Noir wines gave significantly different results to that observed for the Shiraz wines (Figure 6.3). The total colour expressed by the red wines was significantly correlated with only the total polymeric pigments present (Table 6.7). Polymeric pigments appeared to be the major contributing factor to the total colour expression at any particular time interval.

After fermentation:

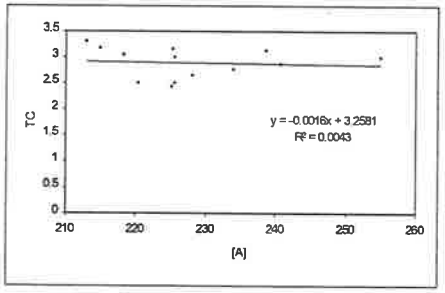

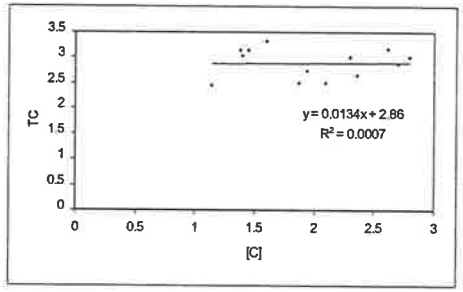

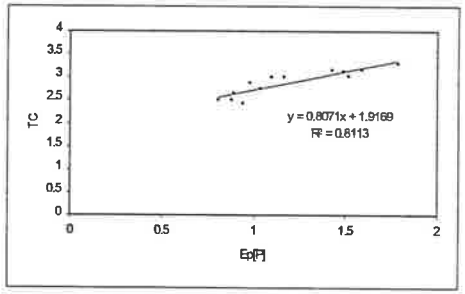

After 6 months ageing:

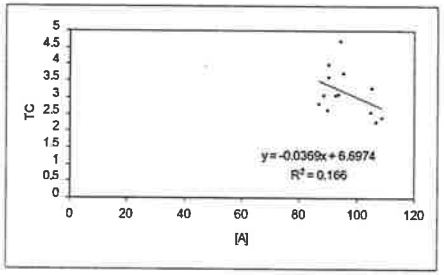

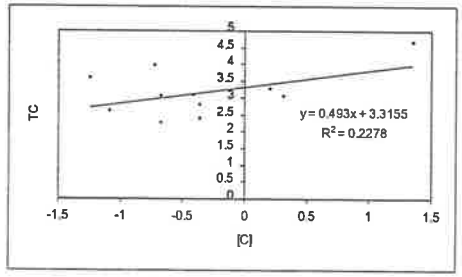

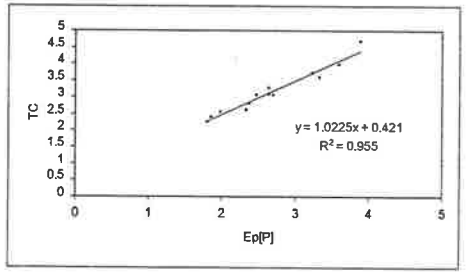

After 12 months ageing:

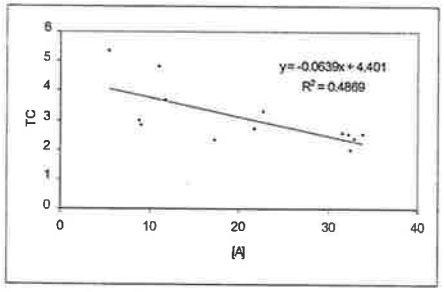

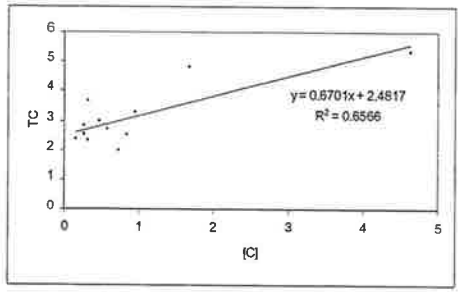

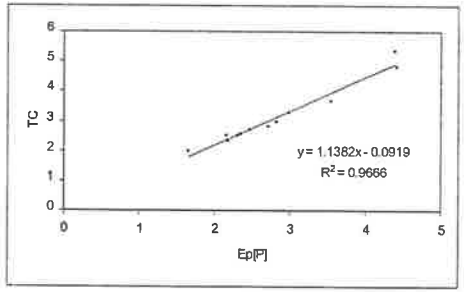

Figure 6.3 Relationship between anthocyanin [A] (mgL^{-1}), copigment complex [C] (mgL^{-1}), polymeric pigment Ep[P] (AU) and the total colour expression (AU) of Pinot Noir wines. R^2 values of greater than 0.608 indicate significance at the 0.1% level ***.

Table 6.7 Correlation coefficient (r) for the relationship between (i) monomeric anthocyanin (A) (mgL^{-1}), (ii) copigment complex (C) (mgL^{-1}) and (iii) polymeric pigment concentration (Ep[P]) (AU) with total colour expression for a set of Pinot Noir wines.

	After fermentation	*After 6 months ageing*	*After 12 months ageing*
[A]	-0.0653	-0.4074	-0.698**
[C]	0.0256	0.4773+	-0.6978(outlier present)
Ep[P]	0.9007***	0.9773***	0.9832***

In contrast to the Shiraz wines, copigment complex concentration and anthocyanin concentration did not contribute to the total colour expression of the wines. This may have been a consequence of the small range observed between the wines in respect to copigment complex concentration (section 6.3.1) or it may be partly explained by the difference in the phenolic composition between the wines. Wines made from Pinot Noir grapes do not contain acylated anthocyanins (Gao et al., 1997) and in one study were shown to have low concentrations of quercetin (Goldberg et al., 1998). Therefore, copigmentation such as self-association and intermolecular copigmentation would have been minimal in these wines (Chapter 2). Hence, the copigmentation formulas may not be applicable to red wines that have low concentrations of the anthocyanins and copigments.

The general trend of decreasing copigment complex and anthocyanin concentration with correspondingly increasing polymeric pigment concentration during the 12 months ageing period was similar in the Pinot Noir wines to that observed in the Shiraz wines (Table 6.8). However, the contribution from the polymeric pigment concentration was more predominant in the Pinot Noir wine as evidenced by its significant percentage composition at the three time intervals (Table 6.8).

Table 6.8 Mean values of the concentration of monomeric anthocyanins (A) (mgL^{-1}), copigment complex (C) (mgL^{-1}), polymeric pigment (Ep[P]) (AU), total colour expression (TC) (AU) and the percentage composition of the constituents for a set of Pinot Noir wines.

	After fermentation	*After 6 months ageing*	*After 12 months*
[A]	228.02±11.60	95.81±7.64	20.85±10.84
[C]	1.98±0.55	-0.32±0.67	0.88±1.20
Ep[P]	1.20±0.32	2.68±0.66	2.78±0.86
TC	2.89±0.29	3.16±0.69	3.07±0.99
%[A]	45.28±5.14	18.07±4.71	4.53±2.97
%[C]	13.65±3.92	-2.39±3.80	4.79±4.30
%Ep[P]	41.07±7.42	84.32±4.93	90.67±4.49

6.3.3 Relationships between the measures of monomeric anthocyanin, copigment complex and polymeric pigment at the completion of fermentation and total colour expression after 12 months aging

6.3.3.1 The Shiraz wines

Statistical analysis was performed on the data to determine possible correlations between the degree of copigmentation in the red wine with the other colour parameters as determined by the Somers and Evans, (1977) and Levengood, (1996) methodologies over the 12 months ageing period.

The parameters, which were associated with copigment complex concentration, [C], throughout the aging process were determined. These parameters which were highly significantly correlated ($p < 0.001$), were the measures of polymeric pigment concentration (Ep[P]), total colour (TC) expression and total phenolics (AU) (Table 6.9).

Table 6.9 Correlation matrices of the various parameters measured and calculated by either the Levengood, (1996)[a] or Somers or Evans, (1977)[b] methods for a set of Shiraz wines. Values shown are r (the correlation coefficient for the respective regression analysis). +, *, ** and *** indicate significance at the p<0.1, 0.05, 0.01 and 0.001 level respectively.

	After Fermentation						
	[C] a	*[A] a*	*Ep[P] a*	*%[C] a*	*TC a*	*Total anthocyanin (mg/L) b*	*Total phenol (au) b*
After Fermentation							
[C]	1.000						
[A]	0.923***	1.000					
Ep[P]	0.894***	0.913***	1.000				
%[C]	0.877***	0.687***	0.613***	1.000			
TC	0.989***	0.965***	0.939***	0.808***	1.000		
Total anthocyanin (mg/L)	0.903***	0.947***	0.931***	0.638***	0.942***	1.000	
Total phenol (au)	0.901***	0.949***	0.958***	0.629***	0.946***	0.980***	1.000
After 6 months ageing							
[C]	0.561***	0.540***	0.434**	0.517***	0.549***	0.480**	0.504***
[A]	0.568***	0.558***	0.346*	0.606***	0.543***	0.477**	0.458**
Ep[P]	0.871***	0.932***	0.837***	0.663***	0.903***	0.902***	0.895***
%[C]	0.092	0.033	0.000	0.147	0.064	-0.017	0.025
TC	0.865***	0.907***	0.782***	0.700***	0.884***	0.860***	0.857***
Total anthocyanin (mg/L)	0.333*	0.288+	0.082	0.470**	0.289+	0.198	0.183
Total phenol (au)	0.731***	0.693***	0.668***	0.621***	0.730***	0.664***	0.723***
After 12 months ageing							
[C]	-0.013	-0.025	-0.119	0.100	-0.034	-0.093	-0.096
[A]	0.226	0.222	-0.006	0.366*	0.192	0.105	0.102
Ep[P]	0.682***	0.746***	0.547***	0.598***	0.693***	0.686***	0.659***
%[C]	-0.409**	-0.457**	-0.450**	-0.246	-0.438**	-0.478***	-0.477***
TC	0.587***	0.637***	0.425**	0.557***	0.588***	0.559	0.536***
Total anthocyanin (mg/L)	-0.092	-0.137	-0.328*	0.158	-0.145	-0.267+	-0.255
Total phenol (au)	0.582***	0.512***	0.417**	0.590***	0.552***	0.427**	0.496***

The measure of the concentration of copigment complex at the completion of fermentation was significantly positively correlated at the 0.1% level with polymeric pigment concentration after 6 and 12 months ageing (Figure 6.4 and Figure 6.5).

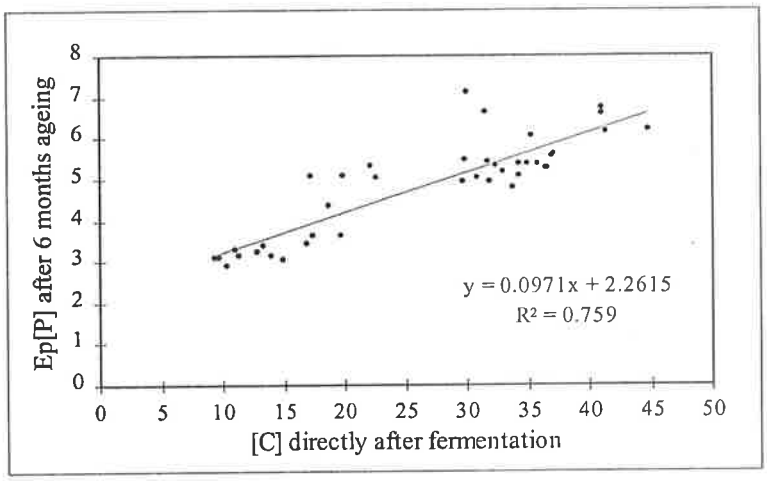

Figure 6.4 The relationship between the concentration of copigment complex (mgL^{-1}) at the completion of fermentation and its concentration of polymeric pigment (Ep[P]) (AU) at 6 months in a set of Shiraz wines.

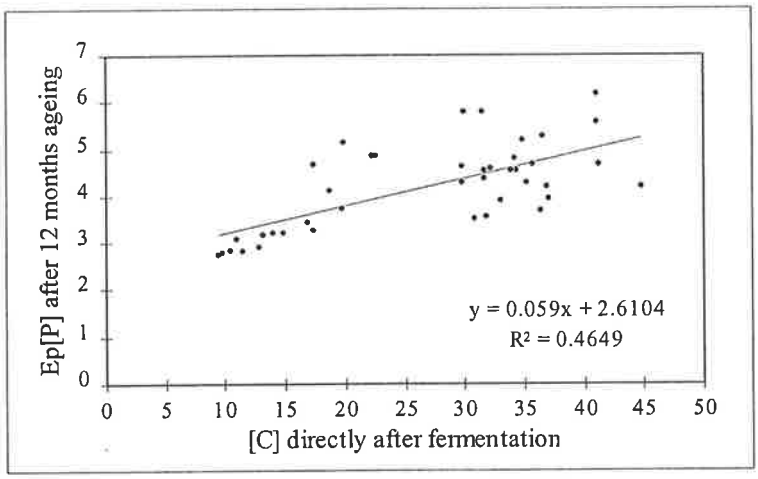

Figure 6.5 The relationship between the concentration of copigment complex (mgL^{-1}) at the completion of fermentation and its concentration of polymeric pigment (AU) at 12 months in a set of Shiraz wines.

Total colour (TC) expression and polymeric pigment concentration after 12 months ageing were positively correlated at the 0.1% level with the concentration of the copigment complex and the total monomeric anthocyanin concentration present at the completion of fermentation. This supports the hypothesis that self-association of the anthocyanins or anthocyanin intermolecular copigmentation with a copigment leads to formation of the colour stable red wine polymeric pigments. Consequently, the more anthocyanins and copigments available to act as substrates in these interactions at the completion of fermentation, the greater the concentration of the polymeric pigments and total colour expressed at 12 months.

In section 6.3.2.1 the importance of the contribution of the polymeric pigments to total colour expression of the Shiraz wines at any particular time interval was highlighted. However, the best indicator directly after fermentation, for predicting the total colour expression after 12 months aging, was that of total monomeric anthocyanin concentration ($r = 0.637$).

6.3.3.2 The Pinot Noir wines

Correlation analysis of the Pinot Noir wines showed that copigmentation in the Pinot Noir wines was not correlated with the other colour parameters throughout the ageing process (Table 6.10).

Table 6.10 Correlation matrices of the various parameters measured and calculated by either the Levengood, (1996)[a] or Somers or Evans, (1977)[b] methods for a set of Pinot Noir wines. Values shown are r (the correlation coefficient for the respective regression analysis). +, *, ** and *** indicate significance at the p<0.1, 0.05, 0.01 and 0.001 level respectively.

	← After Fermentation →					
After Fermentation →	*[C][a]*	*[A][a]*	*Ep[P][a]*	*TC[a]*	*Total anthocyanin (mg/L)[b]*	*Total phenol (au)[b]*
After Fermentation						
[C]	1.000					
[A]	0.227	1.000				
Ep[P]	-0.363	-0.340	1.000			
TC	0.026	-0.065	0.901***	1.000		
Total anthocyanin (mg/L)	0.667**	0.531+	-0.631*	-0.330	1.000	
Total phenol (au)	0.499+	0.285	0.030	0.288	0.737**	1.000
After 6 months ageing						
[C]	-0.109	0.151	-0.269	-0.307	-0.033	-0.368
[A]	0.146	0.017	0.371	0.473+	-0.106	0.123
Ep[P]	0.075	0.347	-0.687**	-0.659*	0.535*	0.081
TC	0.060	0.362	-0.685**	-0.659*	0.498+	0.015
Total anthocyanin (mg/L)	0.103	-0.176	0.589*	0.656*	-0.420	-0.071
Total phenol (au)	0.172	0.527+	-0.438	-0.303	0.615*	0.467+
After 12 months ageing						
[C]	-0.302	-0.051	-0.285	-0.444	0.134	-0.085
[A]	0.113	-0.130	0.528+	0.603*	-0.328	-0.022
Ep[P]	0.137	0.436	-0.617*	-0.537*	0.633*	0.261
TC	0.053	0.357	-0.569*	-0.533*	0.559*	0.204
Total anthocyanin (mg/L)[c]	-	-	-	-	-	-
Total phenol (au)	0.349	0.623*	-0.398	-0.171	0.780***	0.634*

(c) Total anthocyanin (mg/L) concentration after 12 months ageing was negative

The best indicator directly after fermentation, in predicting the total colour expression after 12 months ageing, was that of the polymeric pigment concentration (r = -0.569*). In contrast to the Shiraz wines the relationship was negative, indicating that the more polymeric pigments present at the completion of fermentation, the lower the total colour expression after 12 months ageing.

While copigmentation interactions did occur, they did not appear to be significant in relation to total colour expression. More extensive analysis of Pinot Noir wines would have to be conducted to verify these results.

6.3.4 Relationship between the skin colour of Shiraz grape berries and the wines processed from the grapes

The skin colour (mg anthocyanin/g berry weight) was directly related, at the 0.1% significance level, to the colour measures of the wines at the completion of fermentation (Table 6.11).

Table 6.11 Correlation matrices between the skin colour of Shiraz berry (mg anthocyanin/g berry weight) and the red wine copigmentation measures of Levengood, (1996) and the colour density measures of Somers and Evans, (1977) at the completion of fermentation.

	Skin colour (mg anthocyanin /g berry weight)
[A]	0.9163***
[C]	0.8556***
Ep[P]	0.8808***
TC	0.8963***
%[C]	0.6688***
Colour density	
-finished	0.8733***
-predicted at pH 3.6 (modified for effects of SO_2)	0.9035***

The greater the skin colour of the berry the greater the total colour expression of the corresponding wine at the completion of fermentation (Figure 6.6).

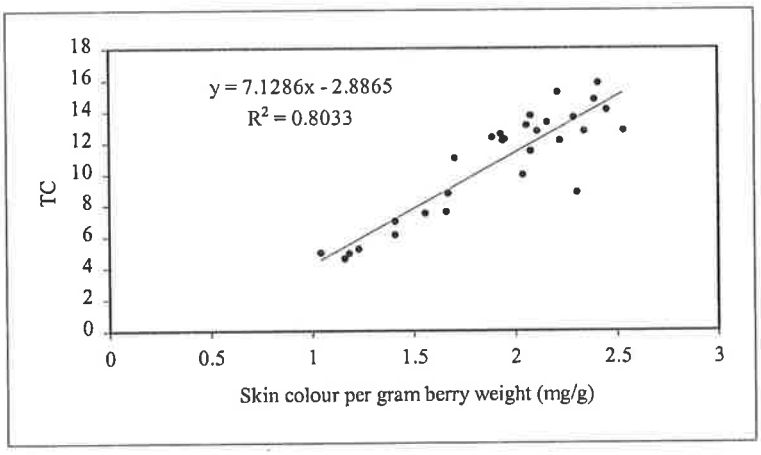

Figure 6.6 The relationship between skin colour per gram berry weight (mgg^{-1}) and the total colour for the set of Shiraz wines at the completion of fermentation.

6.3.5 Relationship between HPLC and UV/visible spectroscopy red wine colour measures

Using a modified HPLC technique developed by Price, (1994) for determining the amount of anthocyanins and polymeric pigment in a wine sample, the concentration of both total anthocyanin and polymeric pigment (expressed as malvidin-3-glucoside equivalents) was

calculated for each sample. An example of a chromatogram of a red wine and the evolution of the polymer peak over time is shown in Figure 6.7.

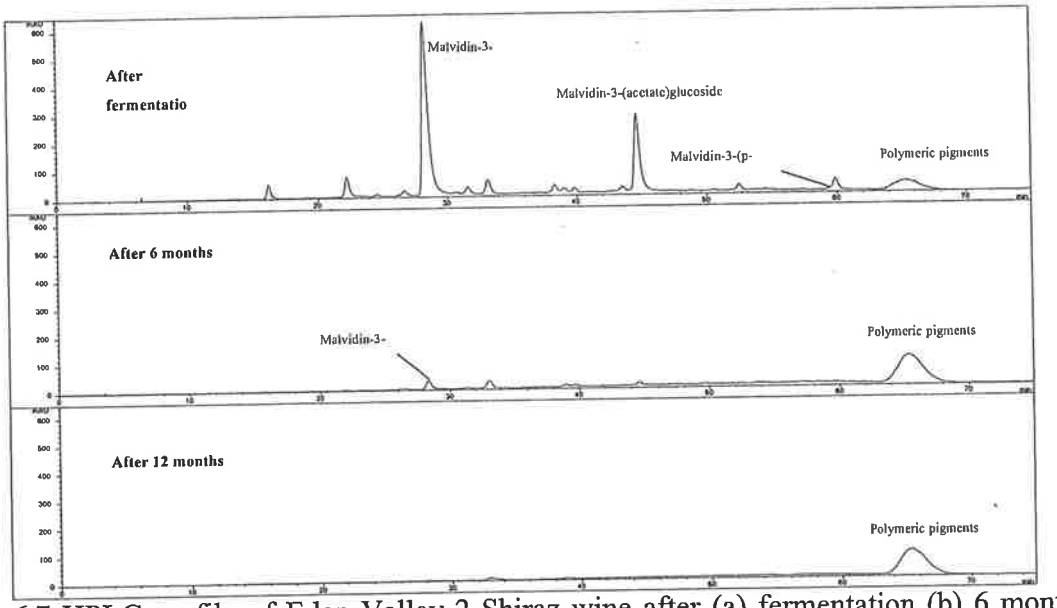

Figure 6.7 HPLC profile of Eden Valley 2 Shiraz wine after (a) fermentation (b) 6 months ageing and (c) after 12 months ageing.

The correlation between this HPLC method and UV/visible spectroscopy was tested to verify the results of the colour parameter measured/derived from the spectroscopic data (Table 6.12 and Table 6.13)

Table 6.12 Correlation matrices between the HPLC and UV/visible spectroscopy methods for determining the total monomeric anthocyanin concentration in a Shiraz wine. Values shown are r (the correlation coefficient for the respective regression analysis). +, *, ** and *** indicate significance at the p<0.1, 0.5, 0.01 and 0.01 level respectively. Values shown in bold are of most interest.

	Total anthocyanins HPLC (mg/L)	*[A] (mg anthocyanin/L)*	*Total anthocyanin (mg/L)*	*Total anthocyanins HPLC (mg/L)*	*[A] (mg anthocyanin/L)*	*Total anthocyanin (mg/L)*
	After fermentation			***After 6 months ageing***		
After fermentation						
Total anthocyanins (mg/L) HPLC	1.000					
[A] (mg anthocyanin/L)[b]	**0.936*** **	1.000				
Total anthocyanin (mg/L)[c]	**0.936*** **	0.947***	1.000			
After 6 months ageing						
Total anthocyanins (mg/L) HPLC	0.244	0.175	0.090	1.000		
[A] (mg anthocyanin/L)[b]	0.597***	0.558***	0.477**	**0.820*** **	1.000	
Total anthocyanin (mg/L[c])	0.330*	0.288+	0.198	**0.908*** **	0.939***	1.00

(a) Total anthocyanins measured as malvidin-3-monoglucoside equivalents

(b) Concentration of monomeric anthocyanins as calculated from the copigmentation formulas

(c) Total anthocyanin concentration as determined by the Somers and Evans, (1977) UV/visible measure

Table 6.13 Correlation matrices between the HPLC and UV/visible spectroscopy methods for determining the polymeric pigment concentration (expressed as malvidin-3-monoglucoside equivalents) in a Shiraz wine. Values shown are r (the correlation coefficient for the respective regression analysis). +, *, ** and *** indicate significance at the $p<0.1$, 0.5, 0.01 and 0.01 level respectively. Values shown in bold are of most interest.

	Polymeric pigments HPLC (mg/L)	*Ep[P] (mg/L)*	*Polymeric pigments HPLC (mg/L)*	*Ep[P] (mg/L)*	*Polymeric pigments HPLC (mg/L)*	*Ep[P] (mg/L)*
	After fermentation		***After 6 months ageing***		***After 12 months ageing***	
After fermentation						
Polymeric pigments HPLC	1.000					
Ep[P] (mg/L)	**0.576*** **	1.000				
After 6 months ageing						
Polymeric pigments HPLC	0.210	0.551***	1.000			
Ep[P] (mg/L)	0.346*	0.837***	**0.673*** **	1.000		
After 12 months ageing						
Polymeric pigments HPLC	0.120	0.447***	0.578***	0.765***	1.000	
Ep[P] (mg/L)	0.113	0.547***	0.541***	0.870***	**0.897*** **	1.000

The concentration of total anthocyanins as determined by HPLC was positively correlated at the 0.1% level with the methods of Somers and Evans, (1977) and also of Levengood, (1996) for calculating total anthocyanin concentration at the completion of fermentation and after 6 and 12 months ageing (Figure 6.8).

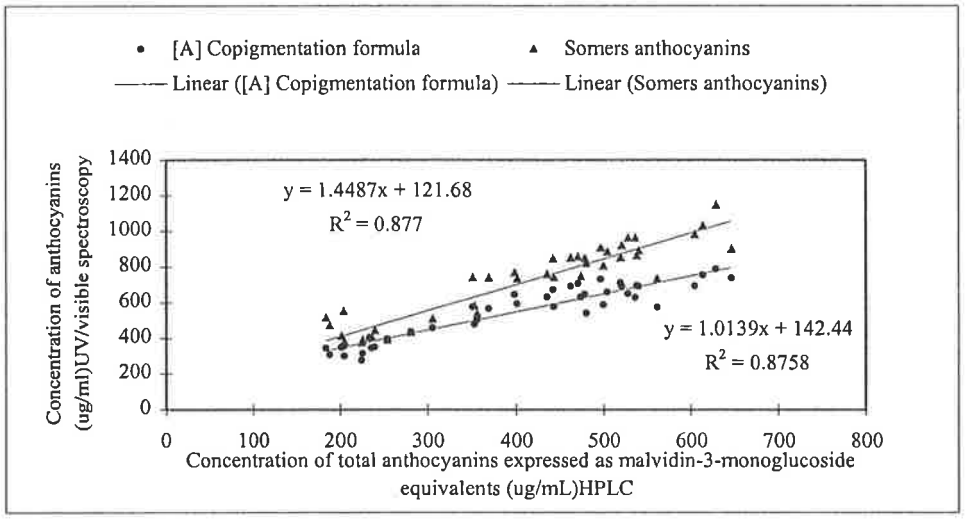

Figure 6.8 The relationship between HPLC and UV/Visible spectroscopy methods of Somers and Evans, (1977) and Levengood, (1996) for determining anthocyanins in a red wine, measured at the completion of fermentation. Statistically significant at the 0.1% level.

The measure of the concentration of total anthocyanins as determined by the visible spectroscopy methods gave values constantly higher than the HPLC method. Bakker et al., (1986) found a similar result and suggested that the higher anthocyanin content obtained by the spectral method of Somers and Evans, (1977) is attributed to partial bleaching of polymeric pigments (anthocyanins condensed with other flavonoids) by bisulphite. Another hypothesis is that the Somers and Evans, (1977) method did not take into account the anthocyanins involved in copigmentation and hence over estimated the total monomeric anthocyanins (Bolton, 2001). The difference between the method of Somers and Evans, (1977) and the copigment formula determination for total monomeric anthocyanin concentration was primarily due to the different extinction coefficients used in the derivation (section 6.3.6). However, the concentration of total monomeric anthocyanin as determined by the copigmentation formulas, [A] was still significantly higher than the concentration as determined by HPLC indicating that the discrepancy between the results was not solely due to copigmentation.

The concentration of polymeric pigment as determined by HPLC was positively correlated at the 0.1% level with the concentration of polymeric pigment (Ep[P]) as determined by UV/visible spectroscopy (Figure 6.8). As the red wine aged and the significance of the polymeric pigments increased, the correlation between the two parameters also increased (values in bold Table 6.13).

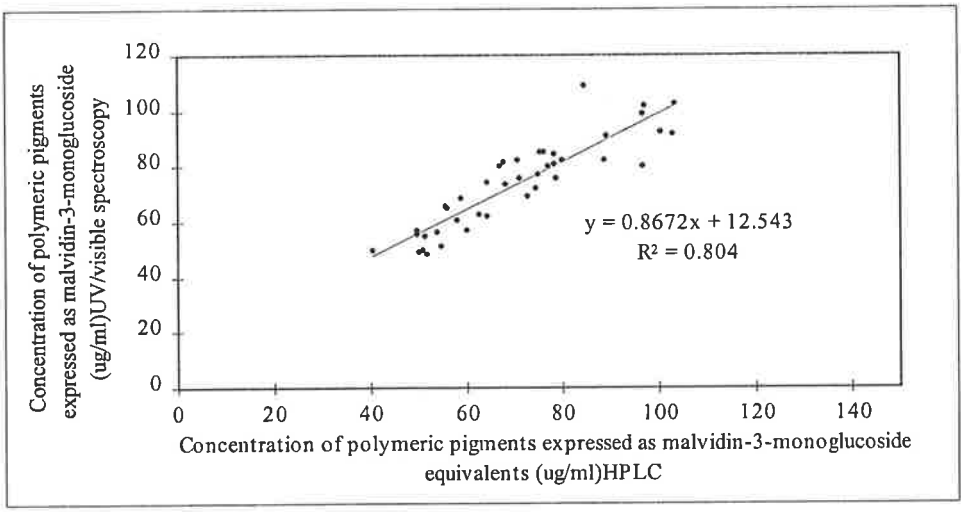

Figure 6.8 The relationship between values of polymeric pigments measured after 12 months ageing as determined by HPLC and the UV/visible spectroscopy methods.

6.3.6 Comparison of total colour as determined by the copigmentation formulas and the Somers and Evans measures

A positive correlation at the 0.1% level was observed between the total red colour of a set of Shiraz wines as determined by the absorbance at 520nm in the presence of acetaldehyde and the copigmentation formulas at the completion of fermentation (Figure 6.9). The relationship was also statistically significant at the 0.1% level after 6 and 12 months ageing, $r^2 = 0.9718$ and 0.9271 respectively.

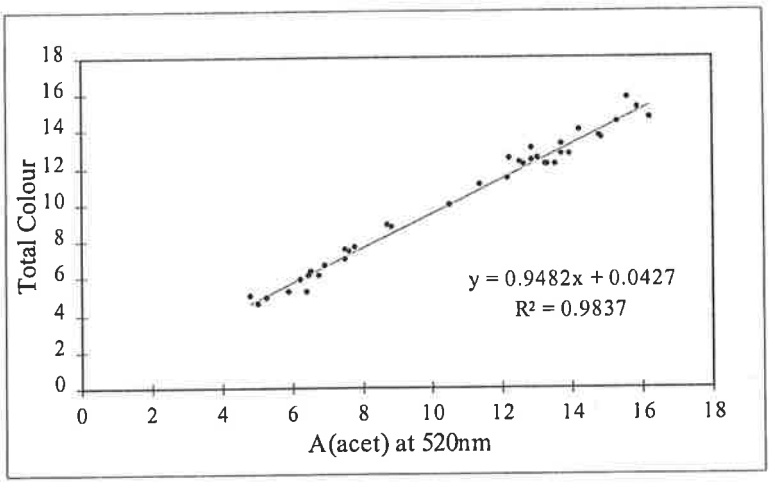

Figure 6.9 The relationship between the Somers and Evans, (1977) spectroscopic measure of total red colour and the total colour as calculated by the copigmentation formulas (Levengood, 1996). Statistically significant at the 0.1% level.

The majority of the red wine samples exhibited slightly larger $A_{520}{}^{acet}$ values compared to the derived total colour (TC). The discrepancy between the two measures for total red colour may be explained by the inherent assumptions made in the copigmentation formulas. Total colour (TC) was calculated as a sum of anthocyanins in the copigment complex, monomeric anthocyanin and polymeric pigment concentration. The individual constituents were calculated as a function of extinction coefficients and pK_H values taken from published data in conjunction with the absorbance data recorded. Hence some inaccuracies may be present in the calculations of the individual constituents due to the use of estimated values.

The measure of total anthocyanins differed between the two spectral methods due to the different extinction coefficients used. The Somers and Evans, (1977) method uses an extinction coefficient value of 0.05 AU/mg whereas Levengood, (1996) uses a value of 0.07 AU/mg. Consequently the total monomeric anthocyanin concentration (with and without accounting for [C]) as determined by the copigmentation formulas was less than that calculated by the Somers and Evans, (1977) method. Somers and Evans, (1977) also accounts for the polymeric pigment response of this component of wine colour to acidification of the wine ($\frac{5}{3}E_{520}^{SO2}$) enabling a better estimation of monomeric anthocyanin colour at pH <1.

Only 95% ± 4% of the total red colour in regards to $A_{520}{}^{SO2}$ was accounted for in the copigmentation formulas of Levengood, (1996). Adjustment of the concentration of total monomeric anthocyanins using the same extinction coefficient and the arbitrary 5/3 factor did not significantly change the percentage of the total colour accounted for in regards to

A_{520}^{SO2} (96.5% ± 4%). The average percentage colour accounted for in regards to the A_{520}^{acet} approached 100% as the wine aged, leading to speculation that it is the anthocyanins in the copigment complex that are not being fully expressed in the derived calculations. It has been suggested that the colourless and yellow coloured species of the anthocyanins may be involved in self-association interactions with the coloured forms (Houbiers et al., 1998). The contribution from the colourless species may not be fully accounted for in the copigment complex calculations. The extinction coefficient associated with the copigment complex may be inaccurate as it uses an estimate of enhancement (3 x 0.066 AU/mg).

The total colour expression of the Pinot Noir wines as determined by the copigmentation formulas and the A_{520}^{acet} were also positively correlated at the 0.1% significance level at all time intervals.

6.3.7 Improving the copigmentation formulas

A slight modification was made to the experimental procedure as outlined by Levengood, (1996) to test the effect of colour bleaching of the anthocyanin by sulphur dioxide in the 20 fold diluted samples. Solutions at a 20-fold dilution were prepared in the absence and presence of acetaldehyde. Calculating an adjusted copigment complex concentration ($A^{20,Acet}$) produced an increase in the corrected absorbance readings. The average reading for all 41 fermentation samples at the completion of fermentation was 5.79 ± 1.61 for the 20 fold diluted samples compared to 6.30 ± 1.71 for the diluted samples with added acetaldehyde. The higher value for the diluted samples with acetaldehyde added, was expected as the anthocyanin component previously bleached by SO_2 was now contributing to total colour.

Statistical analysis of the 20 fold diluted samples with and without the addition of acetaldehyde indicated that the addition of acetaldehyde caused a significant increase in the absorbance measure at the 0.1% level at the completion of fermentation, but at all other times the effect was non significant (Appendix 3). This may be attributed to the high proportion of the monomeric anthocyanins bleached by sulphur dioxide at the completion of fermentation. As the wine ages the concentration of monomeric anthocyanins declines and the effect of sulphur dioxide becomes less pronounced. A recommendation would be to include the addition of acetaldehyde, as it significantly changes the final results calculated for colour expression of a young red wine while not imparting any negative effects on an aged sample.

6.3.8 The relationship between copigmentation in red wines and the wines colour expression using the CIELAB scale

A positive correlation at the 0.1% level was observed between the concentration of the copigment complex in the Shiraz wines with the CIELAB measure of a* (Table 6.14 and Figure 6.10). The positive values of a* for the Shiraz wines indicated that as the concentration of copigment complex increased the colour of the wine increased in red colour. The negative values of b* indicated the wines were exhibiting blue hues. The negative correlation with copigmentation confirms that the greater the copigmentation complex concentration, the bluer the wine. Furthermore the effect of copigmentation caused a decrease in lightness (L).

Table 6.14 Correlation matrices of the CIELAB colour parameters of L, a* and b* and the concentration of copigment complex at the completion of fermentation. Values shown are r(the correlation coefficient for the respective regression analysis). +, *, ** and *** indicate significance at the $p< 0.1$, 0.05, 0.01 and 0.001 level respectively.

	L	*a**	*b**	*[C] after fermentation*	*%[C] after fermentation*
L	1.000				
a*	-0.995***	1.000			
*b**	0.693***	-0.724***	1.000		
[C] after fermentation	-0.878***	0.887***	-0.606***	1.000	
%[C] after fermentation	-0.675***	0.703***	-0.499***	0.877***	1.000

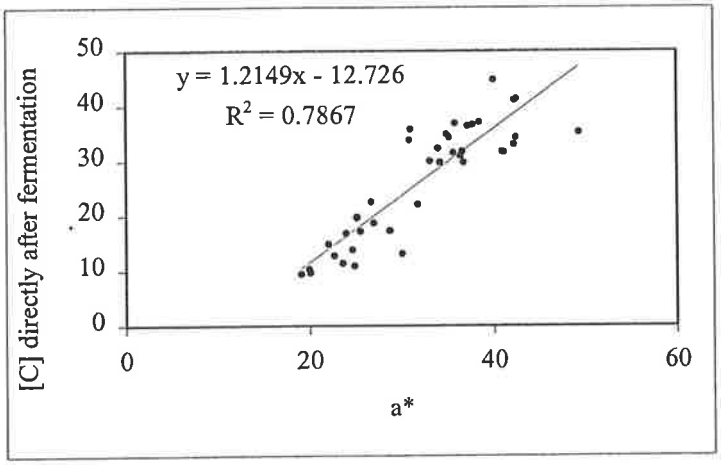

Figure 6.10 The relationship between the chromatic parameter of a* (positive values indicate red colour) and the concentration of copigment complex (mgL^{-1}) at the completion of fermentation.

Analysis of the full spectral profile of the individual wines highlighted the significance of the red and blue shifts relative to each other. The increase in the red colour intensity was the most significant. The increase in red colour expression with increased copigmentation may be directly correlated with the self-association of malvidin-3-monoglucoside, as this type of interaction does not result in an increase in wavelength absorbance maximum (a blue shift) (Chapter 2). The proportion of malvidin-3-(p-coumaryl)glucoside did not significantly differ between the wines. Therefore while the observed blue shifts must be a consequence of both malvidin-3-(p-coumaryl)glucoside self-association (530nm) and intermolecular copigmentation, differences between the wines must be a consequence of intermolecular copigmentation.

In contrast to the Shiraz wines, the wines made from Pinot Noir grapes exhibited no statistically significant correlation between the concentration of copigment complex and the chromatic parameters L, a* and b*. This would have been a consequence of the low variability observed between the wines in regard to copigment complex concentration and also the insignificance of copigmentation in Pinot Noir wines.

6.3.9 Comparison between the colour measures of the red wines after one months heating and 12 months ageing

It was anticipated that after heating a red wine for one month at 45°C the chemical composition of that wine would mimic the wine after 6 or 12 months ageing. If this assumption proved correct then a rapid means of mimicking an aged red wine would be available. Correlation analysis was used to determine relationships (Table 6.15).

With the exception of the Somers and Evans, (1977) measure of total anthocyanin there was positive correlation at the 0.1% significance level for all the colour parameters between one months heating and 6 months ageing. Correlation between heating of the Shiraz wine for one month and the wine after 12 months ageing was observed with polymeric pigment concentration and the total colour measure. As mentioned previously, polymeric pigment concentration at 12 months ageing is significantly correlated with total colour expression. Hence, heating a wine for one month provides a quick means to predict the final polymeric pigment concentration and consequently the total colour expression of the wine after 12 months maturation.

Table 6.15 Correlation matrices between one months heating and 6 and12 months ageing of the Shiraz wines. Values shown are r (the correlation coefficient for the respective regression analysis). +, *, ** and *** indicate significance at the p<0.1, 0.05, 0.01 and 0.001 level respectively.

After one months heating

After one months heating →	*[C]*	*[A]*	*Ep[P]*	*TC*	*Total anthocyanin (mg/L)*	*Total phenol (au)*
After 6 months ageing						
[C]	**0.537*** **	0.471**	0.508***	0.610***	0.449**	0.471**
[A]	0.525***	**0.446****	0.513***	0.602***	0.426**	0.446**
Ep[P]	0.781***	0.746***	**0.800*****	0.938***	0.698***	0.746***
TC	0.785***	0.733***	0.792***	**0.931*****	0.690***	0.733***
Total anthocyanin (mg/L)	0.314*	0.243	0.293+	0.346*	**0.238**	0.243
Total phenol (au)	0.596***	0.547***	0.712***	0.769***	0.531***	**0.547*****
After 12 months ageing						
[C]	**0.062**	-0.096	0.132	0.074	-0.119	-0.096
[A]	0.181	**0.089**	0.312*	0.269+	0.076	0.089
Ep[P]	0.698***	0.569***	**0.648*****	0.775***	0.535***	0.569***
TC	0.606***	0.462**	0.596***	**0.683*****	0.428**	0.462**
Total anthocyanin (mg/L)	-0.100	-0.181	0.021	-0.070	**-0.175**	-0.181
Total phenol (au)	0.369*	0.327*	0.599***	0.564***	0.305*	**0.327***

6.4 Conclusions

The measure of copigmentation gave an indication of its contribution to the total colour expression of a set of Shiraz wines. The contribution of the copigmentation was at its greatest at the completion of fermentation. The agreement between the calculated copigment concentration between the Shiraz wines and model solutions containing a similar total anthocyanin concentration supported the notion that the principal mode of copigmentation in red wines would be self-association. As the wines aged, the polymeric pigment concentration increased at the expense of monomeric anthocyanins and copigment complex. The most dominant component contributing to the total colour expression at any particular time interval was the polymeric pigment concentration. However, the total monomeric anthocyanin concentration at the completion of fermentation was the best predictor of the total colour expression of the wine after 12 months ageing. Colourmetric analysis of the Shiraz wines indicated that the wines exhibited an increased red colour and a blue hue with copigmentation.

The components in the Pinot Noir wines did not engage in copigmentation. The component contributing to the total colour expression of the wine was the polymeric pigment concentration. The best indicator of total colour expression of the wine after 12 months ageing was the polymeric pigment concentration. However it was a negative relationship indicating that the polymeric pigments present at the completion of fermentation were relatively unstable.

The total colour expression of a Shiraz wine at the completion of fermentation was directly correlated with grape berry skin colour (mg of anthocyanin/g of berry weight). The greater the skin colour of the grape berry the greater the total colour expression of the corresponding wine.

The concentration of anthocyanins and polymeric pigment as determined by UV/visible spectroscopy was significantly correlated with their concentration as determined by HPLC. Unless specific constituent information is required, UV/visible spectroscopy is a quick and relatively inexpensive means to determine anthocyanin and polymeric pigment concentration in red wines. Providing important information on the colour and quality of an individual wine. Furthermore, the total potential colour expression of a red wine at 12 months may be predicted by heating the wine at 45°C for one month.

It was recommended that a modification to the experimental procedure for determining copigment complex concentration be made. Acetaldehyde should be added to the 20 fold diluted wine samples to counteract the affect of sulphur dioxide on the bleaching of anthocyanins.

While the copigmentation formulas did account for the contribution of copigmentation interactions to the total colour expression for the Shiraz wines, they did exhibit some limitations when applied to wines with low anthocyanin and copigment concentration such as Pinot wines.

Chapter 7

Summary and conclusions

7.1 Summary

This thesis describes a comprehensive investigation of copigmentation mechanisms that are relevant to red wines made from *V. vinifera* grape berries.

The copigments chosen for the intermolecular copigmentation model studies are common phenolic constituents extracted from grape berries during red wine fermentation. Chlorogenic acid was chosen as a reference standard. The anthocyanins malvidin-3-monoglucoside and malvidin-3-(p-coumaryl)glucoside and the flavan-3-ol seed tannins were extracted and isolated from the skins and seeds respectively of *V. vinifera* grape berries. The procyanidin dimer B3 was synthesised from (±)-taxifolin and (+)-catechin. The solution stabilities and selectivites of the series of copigments toward malvidin-3-monoglucoside and malvidin-3-(p-coumaryl)glucoside were investigated by means of UV/visible spectroscopy. Thermodynamic parameters of copigmentation were derived using the methodology of Brouillard et al., (1989). The copigments which had the greatest influence on the colour expression of the anthocyanin, were the flavonols. The higher oligomeric flavan-3-ols were much better copigments than their monomeric equivalents. Red wine sugars did not exhibit any intermolecular copigmentation with malvidin-3-monoglucoside. In contrast to malvidin-3-monoglucoside, malvidin-3-(p-coumaryl)glucoside did not form intermolecular dimer copigment complexes.

One of the most important findings described in this thesis was the importance of malvidin-3-monoglucoside self-association. An equivalent addition of malvidin-3-monoglucoside acting as a copigment gave in general a ten-fold increase in colour expression relative to the other copigments. Furthermore, malvidin-3-(p-coumaryl)glucoside exhibited approximately twice the colour expression than the non-acylated malvidin-3-monoglucoside at equivalent concentrations. Malvidin-3-(p-coumaryl)glucoside did not form self-associative aggregates. The increased colour expression may be attributed to additional stabilisation by intramolecular copigmentation between the aromatic *p*-coumaric acid substituent on the glucose moiety with the aromatic centres.

A re-evaluation of the mode of copigmentation leading to colour enhancement is proposed. In general copigmentation results in an increase in absorbance and in some cases a slight shift in the absorbance maximum to longer wavelengths. Interaction between two constituents which results in colour enhancement, generally involves the formation of charge transfer complexes with electron delocalisation between the π systems of the individual constituents. The absence of characteristic spectral changes associated with the formation of charge transfer complexes leads to the conclusion that copigmentation colour enhancement is not a direct consequence of interaction. The net driving force of interaction between anthocyanins and either themselves or with copigments involves van der Waals and hydrophobic forces. Copigmentation results in a net decrease in monomeric flavylium ion and/or quinonoidal base thus according to Le Chatelier's principle the equilibrium adjusts to form more of the coloured species.

The conformational alignment of interaction is dependent on electrostatic forces involving attractive interaction between π electrons and the σ framework which outweigh unfavourable contributions such as π electron repulsion. Constituents such as the flavonols, which have π deficient molecular orbitals and in the case of quercetin are planar, reduce the π-π electron repulsion, resulting in face to face or slightly offset interaction. This in turn may result in electron delocalisation between molecular orbitals and explain the observed shift of the absorbance maximum to longer wavelengths.

The copigments with orientation of the B ring out of the plane of the A and C ring system, as demonstrated by *semi empirical* calculations, may in part contribute to their poor copigment complex stability. Furthermore, the increase in intermolecular copigmentation stability with increasing substitution of the flavan-3-ols may be attributed to the increase in cavity size.

Potentiometric titrations provided further information on the influence of intermolecular copigmentation on the equilibrium reactions of malvidin-3-monoglucoside. Malvidin-3-monoglucoside is involved in complex proton transfer reactions involving both monomeric and dimerisation macro and micro ionisation constants. Hence, the calculated ionisation constants of malvidin-3-monoglucoside represented multiple pKs. The ionisation constants of malvidin-3-monoglucoside did not change with copigment addition due to the large buffering capacity of the pKs associated with the coloured forms of malvidin-3-monoglucoside relative to the change in the hemiketal equilibrium.

The addition of seed tannin to malvidin-3-monoglucoside resulted in no change in the chemical shifts of the protons. This is contrary to the observations made by Wigand et al., (1992) where there was a shift in the chemical shifts of the protons of 7-hydroxy-3-4'-dimethoxyflavylium chloride with the addition of gallic acid. This may simply be a concentration effect or the observed change in chemical shift may be due to the use of a non buffered solvent media resulting in a reaction solution with high ionic strength. However ^{1}HNMR did indicate that the quinonoidal base form of malvidin-3-monoglucoside is the most dominant form at pH 3.6.

The presence of the quinonoidal base at wine pH (3.6) was evident in the ^{1}HNMR analysis and implicates the neutral quinonoidal base as the dominant malvidin-3-monoglucoside form involved in intermolecular copigmentation. This would suggest that the pK_a value associated with proton transfer between the flavylium cation and quinonoidal base would be less than 4.25 as reported by Brouillard and Delaporte, (1977). The quinonoidal base is a neutral species, as opposed to the positive flavylium ion, hence copigmentation stacks would not be effected by charge repulsion energies or require a counter anion. The stability constants calculated for copigmentation using the extinction coefficient of the flavylium ion are still valid as the quinonoidal base extinction coefficient is not expected to be significantly different.

The degree of colour enhancement observed with copigmentation is reduced in the presence of potassium bitartrate, ethanol and sulphur dioxide. The higher the concentration of anthocyanin the less the effect of these additives on copigmentation. Furthermore, this highlights the greater colour stability of anthocyanins involved in self-association and intramolecular copigmentation.

For relevance to red wine systems, the relative concentrations of the phenolics must be considered. The concentration of the flavan-3-ols, acids and flavonols in red wines is generally too low to significantly contribute to colour expression by intermolecular copigmentation. A typical red wine contains approximately 800 mgL^{-1} (2.76×10^{-3} $molL^{-1}$ monomeric flavan-3-ol equivalents) total potential copigment phenolic compounds. The concentration of the anthocyanins and their derivatives is approximately 400 mgL^{-1} (8×10^{-4} malvidin-3-monoglucoside equivalents) (Singleton, 1988). Taking into account the maximum possible intermolecular copigmentation, the increase in colour expression ($(A-A_0)/A_0$) would be approximately 45 fold less than that observed with the self-association of the anthocyanins. From this study, it is now known that self-association interactions are preferentially favoured over the intermolecular interactions.

Self-association of malvidin-3-monoglucoside may not account for the blue hues observed in some young red wines. The blue hues may be attributed to contribution from malvidin-3-(p-coumaryl)glucoside, intermolecular copigmentation and possibly other wine pigments that is acetaldehyde bridged polymeric pigments.

The addition of potassium bitartrate, ethanol and sulphur dioxide resulted in a net decrease in copigmentation of malvidin-3-monoglucoside with copigments. The higher the concentration of anthocyanin the less the effect of these variables on copigmentation.

Copigmentation in red wine is dependent on many factors. Perhaps the most important variable is the extractable concentration of both the anthocyanins and copigments. This is very much predetermined by the levels in the grape berries themselves and the relative solubilities of the constituents during the fermentation process. Moreover, winemaking practices to a certain extent may influence extraction rates. It is expected that the copigmentation equilibrium occurring in a young red wine would be complex with many mutually occurring interactions.

A spectral measure of copigmentation was taken to quantify the importance of copigmentation in retention and enhancement of colour expression in two popular Australian red wine varieties. Copigmentation accounts for up to 47% of the colour expression of a young Shiraz red wine. This may in part be attributed to its high anthocyanin concentration and copigment pool. In contrast, the phenolic constituents in the Pinot Noir wine did not engage in copigmentation. The low colour stability of Pinot Noir wines is a direct consequence of its phenolic profile. It lacks the very colour stable acylated anthocyanins and it has a high concentration of monomeric flavan-3-ols and is deficient in the flavanols such as quercetin and quercetin-3-glucoside.

The greater the degree of copigmentation at the completion of fermentation, the more polymeric pigments present after 12 months ageing. This supports the hypothesis that copigmentation is an intermediate step in the formation of the colour stable polymeric pigments.

The work described in this thesis demonstrates that when more anthocyanins are present (and in particular the acylated derivatives) directly after fermentation, the future colour stability of the wine is greater.

Appendices

Appendix 1

Single factor ANOVA to test statistically significant differences between the source of the Shiraz wines.

Total colour [TC]:

Wine	*count*	*sum*	*average*	*variance*
Barossa 1	3	35.604	11.868	2.803
Barossa 2	3	35.661	11.887	0.524
Barossa 3	3	45.749	15.250	0.282
Waikerie Yellow	3	18.342	6.114	0.757
Waikerie Red	3	14.551	4.850	0.044
Nurioopta Non Irrigated	3	33.682	11.227	4.337
Nurioopta Irrigated	3	23.872	7.957	0.502
Coonawarra 1	2	24.154	12.077	0.791
Coonawarra 2	3	39.583	13.194	0.592
Coonawarra 3	3	36.517	12.172	0.001
Coonawarra 4	3	40.598	13.533	0.046
Eden Valley Low Grade	3	20.509	6.836	0.410
Eden Valley High Grade	3	39.594	13.198	1.342
Waite	3	17.250	5.750	0.188
ANOVA				
Source of variation	*df*	*MS*	*Variance*	*Probabilit*
Between groups	13	34.27	37.84	$P<0.001^{***}$
Within groups	27	0.91		

Copigment complex concentration [C]:

Wine	*count*	*sum*	*average*	*variance*
Barossa 1	3	88.003	29.334	4.034
Barossa 2	3	94.356	31.452	2.681
Barossa 3	3	127.030	42.343	4.309
Waikerie Yellow	3	42.137	14.046	10.310
Waikerie Red	3	29.497	9.832	0.268
Nurioopta Non Irrigated	3	91.231	30.410	85.376
Nurioopta Irrigated	3	58.630	19.543	7.453
Coonawarra 1	2	65.514	32.757	17.877
Coonawarra 2	3	98.968	32.989	8.602
Coonawarra 3	3	100.253	33.418	1.108
Coonawarra 4	3	109.118	36.373	1.045
Eden Valley Low Grade	3	51.486	17.162	5.908
Eden Valley High Grade	3	102.468	34.156	36.182
Waite	3	37.432	12.477	0.950

ANOVA				
Source of variation	*df*	*MS*	*Variance ratio*	*Probability*
Between groups	13	308.17	19.51	$P<0.001^{***}$
Within groups	27	15.79		

Appendix 2

Single factor ANOVA to test statistically significant differences between the source of the Pinot Noir wines.

Total colour [TC]:

Wine	*count*	*sum*	*average*	*variance*
Eden Valley 1	3	8.322	2.77	0.0851
Eden Valley 2	3	7.65	2.55	0.0078
Eden Valley 3	2	6.35	3.17	0.0397
Eden Valley 4	3	9.45	3.15	0.0003
Waite	2	5.75	2.89	0.032

ANOVA				
Source of variation	*df*	*MS*	*Variance ratio*	*Probability*
Between groups	4	0.186	5.79	$P<0.05^{*}$
Within groups	8	0.032		

Copigment concentration [C]:

Wine	*count*	*sum*	*average*	*variance*
Eden Valley 1	3	6.15	2.05	0.653
Eden Valley 2	3	6.34	2.11	0.059
Eden Valley 3	2	3.00	1.50	0.021
Eden Valley 4	3	5.44	1.81	0.481
Waite	2	4.74	2.37	0.364
ANOVA				
Source of variation	*df*	*MS*	*Variance ratio*	*Probability*
Between groups	4	0.229	0.66	P=0.64$^{Non\ sign.}$
Within groups	8	0.346		

Appendix 3

Two way ANOVA to test significance of A^{20} vs $A^{20,Aacet}$

	Average	*Variance0*	*df*	*Variance between the treatments*	*Probability*
After fermentation					
$A^{20} + A^{acet}$	6.30	2.91			
A^{20}	5.79	2.59			
			1	32.12	P<0.001***
After 6 months ageing					
$A^{20} + A^{acet}$	6.72	2.35			
A^{20}	6.66	2.26			
			1	1.14	P=0.29 $^{non\ sign.}$
After 12 months ageing					
$A^{20} + A^{acet}$	5.03	1.35			
A^{20}	5.16	1.33			
			1	3.13	P=0.08 $^{non\ sign.}$

References

Abgueguen, O. and Bolton, R. B. The crystallisation kinetics of calcium tartrate from model solutions and wines. *Am. J. Enol. Vitic.* **1993**, *44*, 65-75.

Abraham, R. J., Eivazi, F., Pearson, H. and Smith, K. M. Mechanisms of Aggregation in Metalloporphyrins : Demonstration of a mechanistic dichotomy. *J. Chem. Soc Chem. Commun* **1976**, 698-701.

Adams, J. B. Thermal degradation of anthocyanins with particular reference to the 3-glucosides of cyanidin I. In acidified aqueous solution at 100C. *J. Sci. Food Agric* **1973**, *24*, 747-762.

Albert, A. and Serjeant, E. P. *The determination of ionization constants*; Chapman and Hall Ltd: London, 1971.

Alluis, B. and Dangles, O. Quercetin(=2-(3,4-Dihydroxyphenyl)-3,5,7-trihydroxy-4H-1-benzopyran-4-one) Glycosides and sulfates: chemical synthesis, complexation, and antioxidant properties. *Helv. Chim. Acta* **2001**, *84*, 1133-1156.

Anelli, P. L., Ashton, P. R., Spencer, N., Slawin, A. M. Z., Stoddart, J. F. and Williams, D. J. Self assembling [2]Pseudorotaxanes. *Angew. Chem. Inter. Ed. Eng.* **1991**, *8*, 1036-1042.

Archeir, P., Coen, S. and Roggero, J. P. Phenolic contents of single variety wines. *Sci. Aliments.* **1992**, *12*, 453-466.

Asen, R., Stewart, R. N. and Norris, K. H. Co-pigmentation of anthocyanins in plant tissues and its effect on colour. *Phytochemistry.* **1972**, *11*, 1139-1144.

Asenstorfer, R. E. Isolation, structures and properties of anthocyanins and wine pigments. PhD, Adelaide University, 2001.

Askew, B., Ballester, P., Buhr, C., Jeong, K. S., Jones, S., Parris, K., Williams, K. and Rebek, J. Molecular recognition with convergent functional groups. 6. Synthetic and structural studies with a model receptor for nucleic acid components. *J. Am. Chem. Soc.* **1989**, *111*, 1082-1090.

Bakker, J., Bridle, P., Honda, T. and Kuwano, H. Identification of an anthocyanin occurring in some red wines. *Phytochemistry.* **1997**, *44*, 1375-1382.

Bakker, J., Preston, N. W. and Timberlake, C. F. The determination of anthocyanins in aging red wines: Comparison of HPLC and spectral methods. *Am. J. Enol. Vitic* **1986**, *37*, 121-126.

Bakker, J. and Timberlake, C. F. The distribution of anthocyanin in grape skin extracts of port wine cultivars as determined by high performance liquid chromatography. *J. Sci. Food Agric.* **1985**, *36*, 1315-1324.

Bakker, J. and Timberlake, C. F. Isolation, identification, and characterization of new color-stable anthocyanins occurring in some red wines. *J. Agric. Food Chem.* **1997**, *45*, 35-43.

Baranac, J. M. and Petranovic, N. A. Spectroscopic study of anthocyanin copigmentation reactions. 4. Malvin and apigenin 7-glucoside. *J. Agric. Food Chem.* **1997**, *45*, 1701-1703.

Baranac, J. M., Petranovic, N. A. and Dimitric-Markovic, J. M. Spectroscopic study of anthocyanin copigmentation reactions. *J. Agric. Food Chem.* **1996**, *44*, 1333-1336.

Baranac, J. M., Petranovic, N. A. and Dimitric-Markovic, J. M. Spectroscopic study of anthocyanin copigmentation reactions. 2. Malvin and the nonglycosidized flavone quercetin. *J. Agric. Food Chem.* **1997a**, *45*, 1694-1697.

Baranac, J. M., Petranovic, N. A. and Dimitric-Markovic, J. M. Spectroscopic study of anthocyanin copigmentation reactions. 3. Malvin and the nonglycosidized flavone morin. *J. Agric. Food Chem.* **1997b**, *45*, 1698-1700.

Baudry, D., Ephritikhine, M. and Felkin, H. X-ray structure, conformation, and absolute configuration of 8-bromotetra-O-methyl-(+)-catechin. *J. Chem. Soc. Chem Commun* **1978**, 695-696.

Baumes, R., Cordonnier, R., Nitz, S. and Drawert, F. Identification and determination of volatile constituents in wines from different vine cultivars. *J. Sci. Food. Agric.* **1986**, *37*, 927-943.

Bayer, E., Egeter, H., Fink, A., Nether, K. and Wegmann, K. Complex formation and flower colors. *Angew. Chem. Inter. Ed. Eng.* **1966**, *5*, 791-798.

Benesi, H. A. and Hildebrand, J. H. A spectroscopic investigation of the interaction of iodine with aromatic hydrocarbons. *J. Am. Chem. Soc.* **1949**, *71*, 2703-2707.

Berg, H. W. and Keefer, R. M. Analytical determination of tartrate stability in wine I. Potassium bitartrate. *Am. J. Viti. Enol.* **1958**, *9*, 180-193.

Berke, B., Cheze, C., Vercauteren, J. and Deffieux, G. Bisulphite addition to anthocyanins: revisited structures of colourless adducts. *Tetrahedron Letter* **1998**, *39*, 5771-5774.

Berski, S. and Latajka, Z. On the role of the basis set and electron correlation in the description of stacking interactions. *Comput. Chem.* **1997**, *21*, 347.

Bolton, R. The copigmentation of anthocyanins and its role in the color of red wine- A critical review. *Am. J. Enol. Viti.* **2001**, *52*, 67-87.

Brooks, B. R., Bruccoleri, R. E., Olafson, B. D., States, D. J., Swaminathan, S. and Karplus, M. CHARMM: A program for macromolecular energy, minimisation, and dynamic calculations. *J. Comput. Chem* **1983**, *4*, 187-217.

Brouillard, R. Origin of the exceptional colour stabiltiy of the Zebrina anthocyanin. *Phytochemistry* **1981**, *20*, 143-145.

Brouillard, R. and Dangles, O. Anthocyanin molecular interactions: the first step in the formation of new pigments during wine aging? *Food. Chem.* **1994**, *51*, 365-371.

Brouillard, R. and Delaporte, B. Chemistry of anthocyanin pigments. 2. Kinetic and thermodynamic study of proton transfer, hydration and tautomeric reactions of malvidin 3-glucoside. *J. Am. Chem. Soc.* **1977**, *99*, 8461-8468.

Brouillard, R., Delaporte, B. and Dubois, J. Chemistry of anthocyanin pigments. 3. Relaxation amplitudes in pH-jump experiments. *J. Am. Chem. Soc.* **1978**, *100*, 6202-6205.

Brouillard, R. and Dubois, J. E. Mechanism of the structural transformations of anthocyanins in acidic media. *J. Am. Chem. Soc.* **1977**, *99*, 1359-1364.

Brouillard, R. and El Hage Chahine, J. Chemistry of anthocyanin pigments. 6. Kinetic and thermodynamic study of hydrogen sulfite addition to cyanin. Formation of a highly stable meisenheimer-type adduct derived from a 2-phenylbenzopyrilium salt. *J. Am. Chem. Soc.* **1980**, *102*, 5375-5378.

Brouillard, R and Lang, J. The hemiacetal-*cis*-chalcone equilibrium of malvin, a natural anthocyanin. *Can. J. Chem.* **1990**, *68*, 755-761.

Brouillard, R., Mazza, G., Saad, Z., Albrecht-Gary, A. M. and Cheminat, A. The copigmentation reaction of anthocyanins: A microprobe for the structural study of aqueous solutions. *J. Am. Chem. Soc.* **1989**, *111*, 2604-2610.

Brouillard, R., Wigand, M. and Cheminat, A. Loss of colour, a prerequisite to the plant pigmentation by flavonoids. *Phytochemistry.* **1990**, *29*, 3457-3460.

Brouillard, R., Wigand, M., Dangles, O. and Cheminat, A. pH and solvent effects on the copigmentation reaction of malvin with polyphenols, purine and pyrimidine derivatives. *J. Chem. Soc. Perkin Trans II.* **1991**, 1235-1241.

Buckingham, A. D. *Intermolecular interactions : from diatomics to bioploymers*; Wiley: Chichester, 1978.

Burley, S. K. and Petsko, G. A. Dimerisation energetics of benzene and aromatic amino acid side chains. *J. Am. Chem. Soc.* **1986**, *108*, 7995-8001.

Burley, S. K. and Petsko, G. A. Weakly polar interactions in proteins. *Advances in protein chemistry* **1988**, *39*, 125-189.

Calderon, A. A., Garcia-Florenciano, E., Munoz, R. and Ros-Barcelo, A. Gamey grapevine peroxidase: Its role in vacuolar anthocyani(di)n degradation. *Vitis* **1992**, *31*, 139-147.

Cheminat, A. and Brouillard, R. PMR investigations of 3-0-(b-D-glucosyl)malvidin structural transformations in aqueous solutions. *Tetrahedron. Lett* **1986**, *27*, 4457.

Chen, L. and Hrazdina, G. Structural aspects of anthocyanin-flavonoid complex formation and its role in plant colour. *Phytochemistry* **1981**, *20*, 297-300.

Claessens, C. and Stoddart, J. F. Review commtary. pi-pi interactions in self-assembly. *J. Phys. Org. Chem* **1997**, *10*, 254-272.

Clark, W. M. *The determination of hydrogen ions*; Bailliere, Tindall and Cox: London, 1928.

Cozzi, F. and Siegel, J. S. Interaction between stacked aryl groups in 1,8-diarylnaphthalenes: Dominance of polar/ over charge transfer effects. *Pure. Appl. Chem* **1995**, *67*, 683-689.

Cram, D. J. Preorganization-from solvents to spherands. *J. Angew. Chem., Int. Ed. Engl* **1986**, *25*, 1039-1134.

Dahl, T. The nature of stacking interactions betwen organic molecules elucidated by analysis of crystal structures. *Acta Chem. Scand* **1994**, *48*, 95-106.

Dallas, C. and Laureano, O. Effects of pH, sulphur dioxide, alcohol content, temperature and storage time on colour composition of a young Portugese red table wine. *J. Sci. Food Agric* **1994**, *65*, 477-485.

Damiani, A., De Santis, P., Giglio, E., Liquori, A. M., Puliti, R. and Ripamonti, A. The crystal structure of the 1:1 molecular complex between 1,3,7,9-tetrmethyluric acid and pyrene. *Acta Crst.* **1965**, *19*, 340-345.

Damiani, A., Giglio, E. and Liquori, A. M. The crystal structure of the 2:1 molecular complex between 1,3,7,9-tetramethyluric acid and 3,4-benzpyrene. *Acta Cryst.* **1967a**, *23*, 675-678.

Damiani, A., Giglo, E., Liquori, A. M., Puliti, R. and Ripamonti, A. Molecular geometry of a 2:1 crystalline complex between 1,3,7,9-tetramethyluric acid and coronene. *J. Mol. Biol.* **1967b**, *23*, 113-115.

Dangles, O. and Brouillard, R. A spectroscopic method based on the anthocyanin copigmentation interaction and applied to the quantitative study of molecular complexes. *J. Chem. Soc Perkin Trans II.* **1992**, 247.

Dangles, O. and Broulliard, R. Polyphenol interactions. The copigmentation case: thermodyamic data from temperature variation and relaxation kinetics. Medium effect. *Can. J. Chem.* **1992**, *70*, 2174-2189.

Dangles, O. and Elhajji, H. Synthesis of 3-Methoxy- and 3-(b-D-Glucopyranosyloxy)flavylium ions. Influence of the flavylium substitution pattern on the reactivity of anthocyanins in aqueous solutions. *Helv. Chim. Acta.* **1994**, *77*, 1595-1610.

Dangles, O., Saito, N. and Brouillard, R. Anthocyanin intramolecular copigment effect. *Phytochemistry.* **1993a**, *34*, 119-124.

Dangles, O., Saito, N. and Brouillard, R. Kinetic and thermodynamic control of flavylium hydration in the pelargonidin-cinnamic acid complexation. Origin of the extraordinary flower color diversity of *pharbitis nil*. *J. Am. Chem. Soc.* **1993b**, *115*, 3125-3132.

Darias-Martin, J., Carrillo, M., Diaz, E. and Bolton, R. B. Enhancement of red wine colour by prefermentation addition of copigments. *Food. Chem.* **2001**, *73*, 217-220.

Davies, A. J. and Mazza, G. Copigmentation of simple and acylated anyhocyanins with colorless phenolic compounds. *J. Agric. Food Chem.* **1993**, *41*, 716-720.

Davies, M. T. A universal buffer solution for use in ultra-violet spectroscopy. *J. Am. Chem. Soc* **1959**, *84*, 248-251.

Dewer, M. J. S. and Thiel, W. Ground states of molecules 38. The MNDO method. Approximations and parameters. *J. Am. Chem. Soc.* **1977**, *99*, 4899-4907.

Dufour, C. and Sauvaitre, I. Interactions between anthocyanins and aroma substances in a model system. Effect on the flavor of grape-derived beverages. *J. Agric. Food Chem* **2000**, *48*, 1784-1788.

Einstein, F. W. B., Kiehlmann, E. and Wolowidnyk, E. K. Structure and nuclear magnetic resonance spectra of 6-bromo-3,3',4',5,7-penta-*O*-methyl catechin. *Can. J. Chem.* **1985**, *63*, 2176.

Escribano-Bailon, T., Gutierrez-Fernandez, Y., Rivas-Gonzalo, J. C. and Santos-Buelga, C. Characterization of procyanidins of Vitis vinifera variety Tinta del Pais grape seeds. *J. Agric. Food Chem.* **1992**, *40*, 1794-1799.

Es-Safi, N., Fulcrand, H., Cheynier, V. and Moutounet, M. Competition between (+)catechin and (-)epicatechin in acetaldehyde-induced polymerization of flavanols. *J. Agric. Food Chem.* **1999**, *47*, 2088-2095.

Etievant, P. X. Volatile phenol determination in wine. *J. Agric. Food Chem.* **1981**, *29*, 65-67.

Figueiredo, P., Elhabiri, M., Toki, K., Saito, N., Dangles, O. and Brouillard, R. New aspects of anthocyanin complexation. Intramolecular copigmentation as a means for colour loss? *Phytochemistry.* **1996**, *41*, 301-308.

Figueiredo, P. and Pina, F. Formation of anthocyanin ion-pairs. A copigmentation effect. *J. Chem. Soc. Perkin. Trans II* **1994**, 775-778.

Foresman, J. B. and Frish, A. *Exploring chemistry with electronic structure methods*, 2 ed.; Gaussian Inc: Pittsburg, 1996.

Francia-Aricha, E. M., Guerra, M. T., Rivas-Gonzalo, J. C. and Santos-Buelga, C. New anthocyanin pigments formed after condensation with flavanols. *J. Agric. Food Chem.* **1997**, *45*, 2262-2266.

Frisch, M. J., Trucks, G. W., Schlegel, H. B., Gill, P. M. W., Johnson, B. G., Robb, M. A., Cheeseman, J. R., Keith, T. A., Petersson, G. A., Montgomery, J. A., Raghavachari, K., Al-Laham, M. A., Zakrzewski, V. G., Ortiz, J. V., Foresman, J. B., Ciozlowski, J., Stefanov, B. B., Nanayakkara, A., Challacombe, M., Peng, C. Y., Ayala, P. Y., Chen, W., Wong, M. W., Andres, J. L., Replogle, E. S., Gomperts, R., Martin, R. L., Fox, D. J., Binkley, J. S., Defrees, D. J., Baker, J., Stewart, J. P., head-Gordon, M., Gonzalez, C. and Pople, J. A. *Gaussian 94 (Revision A.1)*; Gaussian Inc.: Pittsburgh, 1995.

Fronczek, F. R., Gannuch, G., Mattice, W. L., Tobiason, F. L., Broeker, J. L. and Hemingway, R. W. Dipole Moment, solution, and solid state structure of (-)-epicatechin, a monomer unit of procyanidin polymers. *J. Chem. Soc. Perkin Trans II* **1984**, 1611.

Fronczek, F. R., Mattice, W. L., Mcgraw, W., Steynberg, J. P. and Hemingway, R. W. Crystal structure, conformational analysis, and molecular dynamics of tetra-*O*-methyl-(+)-catechin. *Bioploymer* **1993**, *33*, 275.

Fulcrand, H., Benabdeljalil, C., Rigaud, J., Cheynier, V. and Moutounet, M. A new class of wine pigments generated by reaction between pyruvic acid and grape anthocyanins. *Phytochemistry.* **1998**, *47*, 1401-1407.

Fulcrand, H., Doco, T., Es-Safi, N.-E., Cheynier, V. and Moutounet, M. Study of acetaldehyde induced polymerisation of flavan-3-ols by liquid chromatography-ion spray mass spectrometry. *J. Chromatogr. A.* **1996a**, *752*, 85-91.

Fulcrand, H., dos Santos, P. J. C., Sarni-Manchado, P., Cheynier, V. and Favre-Bonvin, J. Structure of new anthocyanin-derived wine pigments. *J. Chem. Soc. Perkin Trans 1.* **1996b**, 735-739.

Gans, P., Sabatini, A. and Vacca, A. SUPERQUAD: An improved general program for computation of formation constants from potentiometric data. *J. Chem. Soc. Dalton Trans* **1985**, 1195-1200.

Gao, L., Girard, B., Mazza, G. and Reynolds, A. G. Changes in anthocyanins and color characteristics of Pinot Noir wines during different vinification processes. *J. Agric. Food Chem.* **1997**, *45*, 2003-2008.

Gläbgen, W. E., Wray, V., Strack, D., Metzger, J. W. and Seitz, H. U. Anthocyanins from cell suspension cultures of *Daucus carota*. *Phytochemistry.* **1992**, *31*, 1593-1601.

Goldberg, D. M., Karumanchiri, A., Tsang, E. and Soleas, G. J. Catechin and epicatechin concentrations of red wines: Regional and cultivar-related differences. *Am. J. Enol. Vitic* **1998a**, *49*, 23.

Goldberg, D. M., Tsang, E., Karumanchiri, A. and Soleas, G. J. Quercetin and p-coumaric acid concentrations in commercial wines. *Am. J. Enol. Vitic* **1998b**, *49*, 142-151.

Goto, T. Structure, stability and color variation of natural anthocynins. *Progress Chem. Org. Nat. Product* **1987**, *52*, 113-118.

Goto, T., Hoshino, T. and Takase, S. A proposed structure of commelinin, a sky blue anthocyanin complex obtained from the flower petals of commelina. *Tetra Lett* **1979**, 2905-2911.

Goto, T. and Kondo, T. Structure and molecular stacking of anthocyanins-flower color variation. *Angew. Chem. Int. Ed. Eng.* **1991**, *30*, 17.

Goto, T., Tamura, H., Kawai, T., Hoshino, T., Harada, N. and Kondo, T. Chemistry of metalloanthocynins. *Annal. NY. Acad. Sci* **1986**, *471*, 155-160.

Grant, G. H. and Richards, W. G. *Computational chemisrty*; Oxford University Press: Oxford, 1996.

Harborne, J. B. *The Flavonoids - Advances in research since 1980*; Chapman and Hall: London, New York, 1988.

Haslam, E. Review. Symmetry and promiscuity in procyanidin biochemistry. *Phytochemistry.* **1977**, *16*, 1625-1640.

Haslam, E. *Plant Polyphenols, Vegetable Tannins Revisited*; Cambridge University Press: Cambridge, 1989.

Haslam, E. *Practical Polyphenolics. From structure to molecular recognition and physiological action*; Cambridge University Press: Cambridge, 1998.

Hehre, W. J. and Huang, W. W. *Chemistry with computation. An introduction to spartan*; Wavefunction: California, 1995.

Hoshino, T. An approximate estimate of self association constants and the self stacking conformation of malvin quinonoidal bases studied by 1H NMR. *Phytochemistry.* **1991**, *30*, 2049-2055.

Hoshino, T. Self-association of flavylium cations of anthocyanin 3,5-diglucosides studied by circular dichroism and 1H NMR. *Phytochemistry* **1992**, *31*, 647-653.

Hoshino, T. and Matsumoto, U. Evidences of the self association of anthocyanins I. Circular dichrism of cyanin anhydrobase. *Tetrahedron. Lett.* **1980**, *21*, 1751-1754.

Hoshino, T., Matsumoto, U. and Goto, T. Self association of some anthocyanins in neutral aqueous solution. *Phytochemistry.* **1981a**, *20*, 1971-1976.

Hoshino, T., Matsumoto, U., Goto, T. and Harada, N. Evidence for the self association of anthocyanins IV. PMR spectroscopic evidence for the vertical stacking of anthocyanin molecules. *Tetrahedron. Lett.* **1982**, *23*, 433-436.

Hoshino, T., Matsumoto, U., Harada, N. and Goto, T. Chiral exciton coupled stacking of anthocyanins: Interpretation of the origin of anomalous CD induced by anthocyanin association. *Tetrahedron. Lett.* **1981b**, *22*, 3621-3624.

Houbiers, C., Lima, J. C., Macanita, A. L. and Santos, H. Color stabilisation of malvidin 3-glucoside: self aggregation of the flavylium cation and copigmentation with the Z-chalcone form. *J. Phys. Chem B* **1998**, *102*, 3578-3585.

Hsu, P., Hodel, M. R., Thomas, J. W., Taylor, L. J., Hagedorn, C. H. and Hodel, A. E. Structural requirements for the specific recognition of an m7G mRNA cap. *Biochem.* **2000**, *39*, 12730-13736.

Hunter, C. A. Sequence-dependent DNA structure. The role of base stacking interactions. *J. Mol. Biol.* **1993**, *230*, 1025-1054.

Hunter, C. A., Leighton, P. and Sanders, J. K. M. Allosteric ligand binding to cofacial metalloporphyrin dimers : the mechanism of porphyrin disaggreagation. *J. Chem. Soc. Perkin Trans I* **1989a**, 547-552.

Hunter, C. A. and Sanders, J. K. M. The nature of p-p interactions. *J. Am. Chem. Soc.* **1990**, *112*, 5525.

Hunter, C. A., Sanders, J. K. M. and Stone, A. J. Exciton coupling in porphyrin dimers. *Chem. Phys.* **1989b**, *133*, 395-404.

Iland, P. *ASVO Oenology seminar, Adelaide*; Australian society of viticulture and oenology, p 40-41.

Iland, P., Ewart, A., Sitters, J., Markides, A. and Bruer, N. *Techniques for chemical analysis and quality monitoring during winemaking*; Patrick Iland Wine Promotions: Adelaide, 2000.

Karlström, G., Linse, P., Wallqvist, A. and Jönsson, B. Intermolecular potentials for the H2O-C6H6 and the C6H6-C6H6 systems calculated in an ab initio SCF CI approximation. *J. Am. Chem. Soc.* **1983**, *105*, 3777.

Katritzky, A. R., Szafran, M., Malhotra, N., Chaudry, S. U. and Anders, E. Aromaticity as a quantitative concept Part V: A comparison of semi-empirical methods for the calculation of molecular geometries of heteroaromatic compounds and application of AM1 and MNDO methods to the calculation of Bird's aromaticity indices. *Tetrahedron Computer Methodology* **1990**, *3*, 247-269.

Kennedy, J. A. and Jones, G. P. Analysis of proanthocyanidin cleavage products following acid-catalysis in the presence of excess phloroglucinol. *J. Agric. Food Chem* **2000**.

Kondo, T., Yoshida, K., Nakagawa, A., Kawai, T., Tamura, H. and Goto, T. Structural basis of blue-colour development in flower petals from *Commelina communis*. *Nature* **1992**, *358*, 515-518.

Kurtin, W. E. and Song, P. S. Electronic structures and spectra of some natural products of theoretical interest-I. *Tetrahedron* **1968**, *24*, 2255-2267.

Lazarus, S. A., Adamson, g. E., Hammerstone, J. F. and Schmitz, H. H. High-performance liquid chromatography/mass spectroscopy analysis of proanthocyanidins in foods and beverages. *J. Agric. Food Chem.* **1999**, *47*, 3693-3701.

Levengood, J. Copigmentation in Cabernet Sauvignon. M.S, University of California, 1996.

Levy, L. and Robinson, R. Experiments on the synthesis of anthocyanin. Part IX. Synthesis of oxycoccicyanin chloride. Observations on the distribution numbers of the anthocyanins. *J. Chem. Soc.* **1931**, *1931*, 2715-2722.

Liao, H., Cai, Y. and Haslam, E. Polyphenol interactions. Anthocyanins: Co-pigmentation and colour changes in red wines. *J. Sci. Food. Agric.* **1992**, *59*, 299-305.

Linder, P. W. and Voye, A. Potentiometric investigations of the equilibria between caffeic acid and copper(II), zinc(II), iron(II) and hydrogen ions in aqueous solution. *Polyhedron.* **1987**, *61*, 53-60.

Linskens, H. F. and Jackson, J. F. *Wine analysis*; Springer-Verlag: Berlin, 1988.

Litcher, V. Influence of oxidation processes on the development of the taste and flavour of wine distillates. *Am. J. Enol. Viti* **1989**, *40*, 31-35.

Lu, T. S., Saito, N., Yokoi, M., Shigihara, A. and Honda, A. Acylated pelargonidin glycosides in the red-purple flowers of *Pharbitis nil*. *Phytochemistry.* **1992**, *31*, 289-295.

Malien-Aubert, C., Dangles, O. and Amiot, M. J. Color stability of commercial anthocyanin-based extracts in relation to the phenolic composition. Protective effects by intra and intermolecular copigmentation. *J. Agric. Food Chem* **2001**, *49*, 170-176.

Malone, J. F., Murray, C. M., Charlton, M. H., Docherty, R. and Lavery, A. J. X-H...p (phenyl) interactions. Theoretical and crystallographic observations. *J. Chem. Soc., Faraday Trans.* **1997**, *93*, 3429.

Markakis, P. *Anthocyanins as food colours*; Academic Press: New York, 1982.

Markovic, J. M. D., Petranovic, N. A. and Baranac, J. M. A spectroscopic study of the copigmentation of malvin with caffeic and ferulic acids. *J. Agric. Food Chem.* **2000**, *48*, 5530-5536.

Mazza, G. and Brouillard, R. Cyanidin 3,5-diglucoside and four 3-deoxyanthocyanins in aqueous solutions. *J. Agric. Food Chem.* **1987**, *35*, 422-426.

Mazza, G. and Brouillard, R. The mechanism of co-pigmentation in aqueous solutions. *Phytochemistry.* **1990**, *29*, 1097-1102.

Melo, M.J., Moncada, M.C and Pina, F. On the red colour of raspberry (*Rubus idaeus*). *Tetrahedron. Lett.* **2000**, *41*, 1987-1991.

Miniati, E., Damiani, P. and Mazza, G. Copigmentation and self-association of anthocyanins in food model systems. *Ital. J. Food Sci.* **1992**, *2*, 109-116.

Mirabel, M., Saucier, C., Guerra, C. and Glories, Y. Copigmentation in model wine solutions: occurrence and relation to wine aging. *Am. J. Enol. Vitic* **1999**, *50*, 211-218.

Mistry, T. V., Cai, Y., Lilley, T. H. and Haslam, E. Polyphenol interactions. Part 5. Anthocyanin copigmentation. *J. Chem. Soc Perkin Trans II* **1991**, 1287-1296.

Mulliken, R. S. Molecular compounds and their spectra II. *J. Am. Chem. Soc.* **1952**, *74*, 811-824.

Nagel, C. W. and Wulf, L. W. Changes in the anthocyanins, flavonoids and hydroxcinnamic acid esters during fermentation and ageing of merlot and cabernet sauvignon. *Am. J. Enol. Vitic.* **1979**, *30*, 111-116.

Newcomb, L. F. and Gellman, S. H. Aromatic stacking interactions in aqueous solution: evidence that neither classical hydrophobic effects nor dispersion forces are important. *J. Am. Chem. Soc.* **1994**, *116*, 4993-4994.

Nishio, M., Umesawa, Y., Hirota, M. and Takeuchi, Y. The Ch/p interaction: Significance in molecular recognition. *Tetrahedron.* **1995**, *51*, 8665.

Okano, T., Uekama, K. and Taguchi, E. Electronic properties of N-heteroaromatics. XXXV. Futher observations on the charge transfer interaction of the carcinogen, 4-nitroquinoline 1-oxide, with DNA and deoxyribonucleosides: analysis of the visible difference bands. *Gann* **1969**, *60*, 295-305.

Pauling, L. *The nature of the chemical bond and the structure of molecules and crystals*; Cornell University Press: Ithaca, 1960; Vol. 3.

Pawliszyn, J., Szczesniak, M. M. and Scheiner, S. Interactions between aromatic systems: Dimers of benzene and *s*-tetrazine. *J. Phys. Chem.* **1984**, *88*, 1726.

Pekic, B., Kovac, V., Alonso, E. and Revilla, E. Study of the extraction of proanthocyanidins from grape seeds. *Food. Chem.* **1998**, *16*, 201-206.

Porter, L. J., Hrstich, L. N. and Chan, B. G. The conversion of procyanidins and prodelphinidins to cyanidin and delphinidin. *Phytochemistry.* **1986a**, *25*, 223-230.

Porter, L. J., Wong, R. Y., Benson, M., Chan, B. G., Vishwanadhan, V. N., Gandour, R. D. and Mattica, W. L. Conformational analysis of flavans: 1H N.m.r. and molecular mechanical (MM2) studies of the benzpyran ring of 3',4',5,7-tetrahydroxyflavan-3-ols: the crystal and molecular structure of the procyanidin (2R,3S,4R)-3',4',5,7-tetramethyoxy-4-(2,4,6-trimethoxyphenyl)flavan-3-ol. *J. Chem. Res. (S)* **1986b**, 86-87.

Price, S. F. Sun exposure and flavonols in grapes. PhD, Oregon State University, 1994.

Price, S. L. and Stone, A. J. The electrostatic interactions in van der Waals complexes involving aromatic molecules. *J. Chem. Phys.* **1987**, *86*, 2859-2868.

Rathore, R., Lindeman, S. V. and Kochi, J. K. Charge-transfer probes for molecular recognition via steric hinderance in donor-acceptor pairs. *J. Am. Chem. Soc.* **1997**, *119*, 9393-9404.

Ribereau-Gayon, P. The chemistry of red wine colour. In *Chemistry of winemaking*; A. Webb, Ed.; American Chemical Society: Washinigton D.C, 1973; pp 50-87.

Ricardo da Silva, Jorge, M., Rigaud, J., Cheynier, V., Cheminat, A. and Moutounet, M. Procyanidin dimers and trimers from grape seeds. *Phytochemistry.* **1991a**, *30*, 1259-1264.

Ricardo da Silva, J. M., Bourzeix, M., Cheynier, V. and Moutounet, M. Procyanidin composition of Chardonnay, Mauzac and Grenache blanc grapes. *Vitis* **1991b**, *30*, 245-252.

Rigaud, J., Escribano-Bailon, M. T., Prieur, C., Souquet, J. M. and Cheynier, V. Normal-phase high-performance liquid chromatographic separation of procyanidins from cacao beans and grape seeds. *J. Chromatogr.* **1993**, *654*, 255-260.

Ritchey, J. G. and Waterhouse, A. L. A standard red wine: Monomeric phenolic analysis of commercial cabernet sauvignon wines. *Am. J. Enol. Vitic.* **1999**, *50*, 91-100.

Rivas-Gonzalo, J. C., Bravo-Haro, S. and Santos-Buelga, C. Detection of compounds formed through the reaction of malvidin-3-monoglucoside and catechin in the presence of acetaldehyde. *J. Agric. Food Chem.* **1995**, *43*, 1444.

Robinson, G. and Robinson, R. A survey of anthocyanins. I. *Biochem* **1931**, *25*, 1687-1690.

Roehri-Stoeckel, C., Gonzalez, E., Fougerousse, A. and Brouillard, R. Synthetic dyes: simple and original ways to 4-substituted flavylium salts and their corresponding vitisin derivatives. *Can. J. Chem.* **2001**, *79*, 1173-1178.

Romero, C. and Bakker, J. Interactions between grape anthocyanins and pyruvic acid, with effect of pH and acid concentration on anthocyanin composition and color in model solutions.*J. Agric. Food Chem.* **1999**, *47*, 3130-3139.

Rossi, M., Rickles, L. F. and Halpin, W. A. The crystal and molecular structure of quercetin: A biologically active and naturally occurring flavonoid. *Bioorg. Chem.* **1986**, *14*, 55.

Saenger, W. *Principles of nucleic structure*; Spinger-Verlag: New York, 1984.

Saito, N., Osawa, Y. and Hayashi, K. Platyconin, a new acylated anthocyanin in chinese bell flower, *platycodon grandiflorum*. *Phytochemistry.* **1971**, *10*, 445-447.

Santos, H., Turner, D. L., Lima, J. C., Figueiredo, P., Pina, F. S. and Macanita, A. L. Elucidation of the multiple equilibria of malvin in aqueous solution by one and two dimensional NMR. *Phytochemistry* **1993**, *33*, 1227-1232.

Saucier, C., Little, D. and Glories, Y. First evidence of acetaldehyde-flavanol condensation products in red wine. *Am. J. Enol. Vitic* **1997**, *48*, 370-373.

Scheffeldt, P. and Hrazdina, G. Copigmentation of anthocyanins under physiological conditions. *J. Food Sci.* **1978**, *43*, 517520.

Scott, A. I. *Ultrviolet spectra of natural products*; Pergamon Press: Oxford, 1964.

Sigel, H., Malini-Balakrishnan, R. and Häring, U. K. Ternary complexes in solution. Influence of organic solvents on intramolecular aromatic ring stacks in aqueous mixed ligand metal ion complexes. Opposing solvent effects. *J. Am. Chem. Soc.* **1985**, *107*, 5137-5148.

Singleton, V. Wine Phenols. In *Modern Methods of Plant Analysis.*; H. Linskens and J. Jackson, Eds., 1988; pp 173-218.

Singleton, V. L. and Trousdale, E. K. Anthocyanin-tannin interactions explaining differences in polymeric phenols between white and red wines. *Am. J. Enol. Vitic.* **1992**, *43*, 63-70.

Skoog, D. A., Holler, F. J. and Nieman, T. A. *Principles of instrumental analysis*; Saunders College: Philadelphia, 1998.

Slifkin, M. A. Charge-transfer interactions of nucleic acid derivatives. *Biochim. Biophys. Acta.* **1965**, *103*, 365-373.

Somers, T. C. The polymeric nature of wine pigments. *Phytochemistry* **1971**, *10*, 2175-2186.

Somers, T. C. and Evans, M. E. Spectral evaluation of young red wines: anthocyanin equilibria, total phenolics, free and molecular SO2, "chemical age". *J. Sci. Food. Agric.* **1977**, *28*, 279-287.

Somers, T. C. and Pocock, K. F. Evolution of red wines III. Promotion of maturation phase. *Vitis* **1990**, *29*, 109-121.

Somers, T. C. and Verette, E. *Phenolic composition of natural wine types*; Springer-verlag: Berlin, 1988; Vol. 6.

Somers, T. C. and Wescombe, L. G. Evolution of red wines II. An assessment of the role of acetaldehyde. *Vitis* **1987**, *26*, 27-36.

Song, P. S., Moore, T. A. and Sun, M. Excited states of some plant pigments. In *The chemistry of plant pigments*; C. O. Chichester, Ed.; Academic Press: New York, 1972; pp 33-74.

Spek, A. L., Kojic-Prodic, B. and Labadie, R. P. Structure of (-)-epicatechin : (2R,3R)-2-(3,4-Dihydroxyphenyl)-3,4-dihydro-2H-1-benzopyran-3,5,7-triol, C15H14O6. *Acta Cryst.* **1984**, *C40*, 2068.

Steinke, R. D. and Paulson, M. C. The production of steam-volatile phenols during the cooking and alcoholic fermentation of grain. *J. Agric. Food Chem.* **1964**, *12*, 381-387.

Swain, T. and Hillis, W. E. The phenolic constituents of Prunus domestica I. the quantitative analysis of phenolic constituents. *J. Sci. Food Agric.* **1959**, *10*, 63-68.

Szent-Gyorgyi, A. *Bioenergetics*; Academic Press: New York, 1957.

Terahara, N., Saito, N., Honda, T., Toki, K. and Osajima, Y. Acylated anthocyanins of *Clitoria ternatea* flowers and their acyl moieties. *Phytochemistry.* **1990**, *29*, 949-953.

Timberlake, C. Anthocyanins-occurrance, extraction and chemistry. *Food Chem.* **1980**, *5*, 69-80.

Timberlake, C. F. and Bridle, P. Flaylium salts, anthocyanidins and anthocyanins 1. Structural transformations in acid solutions. *J. Sci. Food Agric* **1967**, *18*, 473-478.

Timberlake, C. F. and Bridle, P. Interactions between anthocyanins, phenolic compounds, and acetaldehyde and their significance in red wines. *Am. J. Enol. Vitic* **1976**, *27*, 97-105.

Timberlake, C. F. and Bridle, P. Anthocyanins: Colour augmentation with catechin and acetaldehyde. *J. Sci. Food. Agric.* **1977**, *28*, 539.

Vivas, N. and Glories, Y. Role of oak wood ellagitannins in the oxidation process of red wines during aging. *Am. J. Enol. Vitic* **1996**, *47*, 103-107.

Weinges, K. and Piretti, M. V. Isolierung des $C_{30}H_{26}O_{12}$ procyanidins B1 ans weintrauben. *Liebigs Ann. Chem. Dtsch.* **1971**, *748*, 218-221.

Wigand, M. C., Dangles, O. and Brouillard, R. Complexation of a fluorescent anthocyanin with purines and polyphenols. *Phytochemistry.* **1992**, *31*, 4317-4324.

Williams, J. H. The molecular electric quadrupole moment and solid state architecture. *Acc. Chem. Res* **1993**, *26*, 593-598.

Williams, M. and Hrazdina, G. Anthocyanins as food colorants: Effect of pH on the formation of anthocyanin-rutin complexes. *J. Food Sci.* **1979**, *44*, 66-68.

Willstatter, R. and Zollinger, E. H. XVI. Uber die Farbstoffe der Weintraube und der Heiderbeere, II. *Annalen* **1916**, *412*, 195-216.

Wilska-Jezka, J. and Korzuchowska, A. Anthocyanins and chlorogenic acid copigmentation - influence on the colour of strawberry and chokeberry juices. *Z Lebensm Unters Forsch* **1996**, *203*, 38-42.

Wilson, B. and Allen, M. Phenolic polymerisation and copigmentation. *The Australian Grapegrower and Winemaker Ann Tech Issue* **1994**, *18*.

Wright, L. D. and McCormick, D. B. Charge-transfer complexations among biochemically reactive compounds. *Experientia* **1964**, *20*, 501-502.

Yoshitama, K. Blue and purple anthocyanins isolated from the flowers of *Tradescantia reflexa*. *Bot. Mag. Tokyo* **1978**, *91*, 207-212.

Zimmerman, S. C., VanZyl, C. M. and Hamilton, G. S. Rigid molecular tweezers: preorganized hosts for electron donor-acceptor complexation in organic solvents. *J. Am. Chem. Soc.* **1989**, *111*, 1373-1381.